20th Himalaya-Karakoram-Tibet workshop, HKT 20 = HKT 20 ème colloque Himalaya-Karakoram-Tibet : Aussois, 29-03, 01-04 2005 : special extended abstracts volume = Volume de résumés étendus

Georges Mascle, Jérôme Lavé

ISSN 0993-796X

GEOLOGIE ALPINE

MEMOIRE H.S. N° 44

20TH HIMALAYA-KARAKORAM-TIBET WORKSHOP HKT 20

HKT 20 20ÈME COLLOQUE HIMALAYA-KARAKORAM-TIBET

Aussois 29-03 01-04 2005

Special Extended Abstracts Volume

Volume de Résumés Etendus

GEORGES MASCLE AND JÉRÔME LAVÉ EDITORS

2005

LGCA LABORATOIRE DE GÉODYNAMIQUE DES CHAÎNES ALPINES

Science de la Terre
LYON

GÉOLOGIE ALPINE

EDITÉ PAR LE LABORATOIRE DE
GÉODYNAMIQUE DES CHAÎNES ALPINES

MÉMOIRE H.S. N° 44

20TH HIMALAYA-KARAKORAM-TIBET WORKSHOP
HKT 20

HKT 20 20ÈME COLLOQUE
HIMALAYA-KARAKORAM-TIBET

Aussois 29-03 01-04 2005

Special Extended Abstracts Volume

Volume de Résumés Etendus

GEORGES MASCLE AND JÉRÔME LAVÉ EDITORS

HKT 20 Organizing Committee

J.M. Bertrand (CNRS LGCA, Université de Savoie, Chambéry);
S. Guillot (CNRS, Université Claude Bernard, Lyon);
F. Jouanne (CNRS LGCA, Université de Savoie, Chambéry);
J. Lavé (CNRS LGCA, Université Joseph Fourier, Grenoble);
P.H. Leloup (CNRS, Université Claude Bernard, Lyon);
G. Mascle (LGCA, Université Joseph Fourier, Grenoble);
A. Pêcher (LGCA, Université Joseph Fourier, Grenoble)

HKT 20 Scientific Committee

E. Appel (Tübingen University, Germany);
K. Arita (Hokkaido University, Sapporo, Japan);
N. Arnaud (Université de Montpellier, France);
J.P. Burg (ETH Zürich, Switzerland);
Y. Chen (Université d'Orléans, France);
C. France-Lanord (CRPG, Nancy, France);
E. Garzanti (Milano University, Italy);
P. Molnar (Colorado University, USA);
J.L. Mugnier (Observatoire de Grenoble, France);
Y. Najman (Lancaster University, UK);
P. O'Brien (PotsdamUniversity, Germany);
A. Paul (Observatoire de Grenoble, France);
G. Poupinet (Observatoire de Grenoble, France);
M. Strecker (PotsdamUniversity, Germany);
P. Tapponnier (IPG Paris, France);
I. Villa (Bern University, Switzerland).

Science de la Terre
LYON

HKT 20

20th Himalaya-Karakoram-Tibet Workshop
Aussois March 29-April 1, 2005

Special Extended Abstracts Volume
Volume de Résumés Etendus

GEORGES MASCLE AND JÉRÔME LAVÉ EDITORS

Aknowledgements

The organizers of the workshop are grateful for the financial and/or technical support received from the following sponsors

Remerciements

Les organisateurs du colloque remercient de leur aide financière et/ou technique les organismes suivants

Centre National de la RechercheScientifique (CNRS)
Ministère de l'Education Nationale, de l'Enseignement Supérieur et de la Recherche
Université Joseph Fourier, Grenoble
Université Claude Bernard, Lyon
Université de Savoie, Chambéry-Annecy
Observatoire des Sciences de l'Univers de Grenoble (OSUG)
Région Rhône-Alpes
Municipalité d'Aussois
International Lithosphere Program (ILP)
Fédération Françaises des clubs alpins et de montagne (Club Alpin Français)

THE BANGONG-NUJIANG SUTURE BETWEEN GERTSE AND DONG TSO (84°- 85°E) CENTRAL TIBET

[a]Jonathan C. Aitchison, [a]Jason Ali, [b]Badengzhu, [a]Aileen M. Davis, [a]Dei Faustino, [a]Lan Hui, [a]Smriti Safaya, [a]Iain Ross and [c]Zeng Qinggao

[a]Tibet Research Group, Department of Earth Sciences, University of Hong Kong, Pokfulam Road, Hong Kong SAR, CHINA

[b]Geological Team # 2, Tibet Geological Survey, Lhasa, Tibet, CHINA

[c]Tibet Geological Survey, Tibet Bureau of Land and Resources, Lhasa, Tibet, CHINA

The Bangong-Nujiang suture crosses central Tibet marking where Meso-Tethyan oceanic lithosphere, that once separated the Lhasa and Qiangtang terranes, was consumed by Late Jurassic to Early Cretaceous subduction. Although several models speculate on the development of this suture, few constraints on its geology are published. For example, the dimensions and temporal duration of the Meso-Tethys Ocean as well as the timing of its closure are poorly constrained. Field investigations were carried in 2000, 2002, and 2004 by the Tibet Research Group of The University of Hong Kong in the Gertse to Dong Tso region as part of an on-going research program.

Field data indicate southward emplacement of an ophiolitic nappe of suture zone rocks onto the Lhasa terrane. The suture itself is marked by a series of steeply dipping south-directed thrust faults. From north to south across the suture, the following lithologies can be observed. The continental sediments along the northern margin of the suture are in fault contact with southern Qaintang terrane rocks that are juxtaposed against thick successions of locally ankaramitic alkaline pillow basalts overlain by limestones. The presence of rugose corals indicates a Paleozoic age. This terrane is thrust southwards over the base (north) of an ophiolitic section at a zone of serpentinite-matrix mélange, which is dominated by ultramafic blocks in the footwall. Amphibolite blocks, which occur within this zone are regionally extensive. Locally the serpentinites have experienced significant silica-carbonate alteration. Small felsic stocks locally intrude harzburgitic ultramafic rocks at the base of the ophiolite. Traversing up-section through the ophiolite section, cumulate ultramafics, isotropic and layered gabbros, a well preserved sheeted dike section and pillow basalts are encountered. Chert is locally present although it is typically highly altered. South of the suture an extensive nappe of ophiolitic mélange has been thrust southwards over Late Mesozoic orbitolinid-bearing limestones. This nappe is dominated by serpentinite matrix mélange. It contains similar lithologies to those observed along the main suture including amphibolites, which are extensive near Largu Tso. Chert blocks within the mélange have yielded a Jurassic radiolarian fauna.

Calc-alkaline volcaniclastic rocks including andesitic lahars, pyroclastic flows and dacitic ignimbrites also crop out along the suture. They are overlain by conglomerates, the initial derivation of which was mostly from the volcanics, with higher units derived from other lithologies in the region.The suture is a zone of active tectonism with several neotectonic features cutting the area. Work is still at a preliminary stage and we expect further details of sedimentology, micropaleontology, geochemistry, geochronology, and paleomagnetism to follow.

GREATER INDIA: A REVIEW

JASON R. ALI (1) AND JONATHAN C. AITCHISON (1)

(1) Department of Earth Sciences, University of Hong Kong, Pokfulam Road, Hong Kong, China

"Greater India" is an eighty-year-old concept that has been used by geoscientists in plate tectonic models of the India-Asia collision system. Numerous authors working on the orogen and/or plate models of the broader region have added various sized chunks of continental lithosphere to the now northern edge of their reconstructed Indian plate. Prior to plate tectonic theory, Emile Argand (1924) and Arthur Holmes (1965) thought that the Himalayan Mountains and Tibetan Plateau had been raised due to the northern edge of the Indian craton under-thrusting the entire region. After plate tectonic theory began to be widely received, Greater India took on one of two different roles. A relatively small group of modelers added various amounts of plate to India as part of their reconstructions of eastern Gondwana. In contrast, a larger group of workers used India-plate extensions as a means of allowing initial contact between the sub-continent and the Eurasian backstop plate in southern Tibet to take place at various times between the Late Cretaceous and late Eocene in what we call "fill-the-gap" solutions. The Indian craton and the southern edge of Eurasia were almost invariably some distance from one another when the collision was supposed to have started; extensions to the sub-continent were used to circumvent the problem.

In this review, we exhume and re-examine the key Greater India proposals. From our analysis, it is clear that many proponents have ignored key information regarding the sub-continent's break-up position within Gondwana *and* the bathymetry of the Indian Ocean west of Australia, in particular the Wallaby-Zenith Plateau ridge and the Wallaby-Zenith Fracture Zone. It is our contention that the Indian plate likely extended only ~1000 km "north" of the central part of the Main Boundary Thrust, up to the Wallaby-Zenith Fracture Zone. Two interesting facts emerge. First, and ignoring issues that have been raised regarding this type of model, the under-thrusting/-plating proposals in which the extension to Greater India is based on the elevated portion of the Himalaya-Tibet area can be accommodated reasonably well when the sub-continent plus appendage is repositioned back in Gondwana. Second, some of the recently derived geophysical models depicting subducted Indian lithosphere beneath Tibet are broadly compatible with the suggested upper limit for the sub-continent's northern appendage. Models requiring more than ten degrees of northward extension are likely wrong. Related information concerning the position of southern Eurasia at the time of the collision will also be summarized as this impacts on the "fill-the-gap" type Greater India proposals.

REGIONAL TECTONIC CORRELATION OF CENTRAL SECTOR OF THE HIMALAYA

Kazunori ARITA (1) and Lalu Prasad PAUDEL(1, 2)

(1) Department of Earth and Planetary Sciences, Graduate School of Science, Hokkaido University, Sapporo, 060-0810, Japan.
(2) Central Department of Geology, Tribhuvan University, Kirtipur, Kathmandu, Nepal.

The Nepal Himalaya as well as Kumaun in India occupies a central sector of the Himalayan arc and shows crucial and typical foreland fold-and-thrust tectonics in the Himalaya after the India-Eurasia collision ca. 50 Ma. The geological and structural correlations of the central sector, however, have not yet been brought to a settlement. We try to correlate the geology and tectoncis of the Nepal Himalaya to Kumaun Himalaya and to discuss tectonics of the central sector of the Himalaya.

One of the key points to understand the Himalayan tectonics is the Main Central Thrust (MCT). The original MCT proposed by Heim and Gansser (1939) is the Lower MCT in our sense and is equivalent to the Munsiari Thrust in Kumaun (Valdiya, 1980). The Upper MCT is a real boundary separating the Lesser Himalayan meta-sediments (LHS) of the footwall from the Higher Himalayan Crystallines (HHC) of the hanging wall. The MCT zone between these two thrusts, variable both in thickness and width, is quite different in metamorphic grade and deformation degree from the overlying HHC (Paudel and Arita, 2002) and plays a role as a sliding zone of southward thrusting of the HHC. The rocksequence lithostratigraphically equivalent to those of MCT zone is often distributed in the LHS zone in the south as nappes and klippes and they are sometimes lack of the overlying HHC. In western Nepal the Karnali klippe consisting of the HHC and the overlying Tethyan sediments is underlain by the MCT zone with a thrust. The Karnali klippe continues westward to form the Almora kippe. The Almora klippe also is underlain by the MCT zone which is named the Ramgarh zone in Kumaun.

The nappes and klippes tectonically overlying the LHS zone in the central sector of the Himalayan arc are composed of rock sequence of the MCT zone and/or the HHC zone with or without the Tethyan sediments although they are called various names in places. This is likely considered to be owing to that the Upper MCT cuts the different lithostratigraphic horizon of the overlying the Higher Himalayan Crystalllines and the Tethyan sediments

References

HEIM, A. & GANSSER, A. 1939. *Mem. Soc. Helv. Sci. nat.*, **73**, 1-245.
PAUDEL, P. & ARITA K., 2000. *J. Asian Earth Sci.*, **18**, 561-584.
VALDIYA, K. S.,1980. Geology of Kumaun Lesser Himalaya. Wadia Institute of Himalayan Geology.

GEOLOGY, MAGMATISM AND DEFORMATION IN WEST-CENTRAL TIBET, ALONG THE LONGMU-CO LAKE.

NICOLAS ARNAUD (1), PHILIPPE H. LELOUP (2), STÉPHANE GUILLOT(2), JEAN LOUIS PAQUETTE (3),FRANCK VALLI4), GWELTAZ MAHEO(5), HAIBING LI (6), ZHIQIN XU(6), ROBIN LACASSIN (4), AND PAUL TAPPONIER(4)

1 Lab. Dynamique de la Lithosphère, UMR 5573 CNRS, ISTEEM et Univ. Montpellier 2, Pl. Eu. Bataillon, cc.066, 34095 Montpellier, France.
2 : Laboratoire de Dynamique de la Lithosphère (UCB-Lyon), CNRS UMR 5570 2 rue Raphaël Dubois, 69622 Villeurbanne Cedex
3 Lab. Magmas et Volcans, UMR 6524 CNRS, Univ. B. Pascal, 5 rue Kessler, 63000 Clermont-Ferrand, France
4 : Laboratoire de Mécanique de la Lithosphère, IPG Paris et Univ. Paris 7, France;
5 : Geol. Planet. Sci. Division,California Institute of Technology, Pasadena CA 91125
6 : Inst. of Geology, CAGS Beijing, China

As few basement geology is exposed in Tibet, this makes difficult any discussion on the shape and age of pre-Cenozoic events (oceanic sutures , geometry of blocks and deformations),. Here we present new geological data from western Tibet, near the LongMu Co (LMC) lake close to the Kashgar – Shiquanhe (Ali) road, that shed some light on the earlier geological history of that part of Tibet.

South of the Long Mu and Jingyu Lakes, the LongMu range forms a significant relief corresponding to a magmatic and metamorphic range It is bounded to the north by strands of the active left-lateral Goza fault. Most of the range consists of limestones, flysches, metabasalts, diabases, gabbros, granodiorites, acid volcanics and ultramafic rocks, as well as staurolite bearing schists. These rocks correspond to a paleo-continental volcanic arc, the LongMu arc, possibly marking a suture zone. The LongMu arc is intruded by leucocratic granites that exhibit a steep E-W foliation. The granites are muscovite rich and preserve a magmatic assemblage of Qz+Kfd+Pl+Mus±Bio. Deformation is fairly developed in thin section and shows plastic recrystalization of quartz with migrating sub grains. Magmatic muscovites are kinked or truncated along shear planes and partly recrystalized along their bordures forming new grains of few microns size. Biotites, when they existed at the magmatic stage, are severely retrogressed. These observations are in agreement with a fairly low pressure medium temperature deformation around 400°C (White, 1976). Deformation fades out rapidly and the south easternmost granites are un-deformed.

The LMC active left-lateral fault trends E-W and bound the LMC Range to the north. South of the active fault trace, the LMC fault zone corresponds to a ~1.5 km wide zone of intensively folded and sheared sedimentary rocks: Red Beds of probable Cretaceous age, conglomerates and schists. The LMC fault zone cross-cut NE trending thrusts that affect both the granodiorites and the leucocratic granite.

The U/Pb age of the leucocratic granites is very unprecise but points to a late Paleozoic minimum intrusion time, while some parts of the zircons are inherited from an older basement of ca 2.4 Ga. $^{40}Ar/^{39}Ar$ dating yields mica cooling ages of 102 Ma both in the undeformed and the deformed facies and thus indicate that the E-W foliation was acquired prior to the late Cretaceous. Modeling of K-feldspars $^{40}Ar/^{39}Ar$ ages show rapid cooling just after emplacement, followed by a period of protracted cooling and finally a much faster cooling starting at ca 55 Ma.

We propose that the LongMu arc marks the suture between the Kunlun and Qiangtang blocks, and thus could be a western prolongation of the Jinsha suture. Recognition of the Jinsha/ Longmu suture in western Tibet will allow using it as a Mesozoic and Cenozoic deformation marker. The late deformation of the leucogranites may be associated to Cretaceous strike slip movements along the Longmu range, as already reported along parts of the presently active Altyn Tagh and Kunlun The fact that the active Goza fault locally follows an old suture and possibly a cretaceous deformation zone shows that Tertiary strike slip faults may have re-oriented or re-activated weakness zones along some parts of their path. Finally the rapid cooling at 55 Ma suggests an early Tertiary period of exhumation, which could be a far-reaching, early, effect of the India-Asia collision.

CARBONATE PLATFORMS THROUGH TIME AND SPACE IN THE SPITI BASIN

T.N. BAGATI

Sedimentology Group, Wadia Institute of Himalayan Geology, Dehra Dun-248001(UA)

Spiti basin occupies an area of about 35,000 Sq Km in the North-Western Higher Himalaya between Latitudes 31°30' and 34° 20' and east Longitudes 75°50' and 79°00' and exposes about 10 km mostly fossiliferous Cambrian to Cretaceous sediments. It rests on Precambrian basement with relatively continuous sediments and two major sedimentation breaks are conspicous (e.g. cambro-ordovician and Hercynian gap). The first major carbonate episode in this part of tethyan sea was observed in Silurian followed by lower carboniferous. The carbonates in palaeozone are only 700 m thick while Mesozoic is 2.3 km thick (dominant between Scythian-Oxfordian). Lithostratigraphy, facies distribution, sedimentary characteristics, faunal assemblage, microfacies analysis and geochemistry suggest varied and complex depositional milieu, basin morphology and tectonic setting during Silurian (Pin Dolomite Formation), Lower Carboniferous (Lipak Formation), Triassic and Jurassic (Lalung Group, Scythian-Oxfordian).

Silurian (Pin Dolomite Formation) carbonate episode represents episodic reefal complexes, ooid shoals and tidal facies on the platform setting. Overall facies, microfacies, fauna and flora indicate supratidal to subtidal depositional milieu and patch reefs. The shallowing and deepening are associated with mud banks and are generally dolomite rich episodes. Lipak Formation (Lower Carboniferous) represents the second major phase of carbonate accumulation during Palaeozoic Era with emergence of some parts of the basin which resulted in deposition of sediments in the isolated platforms. Tidal deposits, ooid shoals with mudstone and evaporates suggest frequent shallowing and deepening events and presence of lagoons in latitude falling between 5-25°.

The Lalung Group (Mesozoic Era) carbonates are dominant from Scythian to Lower Oxfordian and are about 2.3 km thick. It represents complex facies association, basin morphology and geometry. The facies relationship, faunal distribution, microfacies analysis, field relationship and geochemistry indicate deep-shallow-deep water facies during Mesozoic. It was deposited in the passive margin setting with carbonate platform to basin facies. Scythian to Oxfordian platform is represented by drowned platform, rimmed shelf, ramp, lagoonal facies and reefal complexes. The incipient drowned platform during Scythian – Anisian shows deeper water facies assemblage. Shallow tidal to deeper shelf during Ladinian to Early Oxfordian was associated with reefal complexes, ooid shoals, lagoonal facies and complex deposition milieu and in the northeastern part the basin facies developed. The reefal complex during Rhaetian acted as barrier reefal complex and separated the basin carbonate-mudstone facies in the north from the platform carbonates in the south. The barrier reef complex shows presence of frame builders (viz; corals, algae, crinoids, ostrocodes, echinoids, stromatoporoids etc.) and is represented by back reef, central reef and fore reef. The geochemistry shows high concentration of Sr in the deeper water facies assemblage and reefal complexes.

The overview of carbonate accumulation in the spiti basin shows presence of shallow and wide platform in the epicontinental sea with reefal complexes, ooid shoals and tidal deposit during Silurian (Pin Dolomite Formation) and isolated platforms during Early Carboniferous (Lipak Formation). Palaeotethys - Silurian and Early Carboniferous was generally shallow, wide and sea level changes were common and was confined between 5° and 2° south of equator. Mesotethys – Scythian to Oxfordian (Mesozoic) represent very extensive platform and basin facies in the north. Barrier reef complex, patch reefs, drowning of platforms were common and the shallow tidal to deeper facies assemblage indicates interplay of tectonics and sea level changes (drifting phase?).

THE X-RAY DIFFRACTION STUDIES OF HUNZA RUBY AND ITS HOST ROCKS EXPOSED IN KARAKORAM RANGE.

S.R.H. BAQRI AND A. UL HAQUE

Earth Sciences Division, Pakistan Museum of Natural History (Pakistan Science Foundation) Garden Avenue, Shakarparian, Islamabad 44000, Pakistan.

Beautiful isolated pinkish red crystals of ruby and reddish pink crystals of garnets are found in the coarsely crystalline white limestones/marbles of Baltit Group, exposed in the Karakoram Range, at Aliabad, Hunza, on the main Karakoram Highway. The coarsely crystalline limestones display direct contact with the granites and granodiorites of the Karakoram Batholith of Tertiary age. The X-ray diffraction patterns of the Hunza ruby were compared with the patterns given by the corundum and gave more or less similiar hkl reflections and respective intensities. The host rock (coarsely crystalline limestones) gave all the hkl reflections and respective intensities of a calcite. The densities of the ruby and the calcite of the host rocks were observed as 4.05 gm/cm^3 and 2.687 gm/cm^3, respectively. The Hunza ruby originated due to the contact metamorphism of limestones as a result of the intrusion of the Karakoram Batholiths into the Baltit Group of Pre-Cambrian/Permian age. The aluminum and Magnesium rich solutions concentrated into the cavities and pores of the associated limestones and gave rise to the beautiful crystals of ruby and garnets.

CONTINUOUS AND EPISODIC EXHUMATION OF THE CENTRAL HIMALAYAS FROM DETRITAL ZIRCON FISSION-TRACK ANALYSIS OF SIWALIK SEDIMENTS, NEPAL

Matthias BERNET, Peter VAN DER BEEK, Pascale HUYGHE, and Jean-Louis MUGNIER

Laboratoire de Géodynamique des Chaînes Alpines, Université Joseph Fourier, Grenoble, France

The record of orogenic cooling and exhumation is preserved in foreland basins adjacent to convergent mountain belts (e.g. Zeitler et al. 1986). These basins hold sediments that contain detrital apatite, zircon and mica that can be dated with various low-temperature thermochronologic techniques such as (U-Th)/He, fission-track or Ar/Ar dating. We present here a study of the Miocene to Pliocene Siwalik Group, which encompasses the Neogene foreland basin deposits of the Himalayas, to determine long-term exhumational history of the central Himalayas. So far the exhumation history for this part of the Himalayas has been poorly constrained. For this reason we analyzed detrital zircon of 24 samples collected from modern river sediment and sandstone of magneto-stratigraphically controlled sections of the Siwaliks near Karnali, Surai Khola, and Tinau Khola in western and central Nepal (Fig. 1A).

The zircons were dated with the fission-track method in order to estimate long-term exhumation rates using the lag-time concept (cooling age – depositional age) and for analyzing the overall pattern of exhumation (Bernet et al. 2001). The advantage of using zircon fission-track analysis is that zircon is not easily reset after deposition in a basin because of its relatively high closure temperature of ~ 240°C (Hurford 1986; Brandon et al. 1998), therefore retaining original cooling ages. On the other hand the closure temperature is not as high as for the Ar/Ar system (~350-420°C) (von Eynatten and Wijbrans 2003), which leads to highly smoothed exhumation rate estimates.

All our samples where dated with external detector method and using multiple mounts with different etch times per sample to allow detection of the full grain-age spectrum. The results were analyzed with BINMOFIT to decompose the observed grain-age distributions into major grain-age components or peaks (Brandon 1996). Our data indicate three main age groups, which are found consistently in our samples. The oldest age group shows fairly constant peak ages between 80-120 Ma and is a typical example of a static peak, which demonstrates recycling of zircon with pre-Himalayan cooling ages (Fig. 1B). These zircons were likely derived from Tethyan Himalaya sedimentary rocks or non-reset parts of the Lesser Himalayas. The second age group reflects a second static peak at 15-18 Ma, which is observed in each sample (Fig. 1B). This peak may be related to a fast exhumation and cooling event associated with possible slab break-off around 18 Ma and/or with episodic movement along major thrust-faults, such as the Main Central Thrust. Sources for theses zircons include reset parts of the Lesser Himalayas and possibly the Miocene Leucogranites in the High Himalayas. The youngest age group displays a moving peak with a relatively constant lag-time of 4 +/-1 m.y., which translates into a long-term exhumation rate of 1-1.5 km/m.y. This peak first appears around 11 Ma (Fig. 1B) and is evidence of continuous exhumation in the central Himalayas, probably driven by fluvial erosion and river incision in the High Himalayas.

Currently we are analyzing the same single zircons of the two younger age groups with the U-Pb method, because U-Pb dating helps us with provenance discrimination between Lesser Himalayan and Greater Himalayan sources or with identifying zircon derived from Miocene Leucogranites.

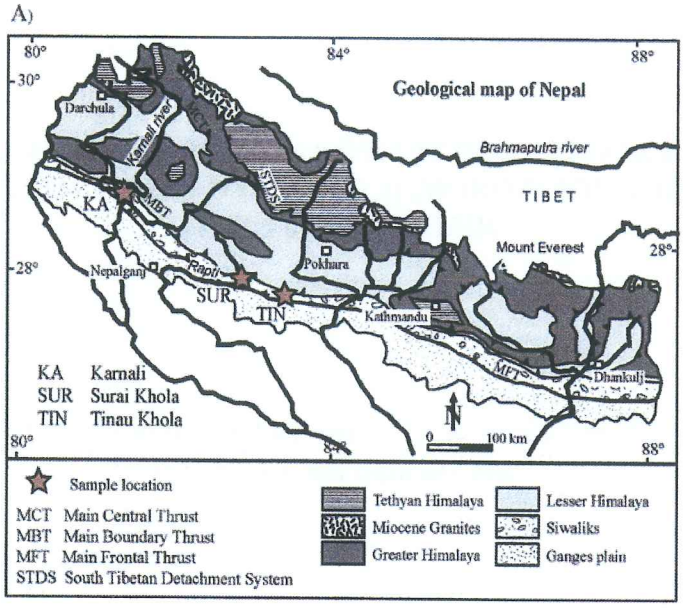

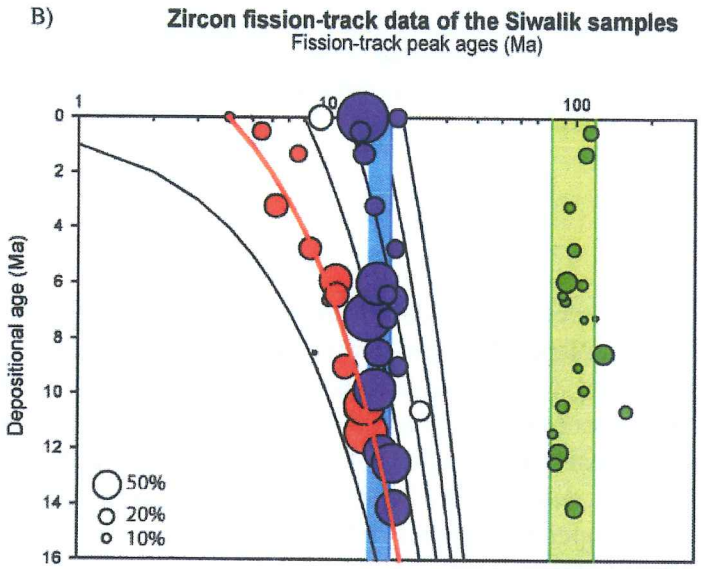

References:

BERNET, M., ZATTIN, M, GARVER, J.I., BRANDON, M.T., AND VANCE, J.A., 2001, Steady-state exhumation of the European Alps: *Geology*, **29**, 35-38.

BRANDON, M.T., 1996, Probability density plot for fission track grain-age samples: *Radiation Measurements*, **26**, 663-676.

BRANDON, M.T., RODEN-TICE, M.K., AND GARVER, J.I., 1998, Late Cenozoic exhumation of the Cascadia accretionary wedge in the Olympic Mountains, northwest Washington State: *Geological Society of America Bulletin*, **110**, 985-1009.

HURFORD, A.J., 1986, Cooling and uplift patterns in the Lepontine Alps, South Central Switzerland and an age of vertical movement on the Insubric fault line: *Contributions to Mineralogy and Petrology*, **92**, 413-427.

VON EYNATTEN, H., AND WIJBRANS, J.R., 2003, Precise tracing of exhumation and provenance using the $^{40}Ar/^{39}Ar$ geochronology of detrital white mica: the example of the Central Alps, *in* McCann, T., and Saintot, A., eds., Tracing Tectonic Deformation Using the Sedimentary Record: *Geological Society [London] Special Publications*, **208**, 289-305.

ZEITLER, P.K., JOHNSON, M.N., BRIGGS, N.D., AND NAESER, C.W., 1986, Uplift history of the NW Himalaya as recorded by fission-track ages of detrital Siwalik zircons, in Jiqing, H., ed., Proceedings of the Symposium on Mesozoic and Cenozoic Geology: Beijing, Geological Publishing House, 481-494.

LOOKING FOR SPATIAL AND TEMPORAL VARIATIONS OF INTERSEISMIC STRAIN FROM GPS MONITORING (CGPS AND CAMPAIGN DATA) ACROSS THE HIMALAYA OF NEPAL

Pierre BETTINELLI (1), Mireille FLOUZAT (1) , Jean-Philippe AVOUAC (2), Laurent BOLLINGER (1) and Madhab Raj PANDEY (3)

(1) Commissarait à l'Energie Atomique, Laboratoire Détection et Géophysique, 91680 Bruyères-Le-Châtel, France.
(2) Geological and Planetary Sciences, California Institut of Technology, Pasadena 91125 (CA), USA.
(3) National Seismological Center, Department of Mines and Geology, Lainchaur, Kathmandu, Nepal.

We analyse several sources of GPS data from geodetic monitoring of current shortening across the Himalaya of central Nepal. The data set includes: campaign measurements from 1995, 1998 and 2000 realized by LDG, CIRES, Idylhim networks [Jouanne et al., 2004 & Larson et al., 1999]; data from three permanent GPS stations that have been operated continuously since 1997 [Flouzat et al., 2002] along a transect at the latitude of Kathmandu ; sporadic data from one continuous GPS (cGPS) station at Nagarkot; data from the DORIS station at EVEB. The continuous observations of the DASE-DMG network operated since 1997, appears to be a particularly dense temporal constrain on the interseismic velocity field.

In order to avoid possible seasonal effects from long baselines, the cGPS data were processed with Bernese software relative to the IGS station at Lhasa. The data are combined and expressed in the same ITRF2000 reference frame. The processing strategy is discussed. They were next referenced to stable India motion relative to Lhasa and plate solutions for the motion of India in ITRF2000. Seasonal variations observed within the time series are discussed.

The data were then modeled using first a simple 2-D creeping dislocation embedded in an elastic half space model [Singh & Rani, 1993], and second, compare then to a finite element model which accounts for the thermal structure of the range and the temperature-dependant rock rheology [Cattin & Avouac, 2001]. Depending on model assumptions, the shortening rate across the range is estimated between 15 and 21mm/yr, a value that is comparable, though slightly lower than the 21±1.5mm/yr long term slip rate on the MHT derived from long term (Holocene) geological observations [Lavé et Avouac, 2000].

(References)

Avouac, J.P., Mountain Building, Erosion, and the Seismic Cycle in the Nepal Himalaya, Advances in Geophysics, 46, 2003.

Beutler G., Brockmann E., Dach R., Fridez P., Gurtner W., Hugentobler U., Johnson J., Mervart L., Rothacher M., Shaer S., Springer T. and Weber R., Bernese GPS Software Version 4.2.,Astronomical Institute, University of Berne,pp 436, 2001.

Bilham, R., The elusive height of Mount Everest: Everest, National Geographic Society, 26-27, 1997.

Bilham, R., F. Blume, R. Bendick, and V.K. Gaur, Geodetic constraints on the translation and deformation of India: Implications for future great Himalayan earthquakes, Current Science, 74 (3), 213-229, 1998.

Bollinger, L., J.P. Avouac, R. Cattin, and M.R. Pandey Stress buildup in the Himalaya, Journal of Geophysical Research, 109 (B11405), doi:10.129/2003JB002911, 2004.

Brown, L.D., et al., INDEPTH deep seismic reflection observation of a regionally extensive high-amplitude basement reflector, and associated "bright spots" beneath the northern Yadong-Gulu rift, Tibet, Science, 274, 1688-1690, 1996.

Cattin, R., and J.P. Avouac, Modeling mountain building and the seismic cycle in the Himalaya of Nepal, Journal of Geophysical Research-Solid Earth, 105 (B6), 13389-13407, 2000.

Chen, Q.Z., J.T. Freymueller, Q. Wang, Z.Q. Yang, C.J. Xu, and J.N. Liu, A deforming block model for the present-day tectonics of Tibet, Journal of Geophysical Research-Solid Earth, 109 (B1), art. no.-B01403, 2004.

Dong, D., Fang, P., Bock, Y., Cheng, M. K., Miyazaki, S., Anatomy of apparent seasonal variations from GPS-derived site position time series, Journal of Geophysical Research, vol.107, no.4, 13 pp., 2002.

Flouzat, M., Avouac, J.P., Durette, B., Bollinger, L., Heritier, T., Jouanne, F. and Pandey, M., Interseismic deformation across the Himalaya of Central Nepal from GPS measurements, AGU Fall Meeting, 2002.

Jackson, M., and R. Bilham, 1991-1992 GPS measurements across the Nepal Himalaya, Geophysical Research Letters, 21, 1169—1172, 1994a.

Jackson, M., and R. Bilham, Constraints on Himalaya deformation inferred from vertical velocity fields in Nepal and Tibet, J. Geophys. Res., 99, 13897—13912, 1994b.

Jouanne, F., J.L. Mugnier, J.F. Gamond, P. Le Fort, M.R. Pandey, L. Bollinger, M. Flouzat, and J.P. Avouac, Current shortening across the Himalayas of Nepal, Geophysical Journal International, 157 (1), 1-14, 2004.

Jouanne, F., J.L. Mugnier, M. Pandey, J.F. Gamond, P. Le Fort, P. Serrurier, C. Vigny, J.P. Avouac, and I. members., Oblique convergence in Himalaya of western Nepal deduced from preliminary results of GPS measurements, Geophys. Res. Lett., 26, 1933—1936, 1999.

Larson, K.M., and e. al., Kinematics of the India-Eurasia collision zone from the GPS measurements, J. Geophys. Res., 104, 1077—1093, 1999.

Lavé, J., and J.-P. Avouac, Active folding of fluvial terraces across the Siwaliks Hills, Himalayas of central Nepal, Journ. Geophys. Res., 105, 5735—5770, 2000.

Molnar, P., and M.R. Pandey, Rupture zones of great earthquakes of the Himalayan region, Indian Academy of Sciences (Earth and Planetary Science), Volume 98 (1), 61-70, 1989.

Nelson, K.D., W. Zhao, L.D. Brown, and e. al., Partially molten middle crust beneath southern Tibet: Synthesis of Project INDEPTH Results, Science, 174, 1684—1688, 1996.

Perfettini, H., and J.P. Avouac, Stress transfer and strain rate variations during the seismic cycle, Journal of Geophysical Research-Solid Earth, 109 (B6), 2004.

Sella, G.F., T.H. Dixon, and A.L. Mao, REVEL: A model for Recent plate velocities from space geodesy, Journal of Geophysical Research-Solid Earth, 107 (B4), art. no.-2081, 2002.

Singh, S.J., and S. Rani, Crustal deformation associated with two-dimensional thrust faulting., Journal of Physics of the Earth., 41, 87-101, 1993.

Socquet, A., C. Vigny, W. Simons, and N. Chamot-Rooke, Accomodation of the relative motion between India and Sunda determined by GPS, J. Geophys. Res., 2003 submitted.

SOPAC, University of California San Diego, http://sopac.ucsd.edu/

Vergne, J., R. Cattin, and J.P. Avouac, On the use of dislocations to model interseismic strain and stress build-up at intracontinental thrust fault, Geophysical Journal International, 147, 155—162, 2001.

Willis, P., M. Heflin (2004), External validation of the GRACE GGM01C, gravity field using GPS and DORIS positioning results, Geophys. Res. Lett., 31, 13, L13616, doi:10.1029/2004GL020038.

Zhao, W., K.D. Nelson, and p.I. Team, Deep seismic-reflection evidence continental underthrusting beneath southern Tibet, Nature, 366, 557—559, 1993.

Zhao, W., Nelson, K. D. and project INDEPTH Team, Deep seismic-reflection evidence continental underthrusting beneath southern Tibet, Nature, 366, 557-559, 1993.

RAMAN SPECTROSCOPY OF CARBONACEOUS MATERIAL (RSCM) THERMOMETRY AS A NEW TOOL FOR GEODYNAMICS: APPLICATION TO THE LESSER HIMALAYAS OF NEPAL

Olivier BEYSSAC (1), Bruno GOFFÉ (1), Laurent BOLLINGER (2) and Jean-Philippe AVOUAC (3)

(1) Laboratoire de Géologie, Ecole Normale Supérieure, Paris, France (mailto Olivier.Beyssac@ens.fr)
(2) Laboratoire de Géophysique, Commissariat à l'Energie Atomique, Bruyères le Châtel, France
(3) Geological and Planetary Sciences division, Caltech, Pasadena, USA

The determination of metamorphic conditions is critical in understanding mountain-building processes. However, all collisional mountain belts contain large volumes of accreted sediments generally lacking metamorphic index minerals and are therefore not amenable to conventional petrologic investigations. By contrast, these units are often rich in carbonaceous material, allowing for determining thermal metamorphism through Raman spectroscopy of carbonaceous material (RSCM method), a technique that has been recently calibrated (Beyssac et al., 2002). During diagenesis and metamorphism, carbonaceous material (hereafter CM), present in the initial sedimentary rock, is progressively transformed into graphite (graphitization). The corresponding progressive evolution of the degree of organization of the CM is considered to be a reliable indicator of metamorphic grade, and more specifically of temperature. Because of the irreversible character of graphitization (CM is tending toward the thermodynamic stable phase which is graphite), CM structure is not sensitive to retrograde metamorphism and therefore primarily depends on the maximum temperature reached during metamorphism, whatever the retrograde history of the sample. It also has been observed that samples collected from neighbouring outcrops with clearly different strain have the same degree of graphitization, indicating that deformation does not significantly affect the structural organization of the CM.

The first-order Raman spectrum of disordered CM exhibits a graphite G band at 1580 cm^{-1}, E2g2 mode corresponding to in-plane vibration of aromatic carbons, and several defect bands, corresponding to "physico-chemical defects". The structural organization of CM can be quantified through the R2 parameter defined as the relative area of the main defect band D1 (R2= D1/(G+D1+D2) peak area ratio). A linear correlation between this R2 parameter and metamorphic temperature was calibrated using samples from different regional metamorphic belts with well-known P-T conditions in the range 330-650°C (RSCM method – Beyssac et al. 2002). RSCM can be applied to metasediments of pelitic lithology in which CM precursor is mainly a kerogen mixed with minor hydrocarbons trapped during diagenesis. The uncertainty on temperature is ± 50°C due to uncertainties on petrologic data used for the calibration. The relative uncertainties on temperature are much smaller, probably around 10-15°C (Beyssac et al, 2004), allowing for estimating quite accurately thermal metamorphic gradients (Bollinger et al. 2004).

A first application of the RSCM method to the study of thermal metamorphism through the Lesser Himalaya (LH) of Central and Far-Western Nepal will be presented. The Lesser Himalaya is one of the problematic cases cited above with a very poor mineralogy, but at a key structural position within the Himalayan system that allows for considering LH as diagnostic of the overall thermal structure of the orogen. This study demonstrates the performance of the technique, and reveals that the LH has undergone a large-scale thermal metamorphism, with temperature decreasing progressively from about 540°C at the top to less than 330°C within the deepest exhumed structural levels (Fig. 1).

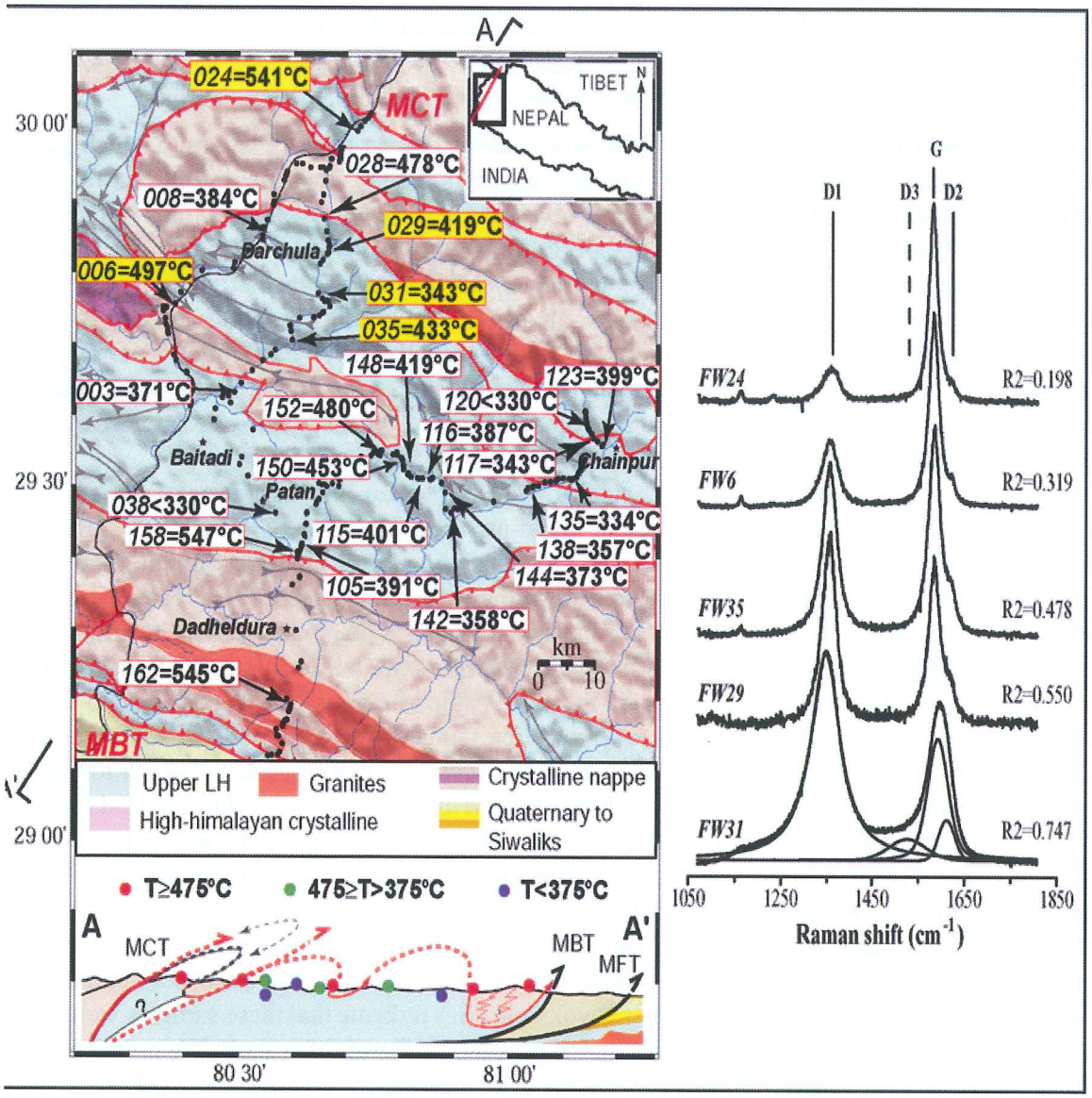

Fig. 1: Geological map of far-western Nepal showing the major tectonostratigraphic zones and tectonic contacts. For each sample: label and mean RSCM temperature are given. The upper right inset shows location of the studied area at the scale of Nepal. The samples for which a Raman spectrum is depicted are indicated with a yellow label. (LH: Lesser Himalaya). Lower inset shows a simplified NE-SW cross-section AA' with temperature and main thrusts (MCT: main central thrust, MBT: main boundary thrust, MFT: main frontal thrust). Examples of Raman spectra obtained from samples collected in far-western Nepal. An example of spectral decomposition by the fitting procedure is given for the less organized sample (FW31). Position of the graphite G band and D1, D2, D3 defects bands are indicated. For each spectrum, the value of the mean R2 ratio (R2 = D1 / [G+D1+D2] peak area ratio) obtained after 10 decompositions is given. (Modified from Beyssac et al., 2004)

References

- BEYSSAC O., GOFFÉ B., CHOPIN, C. AND ROUZAUD J.N. 2002. *J. of Met. Geol.*, 20, 859-871.
- BEYSSAC O., BOLLINGER L., AVOUAC J.P. ET GOFFÉ B. 2004. *EPSL*, 225, 233-241.
- BOLLINGER, L., AVOUAC, J.P., BEYSSAC, O., CATLOS, E.J., HARRISON, T.M., GROVE, M., GOFFÉ, B., AND SAPKOTA, S. (2004) *Tectonics,* VOL. 23, TC5015, doi:10.1029/2003TC001564.

SIMULTANEOUS ISLAND AND CONTINENTAL ARC MAGMATISM IN NORTHWEST TRANS-HIMALAYA, LADAKH, INDIA: INFERENCE FROM ^{40}AR-^{39}AR STUDY

Rajneesh BHUTANI (1) and Kanchan PANDE (2)

(1) Department of Earth Sciences, Pondicherry University, Pondicherry, India
(2) Department of Earth Sciences, Indian Institute of Technology, Mumbai, India

Magmatism in trans-Himalaya is characterized by the calc-alkaline batholith which outcrops all along the northern margin of ~2500 km long mountain belt. The northwestern region of trans-Himalaya in Pakistan and Ladakh in India however, has several narrow longitudinal volcanic belts on the either flanks of trans-Himalayan batholith. At least three different volcanic belts, apart from the volcanics of ophiolitic mélange of two suture zones, have been identified in the Ladakh region in India. These are known as Dras volcanics, Shyok volcanics and Khardung volcani cs. Though plutonic magmatism in the Trans-Himalayan batholith is usually attributed to the subduction process, the volcanic belts may present different tectonic settings and hence different magmatic processes. Results of an Ar-Ar thermochronological study indicate that these magmatic rocks record evidences for tectono-thermal events ranging from pre-, syn- to post-collision.

A sample of basalt from Dras volcanics yields a plateau-like whole rock age of ~ 85 Ma. Dras volcanics are showed to have formed in island-arc tectonic setting (Clift et al 2000, Rolland et al 2000). However, the Shyok volcanic belt on the northern side of the Ladakh batholith, which is distinct from the Dras volcanics, did not yield any reliable formation ages. The apparent age-spectra clearly indicate post-collision thermal disturbances. It has been demonstrated earlier (Bhutani et al 2003) that Shyok Volcanics are affected thermally by strike-slip faulting along the Karakoram fault at ~14 Ma ago. The emplacement age of these volcanics however, been constrained by other geological evidences, such as presence of Orbitolina fauna, to be early Mid- to Late-Cretaceous (Pudsey 1986, Reuber 1989, Rolland 2000). Shyok volcanics are in tectonic juxtaposition with the contrasting acidic Khardung volcanics which are exposed in the form of thick rhyolitic and ignimbrite flows on the northern flanks of Ladakh batholith. The chemistry and explosive nature of these volcanics indicate that these are emplaced on a thickened continental crust. The whole rock plateau-ages of two rhyolite samples are 52.8±0.9 and 56.4±0.4 Ma. We interpret these ages to be the age of emplacement over thickened margin of the continental crust, which appears to be coeval with the initiation of the collision between the Indian and Asian plate. The absence of post-emplacement thermal affects in these samples unlike the Shyok volcanics indicate that these samples were present in different tectonic setting at the time of faulting along the Karakoram fault. We propose that the two volcanic belts of contrasting nature were brought together in juxtaposition by the Karakoram strike slip faulting at ~14 Ma. The plutonic magmatism as represented by the Ladakh batholith continued from Cretaceous to as late as ~29 Ma ago. Post-collision phase of the magmatism is recorded by the late leucogranite intrusion; probably resulted by the partial melting of the thickened crust (Bhutani et al 2004). The three volcanic belts and the plutonic magmatism therefore provide a record of the evolution of the India-Asia collision zone.

We propose the following sequence of magmatism in the northwest Himalaya- Simultaneous island and continental arc magmatism occurred during ~100 to 52 Ma. The island arc magmatism is represented by the Dras volcanics while the continental arc magmatism is manifested in the plutonic Ladakh batholith. The end of the subduction related continental arc magmatism is probably recorded by the acidic Khardung volcancis. The Shyok volcanics along with the ophiolitic mélange of the Shyok suture zone of the northern Ladakh probably represent the small part of oceanic crust of the Asian plate prior to the collision. Rolland et all 2000 earlier proposed the progressive maturing of the arc from west to east on the basis of geochemical differences between the Shyok volcanics in northwest Pakistan and Khardung volcanics in northern Ladakh.

We also envisage a similar scenario and further propose that the pre-collision plate boundary of the Asian plate was such that it had a small oceanic crust in western margin of the plate and rest was continental plate. Hence the island arc and continental arc magmatism took place simultaneously and independently. The present day tectonomorphology of trans-Himalaya was achieved after the Karakoram fault activation at ~14 Ma ago. This model also explains all the available geological and geochemical evidences (Fig.1).

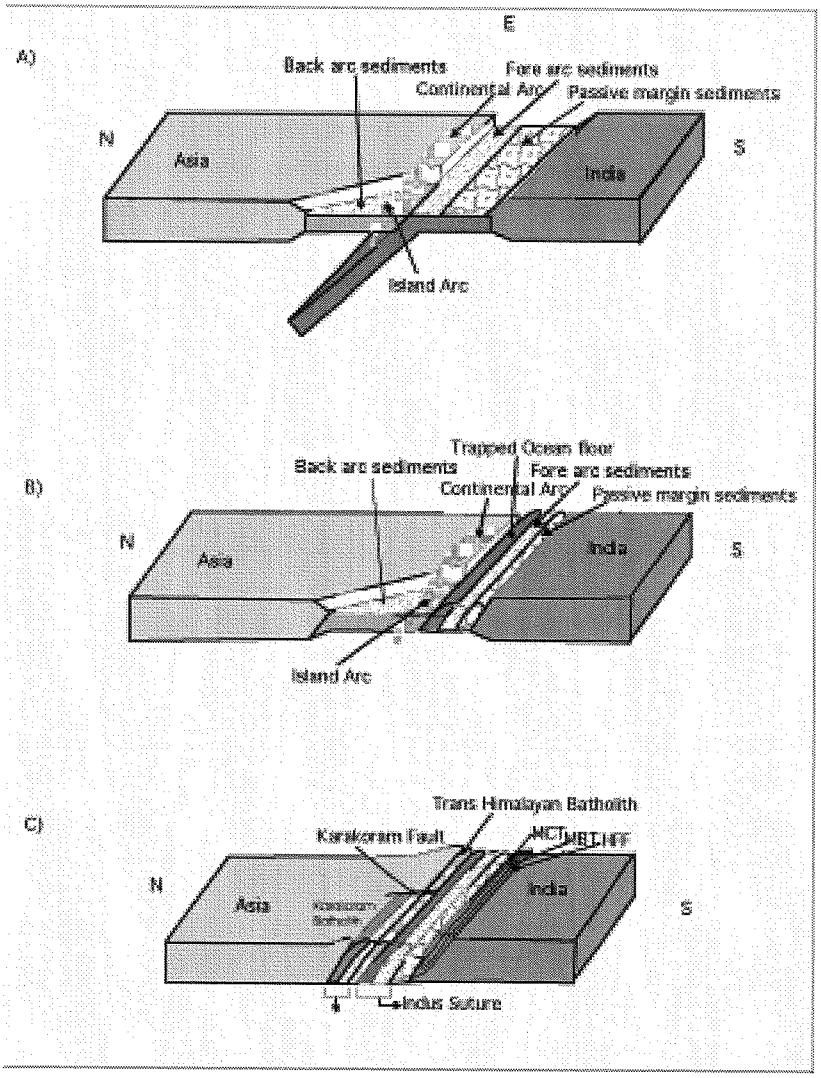

Fig. 1 Cartoon diagram showing the evolution of the southern margin of the Asian plate. (A) Pre-collision boundary of the southern margin of Asian plate was partly oceanic at western end which subsequently gave rise to island arc magmatism and the back arc sedimentation while at the same time the continental margin of the plate was having the continental arc magmatism. (B). The Indus Suture closed as the Tethys ocean completely subducted , it compressed the small part of the oceanic crust along the Asian margin and caused the breakage along the continent-oceanic boundary. (C). The small part of the oceanic plate along the Asian continental plate formed the Shyok Suture Zone with the characteristic ophiolites and flyschoids. The boundary between the continent and ocean later acted as plane of weakness to facilitate the formation of Karakoram Fault.

References

BHUTANI R.., PANDE K. & DESAI N. 2003. *Current Science* 84. 1454-1458.

BHUTANI R., PANDE K. & VENKATESAN T.R. 2004 *Proc. Indian Acad. Sci.* (Earth and planet. Sci.) 113.

CLIFT P.D., DEGNAN P.J., HANNIGAN R. & BLUSZTAJN J., 2000. *GSA Bull.* 112. 450-466.

PUDSEY C.J. 1986. *Geol. Mag.* 123. 405-23

REUBER I. 1986. *Nature* 321. 592-596.

ROLLAND Y., PECHER A., & PICARD. C, 2000. *Tectonophysics* 325. 145-173.

CHEMISTRY OF THE SILICATE PHASES FROM THE CHILAS COMPLEX, KOHISTAN MAGMATIC ARC, NORTHERN PAKISTAN

R. BILQEES (1), M. Q. JAN (2) and M.A. KHAN (3)

1 Pakistan Council of Scientific and Industrial research Laboratories, Peshawar, Pakistan
2 Department of Geology, University of Peshawar, Pakistan
3 National center of Excellence in Geology, University of Peshawar, Pakistan

The Chilas complex is an important element of the Kohistan magmatic arc. Covering 8000 km^2 area, it stretches for 200 km from the Nanga Parbat to western Dir. It is thought to have been emplaced 85 Ma ago during the rifting of the arc after collision with the Karakoram plate. Over 85 % of the complex comprise homogeneous gabbronorites (MGN) with local, minor layers of pyroxenites and anorthosite. Within these are emplaced small bodies (<10 km^2) of ultramafic-mafic-anorthositic (UMA) rocks, mostly in the eastern part of the complex. The UMA rocks may contain olivine Cr- and/ or Al-spinel but no biotite, whereas the MGN contain biotite, and Fe- Ti-oxides but no olivine and spinel. The UMA commonly show well-developed layering and several syndepositional structures suggestive of emplacement in tectonically active areas. Thousands of microprobe analyses show that the UMA rocks are characterized by mineral phases more magnesian and more aluminian than those of the MGN rocks are.. In the UMA, plagioclase ranges from An_{85} to $An_{100.}$, olivine from Fo_{71} to Fo_{94}, orthopyroxene from En_{58} to En_{84}, whereas clinopyroxene is diopsidic and amphibole is tschermakitic- and pargasitic-hornblende. In the MGN, plagioclase is An_{40}–An_{70}, orthopyroxene $En_{50\ 68,}$ clinopyroxene is diopsidic to augite and amphibole is generally hornblendic.

High modal abundance of orthopyroxene, magnetite and ilmenite and Mg-Fe-Alk variations (Fig.1) indicate a calc-alkaline origin for the MGN. Projection of the pyroxene compositions on Mg-Fe-Ca face and their Ti and Cr contents suggest an island arc affinity for the Chilas. The restricted range of olivine compositions and the coexistence of olivine and pyroxenes with highly calcic plagioclase in the UMA association are comparable with other island arc cumulates. The rather low Cr-number in the Cr-spinel and the field evidence suggest the emplacement of the complex in extensional environment during the arc rifting.

The Al and Fe-Mg contents of the pyroxene indicate a transition between igneous and metamorphic domains. The mineral assemblages and two-pyroxene geothermometery show medium-P re-equilibration either during cooling or granulite facies conditions. Subsolidus reaction between calcic plagioclase and olivine has resulted in the development of coronas of orthopyroxene±clinopyroxene+hornblende+spinel in the UMA association. Hydration of the complex along shear zones in many places has resulted in the formation of amphibolites, hornblende-rich rocks, and local greenschist facies assemblages. The highly calcic plagioclase in the UMA may be a result of high P_{H2O} or high Ca/Na ratio of the magma. The scarcity of primary hydrous minerals in MGN the complex, however, is suggestive of anhydrous magma.

The huge volume and local petrographic and chemical variations suggest that the complex has been built by the emplacement of several batches of very similar magma. The general absence of layering and other inhomogeneities, in the MGN series may be due either to 1) viscous nature of magma, 2) obliteration of layering due to shearing and subsequent high temperature annealing 3) an open magma chamber, or 4) the turbulence in the magma chamber.

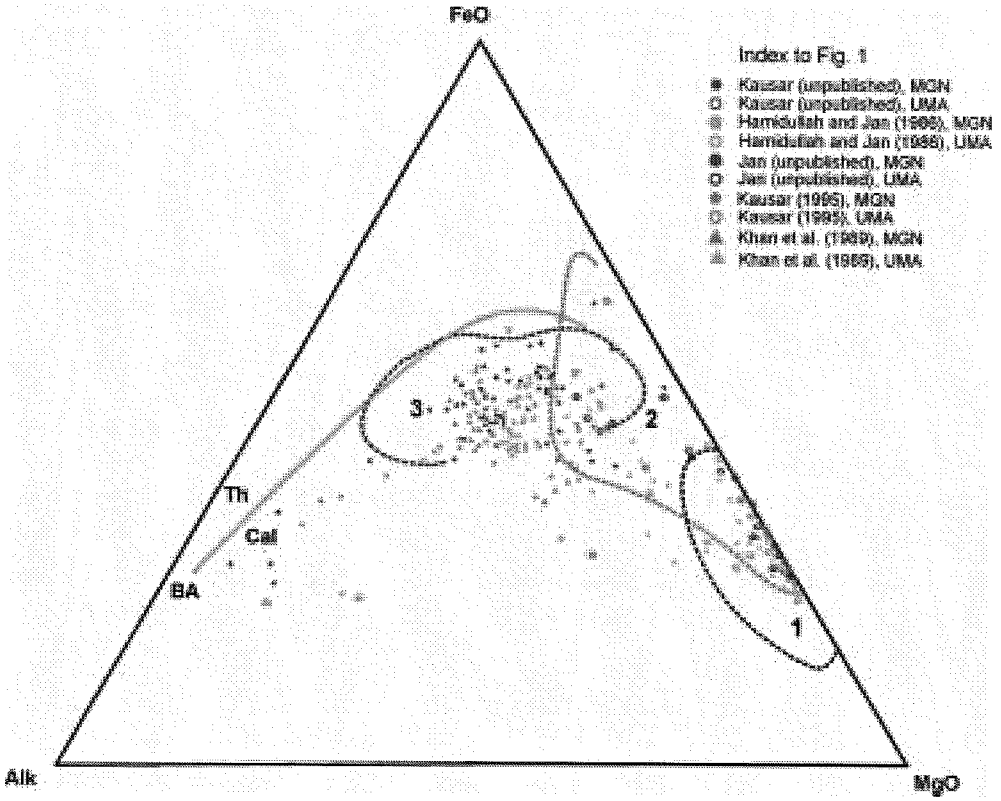

Fig. 1. AFM diagram for Chilas complex rocks. Fields from Island arc cumulates=1, and non-cumulates =2, shown for comparison (after Beared, 1986). Dashed line 'BA' divides the Calc-alkaline and tholiites fields of Barakar and Arth (1976). '1' denotes the field of Coleman (1977) for ophiolites.

REFERENCES

1. BARKER, E. & ARTH, J.G. 1976. *Geology*, **4**, 596-600

2. BEARD, J.S. 1986. *Geology*, **14**, 845 –851.

3. COLEMAN, R. G., 1977. Ophiolites- Ancient oceanic lithosphere. Springer-Verlag

4. HAMIDULLAH, S. & JAN, M.Q., 1986. Geological Bulletin, Univ. Peshawar 19, 157-182.

5. JAN, M. Q., & HOWIE, R.1981. A. *The Geological Bulletin of the Punjab University*, 16,1-10.

6. KHAN, M. ASIF, JAN, M. QASIM, WINDLEY, BRIAN F., TARNEY, JOHN, THIRLWALL, MATTHEW F., *Special Paper - Geological Society of America*, 232, p. 75-94, 1989.

7. KAUSAR, A.B., 1995. *Geologica 1*, 1-14.

THE ULTRAMAFIC SEQUENCE OF SAPAT (NE PAKISTAN): A KEY IN UNDERSTANDING ARC BUILDING PROCESSES AND SUTURING KINEMATICS

Pierre BOUILHOL (1), Jean-Pierre BURG (1), Jean-Louis BODINIER (2), Shahid HUSSAIN (3), Hamid DAWOOD(3)

(1) Geological institute, ETH, Zurich, Switzerland
(2) Laboratoire de Tectonophysique, University of Montpellier, France
(3) Pakistan Museum of Natural History, Islamabad, Pakistan

The Sapat mafic-ultramafic Complex occurs along the Indus Suture Zone in Pakistan, to the east of Besham and southwest of Chilas (Fig.1). As such, it shares the same structural level as the well-known Jijal section, to the north of Besham.

The Sapat Complex is one of the little documented segments of the suture zone. This Complex is famed for the exceptional gem olivine, which occurs in tension gashes opened in partly serpentinized dunites (Jan et al., 1996; Kausar and Khan, 1996). The complex was described as a layered sequence of cumulate dunites, pyroxenites, anorthosites and gabbros (Jan et al., 1993; Khan et al., 1995) and was thus considered as lateral equivalent to the mafic-ultramafic section of the Jijal Complex (Khan et al., 1998; Searle et al., 1999). Spinel from dunite have signature of supra-subduction fore-arc setting (Khan et al., 2004).

We document fundamental differences between Sapat and Jijal and show that kinematic, petrological and geochemical information on Sapat will provide new constraints on the tectonic and magmatic processes that took place at the front of the Kohistan Arc, and/or during its early evolutionary stages.

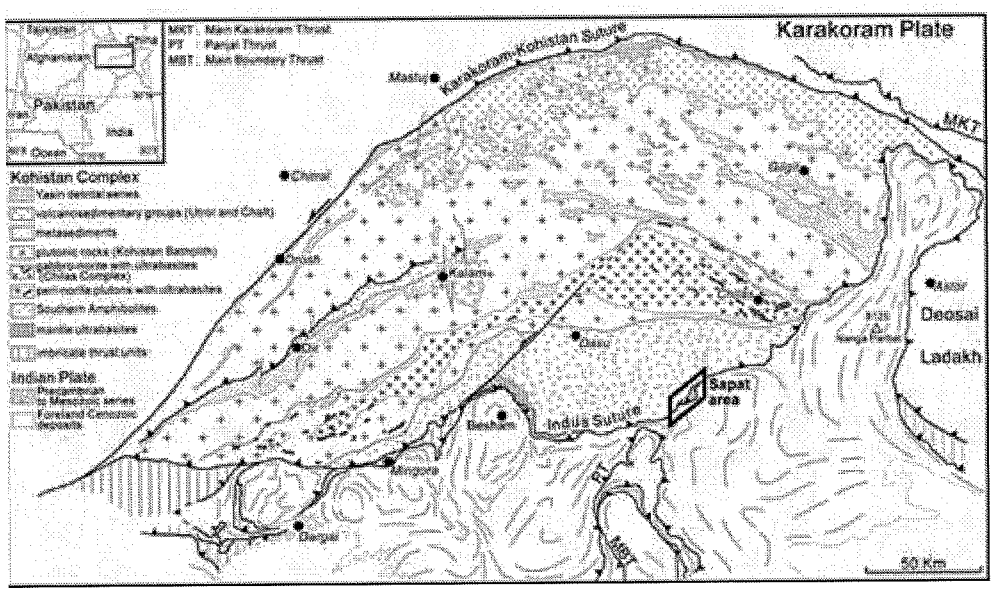

FIGURE 1: Sketch map of the Kohistan Terrane with location of the investigation area (Sapat)

At the base of the complex, the suture zone includes low-grade graphitic schists. Shear planes and asymmetry of mesoscopic folds are consistent with normal-faulting related to the back-sliding of the Kohistan terrane, as reported elsewhere. The tectonic contact between graphitic schist and the Sapat dunite is a ~3m gouge zone in which rare calcschists contain emerald. Two units are identified in the Sapat Complex:

The lower, southern unit is composed of a lens-shaped, up to 600m thick dunite body extending over 12 km along the suture zone. Within this body, the chromite content seems to increase upward to the north.

Serpentinization is more penetrative close to the main contact where shear planes indicate a top-to-the SW, sinistral strike-slip movement consistent with back sliding identified in the underlying low-grade schists.Gem olivine crystallized in association with talc, clinochrysotile, calcic amphiboles, carbonates and other mineral phases in centimeters-wide and meters-long veins formed in the massive, chromite-bearing dunite, (Fig. 2a.). These veins are generally dipping 60°W with an average EW strike-direction, and are cut by N060 steep normal faults. These veins reflect fluid circulation in the mantle during subduction or during early exhumation

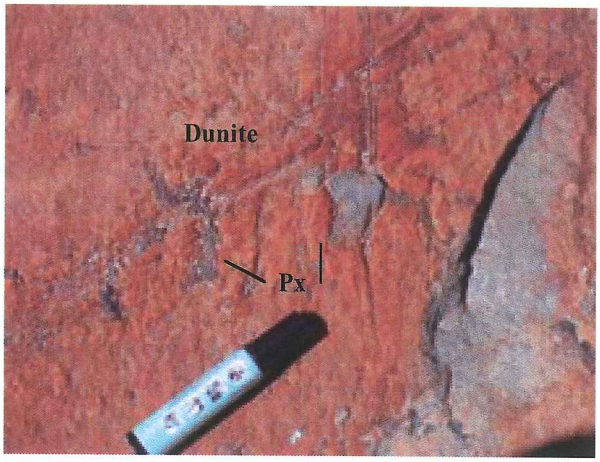

Figure 2a: vein containing crystallized gem olivine

Figure 2b: corroded pyroxene documenting partial melting of pyroxenites

The contact with the overlying upper northern units is characterised by mylonitic serpentine.

The upper, northern units include scattered bodies of intimately associated dunites, wehrlites and coarse-grain pyroxenites, including spectacular pegmatitic facies with clinopyroxene crystals up to 50 cm in size, enclaved into medium and fine-grained layered gabbros and associated veins of quartz- and mica-bearing pegmatites. Structural relationships indicate that the gabbros have intruded the km-sized dunite-wehrlite-pyroxenite lenses. The primary (igneous) gabbro mineralogy was replaced by metamorphic assemblages of the amphibolite facies, grading upwards into the greenschist facies.

The ultramafic rocks are less affected by metamorphic recrystallization and generally preserve primary textures. We document a great variety of igneous and melt-rock reaction structures, as well as cumulate textures in wehrlites. However, in the cumulate wehrlite, intercumulus olivine appears to be residual, being transported as a mush by melt. We conclude that the wehrlites and pyroxenites were likely formed by reaction between pre-existing dunites and infiltrated melts. In addition, some dunites were clearly formed belatedly as solid residues after partial melting of a wehrlite protolith (Fig. 2b). This suggests that complex melt redistribution processes have taken place within the dunite-wehrlite-pyroxenite association.

In conclusion, Sapat has locally preserved exceptional igneous and melt-rock reaction textures. Owing to the lack of granulite facies metamorphism, to the occurrence of gem olivine and to the scarcity of hornblendites, the Sapat Complex is markedly different from Jijal and provides additional clue to document the early evolutionary stages of the Kohistan Arc and the nature of primary mantle melts. It also provides important constrains on the kinematics involved in the early suturing phases and paleo-stress tensors that controlled the gem-bearing veins and the suture-associated faulting.

RIVER PROFILES, TECTONICS AND CLIMATE IN THE GREAT PAMIR INDENTER OF CENTRAL ASIA.

M. E. BROOKFIELD
Land Resource Science, Guelph University, Guelph, Canada N1G 2W1
mbrookfi@lrs.uoguelph.ca

Collision orogens developed between two plates result not only in shortening, uplift and erosion of the rocks, but also compression, uplift and modification of the drainage systems (Summerfield, 1991). Many studies now relate orogenic uplifts to the interaction of plate compression with isostatic changes due to active denudation (Jamieson and Beaumont, 1989; England and Molnar, 1990). In this paper I outline the relationships between river profiles, drainage patterns, tectonics and climate during the indentation of Asia in the Pamir range and adjacent areas: it extends a previous study of rivers draining south (Brookfield, 1999).

The reasons for choosing the Pamir are the following.

a) The indentation is relatively simple and can thus be modelled with a relatively simple rigid indentation model (Peltzer and Tapponnier, 1988). The major complication is due to the different behaviour of the western and eastern edges of the indenter. The western edge involves mostly ductile deformation of the Tadjik back-arc basin to form a fold and thrust belt (Leith and Alvarez, 1985). The eastern edge involves strong shearing between continental crust of the Pamir and Tarim basins to form a complex collisional transform zone (marked by the Karakoram and associated faults) linking the Pamir arc with the Himalaya (Peltzer and Tapponnier, 1988).

b) The compression pattern is relatively simple and various tectonic units can mostly be traced from west to east across the Pamir indenter. Individual tectonic elements and ancient sedimentary basins can be followed almost continuously from the hardly compressed Afghan area through the highly compressed Pamir indent into the less compressed Tibetan plateau area (Brookfield, 1993).

c) The displacements are enormous, relatively recent, and measurable. The Pamir arc only started developing in the Miocene around 20 ma. Since then over 800 km of internal shortening has occurred between the Indian shield and the Tien Shan (Dewey et al., 1989). Most of this post-Oligocene shortening occurred in the Pamir arc itself. And because of this, the earlier progressive Paleocene - Oligocene collisions of India with magmatic arcs south of Asia can be followed in some detail in the Pakistan Himalaya though not in the Indian Himalaya (Treloar et al., 1991).

d) The river profiles and courses can be directly related to the major tectonic development of the arc, modified by the influence of Quaternary climatic change (Molnar and England, 1990).

The main drainage divide is along the crest of the fundamentally Mesozoic Hindu Kush and Karakoram ranges and extensions. Despite the late Cenozoic uplift of the Pamir, only the Pyandzh river cuts across the Pamir range in a course that corresponds with a geophysical but not a geological boundary. The rest of the rivers, with a few exceptions, tend to run in valleys parallel to the arc, except to the west and east. To the west, in northern Afghanistan the rivers still run northward from the westward extension of the Hindu Kush. To the east the main rivers have headwaters far within the Tibetan plateau and cut, with incredibly steep gradients across the Kun Lun and related ranges - testifying to the latest Tertiary development of this range.

REFERENCES

Brookfield, M. E., 1993. Special Publication of the International Association of Sedimentologists, 20: 13-35.
Brookfield, 1998. Geomorphology, 22: 285-312.
Dewey, J.F., Cande, S. and Pitman III, W.C., 1989. Eclogae geologica Helvetica, 82: 717-734.
England, P. and Molnar, P., 1990. Geology, 18: 1173-1177.
Jamieson, R.A. and Beaumont, C.J., 1989.Geological Society of London Special Publication, 43: 117-129.
Leith, W. and Alvarez, W., 1985. Geological Society of America Bulletin, 96: 875-885.
Molnar, P. and England, P., 1990. Nature, 346: 29-34.
Peltzer, G. and Tapponnier, P., 1988.Journal of Geophysical Research, 93 B10: 15,085-15,117.
Summerfield, M.A., 1991. Global Geomorphology. Longman, London.
Treloar, P.J., Rex, D.C. and Williams, M.P., 1991. Geological Magazine, 128: 465-478.

Note Page

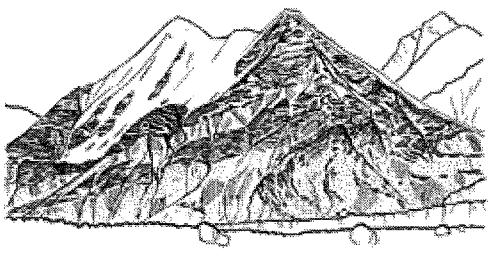

Makalu, Bordet, 1954

PRE-COLLISION TILT OF CRUSTAL BLOCKS IN EXTENDED ISLAND ARCS: STRUCTURAL EVIDENCE IN THE KOHISTAN ARC

Jean-Pierre BURG, Oliver JAGOUTZ, Hamid DAWOOD[1], Shahid S. HUSSAIN[1]

Geologisches Institut, ETH and University Zurich, Sonneggstrasse, 5, CH 8092 Zurich, Switzerland
[1] Pakistan Museum of Natural History, Garden Avenue, Shakarparian, 44 000 Islamabad, Pakistan

Mapping, based on compositional differences recognized in the field and in thin sections and subsequent colour differences on various channel combinations of satellite data, identified a multiple intrusion system within the gabbronoritic-ultramafic Chilas complex. This Complex has intrusive contacts to the north with metasediments and metavolcanites, probably both belonging to the so-called Jaglot Group, and plutonic rocks possibly belonging to the early magmatic phases of the Kohistan Batholith, and to the south with the Southern Amphibolites (Treloar *et al.* 1996; Searle *et al.* 1999). The plutonic bodies identified from field and satellite mapping as parts of the Chilas Complex have length >10 times longer than width. Contacts are mostly concordant with the mesoscopic layering, yet display local unconformities at both mesoscopic and map-scale, as described above.

Orientation data of primary igneous fabrics were identified from both field and microscopy observation. Primary fabrics represent flow-related structures ranging from faint mineral preferred orientation in otherwise massive, homogeneous rocks to composition layers particularly prominent in the vicinity of elongated, generally concordant ultrabasic bodies (Jan *et al.* 1984). The absence of crystal-plasticity deformation features in conventional thin sections indicates that even pronounced layering with slump-folds and geopetal structures (Khan *et al.* 1989; Sawada *et al.* 1994) represents planar concentration domains inherited from magmatic processes. Interlayered lithologies show syn-deposition faults, erosional contacts, cross-bedding and magmatic breccias that reflect very dynamic, multiphase magmatic activity. Cross-cutting relationships in such structures may represent mesoscale equivalent to map-scale, discordant foliation trajectories in zones where neither shear zone nor fault is apparent. They reveal internal magmatic contacts undetectable away from layered and truncated zones. This observation suggests that the widespread granoblastic texture was homogenized by post-truncation annealing. Cross-cutting relationships between variable lithologies indicate that the gabbronorite is a multiple magma complex accumulated through repeated injections of magma pulses of similar composition.

The magmatic foliation is generally parallel to the trend of the Chilas Complex, its internal layering and its contacts, and the lineation plunges steeply. Subvertical lineations and syn.magmatic normal faults support the hypothesis that the Chilas Complex was emplaced in an extensional environment (Khan *et al.* 1993; Burg *et al.* 1998). Two main domains are distinguished from the orientation of planar flow markers and foliations. The northern, Chilas-Kandiah domain dips dominantly SSW, which implies that the Kohistan Batholith is the footwall and the Southern Amphibolites the hanging wall of the Chilas intrusion. The western, Kandiah-Dir domain strikes SSW-NNE and is subvertical to WNW-dipping.

We challenge the interpretation of a horizontal lopolith at the contact interface between sediments of the Kohistan Batholith and the Southern Amphibolites later tilted to the measured, steep attitude. from three types of arguments.

Firstly, tilt to near-vertical in an upright, isoclinal fold of some tens of kilometres amplitude is mechanically impossible and would involve intense, vertical foliation along the hinge zone. Such a foliation does not exist and the two theoretical limbs display lithologies and metamorphic grades that cannot be correlated. Secondly, tilt of a thick crustal block around a horizontal axis is equally implausible owing to the lack of evidence for a vertical crustal sequence: sediments and volcanites are well documented on both sides of the Chilas Complex. Thirdly, metamorphic pressures to the south (the floor) of the supposed 30 km thick Chilas lopolith should beabout 1.0 GPa

higher than those in the eventual roof, to the north. Sediments and metavolcanites of the Southern Amphibolites are in places low to medium grade, which precludes a crustal pile of > 30 km above them. Thermobarometry on a metapelite from the northern border of the Chilas Complex yielded peak metamorphic conditions of ca. 0.7 GPa at ca. 700°C (Jagoutz 2004). Pressure-temperature estimates on Southern Amphibolites range from 0.7 to 1.0 GPa at 650-850°C (Anczkiewicz & Vance 2000)(Treloar *et al.* 1990)(Zeilinger 2002). Therefore, the interpretation of a large, originally horizontal lopolithic gabbronorite is at odds with the geological information. It is also at odds with the classical view that the Kohistan Arc, including the Chilas Complex, has been tilted northward by about 30° after India – Kohistan collision. Indeed, if presently sub-vertical foliations and contacts are back-tilted southward to restore a near pre-collision attitude, then the Chilas Complex was dipping about 60°N.

We further argue that the structural information contained in sets of the latest hornblende-plagioclase pegmatite veins hints at the Chilas Complex being originally even steeper than the 60° dip estimate. Foliation-parallel and foliation and/or lineation-normal hornblende-plagioclase pegmatite veins represent cross and longitudinal joints originated when the magma cooled. These pegmatite veins indicate that brittle deformation occurred in the presence of residual melt during intrusion of the main body and are not considered in this discussion. Later, hornblende-bearing pegmatite dykes bear no simple relationship to the magmatic fabric. Their remarkably planar shapes with very large length/width ratios (> 500) and lack of vein-parallel offsets of earlier structures indicate that those veins represent fluid-filled extensional fractures that formed when the Chilas magmas and early hornblende-pegmatite veins were solidified, yet still containing a very small melt fraction. Such single, linear fractures tend to open perpendicular to the least principal stress and dilate parallel to the maximum principal stress. These late vein sets have a wide range of strikes that would require different horizontal rotation axes (parallel to the various strike directions) which, by chance, would each have the ad-hoc orientation to bring individual vein sets to near-vertical dips. The regional continuity of host rock structures (magmatic foliations in particular) excludes the existence of separate blocks and multiple, horizontal rotation axes. An important corollary is that the vertical veins have not or little been rotated since they formed; consequently, the magmatic structures in the host Chilas Complex, away from the Nanga Parbat Syntaxis, are in a near-original attitude, eventual rotations around vertical axes excepted. As a matter of fact, the extensional nature of the Chilas Complex is theoretically consistent with a vertical greatest principal stress. We conclude that the Chilas body was initially south-dipping.

On a bulk southward-dipping fault, like the Chilas body, one expects antithetic rotation resulting in a bulk northward dip of the hanging wall. We suggest that the general attitude of the Southern Amphibolites is essentially inherited from rollover tilting, which took place when the Chilas Complex was emplaced at about 85 Ma.

ANCZKIEWICZ R. & VANCE, D. 2000. *Geological Society Special Publication, London,* **170**. 321-331.
BURG J.-P., BODINIER, J.-L., CHAUDHRY, M.N., HUSSAIN, S. & DAWOOD, H. 1998. *Terra Nova* **10**, 74-80.
JAGOUTZ O. 2004. Unpublished PhD thesis, ETH.
JAN Q.M., KHATTAK, M.U.K., M.K., P. & WINDLEY, B.F. 1984. *Geological Bulletin, University of Peshawar* **17**, 153-169.
KHAN M.A., JAN, M.Q., WINDLEY, B.F., TARNEY, J. & THIRLWALL, M.F. 1989. *Geological Society of America, Special Paper* **232**, 75-93.
KHAN M.A., JAN, M.Q. & WEAVER, B.L. 1993. Geological Society Special Publication, London, **74**. 123-138.
SAWADA Y., KAUSAR, A.B., KUBO, K., TAKAHASHI, Y. & TAKAHASHI, Y. 1994. *Earth Science* **48**, 33-38.
SEARLE M.P., KHAN, A.M., FRASER, J.E., GOUGH, S.J. & JAN, Q.M. 1999. *Tectonics* **18**, 929-949.
TRELOAR P.J., BRODIE, K.H., COWARD, M.P., JAN, M.Q., KHAN, M.A., KNIPE, R.J., REX, D.C. & WILLIAMS, M.P. 1990. In: *Exposed cross-sections of the continental crust* (edited by Sallisbury M.H. & Fountain D.M.). Kluwer Academic Press, Amsterdam, 175-214.
TRELOAR P.J., PETTERSON, M.G., QASIM JAN, M. & SULLIVAN, M.A. 1996. *Journal of the Geological Society of London* **153**, 681-693.
ZEILINGER G. 2002. Unpublished PhD thesis, ETH.

HIGH GRADE SHEAR ZONES IN THE CORE OF THE HIMALAYAN BELT (WESTERN NEPAL): CONSEQUENCES ON THE EXHUMATION OF THE HIGHER HIMALAYAN CRYSTALLINES

Rodolfo CAROSI (1), Chiara MONTOMOLI (1), Dario VISONÀ (2)

- (1) Università di Pisa, Dipartimento di Scienze della Terra, via S. Maria, 53, 56126 Pisa, ITALY; e-mail: carosi@dst.unipi.it, montomoli@dst.unipi.it
- (2) Università di Padova, Dipartimento di Mineralogia e Petrologia, c.so Garibaldi 37 35122 Padova, ITALY

The Himalayan belt in Western Nepal is characterized by the occurrence of four main tectonic units that from the bottom to the top are represented by the Lesser Himalaya (LH), the Lesser Himalayan Crystalline (LHC), the Higher Himalayan Crystalline (HHC) and the Tibetan Sedimentary Sequence (TSS) (Fuchs and Frank, 1970).

The HHC is regarded as an extruding wedge of crystalline rocks bounded at the base by the top-to-the SW Main Central Thrust and at the top by the top-to-the NE South Tibetan Detachment System (Burchfiel et al., 1992; Hodges et al., 1992; Grasemann et al., 1999; Gruijc et al., 1996; 2002).

The HHC is usually regarded as a unitary high-grade crystalline unit with similar tectonic and metamorphic features all over the Himalayan belt (Le Fort, 1975). Most of researches have been concentrated on its upper and lower tectonic boundaries because of their primary role in the exhumation of the unit. However, some structural discontinuities, such as shear zones, thrusts and normal faults have been reported within the HHC, with different roles with respect to the exhumation history, from Bhutan (Davidson et al., 1997; Grujic et al., 2002) to Nepal (Vannay & Hodges, 1996; Hodges et al., 1996; Mcfarlane, 1993; Maruo and Kizaki, 1981; Searle, 1999; Goscombe and Hand, 2000).

The superb exposure of the crystalline units in Lower Dolpo (western Nepal) allowed to unravel their structural and kinematic evolution and to identify a ductile, high-temperature, shear zone located in the middle portion of the HHC, in the Gorpung Khola valley.

The shear zone (Toijem Shear Zone) is localized at the boundary between Formations 1 and 2. Shear planes dip to the NE and kinematic indicators show a top-to-the SW sense of shear.

HHC underwent an Eohimalayan phase of metamorphism reaching, in the study area, the kyanite grade followed by a Neohimalayan phase testified by abundant growth of sillimanite on shear planes during the exhumation.

Geometric, kinematic and petrological data indicate that the high-temperature Toijem Shear Zone developed during the exhumation of the HHC enhancing the decompression of the hanging-wall and the emplacement of leucogranite dykes and sills.

It is worth noting that the "compressional" Toijem Shear Zone developed in a very thin section of the HHC and it did not caused repetition in the crystalline unit.

The localization of the shear zone can be triggered by major lithological boundaries among the Formations of the HHC. Once activated in the earlier stages of exhumation, the shear zone affects the velocity path of the extruded unit enhancing the velocity of extrusion of the hanging-wall that moved faster upward and southward with respect to the footwall rocks.

BURCHFIEL B.C., CHEN Z., HODGES K.V., LIU Y., ROYDEN L.H., CHANGRONG D. & XU L. 1992. Geol. Soc. Am. Spec. Paper, 269. 41.
DAVIDSON C., GRUJIC D. E., HOLLISTER L. S. & SCHMID S. M. 1997. J. METAM. GEOL., 15. 593–612.
GOSCOMBE B. & HAND M. 2000. J. Petrol., 41 (12). 1673-1719.
GRASEMANN B., FRITZ H. & VANNAY, J.C. 1999. J. Struct. Geol., 21. 837–853.
GRUJIC D., CASEY M., DAVIDSON C., HOLLISTER L., KUNDIG K., PAVLIS T. & SCHMID S. 1996. Tectonophysics, 260. 21–43.
GRUJIC D., HOLLISTER L., & PARRISH R.R. 2002. Earth Planet. Sci. Letters, 198. 177–191.
HODGES K.V., PARRISH, R.R., HOUSH T.B., LUX D.R., BURCHFIEL B.C., ROYDEN L.H. & CHEN Z. 1992. *Science*, **258**. 1466- 1470.
HODGES K.V., PARRISH R.R. & SEARLE M.P. 1996. *Tectonics*, **15**. 1264-1291.
MACFARLANE, A. M., 1993. *Tectonics*, **12/4**. 1004-1025.
MARUO, Y. & KIZAKI, K. 1983. *In Granites of Himalayas, Karakorum and Hindu Kush (Edited by Shams F.A.)*. Institute of Geology, Punjab University, Lahore, 271-286.
SEARLE M. P. 1999. *J. Geol. Soc. London*, **156**. 227-240.
VANNAY J.C. & HODGES K. 1996. *J. Metam. Geol.*, **14**. 635-656.

KINEMATIC AND TECTONIC EVOLUTION OF THE MAIN CENTRAL THRUST ZONE IN LOWER DOLPO (WESTERN NEPAL)

Rodolfo CAROSI (1), Chiara MONTOMOLI (1), Giovanni RUGGIERI (2)

(1) Università di Pisa, Dipartimento di Scienze della Terra, via S. Maria, 53, 56126 Pisa, Ialy

(2) Istituto di Geoscienze e Georisorse - CNR, Area della Ricerca, Via Moruzzi 1, 56124 Pisa, Italy.

The Main Central Thrust Zone (MCT) in Lower Dolpo (Western Nepal) affects both the lower part of the Higher Himalayan Crystallines (HHC) and the upper part of the underlying Lesser Himalayan Sequence (LH) giving rise to a thick zone of penetrative mylonitic deformation.

A sudden change in lithology, from the upper migmatitic gneiss and kyanite-bearing gneiss to a lower complex made by garnet-bearing micaschists, white quartzites, amphibolites, paragneisses and phyllites marks the boundary between the HHC and the LH.

In the MCT zone an inverted metamorphic field gradient has been confirmed both at the meso- and microscale and biotite, garnet, staurolite and kyanite are found progressively upward in the sequence. The metamorphic minerals are deformed in the mylonites that show a low-grade metamorphic re-equilibration. Kyanite is bent and sometimes stretched with open spaces filled by muscovite and quartz.

Shear along the MCT zone and the STDS (Burchfiel et al., 1992) and erosion in the front of the belt (Beaumont et al., 2001) allowed the ductile extrusion of the HHC from depth up to the higher structural levels either as a ductile wedge (Hodges et al., 1992) or by channel flow (Gruijc et al., 1996; 2002). This path has been recorded in the MCT zone by a spectacular main ductile fabric overprinted by later ductile/ brittle and brittle shear zones.

The ductile deformation developed under non-coaxial deformation in which stable porphyroclast analysis, following Passchier (1987) and Wallis (1995), points to simple shear and pure shear acting together during exhumation and to an increase in simple shear component of deformation approaching the high strain zone. Shear planes strike N110-120 and moderately to steeply dip to the NE: stretching lineation trend N40-50 and plunge 50-60° to the NE. Kinematic indicators indicate a top-to-SW sense of shear.

In Lower Dolpo brittle reverse faults have been recognized overprinting the mylonites of MCT zone. They are associated to centimetre up to decimetre thick cataclasites and drag folds pointing to a top-to-the SW sense of shear. Foliated cataclasites are often associated to shear planes as well as Riedel shears. These brittle structures testify a later compressive reactivation of the MCT zone after the main ductile phase at upper structural levels (Mcfarlane, 1993; Harrison et al., 1997; Catlos et al., 2002; 2004).

To constraint the P-T conditions during the ductile to brittle tectonic evolution of the MCT zone fluid inclusion analyses have been performed on quartz lenses from kyanite bearing gneiss and micaschists sampled from the Main Central Thrust Zone.

The studied fluid inclusions, found either in isolated clusters and along trails, are two-phase (liquid water + liquid carbonic fluid) at room temperature. They usually show a constant ratio between the liquid water and the carbonic fluids and they are characterized by quite regular negative crystal shapes even if sometimes irregular morphologies have been observed. Preliminary microthermometric analyses point CO_2 homogenization temperature (Th-CO_2) ranging between 9.7 and 11.8 °C, while CO_2 melting temperature (Tm-CO_2) is always below the triple point of the pure CO_2 and varies between –58.6 and –59°C, suggesting the presence of CH_4 and/or N_2 coexisting with CO_2. Clathrate dissociation temperatures have been observed between 10.2 and 10.6°C. The isochores for representative fluid inclusions, computed using Bakker's (1999) method, based on the adaptation of Bowers and Helgeson's (1983) equation of state, compared with the geothermobarometric data and mineral assemblages in the host rock, indicate lower pressure- temperature conditions for their trapping in accordance with the retrograde P-T evolution found in the MCT zone of Garhwal Himalaya (Sachan et al., 2001).

The study sector of the MCT zone recorded a metamorphic event at higher PT conditions up to amphibolite facies followed by a lower grade metamorphism and deformation acquired during exhumation reaching the PT conditions of 2-4 Kbar and 300-400°C at nearly 14-17 Ma (Carosi et al., in prep.; Vannay & Hodges, 1996).

The presence of reverse thrusts overprinting the mylonites of the MCT zone could also suggest that deformation after the MCT activity proceeded both toward the foreland and by out of sequence thrusts.

BAKKER R.J. 1999. *Chem. Geol.*,**154**, 225-236.
BEAUMONT C., JAMIESON R.A., NGUYEN M.H. & LEE B., 2001. *Nature*, **414**. 738-742.
BOWERS T.S. & HELGESON H.C. 1983. *Geochim. Cosmochim. Acta*, **47**, 1247-1275.
BURCHFIEL B.C., CHEN Z., HODGES K.V., LIU Y., ROYDEN L.H., CHANGRONG D. & XU L. 1992. *Geol. Soc. Am. Spec. Paper*, **269**. 41.
CATLOS E.,J., HARRISON T.M., MANNING C.E., GROVE M., RAI S.M., HUBBARD M.S. & UPRETI B.N. 2002. *J. Asian Earth. Sci.*, **20**. 459-479.
CATLOS E.J., DUBEY C.S., HARRISON T.M. & EDWARDS M.A., 2004. *J. Metam. Geol.*, **22**. 207-226.
GRUJIC D., CASEY M., DAVIDSON C., HOLLISTER L., KUNDIG K., PAVLIS T. & SCHMID S. 1996. *Tectonophysics*, **260**. 21–43.
GRUJIC D., HOLLISTER L. & PARRISH R.R. 2002. *Earth Planet. Sci. Letters*, **198**. 177–191.
HODGES K.V., PARRISH, R.R., HOUSH T.B., LUX D.R., BURCHFIEL B.C., ROYDEN L.H. & CHEN Z. 1992. *Science*, **258**. 1466- 1470.
HARRISON T.M., RYERSON F.J., LE FORT P., YIN A., LOVERA O.M. & CATLOS E.J., 1997. *Earth Planet. Sci. Letters*, **198**. 177-191.
MACFARLANE, A. M., 1993. *Tectonics*, **12/4**. 1004-1025.
MARUO, Y. & KIZAKI, K. 1983. *In Granites of Himalayas, Karakorum and Hindu Kush (Edited by Shams F.A.)*. Institute of Geology, Punjab University, Lahore, 271-286.
PASSCHIER C. W. 1987. *J. Struct. Geol.*, **9**. 679-690.
SACHAN H.K., SHARMA R., SAHAI A & GURURAJAN N.S., 2001. *J. Asian Earth. Sci.*, **19**. 207-221.
VANNAY J.C. & HODGES K. 1996. *J. Metam. Geol.*, **14**. 635-656.
WALLIS R. S. 1995. *J. Struct. Geol.*, **17**. 1077-1093,

ISOTOPIC MAPS OF HIMALAYAN UNITS – A FRAMEWORK FOR METAMORPHIC ANALYSIS OF CHANNEL FLOW

Jennifer CHAMBERS (1), Mark CADDICK (2), Andy RICHARDS (1), Tom ARGLES (1), Nigel HARRIS (1), Randy PARRISH (3),

(1) Department of Earth Sciences, The Open University, Milton Keynes MK7 6AA, UK
(2) Institute for Mineralogy and Petrography, ETH Zentrum, 8092 Zurich, Switzerland
(3) NERC Isotope Geosciences Laboratory, British Geological Survey, Keyworth, Notts NG12 5GG, UK

The major tectonic units of the Himalayas have been successfully mapped in several areas of the orogen using a combined isotopic studies approach (e.g. Ahmad et al., 2000; Parrish & Hodges, 1996; Richards *et al.*, this volume; Robinson et al., 2001). An invaluable result of this work is that the boundaries between several distinct units are well-defined, thus providing a sound framework for other studies.

This approach has recently been applied to the Sutlej Valley of NW India. Here the Lesser Himalayan Series (LHS) is bounded to the north by a 1-2 km wide mylonite zone defining the Main Central Thrust (MCT: (Vannay & Grasemann, 1998). The High Himalayan Crystalline Series (HHCS, locally called the Vaikrita Group) overthrusts the LHS along this shear zone. The contrasting isotopic signatures of the LHS and HHCS clearly identify the MCT as a major protolith boundary (Richards *et al.*, this volume). The top of the HHCS is marked by the Sangla detachment (the local equivalent of the South Tibetan detachment system), above which lies the Kinnaur Kailas granite (also known as the Akpa granite). This granite is in turn overlain by the Haimanta Group (the basal part of the Tethyan Sedimentary sequence).

The integration of detailed mapping techniques with metamorphic constraints is invaluable to our understanding of orogens. Pressure-temperature-time (P-T-t) paths illustrate how rocks now at the surface have undergone burial and subsequent exhumation. Knowing to which tectonic unit a derived P-T-t path applies is critical when evaluating exhumation models for the HHCS and surrounding units. One such exhumation model is the channel flow model (Beaumont et al., 2001). Thermo-mechanical modelling of channel flow predicts characteristic P-T-t paths for upper LHS rocks, and lower and upper HHCS rocks (Beaumont et al., 2001; Jamieson et al., 2004). These predictions can be tested against empirical results from field observations/sampling.

A metamorphic study in the Sutlej Valley (Caddick, 2004), has recently generated a number of P-T-t paths for samples from the Sutlej valley, by combining P-T pseudosections with accessory phase geochronometry. However, since most of these samples were collected from the HHCS and contain compositionally homogenised garnets, more data are required to evaluate the merit(s) of the channel flow model. Therefore, plans for forthcoming fieldwork in the Sutlej Valley involve sampling units adjoining the upper and lower boundaries of the HHCS (i.e. the Haimanta Formation, and the Jutogh Group of the Lesser Himalaya). The study will construct pseudosections for samples bearing garnet with prograde zoning, in conjunction with Sm-Nd dating of leached garnet and accessory phases. The advantages of this strategy are that it will yield detailed information on the burial and heating phase of samples as well as their exhumation history; it will avoid homogenised garnets from the core of the HHCS which provide limited prograde data; and it will allow comparison of the results with those predicted by the thermo-mechanical channel flow model (Beaumont et al., 2001; Jamieson et al., 2004).

References

Ahmad, T., Harris, N., Bickle, M., Chapman, H., Bunbury, J. & Prince, C., 2000. *Geol. Soc. A.m Bull.*, **112**, 467-477.
Beaumont, C., Jamieson, R. A., Nguyen, M. H. & Lee, B., 2001. *Nature*, **414**(6865), 738-742.
Caddick, M., 2004. *Unpublished Thesis, Cambridge University, Cambridge.*
Jamieson, R. A., Beaumont, C., Medvedev, S. & Nguyen, M. H., 2004. *Journ.Geoph. Res.*- **109**(6), art. no.-B06407.
Parrish, R. R. & Hodges, K. V., 1996. *Geol. Soc. A.m Bull.*, **108**, 904-911.
Robinson, D. M., DeCelles, P. G., Patchett, P. J. & Garzione, C. N., 2001. *Earth Plan. Sci. Lett.*, **192**(4), 507-521.
Vannay, J. C. & Grasemann, B., 1998. *Schweiz. Miner. Petrog. Mitt.*, **78**(1), 107-132.

Note Page

Rupshu, Stoliczka,1866

STRESS FIELD AND FAULT DEVELOPMENT IN THAKKHOLA HALF GRABEN : A NUMERICAL MODELLING APPROACH

Deepak CHAMLAGAIN* and Daigoro HAYASHI

Department of Physics and earth Sciences, University of the Ryukyus, Okinwa 903-0213, Japan
Corresponding author: dchamlagain@hotmail.com

Since the Eocene collision, the structural evolution of the Himalaya and Tibet have been controlled by three classes of structures (Coleman and Hodges, 1995) e.g. first east-west striking, north dipping thrust systems e.g. Neogene Main Central Thrust (MCT) and Main Boundary Thrust (MBT) system, which strike parallel to the orogen, second east-west striking, north dipping normal faults of the South Tibetan Detachment Fault (STDF) system and third north-south striking normal faults and associated grabens and strike slip features. The third type of structure including grabens of southern Tibet and the Himalayas represent the Cenozoic extensional tectonic phase, which has affected whole Tibet and northernmost part of the Himalaya. Thakkhola half graben, on the crest of the Himalaya, is one of the north trending grabens that define the Neogene structural pattern of the southern margin of the Tibetan Plateau and is seemingly enigmatic feature in a regionally contractional tectonic setting between the colliding plates. Neotectonically, this graben is active and its latest movement is constrained to ca. 17.2 ka (Hurtado et al., 2001). The understanding of the neotectonic stress field and resulting fault pattern is useful constraint to understand its structural configuration and evolutionary history. Therefore, series of 2D elastic, plane-strain, finite element models (FEMs) are generated to simulate the effects of Thakkhola Fault and rock properties on growth of graben faults and their configuration for the Thakkhola half graben evolution.

Our models have successfully shown that the extensional graben faults form at the top of the overburden and propagate downward as we increased extensional displacement (Fig. 1). Simulated models have clearly defined the graben bounding faults and suggest multiple faults on each side of the natural grabens rather than single fault. During progressive extensional displacement depth of faulting increases and deformation is mainly localized in downthrown block both in basement and syntectonic deposits. Syntectonic deposit is, however, characterized by normal faulting in tensional tectonic stress field, which is the characteristic feature of the small-scale graben at post rift deformation stage. The width and depth of graben are primarily controlled by the rheology of the upper elastic layer (syntectonic deposits). The applied rock layer properties are able to deduce the first order characteristics of the Thakkhola half graben. Therefore, this simulation constrains probable values for the rock layer properties controlling the Thakkhola half graben evolution. Assumption of the Thakkhola Fault as a weak zone does not make significant difference on stress field and fault pattern in the half graben basin. Thus it seems that the Thakkhola fault system did not only contribute to development of the half graben. Admittedly, we cannot rule out the effect of basal drag and rheology.

References

Coleman M.E. and Hodges, K 1995. *Nature* 374, 49-50.
Hurtado Jr. J.M., Hodges, K.V. and Whipple, K.X. 2001. *GSA Bulletin* 113, 222-240.

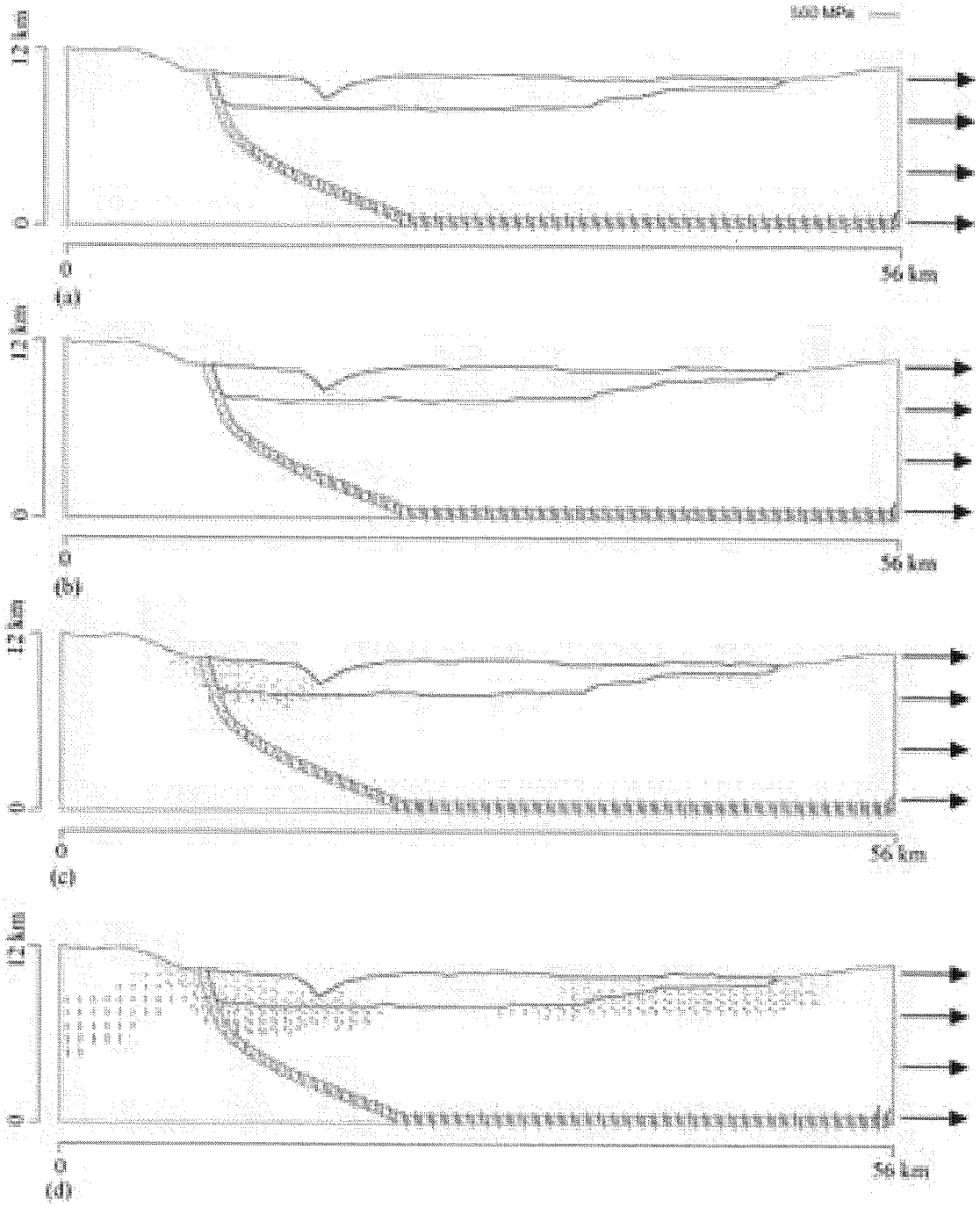

Fig. 1- Failure elements under a (20 m), b (30 m), c (40 m) and d (50 m) horizontal extension with detachment fault.

TIMING OF THE LATE CENOZOIC UPLIFT OF THE CHINESE TIANSHAN CONSTRAINED BY MAGNETOSTRATIGRAPHY AND ROCK MAGNETISM FROM JUNGGAR AND TARIM BASIN

Julien CHARREAU[1], Yan CHEN[1], Stuart GILDER[2], Stéphane DOMINGUEZ[3], Jean-Philippe AVOUAC[4], Sevket SEN[5], and Yongan LI[6]

(1) Institut des Sciences de la Terre d'Orléans
(2) Institut de Physique du Globe de Paris,
(3) Laboratoire Dynamique de la Lithosphère, Université de Montpellier
(4) California Institute of Technology;
(5) Museum of Natural History, Paris
(6) Institute of Geology & Mineral Resources, Bureau of Geology & Mineral Resources of Xinjiang Uygur Autonomous Region
*corresponding author : Julien.Charreau@univ-orleans.fr

The Cenozoic reactivation Tianshan is due to the India-Asia collision. However, its uplifting history remains unclear through several studies have been carried out. The Cenozoic sediments on both sides of the Tianshan are considered as a good recorder of the mountain range building. Because of their continental origin which are difficult to be dated by the paleontology, we carried out two magnetostratigraphic studies along the north and south Tianshan flanks that may provide absolute age of sediments and detailed sedimentation rates believed to be linked to the erosion behavior on the range. To characterize the magnetic mineralogy in terms of nature, shape and orientation, we also performed rock magnetism experiments that permit to track back time-transgressive changes in the sedimentation conditions largely function of tectonic and climate process,.

On the southern flank near Kuche, the north-south Yaha river incises the East-West striking Qiulitage ramp-anticline where Neogene to Quaternary sediments exposed, mainly composed of sandstone and mudstone. 1069 core samples were collected from a 2814-m-thick section. Rock magnetic experiments show that the magnetic remanence is principally carried by magnetite though hematite is negligible. A linear magnetic component is isolated by stepwise thermal demagnetization isolated that decays univectorally toward to the origin. Eighteen magnetic polarity changes were identified that we correlate between ~5.2 and ~12.6 Ma with the reference magnetic polarity time scale. Based on this correlation the sedimentation rate increases from 0.2 mm/yr to 0.38 mm/yr at ~ 11 Ma. We also measured the anisotropy of magnetic susceptibility of the samples. Before ~ 11 Ma the average shape parameter T of the AMS is around 0 meaning that the grains are spherical in shape and far-traveled. By ~11 Ma, T values became greater than 0 meaning that the magnetic grains are oblate in shape and traveled less far. The timing of this change in the T parameter is strongly correlated to a decrease of the bulk susceptibility that likely indicates a modification of the source rock. From the rock magnetic parameters, together with the acceleration of the sedimentation rate, we believe that the uplifting of the southern central Tianshan mountains is probably accelerated by ~ 11 Ma.

On the northern flank we collected 801 samples along the 1559-m-thick Kuitun section where again sediments are fluvio-lacustrine sandstone to mudstone exposed by the incision along the North-south Kuitun He river in the Dushanzi ramp-Antciline. Magnetic experiments (IRM, hysteresis loop, Curie point analyses ...) show that magnetite is the main magnetic carrier. Using both thermal and AF stepwise demagnetization we isolated a linear magnetic component giving 16 polarities changes that we correlate between ~3.1 and ~10.5 Ma. This correlation yields a relatively constant sedimentation rates with an average of 0.21±0.01 mm/yr. Measurements of the AMS show that the magnetic grains are totally oblate in shape with a positive T value from the bottom to the top of the section. Based on the absence of sedimentation rate acceleration and the positive T value we believe that the northern central Tianshan was already uplifting by 10.5 Ma.

More magnetostratigraphic data are needed to improve the understanding on the Cenozoic Tianshan Cenozoic uplifting history.

Note Page

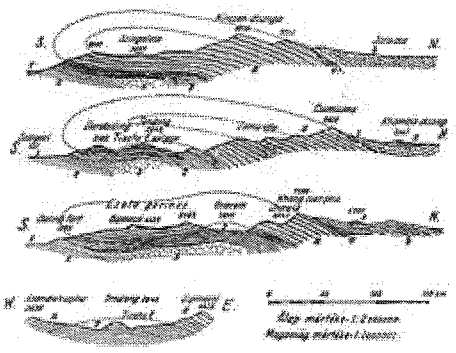

Sikkim, Loczy,1878

INTRAPLATE VOLCANISM ON THE SOUTHERN TETHYAN MARGIN (NORTH ARABIAN AND NORTH INDIAN MARGINS)

François CHAUVET [1], Henriette LAPIERRE [1], Delphine BOSCH [2], Georges MASCLE [1], Jean-Claude VANNAY [3]

1 Laboratoire de Géodynamique des Chaînes Alpines (UMR 5025 CNRS/UJF/US) OSUG, Grenoble, France.
2 UMR CNRS 5568, pl. E. Bataillon 34095 Montpellier, France
2 BFSH2, UNIL, CH 1015, Lausanne, Switzerland.

Several volcanic episodes occur on the southern Tethyan margin during the early stage of its formation. During Lower Carboniferous basaltic dykes are emplaced on the Indian margin in Lahul area in correspondence with a transtensional tectonic event (Vannay and Spring, 1993). This tectono-magmatic episode represents the first indication of the continental break-up. During Permian times, expanded basaltic flows are intercalated either in the platform or in the basin sequences and on both the Arabian and the Indian margins. Finally Late Triassic volcanics are observed solely in distal basinal environment on both margins (Fig. 1).

Petrological, geochemical and isotopical analysis have been performed on selected samples of the different volcanic sequences. Lower Carboniferous (Baralacha La) basaltic dykes exhibit tholeiitic and alkaline affinities ; the tholeiites show an enrichment in light rare earth elements (LREE) and systematic Nb negative and Th positive anomalies. The εNd_i values (+ 2.3 to – 1.3) and Pb isotopes compositions suggest that they derived from the partial melting of an enriched OIB mantle source. The latter is characterized by an HIMU component and is contaminated by an EM1 end member (lower continental crust).

The Permian volcaniscs show a variation of their geochemical and isotopic compositions in relation with their position on both the Arabian and Indian margins. In Himalaya, the Panjal Trapps (platform) exhibit features of continental tholeiites (low Ti content, LREE enrichment, Nb/Ta negative anomalies) deriving from an enriched OIB-type mantle source contaminated by the upper continental crust (high Pb/Pb ratios, low εNd_i values, Fig. 2). In contrast the Drakkar-Po phonolites present the same OIB-type mantle source but are devoid of any contamination. In Oman the sequences of the Arabian platform (Saih Hatat) have features consistent with contamination by the lower crust (low εNd_i values, and Pb isotopic compositions, Group 3 on Fig. 2). In the Hawasina basinal sequences tholeiitic and alkaline afinities have been characterized (respectively Group 1 and Group 2 on Fig. 2). Their isotopic compositions as for Group 3 indicate an OIB-type enriched mantle source, but devoided of any continental contamination (Lapierre et al., 2004).

In Oman, the Triassic volcanics show transitional tholeiitic affinities and isotopic compositions related to an OIB-type mantle source (εNd_i +4 to -3). The negative εNd_i correlated with the Pb/Pb isotopic compositions suggest the involvement of an EM1-type component. The Himalayan samples (Drakkar-Po) present alkaline affinities, related to an OIB-type mantle source (εNd_i +4 to +6).

In conclusion, the early episodes of volcanism on the Southern Tethyan margin are characterized by the influence of enriched mantle sources. The large distribution of the Permian intraplate magmatism with similar geochemical features allow us to propose a relation with the activity of a major plume.

Vannay J.C. and Spring L., Geochemistry of the continentals basalts within the Tethyan Himalaya of Lahul-Spiti and SE Zanskar, NW India, in Treloar P.J. and Searle M.P., (eds), Himalayan Tectonics Geological Society Special Publication, 74, 237-249, 1993.

Lapierre H., Samper A., Bosch D., Maury R.C, Béchennec F., Cotten J., Demant A., Brunet P., Keller F. and Marcoux J., The Tethyan plume : Geochemical diversity of Middle Permian basalts from the Oman rifted margin, Lithos, 74, 167-198, 2004.

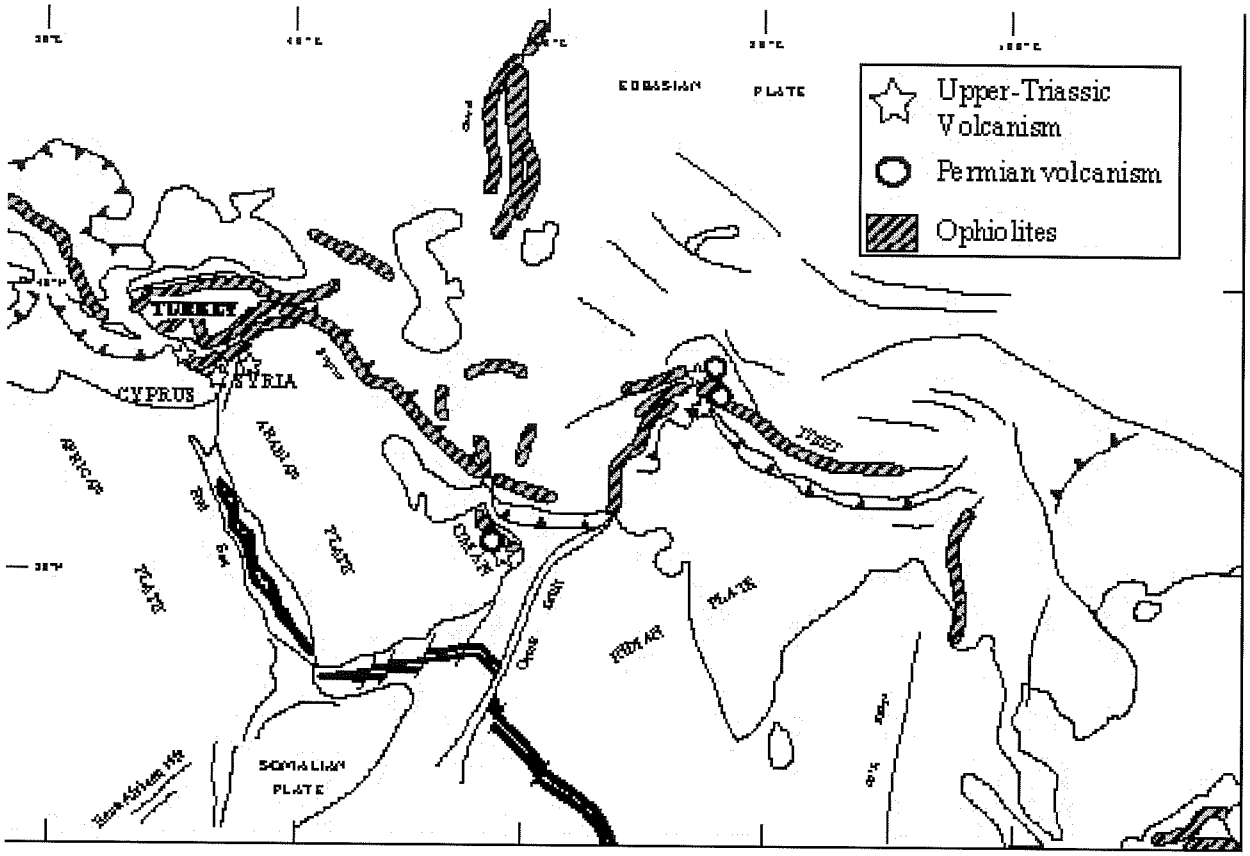

Fig. 1- Location of the Tethyan ophiolites and Permian and Triassic volcanic sequences

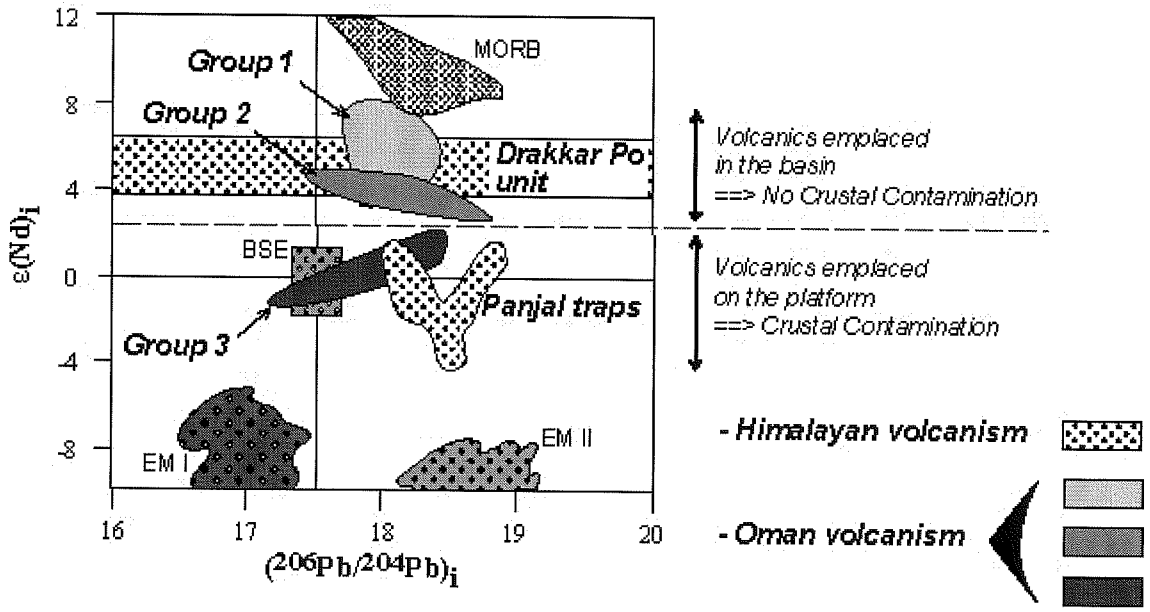

Fig. 2- Synthetic isotopic diagram of the South Tethyan Mid Permian volcanism

SEDIMENTARY RECORD REVEALS UPLIFTING PROCESS OF MOUNTAINS IN NORTHERN EDGE OF THE TIBETAN PLATEAU

Zhengle CHEN, Xiaofeng WANG, Jian LIU

Institute of Geomechanics, Chinese Academy of Geological Sciences, Beijing 100081,P.R. China

The uplift of the Tibetan plateau is controversial for long time. Here, we present new evidence from the sedimentation and stable isotope of calcite-cement in the foreland basin (Fig.1) to discuss the uplifting history of mountains in northern plateau.

1 Sedimentary Record

Cenozoic sediments are widely spread along northern edge of the Tibetan plateau. Our main study area, Jianggalesayi basin (JB), is located at the northwestern front of the Altyn Tagh Mountain (ATM). Four Cenozoic lithologic packages are distinguished. The Paleocene to Eocene rocks are fluvial plain sediments. The lower part of the Oligocene to Miocene Wuqia Formation is also of fluvial plain origin, and the upper part is mainly composed of brown conglomerates and red sandstones, locally interbedded with mudstones, suggesting alluvial fan facies. The Pliocene Atushi Formation consists mostly of yellow conglomerates interbedded with mudstones, indicating pluvial piedmont settings. The Early Pleistocene Xiyu Formation is composed primarily of gray conglomerates, suggesting a rapid talus accumulation tectonic environment. We carefully measured this section, and collected samples for the research in sedimentation and sable isotope, and also for the paleo-magnetic dating (The dating process is still on the way).

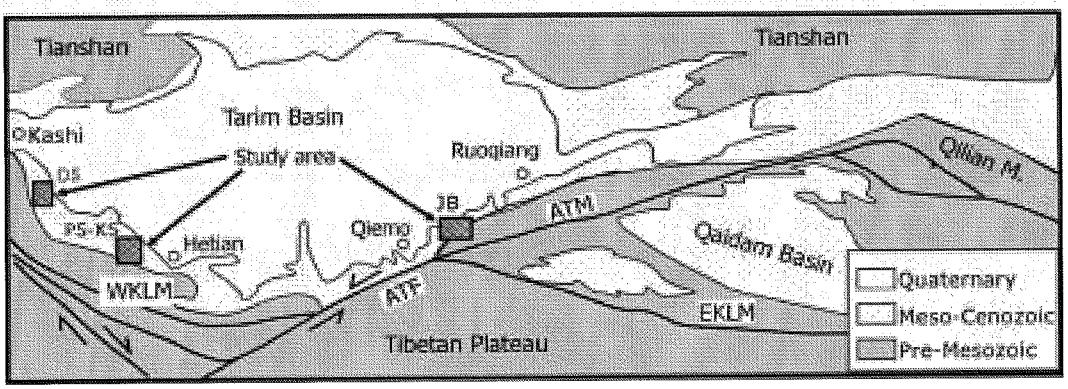

44 sandstones samples for point-counting analyses of detritus under microscope and 47 sites for pebble clast in conglomerate are completed (Fig.2). Lithological assembly and the composition of detritus in sandstone and pebbles in conglomerates reveal the exhumation history of the ATM. Paleozoic double-peak volcanic rocks were firstly denudated during the Paleocene to Eocene, and the difference in topography between the ATM and the JB was small. This difference became large during the late Oligocene to the early Miocene, when the Proterozoic basement imitated to be exposed to the surface and be denudated. The denudation ration increased at the end of the Miocene. The Lower to Middle Proterozoic and Archean basement rocks was then exposed to the surface till the Early Pleistocene when the Xiyu Formation began to deposit. And the much more deeper rocks, such as the ecologite, began to be eroded till to the Middle Pleistocene.

2 Stable Isotope Evidence

The $\delta^{18}O$ value in calcite-cement, as a parameter of climate change, has been proved to be useful in reconstructing the uplift history of mountain (Chamberlain, 2000; Stern,1997). 100 more samples from the Pusikai-keliyang section in the northern front of the western Kunlun mountains and the Damusi section in the northeastern front of the Karakorum mountains were also collected during our field season in 2002 (Fig.1). We took cement from samples by electric drill and applied the method of acid-decomposition for the measurement of $\delta^{18}O$ value in calcite-cement.

Analyses results show that there are three rapid changes of the $\delta^{18}O$ value in the Jianggalesayi Basin. The first one appears at the beginning of the Tertiary. The second one, at boundary age of the Oligocene Wuqia Formation and the Paleocene Kumugeliemu Formation, is characterized by a sharp decrease of the $\delta^{18}O_{smow}$ from 23°Î down to17°Î. And the last one is at the boundary between the lower part with the upper part of the Wuqia Formation (ca. 25Ma), behaving a rapid change of the value from 21.5°Î down to 18°Î. Correspondingly, the $\delta^{13}C$ value also shows a rapid change in the end of the Eocene and the beginning of the Oligocene Wuqia Formation (Ca.35Ma).

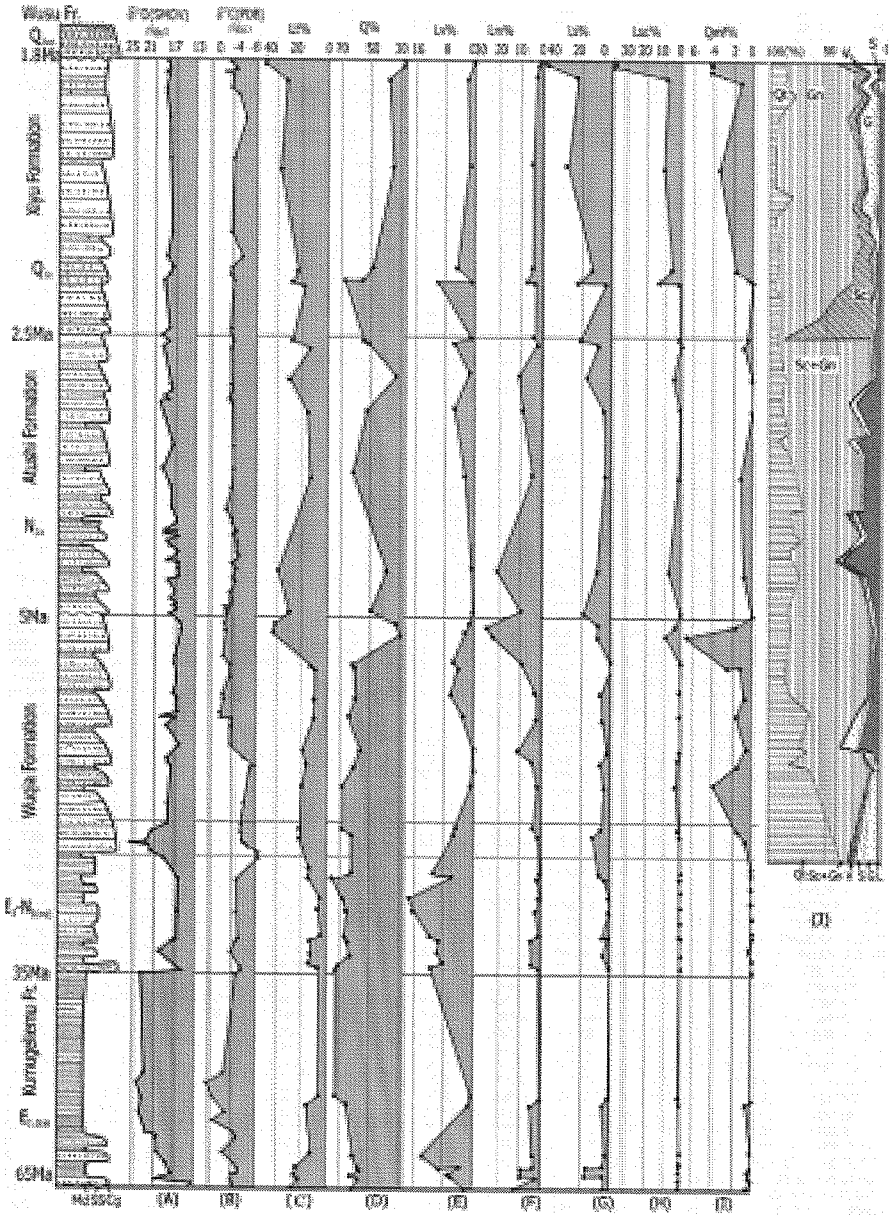

The value of $\delta^{13}C_{PDB}$ rapidly decreased from -1.5°Î down to -5°Î. And a much larger variation of the $\delta^{13}C_{PDB}$ value appears from the beginning of the upper part of the Wuqia Formation (ca.25Ma) till to 16Ma. In Keliyang, and Pusikai sections, there are at least two rapid changes of $\delta^{18}O$ and $\delta^{13}C$ value, similarly as the result in Jiangaglesayi section. The first change appears at the beginning of Tertiary, and the second is at the beginning of the Oligocene. In Damusi section, the result also shows two rapid changes of the $\delta^{18}O$ and $\delta^{13}C$ value. The earlier one occurred at the lower part of the Wuqia Formation and the later one occurred at the middle part of the Wuqia Formation, similarly as that in Jianggelesayi section.

The first change at the beginning of the Tertiary can be explained as the worldwide "boundary event" between the Cretaceous and the Tertiary. The later two changes during the Tertiary can be explained as the response to the uplift of mountains in northern edge of the Tibetan plateau, suggesting that the plateau began to uplift at the early stage of the Oligocene, and a rapid uplift of mountains occurred in early time of the Miocene (ca. 25-23Ma).

3 Discussion and Conclusion

Sedimentation in foreland basin and stable isotope evidence suggest that there are at least three stages of the mountain-uplift in northern edge of the Tibetan plateau. The earliest uplift of mountains initiated from the early time of the Oligocene. The second rapid uplift of mountains occurred at the end of Oligocene to the early of Miocene (ca. 23-25Ma), and much more strongly uplift, the third time uplift, happened at the Late Pliocene to the Early Pleistocene. Our result is fairly consistent with the previous suggestions both by fission track dating of apatite (Wang, 1998; Sobel,1997; Chen, 2001) and paleo-magnetic dating (Zheng, 2000).

Acknowledgements: This study is carried out under the programs of the NNSF of China (No.40102022) and the Major State Basic Research Program of China (No. 2001CB409808 and 2001CB7110013).

References

CHAMBERLAIN C. P., POAGE M. A. 2000. *Geology*, **28.**115-118

Chen Z.L., Zhang Y.Q.&Wang X.F., et al. 2001. *ACTA GEOSCIENCIA SINICA*, **22(5)**.413-418

Edward R. S & Trevor A. D. 1997. *Journal of Geological Research,* **102(B3)**. 5043-5063

Stern L. A., Chamberlain C. P. & Robert C R, et al. 1997. *Geochimica et Cosmochimica Acta*, **61(4)**.731-744

Wang J. 1998. *Geological review*, 44(4).435-442

Zheng H.B., Powell C. & An Z.S. 2000. *Geology*, **28(8).**715-718

PALEOMAGNETIC CONTRAINS ON CENOZOIC MOTION OF THE ALTYN TAGH FAULT, ROTATION OF THE QAIDAM BASIN AND THE NORTHERN EDGE OF TIBETAN PLATEAU

Yan CHEN[1], Stuart GILDER[2] and Vincent COURTILLOT[2]

1 Institut des Sciences de la Terre d'Orléans, Université d'Orléans, France
2 Institut de Physique du Globe de Paris, France

In order to better understand the tectonic evolution of central Asia under the influence of the India-Asia collision, we carried out a paleomagnetic study of about 1600 cores from 115 sites along the Altyn Tagh fault, in the Qaidam and Tarim basins, on the Tibetan plateau and the Yumen area of North China. Samples were mainly collected from Jurassic to Neogene siltstones and sandstones. In most cases stepwise thermal demagnetization unblocks low and high temperature components carried by magnetite and hematite. Low temperature components are north and down directed and lie close to the recent geomagnetic field. High temperature components pass fold and/or reversal tests and likely represent primary remanent magnetizations. The results from Tibetan plateau display a complex pattern of vertical-axis block rotations that are compatible with a tectonic model of clockwise rotation of the Qaidam Basin and concomitant left-lateral slip on the Altyn Tagh fault: (1) two of the ten localities are rotated significantly counterclockwise; they lie adjacent to the Altyn Tagh fault zone, consistent with the idea that left-lateral strike-slip motion occurred along it. The age of counterclockwise rotation near the eastern extremity of the fault was dated as younger than 19 Ma; (2) three widely spread areas within the Qaidam Basin exhibit similar and significant clockwise rotations, on the order of 20°, with respect to the North China Block, Tarim and Eurasia. The mean of the three values is thought to represent the total rotation of Qaidam. Because the youngest rocks displaying clockwise rotations are Oligocene, the main phase of Qaidam Basin rotation, and hence shear on the Altyn Tagh fault, took place after or near the end of the Oligocene (~24 Ma). Upper Neogene strata located on the Qaidam Basin are not significantly rotated, thus tectonic deformation acting since the Upper Neogene (~5 Ma) is not resolvable by paleomagnetic methods. Given a 20°±5° clockwise rotation of the Qaidam Basin with respect to the Tarim Basin, the maximum left-lateral displacement on the Altyn Tagh fault since 24 Ma is 500±130 km. The results from Yumen area north piedmont of the Qilian mountains are consistent with those from other areas of the North China block, but significantly different from those from the Qaidam Basin on the southern side of the Qilian Mountains. They suggest that: (1) the Yumen region behaved as a rigid part of the NCB since at least the Early Cretaceous; (2) 740< 500 km of north-south directed convergence has taken place between the NCB and Qaidam,within the Qilian Mountains and (3) extrusion of Qaidam was accompanied by a 23 ±5° relative rotation with respect to North China. This is larger than implied by the maximum left lateral slip on the Altyn Tagh fault system. The same data imply some 1000± 800 km of Cenozoic motion between the Tarim and NCB blocks,which were so far believed to have formed a rigid entity since at least the Jurassic. One interpretation could be that all Tarim and Qaidam Cretaceous paleomagnetic samples from red beds, but not those from Yumen and the NCB, suffered significant inclination shallowing, as observed in Cenozoic red beds from Central Asia. So far, we do not find support for this possibility. Possible tectonic interpretations include: (1) the existence of a large, as yet uncharted, tectonic discontinuity between Tarim and the NCB in the vicinity of the desert corridor near 95-100°E longitude; (2) the occurrence of significant deformation within southwestern Tarim, to the north of Yingjisha where paleomagnetic sites were obtained, or (3) persistent clockwise rotation of Tarim with respect to the NCB, for at least 20 Ma, at the rate found for current block kinematics.

TENFOLD DISPARITY BETWEEN DECADAL INSAR AND MILLENIAL MORPHOCHRONOLOGIC SLIP-RATES ON THE KARAKORUM FAULT.

Marie Luce CHEVALIER*, Paul TAPPONNIER*, F. J. RYERSON, +, R. FINKEL, +, Jérome VAN DER WOERD, **, Haibing LI * °, Qin LIU, ++

* Laboratoire de Tectonique, Mécanique de la Lithosphère, Institut de Physique du Globe de Paris
+ IGPP, Lawrence Livermore National Laboratory, Livermore, USA.
** Institut de Physique du Globe de Strasbourg, France.
°Ministry of Lands and Resources, Beijing
++ Total Exploration , Beijing, China.

The Karakorum Fault is the main dextral strike-slip fault north of the Himalayas. While recent InSAR data are interpreted to suggest that it is barely active, moving at a rate of 1±3 mm/yr, surface exposure dating of moraines and terraces south of Bangong lake suggests it slips ten times as fast. On the west side of the Gar pull-apart (32°3'N-80°1'E, 4365 m- 4760 m), at the foot of the Aliyari Range, we sampled rooted, quartz-rich blocks on two well-defined lateral moraine crests (M1 and M2E) offset right-laterally relative to the valley of the Manikala Daer Glacier. The offsets obtained from retro-deformation of 1 m-resolution IKONOS images are 220 ± 10 m and 1520 ± 50 m, respectively. Twenty-seven samples were dated with cosmogenic ^{10}Be. The exposure ages fall in distinct clusters: 21 ± 0,1 ka and 40 ± 3 ka on M1, and 140 ± 5,5 ka and 180 ± 14 ka on M2. The ages of maximum sample abundance correlate well with the ages of the coldest periods derived from proxy paleo-temperature records (SPECMAP), suggesting that the Manikala glacier abandoned M1 and M2E northeast of the fault at the end of the LGM and penultimate glacial maximum (late stage 6), respectively, and that the ages are little affected by erosion. Pairing the abandonment ages of the moraines with their offsets yields concordant dextral slip-rates of 10.9 ± 0.6 and 10.5 ± 0.5 mm/yr. The resulting, average slip rate (10,7±0,7 mm/yr) in the last 150 ka is comparable to the geological rate obtained by Lacassin et al., [2004] (10 ± 3 mm/yr in the last 34 Ma) and to the GPS geodetic rate determined by Banerjee and Burgmann, [2002] (11 ± 4 mm/yr). It is over twice that measured in India by Brown et al., [2002] (4 ± 1 mm/yr). The ≈ 11 mm/yr slip-rate along the Ayilari range should be considered a minimum because the site is situated on one side of the Gar pull-apart and two branches of the Karakorum fault system splay off into that pull-apart. Cosmogenic exposure dating of other geomorphic features north and south of Gar corroborates this millennial slip-rate, implying that Tibet moves southeastwards by at least 1cm/yr relative to the Ladakh Himalayas. That the GPS and InSAR values differ by a factor of ten suggests that strong monsoonal tropospheric effects might bias the InSAR data. If the tenfold disparity between decadal and millennial rates is real, however, then it might reflect slip-rate fluctuations over periods comparable to or longer than the seismic cycle, reflecting the mechanical behavior of the fault zone integrated over the entire lithosphere.

MARINE SEDIMENTARY RESPONSE ACROSS THE PALEOCENE-EOCENE THERMAL MAXIMUM (PETM) AT TINGRI, SOUTHERN TIBET

Cecily O.J. CHUN (1), Zhifei LIU (2), Margaret L. DELANEY (1), Xianghui LI (3), and Xinrong CHENG

(1) Ocean Sciences/Institute of Marine Sciences, University of California, Santa Cruz, 95064 USA
(2) Laboratory of Marine Geology, Tongji University, Shanghai 200092, China
(3) Institute of Sedimentary Geology, Chengdu University of Technology, Chengdu 610059, China

The Paleocene-Eocene Thermal Maximum (PETM), ~55 million years ago, is one of the most prominent transient warming intervals in Earth's history. The ocean's surface temperature increased rapidly by 8-10 °C at high latitudes and 4-5 °C in the tropics during a period of < 40 k.y., then cooled again (Zachos et al., 2003). A sudden large increase of carbon dioxide in the atmosphere, possibly from the rapid release of ~2000 Gt of microbially-produced methane hydrates from the seafloor (Dickens et al., 1995, 1997, 2003), is believed to be the main driver of climate change. Evidence for this theory is the prevalent > 2.5‰ negative carbon isotope excursion (CIE) found in both marine and terrestrial systems (Kennett and Stott, 1991, Koch et al., 1992). This period in Earth history of abrupt and extreme warming, spanning <150 k.y., shows how the Earth, as a system, can respond to such climate change. Understanding the mechanisms allowing the rapid return to more normal conditions can allow us to better predict the effects of modern anthropogenic increases in carbon dioxide and other greenhouse gasses. Previous investigations of the PETM were mainly conducted on sediments from modern oceans and European and American continents (e.g. Kennett and Stott, 1991; Zachos et al., 2003). Asian sites were less often reported because most of the Asian continent was uplifted, making Paleogene marine sediments virtually absent. However, the southern Tethyan region contains carbonaceous and terrigenous shallow-water deposits from the Cretaceous to the Lower Tertiary (see Willems et al., 1996).

We describe the PETM at Tingri in southern Tibet. The Gongzha Section consists of the lower Paleocene Zongpu Formation (deep-grey thin-bedded nodular limestone and grey medium- to thin-bedded bioclastic limestone) and the upper Eocene Zhepure Formation (gray medium- to thick-bedded limstone) (Figure 1). The obvious replacement of benthic forminiferal assemblages *Lockhartia* community by *Alveolina* community indicates the approximate position at ~ 30 m above the base of the section, for the Paleocene-Eocene (PE) boundary (Willems et al., 1996, Li et al., 2002). Our work is the first attempt to measure the bulk carbon and oxygen isotopes, and magnetic susceptibility changes across the section. We also use sedimentary phosphorus (P) concentrations and calcium carbonate measurements along with trace metal enrichment factors (EF) to reconstruct nutrient burial and paleoredox state at Tingri.

Transformations of organic and oxide-associated P to authigenic P in marine sediments at continental margins and open ocean sites occurs during sediment burial (e.g. Anderson et al., 2001 and references within). Distinguishing between the sedimentary pools of bio-available P and detrital P gives us a more accurate understanding of nutrient burial in marine sediments. Calcium carbonate accumulation can indicate local export productivity or the absence of major dissolution events. Redox sensitive metal EF, relative to crustal averages, have the ability to describe the redox chemistry of the overlying water and marine sediments at time of burial. Manganese (Mn) EF >1 indicate oxic conditions, while uranium (U) EF > 1 indicates suboxic or anoxic overlying water conditions.

Our results based on the depth at which the lithology changes from deep-gray thin-bedded nodular limestone to gray medium to thin-bedded bioclastic limestone and the most negative bulk carbon isotope (-5.0‰) indicate the PE boundary is at ~15 m thickness, roughly 10 m lower than Li and Willems both suggest. Background carbon isotope values are +2.0‰. Calcium carbonate weight percent range from a low of 80.7% at 34 m, and high of 99.2% at 39 m. We observe the major decrease in calcium carbonate with a change in lithology, but no major CIE. Mn EF range between

0.5 to 13.1, similar to those observed in a deep-marine PE section located in the Atlantic (Quartini et al., 2004). U EF exceed crustal values throughout the measured section. The negative carbon isotope excursion begins with an initial -4.2 ‰ decrease at ~9.2 m and could represent the true depth of the boundary. However, a more detailed biostratigraphic examination and a higher resolution investigation will be needed to confirm the uncertainty in where to place the PE boundary.

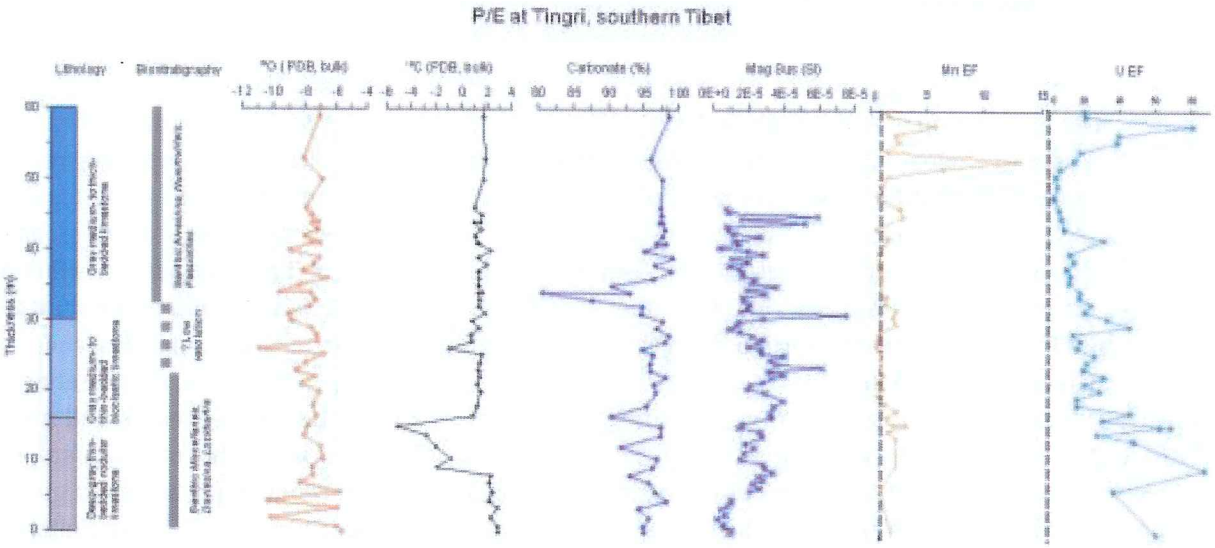

Figure 1. Lithology, biostratigraphic zones (from Li et al., 1996), bulk oxygen and carbon isotopic values, weight percent calcium carbonate, magnetic susceptibility, Mn and U EF plotted versus thickness. Black dashed vertical lines for Mn and U EF are the Mn/Ti and U/Ti enrichment relative to $Mn/Ti_{crust} = 1$ and $U/Ti_{crust} = 1$.

References:

Anderson, L. D., Delaney, M.L., Faul, K. L., Carbon to phosphorus ratios in sediments; implications for nutrient cycling, *Global Biogeochem. Cycles, 15,* 65079, 2001.

Dickens, G.R., Castillo, M.M., and Walker, J.C.G. A blast of gas in the late Paleocene: simulating first-order effects of massive dissociation of oceanic methane hydrate, *Geology, 25*, 259-262, 1997.

Koch, P. L., Zachos, J.C., and Gingerich, P.D., Correlation between isotope records in marine and continental carbon reservoirs near the Paleocene/Eocene boundary, *Nature,* 358, 319-322, 1992.

Li, Xiang-hui, et al., Sedimentary responses to the global event of transitional Paleocene-Eocene boundary in Tingri, Southern Tibet, *Mar Geo & Quart Geo, 22*, 69-74, 2002.

Willems, H., Zhou, Z., Zhang, B., Grafe, K.U., Stratigraphy of the Upper Cretaceous and Lower Tertiary strate in the Tethyan Himalayas of Tibet (Tingri area, China), *Geol. Rundsch,* 85: 723-754, 1996.

Quartini, J. C., Chun, C. O., Delaney, M. L., Zachos, J. C., Tracers of Productivity across the PETM, Walvis Ridge, ODP Sites 1262 and 1263, *EOS Trans. AGU, 85*(47), Fall Meet. Suppl., Abstract PP11B-0562, 2004.

Zachos, J.C. et al, A transient rise in tropical sea surface temperature during the Paleocene-Eocene thermal maximum, *Science, 302*, 1551-1554, 2003

DOES THE ALTYN TAGH FAULT EXTEND BEYOND THE TIBETAN PLATEAU?

Brian J. DARBY (1), Bradley D. RITTS (2), and Yongjun YUE (3)

(1) Department of Geology and Geophysics, Louisiana State University, Baton Rouge, LA, USA; bdarby@geol.lsu.edu
(2) Dept. of Geological Sciences, Indiana University, Bloomington, IN, USA; britts@indiana.edu
(3) Dept. of Geological and Environmental Sciences, Stanford University, Stanford, CA, USA; yongjun@pangea.stanford.edu

The termination of Altyn Tagh fault (Fig. 1) is a critical outstanding problem for understanding the mechanics of Cenozoic deformation resultant from the Indo-Asian collision and mechanisms of Tibetan Plateau formation. Plate-like extrusion models predict high slip rates (>20 mm/yr), and magnitudes, whereas continuum thickening deformation requires lower rates (<10 mm/yr), and magnitudes of slip on major structures. The former model requires the Altyn Tagh fault to extend beyond the plateau or transfer its slip onto other structures, whereas the latter requires the fault to end (slip = 0 km) at the frontal Qilian Shan thrust defining the NE edge of the Tibetan Plateau.

Although recent fault slip-rate data (Yue et al., 2001; 2003; Ritts et al., 2004; this meeting), clearly suggest a two phase evolution, consisting of Oligocene-Early Miocene extrusion and mid-Miocene-Recent shortening and thickening (Ritts et al., this meeting), the mechanism to accommodate an early phase of extrusion beyond the Tibetan Plateau remains problematic given three constraints: 1) the ATF is generally considered to end at the NE corner of the Tibetan Plateau; 2) the amount of extrusion-related Oligocene-Early Miocene slip on the ATF is ~310 km very near the fault's termination near Yumen (Fig. 1; Yue et al., 2003); 3) other structures proposed to accommodate ATF strain near its northeast end (e.g., the Haiyuan fault), do not have the slip magnitudes necessary to have accomplished this (Burchfiel et al., 1991). A remaining mechanism for accommodating lateral extrusion, proposed by Yue and Liou (1999), suggests transfer of left-lateral slip onto the Alxa-East Mongolia fault system, a system of strike-slip faults posited to extend from the northeast end of the ATF to the Sea of Okhostk. This proposed fault system remains largely a tectonic construct; although supported by sparse geological data from southern Mongolia (Johnson, 2004, Johnson and Webb, this meeting) and few geophysical studies (Yue and Liou, 1999); the existence of Tertiary left-lateral faults remains undocumented northeast of the ATF.

We report on a series of newly-recognized and documented E to ENE-striking faults within the Alxa block, NE of the Tibetan Plateau, that are visible on remotely-sensed images and confirmed by field studies (Fig. 1). These structures are demonstrably left-lateral faults based on offset geology and kinematic indicators such as striae and s-c fabrics in fault gouge. Our field data and observations from Landsat and ASTER imagery suggest that the ATF splays in to at least five strike-slip faults east of ~98°E longitude (Yumen; Fig. 1). This change from a single well-developed structure to multiple splays may reflect the transition from juxtaposition of disparate basement terranes west of ~98°E (e.g. Tarim from Qaidam/Qilian terranes) to dissection of the North China block (e.g. the same terrane on both sides of the fault) east of ~98°E (Yumen).

Total slip on post-Cretaceous left-lateral faults in the Alxa region may be greater than 150 km based upon the juxtaposition of numerous different Lower Cretaceous sedimentary basins and tentative correlations of basement units across the structures. Based on timing relationships that we have documented on the southern left-lateral faults in the Alxa region, most of this slip occurred prior to the Miocene. Furthermore, the extremely low estimates of Miocene and younger slip documented in our study suggest that large-scale strike-slip faulting within the Alxa region was effectively restricted to the post-Cretaceous, pre-mid-Miocene, supporting the two-phase model of Yue et al. (2003). The results from previous studies on the ATF and our data from the Alxa region are consistent and indicate that pre-mid-Miocene tectonics of northeast Tibet and the Alxa region

were dominated by lateral extrusion of crustal blocks on large-scale strike-slip faults that include the ATF as well as structures within the Alxa block— some of which project in to southern Mongolia. Miocene to Recent tectonics of northeast Tibet and the Alxa region include relatively slow rates of slip on the ATF (Yue et al., 2003; Zhang et al., 2004), crustal shortening and uplift of the northern Plateau in the Qaidam/ Qilian Shan region (Jovilet et al., 2001; George et al., 2001; Yue et al., 2003), transfer of some slip from the ATF to the Haiyuan fault (Tapponnier et al., 2001), and limited left-slip in the Alxa region, which is linked to normal faulting in the eastern Alxa (Yabrai Shan) and formation of the Ordos graben system.

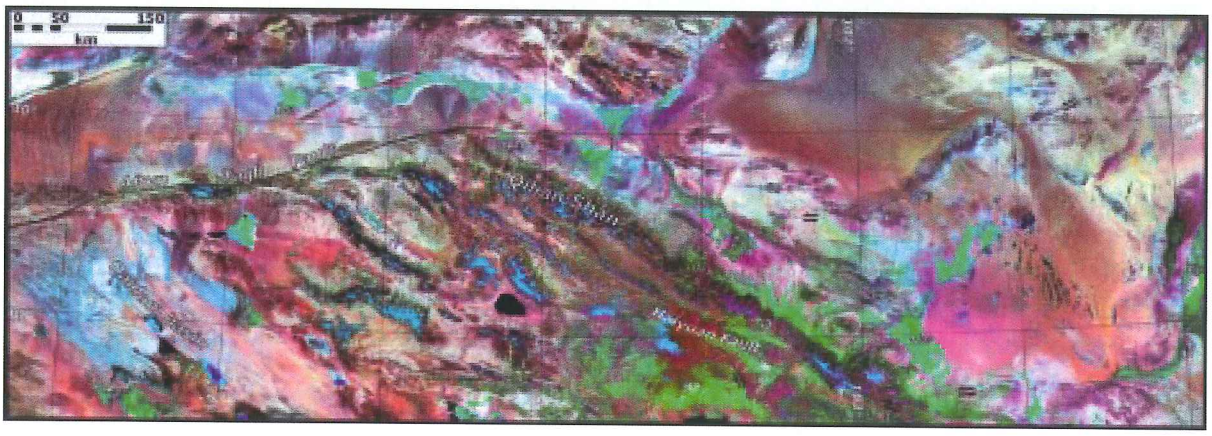

Figure 1: False color composite Landsat TM image of the northern Tibetan Plateau and Alxa region, China. Portions of interpretation from Meyer et al, 1998, and Jovilet et al, 2001. Towns: Bm= Bayan Mod, Dh= Dunhuang, Jc= Jinchang, Ww= Wuwei, Yc= Yinchuan, Ym = Yumen, Yq= Youqi, Zy= Zhangye.

BURCHFIEL B.C., QUIDONG, D., MOLNAR, P., ROYDEN, L., YIPENG, W., PEIZHEN, Z., & WEIQI, Z. 198. *Geology*. **7**. 448-452.

BURCHFIELD, B.C., ZHANG, P., WANG, Y., ZHANG, W., SONG, F., DENG, Q., MOLNAR, P., & ROYDEN, L. 1991. *Tectonics*. **10**. 1091-1110.

GEORGE, A. D., MARCHALLSEA, S. J., WYRWOLL, K. H., CHEN, J., & LU, Y. 2001. *Geology*. **29**. 939-942.

JOHNSON, C.L. 2004. *Basin Research*. **16**. 79-99.

JOLIVET, M., BRUNEL, M., SEWARD, D., XU, Z., YANG, J, ROGER, F., TAPPONNIER, P., MALAVIEILLE, J., ARNAUD, N., & WU, C. 2001. *Tectonophysics*. **343**. 111–134.

MEYER, M., TAPPONNIER, P., BOURJOT, L., METIVIER, F., GAUDEMER, Y., PELTZER, G., GUO, S., & CHEN, Z. 1998. *Geophys. J. Int*. **135**. 1-47.

RITTS, B.D., YUE, Y., & GRAHAM, S.A. 2004. *J. Geol*. **112**. 207-229.

TAPPONNIER, P., XU, Z., ROGER, F., MEYER, B., ARNAUD, N., WITTLINGER, G., & YANG, J. 2001. *Science*. **293**. 1671-1677.

YUE, Y. & LIOU, J.G. 1999. *Geology*. **27**. 227-230.

YUE, Y., RITTS, B.D., & GRAHAM, S.A. 2001. *Int. Geol. Rev*. **43**. 1087-1093.

YUE, Y., RITTS, B.D., GRAHAM, S., WOODEN, J., GEHRELS, G., & ZHANG, Z. 2003. *Earth Planet. Sci. Lett*. **217**. 111-122.

ZHANG, P., SHEN, Z., WANG, M., GAN, W., BÜRGMANN, R, MOLNAR, P., WANG, Q., NIU, Z., SUN, J., WU, J., SUN, H., & YOU, X. 2004. *Geology*. **32**. 809-812.

LESSER HIMALAYAN TERTIARY BEDS OF FAR WEST NEPAL AND THEIR COMPARISON WITH CHAKRATA (SAKNIDHAR) AND RAUTGARA FORMATIONS OF KUMAON, INDIA

Megh Raj DITHAL

Central Department of Geology, Tribhuvan University, Kirtipur, Kathmandu, Nepal
Email: mrdhital@wlink.com.np

Detailed field mapping in Far West Nepal and the adjoining border region of India (Fig. 1) revealed that the red-purple and grey-green sandstone and shale beds of the Rautgara Formation from its type locality near Pancheshwar (Valdiya 1980) continue in the Nepalese territory, and they include lamellibranches and gastropods belonging to the Eocene epoch. The rock succession contains fining-upward fluvial cyclothemes interrupted by intermittent shallow marine deposits.

The Tertiary beds of Far West Nepal are represented by the Chuchura Formation (Fig. 1) made up of red-purple or brown shale interbedded with grey-green sandstone. This formation is sandwiched between the south-dipping North Dandeldhura Thrust (NDT) and the north-dipping Pachkora Thrust. The NDT brings with it schists and gneisses of the Dandeldhura Group and is a continuation of the Almora Thrust sheet in India. On the other hand, the PT brings with it the Patan Formation of slate and quartzite. In this area, the Patan Formation is repeatedly folded and exhibits the features of superposed folding.

Field investigation was also carried out in the Henwal Nadi (near Shivpuri) and Saknidhar (on the Rishikesh–Badrinath Road), where the Chakrata (Saknidhar) Formation is exposed in a window. The detailed traverse and study of sedimentary structures revealed that the rocks are also made up mainly of fining-upward cycles (Fig. 2).

At Saknidhar, the Chakrata (Saknidhar) Formation frequently contains very thick (from 1 to 20 m, and rarely up to 50 m), medium- to very coarse-grained, cross-bedded as well as parallel-laminated, purple and grey-green, mottled sandstone cycles followed by grey-green shale successions. A shale succession is from 3 to 10 m thick. In the sandstone, tiny muscovite flakes are observed. At Saknidhar, large-scale cross-beds (Fig. 3) are also found. The foreset beds contain small ripples. At the bottom of some sandstone beds, 20 to 30 cm wide load casts are also present.

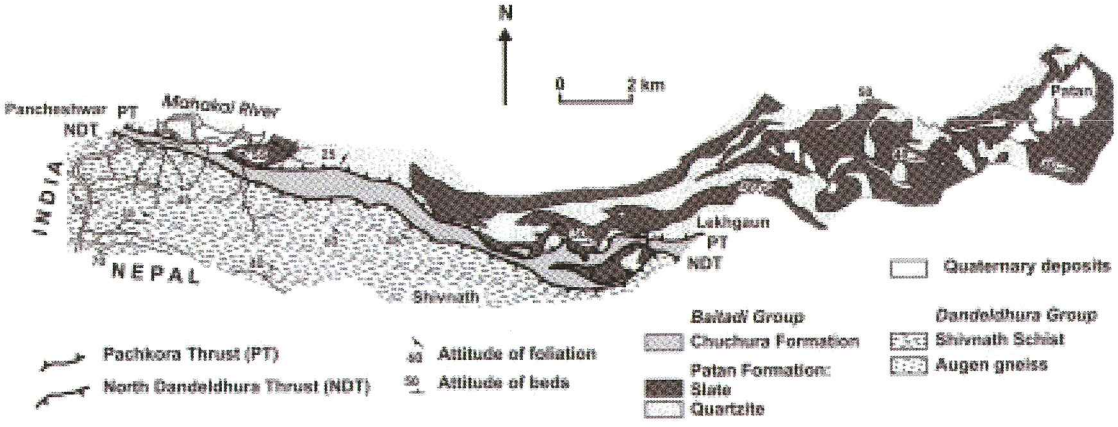

Fig. 1: Geological map of Pancheshwar area in Far West Nepal showing the Tertiary beds of the Chuchura Formation sandwiched between the North Dandeldhura Thrust and the Pachkora Thrust

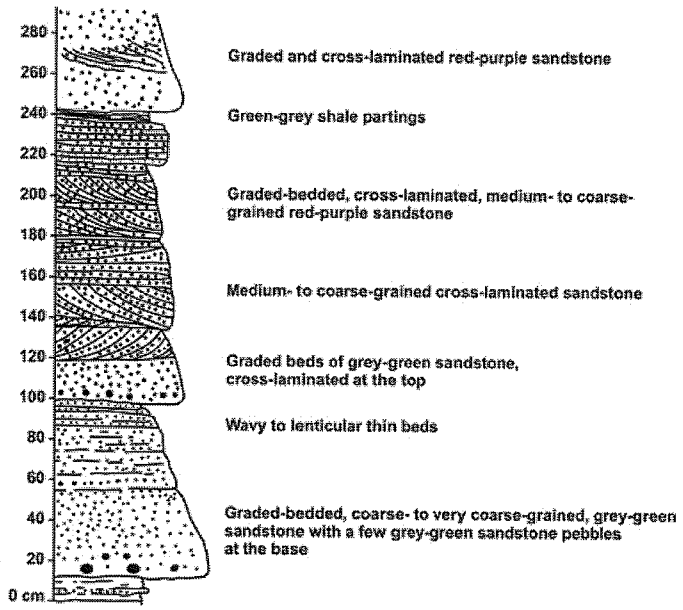

Fig. 2: Graphic log of the sedimentary sequence showing fining-upward cycles with graded bedding, cross-lamination, and parallel laminae at Saknidhar, on the Rishikesh–Badrinath Road, Uttaranchal, India

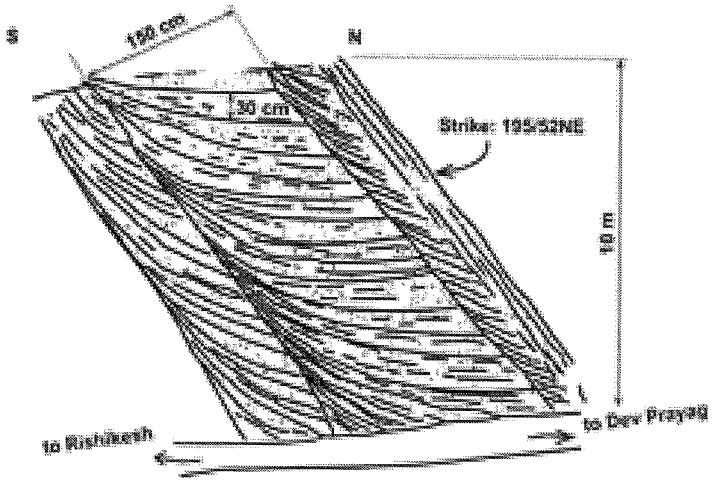

Fig. 3: Sketch of large-scale cross-bedding observed in the Chakrata (Saknidhar) Formation at Saknidhar, on the Rishikesh–Badrinath Road, Uttaranchal, India

All the above sedimentary structures as well as fossils point out to their fluvial and shallow marine environment of deposition. Therefore, there is no evidence of deep marine deposition. Presumably, they are also part of the Lesser Himalayan Tertiary succession, since the identical rocks from the Neelkanth area (east of Rishikesh) have lamellibranches and gastropods and they are mapped as the Eocene Subathu Formation.

Reference

VALDIYA, K. S., 1980. Geology of Kumaon Himalaya, *Wadia Institute of Himalayan Geology, 291 p. (with maps)*

MIXING EVENT BETWEEN THE CRUST AND MANTLE DERIVED MAGMAS: EVIDENCES FROM ZIRCON SURVIDENCES FROM ZIRCON SHRIMP II CHRONOLOGY OF THE CHUSHU PLUTON IN SOUTHERN GANGDESE, TIBET

Guochen DONG[1,2] Xuanxue MO[1,2] Zhidan ZHAO[1,2] Tao CHEN[1] Liangliang WANG[1]

1.China University of Geoscience, Beijing, 100083;
2. Key Lab of Lithospheric Tectonics & Lithoprobing Technology of China University of Geosciences, Beijing, 100083

The Gangdese giant granitoid formed during subduction and collision contains abundant information of geodynamics as a lithoprobe and a window to understand the deep process beneath Tibetan plateau. The granitoid belt extends west to east parallel to the Yarlung Tsangpo suture with 2000 km long by 100 km wide and 110,000 km^2 in area, consisting of mainly diorite, quartz diorite, granodiorite, granite, syenogranite and two-mica granite (Jin & Zhou, 1978; Jin and Xu, 1982). Abundant mafic microgranular enclaves (MMEs) extensively distribute in granitoids of the Gangdese giant magmatic belt, within which the Chushu batholith is the most typical MME-bearing pluton.

The amount and size of MMEs decrease northward away from the Yarlung Tsangpo suture zone. MMEs have igneous texture, rapidly quenched minerals and flow structure, quenched-rims and light color halos showing mass exchange at the contacts between MMEs and its host rocks.Magma mixing are important mechanism of mass-energy exchange between the mantle and the crust and in turn important for accretion of the continental crust and evolution of the lithosphere (Jin and Gao, 1996). Some researches had indicated that the collision was started at about 65Ma, finished at around 45Ma and then transferred to the postcollision stage. Did the intrusions record the exchanging process between mantle and crust during the India-Eurasian continent collision? Key issue to the problem is whether there are obvious mixing between mafic and felsic magmas in the transitional belt of different intrusive rocks. This paper will provide a constraint from geochronology to constrain petrogenesis of MME-bearing granitoids and understand the process.

Based on the detail geological investigation, two sets of magmatic zircons were selected from the samples collected in two outcrops, including granodiorite (host rock), MME and Hb-gabbro in each outcrop to determine their U-Pb ages by SHRIMP II and subsequently Zircon SHRIMP-¢Ú U-Pb dating have been conducted. The analysis results are 50.4°¿1.3Ma, 47.0°¿1.0Ma, 51.2°¿1.1Ma and 49.3°¿1.7Ma, 49.9°¿1.7Ma, 48.9°¿1.1Ma respectively. The data are very similar, indicating the three kinds of rocks formed almost at same time, but did not intrude in separate event in different time. The result exclude the possibility being the refractory solid residue derived from source rock, or xenoliths of host rocks. It chronologically supports that these three kinds of rocks were likely the products of magma mixing in the early-middle Eocene epoch. The composition of granodiorite is close to the acid end member of magma mixing; while the Hb-gabbro is near to the mafic end member and the MME are the incompletely mixed clots of mafic magma while the hot mafic magma was injecting into the relative cold acid magma. It is concluded that partial melting took place and mafic magma formed in the upper mantle of southern Gandese granotoid belt responding to the collision between India-Eurasian continentals in the Eocene epoch (50Ma°¿).

The mafic magma intruded into the bottom of the low crust, resulting in underplating and acid magma forming by partial melting in low crust. Both the crust-derived acid magma and the mantle-derived basic magma mixed and intrude upwards, forming granotoid dominant batholith in southern Gandese, Tibet. The mafic magma underplating and magma mixing may play a key role in crustal accretion of the Gandese and crustal thickening of Tibet.

Key words SHRIMP II age, Granite, Mafic Macro-granular Enclave (MME), Magma-mixing event, Gandese, Chushu pluton

ESTIMATION OF CRUSTAL SHORTENING IN THE HIMALAYA: PROBLEMS AND POSSIBLE SOLUTIONS USING THE MODEL DEFORMATION EXPERIMENTS

Ashok Kumar DUBEY

Wadia Institute of Himalayan Geology 33 General Mahadev singh Road Dehra Dun - 248 001, India

Using the GPS technique, the convergence rates between India and Asia have been obtained from 15 ± 5 mm/yr (Jouane et al., 1999) to 58 ± 4 mm/yr (Bilham et al., 1997). The significantly large variation can be attributed to the fact that the following geological structures, characteristic of the Himalaya, have been ignored in the studies.

1. Development of superposed folds whose hinge lines are oriented in N-S to NE-SW directions indicating maximum compression in E-W to NW-SE directions (i.e. normal to the movement of the Indian plate). These folds occur throughout the Himalayan region.
2. The seismic activities in the region reveal simultaneous development of contrasting geological structures like thrust, normal, and strike-slip faults in the region. For example, the great earthquake of Kangra (4 April 1905, magnitude 8.6 on Richter scale), Uttarkashi earthquakes (20 October, 1991, magnitude 6.5), and Chamoli earthquake (29 March, 1999, magnitude 6.3) show thrust faulting, the concentration of earthquakes in the Leo Pargial area of the Himachal Tethys Himalaya represent normal faulting (Dubey and Bhakuni, 2004), and transverse tectonic zones in the entire Himalayan region and the Karakoram fault suggest strike-slip faulting (Khattri and Tyagi, 1983).

The GPS data have been applied to the entire Himalaya although it is suitable only for the strike-slip faults (i.e. horizontal displacements) because of its inability to accurately measure the vertical displacement. In addition to this, the technique has the following disadvantages.

(i) The model deformation experiments reveal that the true magnitude and direction of the particle movement paths can be determined only by choosing at least two fix points outside the deforming body which is undergoing translation. A single fix point can provide the distance but not the direction of displacement. No such fix points are available and GPS studies are based on location of fix points inside the deforming body.

(ii) The studies are performed over a very short duration of time as compared to the development of natural geological structures.

(iii) The technique ignores folding, and considers the consumption of natural strain by faulting alone.

The results obtained from restoration of cross-sections reveal that the shortening in the Frontal Foothill Belt varies from 22% to 71.33% in different cross-sections. The reasons for the large variation were discussed earlier by Dubey et al. (2001). The present study describes the variation of buckle shortening and layer parallel strain in multilayer profile sections characterized by different fold geometries. Keeping in view of the hard-core geological data, and limitations of the GPS and Balanced cross-section techniques, a model is proposed for the structural evolution of the area. The model can help in prediction of seismicity of the region.

References

BILHAM R., LARSON, K., FREYMULLER, J. and PROJECT IDYLHIM MEMBERS, 1997. *Nature*, **386**, 61-64.

DUBEY, A. K., MISRA, R. AND BHAKUNI, S. S., 2001. *Jour. Asian Earth Sci.*, **19**, 765-775.

DUBEY, A. K.AND BHAKUNI, S. S.., 2004. *Jour. Asian Earth Sci.*, **23**, 427-434.

JOUANNE, F., MUGNIER, J. L., PANDEY M. R., GAMOND, J. F., LE FORT, P., SERRURIER, L., VIGNY, C. AND AVOUAC, J. P., 1999. *Geophysical Research Letters* **26**, 1933-1936.

KHATTRI K. N. AND TYAGI, A. K., 1983. *Tectonophysics,* **96**, 19-29.

LANDSCAPE RESPONSE IN SMALL AND LARGE WATERSHEDS OF CENTRAL NEPAL CONSTRAINED BY THERMOCHRONOLOGY.

M. DUBILLE[1,2], J. LAVÉ[1], R. PIK[2], E. LABRIN[1]

1- LGCA, Grenoble, France.
2- CRPG, Nancy, France

The Nepalese Himalaya present abrupt gradients in precipitation, erosion and deformation. It has been proposed that monsoon precipitation falling on the narrow Himalayan belt, has removed mass and helped to localize deformation since Miocene times through an efficient coupling between tectonic, precipitation and erosion processes. Despite the effective erosion conditions under monsoon climatic setting, the tectonic advection of material is, however, clearly larger than erosional removal (around twice) and leads to a persistent southward migration of the Himalayan arc at a rate of 10-15 mm/yr [Lyon-Caen et Molnar, 1985]. Such migration, associated to the horizontal tectonic advection, is a potential source of disequilibrium in the landscape, in particular between small and large catchments. To document such disequilibrium, we conducted a thermochronological study in a small catchment of Central Nepal, the Mailung valley, a tributary of the Trisuli river, which drains through the MCT zone within the belt of maximum denudation [Lavé and Avouac, 2001]. Dating by several chronometers (FT and (U-Th)/He in apatite, FT in zircons and Ar/Ar in muscovites) provide the opportunity to track the recent evolution of the denudation in this valley compared to adjacent areas drained by larger river networks like the Marsyandi, Buri Gandaki or Trisuli rivers.

The Ar/Ar ages around 5 Myr indicate a Plio-Pleistocene average denudation rate relatively similar to the rates in adjacent large valleys [Catlos et al., 2001] and to the regional large scale patterns. In the lower Mailung valley, the FT ages in apatite and zircons are roughly consistent with the young ages in adjacent large valleys [Burbank et al., 2003, Arita and Ganzawa, 1997]. In contrast, the upper Mailung valley is characterized by cooling ages for the low temperature thermochronometers significantly older than in other larger central Himalayan valleys. In the upper Mailung, the FT ages in apatite range between 1.5 and 3 Myr, and the (U-Th)/He ages in apatite between 1 and 4 Myr, whereas in the Marsyandi valley, the FT ages in apatite reach 0.4-0.5 Myr. Several explanations can be proposed to explain such discrepancy.

Our preliminary results are partly obscured by a poor reproductibility of some data and non-coherent spatial variations that we ascribe to the eventual role of geothermal fluid circulations. For the oldest (U-Th)/He ages, we also strongly suspect analytical bias for the (U-Th)/He ages in apatite. The oldest ages could have been caused by U-Th rich micro-inclusions hidden in apatite crystals (like monazite or zircon) which increased the ^{4}He concentration and calculated ages. Alternatively, such apparent increase in ^{4}He could result from the existence of fluid inclusions containing un-degassed crustal Helium. Both effects are supposed to produce distinct trends in diagrams age/[He] and age/[U], and both trends were identified in different samples.

Our samples were collected at 4000m since Marsyandi's one were coming from 1000 to 2000m elevations. In order to retrieve the potential effect due to the complex interplay between the topography and the isotherms geometry, we have thus performed several numerical simulations using the 3D geothermal modeller PECUBE [Braun, 2002]. A significant part of the discrepancy between the upper Mailung valley and the larger catchments in Central Nepal can indeed be resolved by taking into account the difference in elevation and in isotherms deflexion. However, after corrections, the FT and (U-Th)/He ages are still older than expected by 0.5 to 1 Myr. Such observation would be consistent with the initially envisaged hypothesis that small catchments react and erode slower than large one on the southern flank of the Himalaya. Complementary measurements in Mailung and Buri Gandaki are in progress and new analytic corrections will improve the accuracy of our data and our understanding of the recent evolution of the denudation in the south flank of the Himalayas.

Arita, K., and Y. Ganzawa, Journal of Geography, 106, 156-167, 1997.

Braun, J., *Earth Planet. Sci. Lett.*, 200, 331-343, 2002.

Burbank, D. W., A. E. Blythe, J. Putkonen, B. Pratt-Sitaula, E. Gabet, M. Oskin, A. Barros & T. P. Ojha, *Nature*, 426, 652-655, 2003.

Catlos, E.J. et al., *Journal of Geophysical Research,* 106, 16,177-16,204, 2001.

Lavé J., and J.P. Avouac, *Journal of Geophysical Research,* 106, 26,561-26,592, 2001.

Lyon-Caen, H., and P. Molnar, *Tectonics*, 4, 513-538, 1985.

Note Page

Dong Lung, Dainelli,1934

FROM HIMALAYAN COLLISION TO MAKRAN SUBDUCTION

Nadine ELLOUZ

IFP, dir. Géologie Géochimie, dépt géol. struct., 1-4 Av de bois-préau 92856 Rueil- Malmaison cedex.

A triple junction joins the three Arabian-Eurasian-Indian plates. It is corresponding to the connection between a tectonic accretionary prism (Makran Prism), a transform fault system (Chaman-Ornachnal) along which the northward motion of Indian plate was accommodated and finally, an intra-oceanic transtensional Ridge (Murray Ridge).

The Makran accretionary prism results from the subduction of the Arabian Sea ocean floor beneath the Afghan block microplates now accreted on Eurasian continent. Present-day plate tectonics scheme can be summarised as the evolution of a triple junction between the subduction which has started during Late Cretaceous time, as testified by the initiation of the volcanic arc, after a period of re-organisation and collision of the various micro-blocks with Eurasia.

The trench associated with the subduction was progressively filled by erosion products derived from the relief (mainly the growing Himalayas). Major part of the sediments was transported by the paleo-Indus River and was deposited in the available space (subduction trench, narrow ocean between Afghan and Indian plates). The progressive closure of the space between Afghan and Indian plates, as well as the tectonic involvement of the sediments deposited in the trench, resulted in the migration of the front toward the south and the Southwest, and consequently, the migration of the paleo-Indus delta and fan.

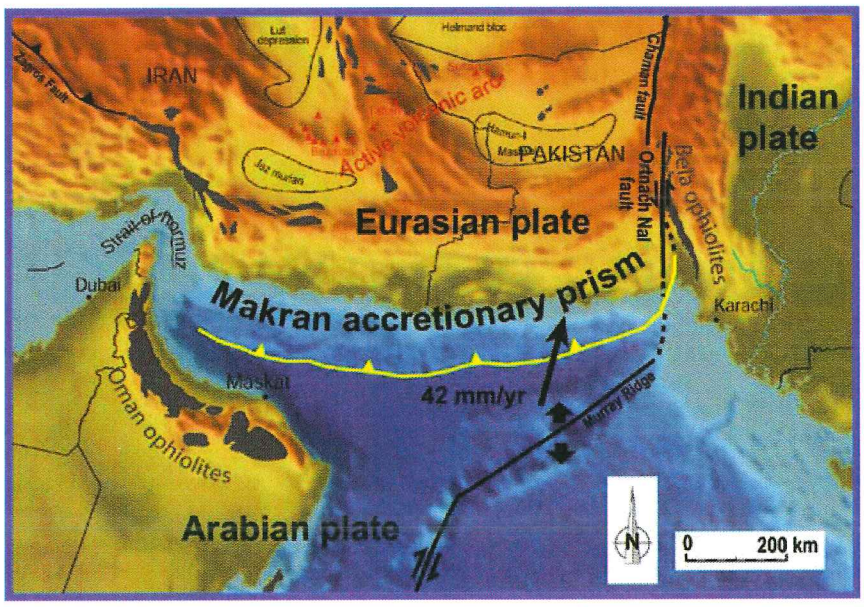

Figure 1: Present-day tectonic plate setting around the Makran accretionary prism

The last step, during the Neogene, relates to the oblique convergence between Afghan and Indian plates, which is accommodated along the left-lateral Chaman-Ornachnal transform zone. During this stage, the Sulaiman and Kirthar ranges developed, inducing the migration of the Indus River farther to the east. At Present, and since Late Miocene time, the Indus delta and fan are located east and south of Karachi, whereas the main offshore sedimentation develops on the Indian Plate, south of a prominent offshore structure, the Murray Ridge. The growing Makran prism itself is located north of the Murray Ridge.

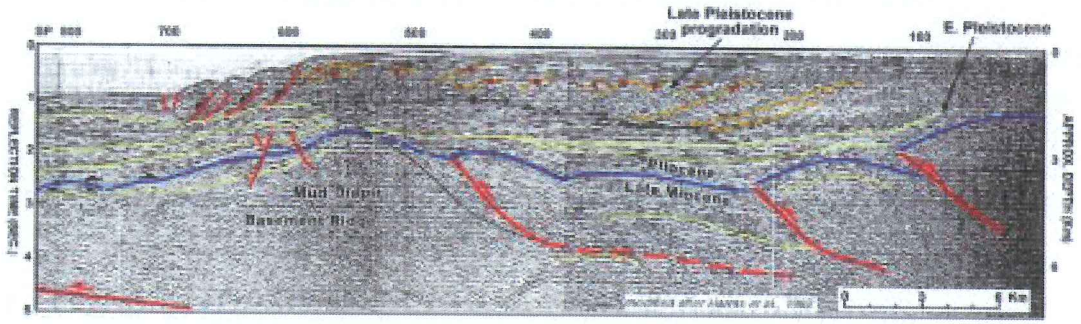

Figure 2: N-S profile south of Gwadar (modified from Harms et al 1992)

The main objectives of our long-term Makran programme, which started with a field trip in 2001, are to study the prism area close to the triple junction of the Makran (Pakistan) through structural and sedimentological analyses, as well as fluid dynamics evaluation. The tectonic evolution and the sedimentary feeding of the prism has been analysed jointly trough time onshore , as well as the consequences of the migration of the Indus paleo-delta since Miocene

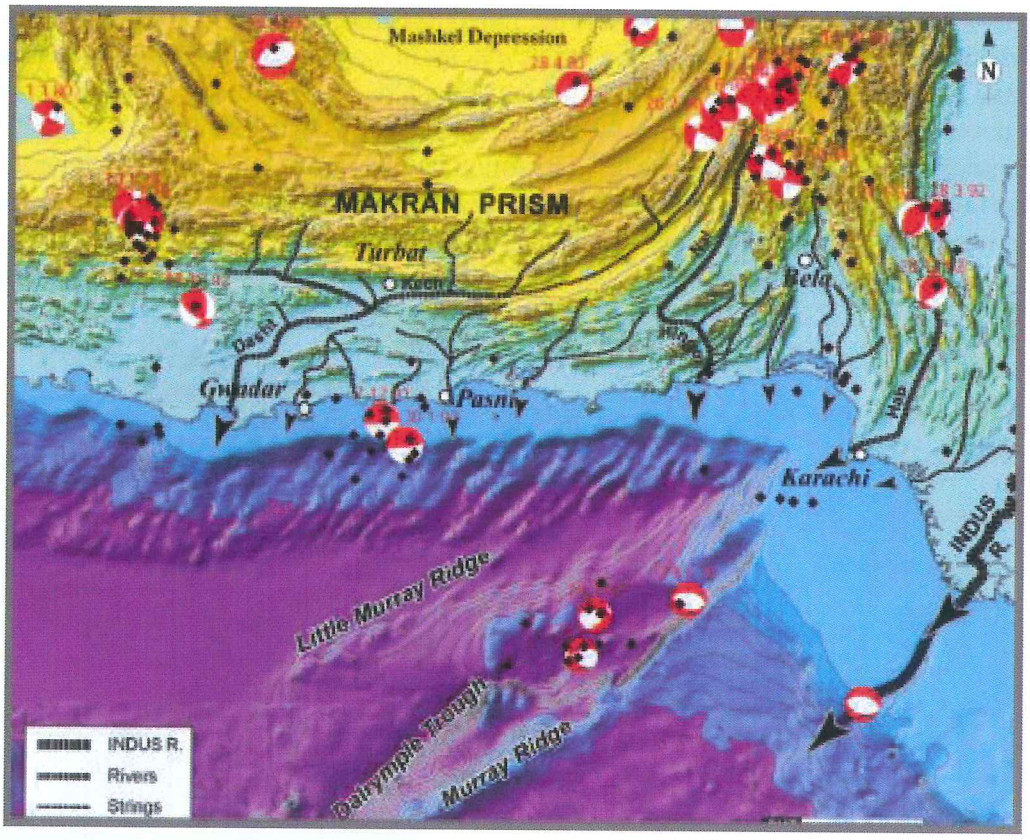

Figure 3: Present-day sedimentary supply of the Makran accretionary prism

During Chamak offshore survey we will focus on the same problematic (described in the next presentation: the CHAMAK survey-offshore frontal part of the Makran prism).

THE CHAMAK SURVEY (PAKISTAN) OFFSHORE FRONTAL PART OF THE MAKRAN PRISM

Nadine ELLOUZ[1], Siegfried LALLEMAND[2], Anne BATTANI[1], Philippe BONING[3], Christophe BURET [4], Raymi CASTILLA[1], Louis CHÉREL[1], Muhammad DANISH[5], Guy DESAUBLIAUX[1], Eric DEVILLE[1], Jérémie FERRAND[1], Alexandra GOURLAN, Syed HASANY[5], Pascale LETURMY[2], Andreas LUGKE[6], Geoffroy MAHIEUX[4], Georges MASCLE(4), Guillemette MÉNOT-COMBES, Nicolas MOUCHOT[4], Peter MUHR[6], Laetitia PICHEVIN[3], Anne-Catherine PIERSON-WICKMANN[8], Philippe ROBION[2], Julien SCHMITZ[1], Aamir HAZHAD[9], Aurélie VANTOER[10], Flavien WAUCHER[1].

[1] IFP, dir. Géologie Géochimie, dépt géol. struct., 1-4 Av de bois-préau 92856 Rueil- Malmaison cedex.
[2] Université de Cergy-Pontoise,
[3] Cerege, UMR 6635, BP 80 Europole de l'Arbois, 13545 Aix-en-Provence cedex
[4] Université de Picardie 33 rue St Leu, 800039 Amiens,
[5] NIO Street 47 block 1, Clifton, Karachi (Pakistan)
[6] BGR Stilleweg 2, 30665 Hannover (Germany)
[7] OSUG, maison des géosciences UMR 5025, BP 53, 38041 Grenoble cedex
[8] Univ. de Rennes1, Geosciences Rennes UMR 6118, av du Gal Leclerc , 35042 Rennes
[9] Pakistany Navy , 11 Liaquat Barracks, Naval Headquarter Karachi (Pakistan)
[10] Univ. de Bordeaux 1, Dept de Géol.&Oceano. UMR 5805, Av des facultés 33405 Talence

Located between the two major collision systems of the Zagros (Iran) and Himalayas (Pakistan-Tibet), the oldest oceanic crust of the Indian ocean is now subducted below the formerly accreted Eurasian blocks. The subduction of this old oceanic crust, composed of the oceanic part of Indian and Arabian plates, probably started close to the Cretaceous-Tertiary boundary as testified by the development of the volcanic arc over Pakistan and Afghanistan borders. The Makran accretionary prism results from the northward motion of the oceanic crust with an average speed of 5cm/year at present. Huge historic seisms, as those registered in 1945, are purely related to compressive focal mechanisms. They are responsible for the emergence of several Islands, linked with the development of mud volcanoes which testifies on the steady overpressure regime imposed at depth.

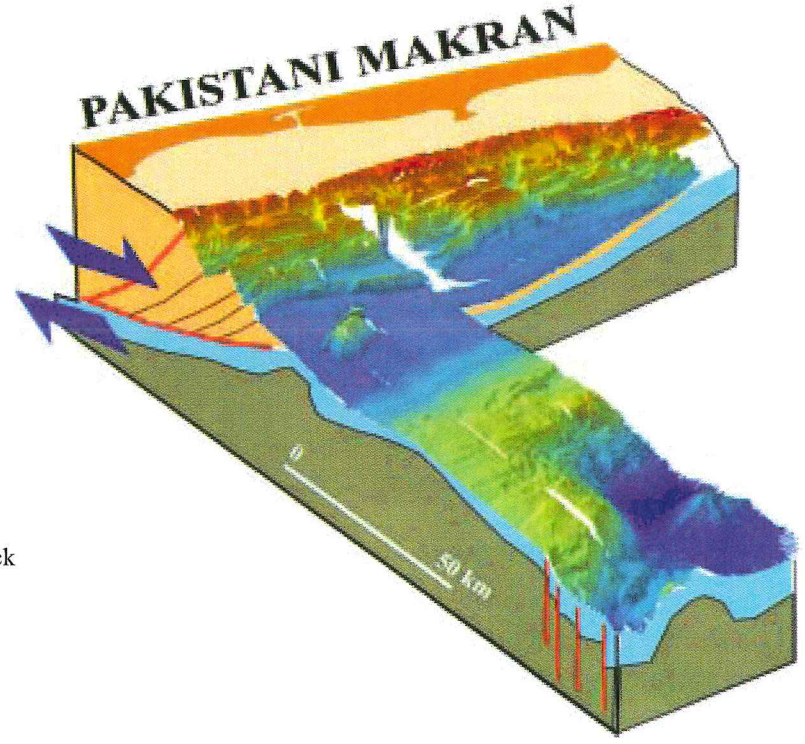

Figure 1: 3D simplified Block of CHAMAK area of acquisition

CHAMAK campaign took place in September October 2004 on the offshore frontal part of the Makran prism in Pakistani waters. The zone covered with bathymetry, seismic acquisitions and coring operations is located between 62°30 E - 65°30^{E} et 23° N et 25°N (Figure 1). Our specific interest on the Makran prism was driven by the following facts: 1) two thirds of the are emerged at present, allowing a detailed structural study onshore, 2) the frontal part is located offshore, where the most recent processes can be analysed, and seems to be more or less linear as far as it joins the transform fault systems 3) the sedimentary rates are varying along strike, due to a change in the location of the sediment supply source - i.e. Indus (draining Himalayan erosion products), or sediment directly produced from erosion of the prism itself, and 4) numerous fluid and gas seepages are described outlining the Pressure and fluid dynamics linked to the horizontal deformation combined with high sedimentary rates.

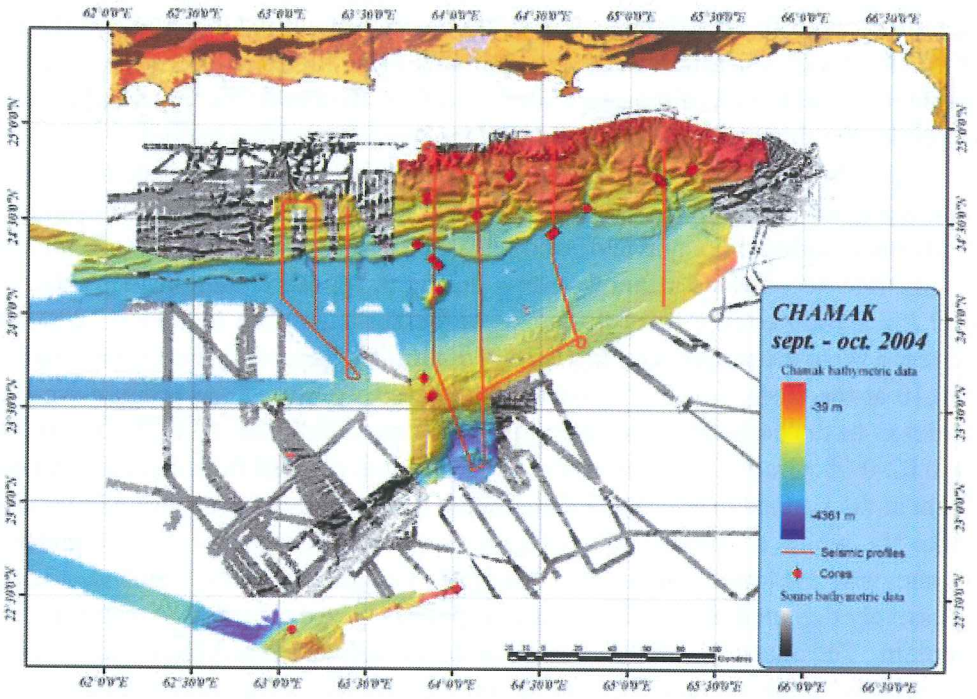

Figure 2: CHAMAK location map of the main acquisitions, bathymetry, seismic profiles and cores

The main objectives are to study an area close to the triple junction of the Makran (Pakistan) through structural and sedimentological analyses, as well as fluid dynamics evaluation. The tectonic evolution and the sedimentary feeding of the prism will be analysed jointly trough time, as well as the consequences of the migration of the Indus paleo-delta since Miocene time. During the CHAMAK survey, a detailed bathymetric map covering 650000Km2 have been picked up (figure 2). For documentation of the recent sedimentation, 27 long cores have been collected, half of them have been recovered by the Calypso giant coring system, privileged tool of the N/O MARION DUFRESNE (IPEV). In order to collected in bottom P/T conditions, the pressure coring system of the BGR, called «Goldorak» has been used 3 times, and we recovered one core at 122b. Gas and waters have been systematically sampled in the cores were necessary.

The results coming out of CHAMAK 1 allow to obtain a good definition and image of the morphology and the 3D geometry of the submerged part of the prism, for the moment poorly documented. The data acquired have been mixed with the Sonne data acquired in 1998 by Geomar and BGR. From seismic data the structural style as well as chronology of the deformation will be analysed . The 27 long cores will provide matter for sedimentology and petrography studies, as well as geochemistry study, comprising organic matter, gas and water analyses.

MODERN FLUX OF EROSION OF THE GANGA BASIN FROM GEOCHEMICAL BUDGET

Christian FRANCE-LANORD (1), Albert GALY(2),
Valier GALY (1), Sunil K. SINGH (3)

(1) Centre de Recherches Pétrographiques et Géochimiques, CNRS, BP 20 54501 Vandoeuvre les Nancy, France - cfl@crpg.cnrs-nancy.fr
(2) Dep. of Earth Sc., University of Cambridge, UK
(3) Physical Research Laboratory, Ahmadabad India

Modern Himalayan erosion fluxes can be approximated from the fluxes carried by rivers draining the Himalaya. Measurements on rivers in Bangladesh provide data on dissolved and particulate fluxes. Both Brahmaputra and Ganga carry suspended particles fluxes that are around 400-500 million tons per year (Mt/yr). Associated dissolved fluxes reach about 40 Mt/yr for each river. The total flux is above 1000 Mt/yr and represents a minimum value, as those measurements do not take into account the floodplain sequestration and the bedload transport. Galy and France-Lanord (2001) used a geochemical budget to approach these fluxes and proposed that they should be approximately equal to that of the suspended load flux. However, the low number of suspended sediment samples for this study seriously limited the precision of this budget.

Here we present new data on river sediments of the Ganga in Bangladesh and in the Gangetic plain that allow a much more reliable assessment of the suspended sediment composition. Sampling has been performed during monsoon periods of 2001, 02 and 04. Sampling includes depth profiling in order to take into account the mineral sorting during transport. Depth profiles show systematic trends: Al_2O_3/SiO_2 ratio evolve from 0.25-0.35 at the surface down to 0.15-0.27 at 10 m depth mainly as a response to the progressive increase of quartz. To the reverse, Fe_2O_3/SiO_2 ratios decrease from 0.08-0.10 at the surface to 0.05-0.08 at depth as a response to the progressive depletion in clays and micas. In the bedload, these ratios are much more extreme: Al_2O_3/SiO_2 = 0.10-0.18 and Fe_2O_3/SiO_2 0.02-0.05. Grain size distribution also evolves in parallel from an unimodal distribution around 20 µm at the surface to a bimodal distribution with a second mode around 200 µm at depth. Elements like Na, which is controlled by plagioclase, and Ca controlled by carbonates do no not show any systematic evolution with depth. Along the Ganga course, the suspended sediments are more progressively depleted in SiO_2 likely as a response to the deposition of quartz rich sediments in the floodplain. The data show that in Bangladesh, the suspended sediments are clearly enriched in Al and Fe relative to the average Himalayan sources. Using a simple geochemical mass balance and assuming steady state erosion of the Himalayan basin, these data imply that the fluxes of bedload transport and floodplain sequestration do represent 50 to 70 % of the suspended load fluxes. This result confirms our preliminary budget and suggests that the Himalayan range drained by the Ganga delivers an erosion flux above 1100 Mt/yr.

Such budget is based on measurements realised over a short period and it is important to question it's representativeness with respect to time. In particular, short-term climatic variability such as glacial-inter-glacial periods should affect the distribution and flux of erosion. Geochemical budget also allow to test the steady state of erosion between chemical and physical erosion. Modern flux of dissolved Na or K, combined with weathering state of sediments, allow to calculate a steady state particulate flux. Such calculation yield sediment fluxes that are twice lower than sediment fluxes measured on the Ganga. This indicates that the steady state hypothesis is not valid between chemical and physical erosion at present. Modern physical fluxes are to high relative to dissolved fluxes. This discrepancy may derive from different factors : (1) modern particle flux is overestimated which is at odd with our budget; (2) dissolved fluxes could be higher during complementary periods such as climatic optimum; (3) the present period favours soil erosion relative to unaltered bedrock which could results from recent deforestation.

A. GALY AND C. FRANCE-LANORD, *Geology* **29**, 23-26, 2001

THE TRIASSIC IN THE KARAKORUM RANGE (PAKISTAN).

Maurizio GAETANI

Dipartimento di Scienze della Terra " A: Desio"
Università degli Studi di Milano, Italia

Rocks of Triassic rocks crops out extensively in the "geological" Karakorum Range over a belt of more than 300 km. They are deformed by regional metamorphism in the Southern/Intermediate metasedimentary belts where only massive dolostones bearing Megalodontids may confidently related to the Triassic. In the Northern Karakorum instead, differentiated environments can be recognized. To the west, from Chitral to the valley of Chillinji, the whole Triassic is represented by shallow water carbonates, often dolomitized, with peritidal cyclic sedimentation. The lowermost part of the Triassic delivered conodonts of Induan age (Perri et al. 2004). Indurate surfaces and karst fillings suggest temporary emersions within a total thickness of the Triassic not exceeding 300 m. At its top, massive packstones packed with *Lithiotis*-like bivalves, indicates the Lower Jurassic.

To the east instead, from the Chapursan and Hunza valleys, the onsetting of the Triassic occurs in deeper water. The area down-warped already in the Permian and the Permian-Triassic boundary occurs in dark-grey marls and slates with occasional mudstone, suggesting a deep, poorly oxygenated environment (Gaetani et al. 1995). A reappraisal of the Wirokhun section with A. Nicora. S. Cirilli and V. Atudorei, allows to fix the P/T boundary with the appearance of a rich pollen assemblage, followed by a conodont assemblage including *H. parvus*. Further conodont levels testifies to the Induan, while gradually carbonate sedimentation recovers to a cyclic dark grey mudstone/marls succession. Also the δC^{13} shift typical for the P/T interval is recorded. The deep water facies continues up to the Ladinian with *Daonella indica* beds. The overlying layers gradually pass to massive carbonates of shallow water with megalodontids, suggesting the Late Triassic.
In the Karakorum Range is recorded the Peri-Gondwana fringe evolution, with the break-up and spreading of the sea-ways between the terranes. There is evidence of block-faulting with emersions and lateral deep waters settings during the Permian and Middle Triassic. The final resumption to shallow conditions testifies instead the approaching to the docking with the Asian margin, resulting in the Eo-Cimmerian (Indosinian) orogeny.

References.

Gaetani M., Angiolini L., Garzanti E., Jadoul F., Leven E. Y., Nicora A., Sciunnach D. (1995)- Permian stratigraphy in the Northern Karakorum, Pakistan. *Riv. It. Pal. Strat.*, 10: 112- 158.

Perri C., Talent J.A., Mawson R. (2004) - Earliest Triassic conodonts from Chitral, Northernmost Pakistan. *Riv. It. Pal. Strat.*, 110:

CONTRASTS IN TEMPERATURE AND HYDRATION OF THE DEEP CRUST ACROSS PRESENT TIBET, AND ECLOGITIZATION (?) OF LOWER CRUSTAL MATERIAL

Audrey GALVE (1), Alfred HIRN (1), Martine SAPIN (1), JIANG Mei (2), Mireille LAIGLE(1), Béatrice DE VOOGD (4), Josep GALLART (3)

(1) Sismologie Expérimentale, UMR 7580 Dpt Sismologie, Institut de Physique du Globe de Paris, 4 place Jussieu 75252 Paris Cedex 05, France
(2) Chinese Academy of Geological Sciences, Baiwanzhuang road, 100037 Beijing, China
(3) Institute of Earth Sciences Jaume Almera, calle Lluis Sole I Sabaris, 08028 Barcelona, Spain
(4) Dept. Sciences de la Terre, Université de Pau, 64000 Pau, France

P and S velocity and attenuation estimates in the lower half of the crust are obtained from a set of wide angle reflection-refraction profiles (Galvé et al., 2002a) in the region of active tectonics at the NE edge of the Tibetan Plateau and discussed together with respect to similar data at its Himalaya-south Tibet edge (Hirn et al., 1984). The quality factor is estimated in the lower half of the crust by accounting for the differential effect on amplitude-frequency observed between waves of different penetrations, and both in P and S modes. Attenuation values allow to exclude a significant proportion of partial melt and to estimate the homologous temperature, ratio of in-situ to solidus absolute temperature. The latter depends on the physical conditions being of dry, wet or dehydration melting, which are found different among the regions, since their in-situ temperatures differ also as estimated from their different Vp for a similar felsic composition.

The material presently in the thickened crust, even its lower part has a felsic composition, upper to middle crustal lithology, and the temperature conditions estimated suggest that basic material that could have underlain it could be eclogitized and does not appear above the seismic Moho, as proposed for Himalayas-South Tibet (Sapin and Hirn, 1997).

Under northern Qang Tang, the felsic material in the lower half of the crust appears as hot and dry, consistently with other evidence (Hacker et al., 2000). Its burial may have occurred earlier or may have been moderate in the postcollisional phase. This is consistent with a model of indentation of the Qang Tang crust by an originally thinner Bayan Har crust to bring part of its crust to greater depth, suggested from imaging the crustal architecture.

Under northern Bayan Har, the material in the lower half of the crust appears as felsic, at low temperature and not dry conditions. This is evidence that it has been transported from a shallower depth, and this recently enough not to be yet dehydrated and temperature equilibrated in a conductive geotherm. It supports a model of recent overriding of the middle crust of the north Kun Lun block to the north independently suggested from the image of crustal architecture.

Himalaya-south Tibet appears bracketed by these two cases in northern Tibet for Vp and temperature conditions, but shows highest attenuation in the lower crust, that is colder but less dry than under northern Qang Tang.

The uncommon joint determination of several parameters: Vp, Vp/Vs, Qp and Qs reveals the composition, the mineralogy and hydration conditions of the lower half of the thickened crust of Tibet and supports the thickening of the Tibetan crust by tectonic superposition, imbrication of originally normal thickness crusts.

A model of lithospheric scale deformation is suggested by Hirn et al. (1984, and this meeting). The interpretations suggested for the position of the interpolate boundary of total subduction under the Himalayas and for the nature of the material above it and beneath the shallowest seismic Moho provide a new framework to discuss the debated interpretation of the deep earthquakes specific of Tibet.

They occur just north of the High Himalayas and north of the Indus-Tsangpo suture at 80-90 km depth, precisely on the transect which section we documented with a Moho significantly shallower from both receiver-functions (Galvé et al., 2002b) and explosion seismology.
The latter documented in addition that in the Tethyan Himalayas only material with upper crustal, felsic lithology is present above the 70 km deep shallowest Moho (Hirn et al., 1984) and this and deeper segments may indeed correspond in places to the top of lower crustal material in course of eclogitization from basic granulites that are metastable since the eclogite-stability field reaches even far shallower for such composition (Sapin and Hirn, 1997). Downdragging of crust or altered uppermost mantle in this imbrication zone provide just the kind of material and conditions that are now considered to produce the intermediate-depth seismicity of oceanic subductions, which sources are caused by dehydration embrittlement. This may give some alternative to considering the occurrence of earthquakes as the measure that the material in which they occur has high strength, which is pursued as the opposing views that the upper mantle is strong and lower crust weak in Tibet and as a general rheological model (Molnar and Chen, 1984; Chen and Yang, 2004), or instead that the lower crust is strong in Himalayas-Tibet, though only the upper crust has strength in a general rheological model (Jackson, 2002).

(REFERENCES)

CHEN W.-P & YANG Z. H. 2004. *Science*, **304**. 1949-1952.
GALVE A., HIRN A., JIANG M., GALLART J., DE VOOGD B., LEPINE J.-C., DIAZ J., WANG Y. & QIAN H. 2002a. *Earth Planet. Sci. Lett.*, **203**. 35-43.
GALVE A., SAPIN M., HIRN A., DIAZ J., LEPINE J.-C., LAIGLE M., GALLART J. & JIANG M., 2002b. *Geophys. Res. Lett.*, **29** (24). 2182. doi:10.1029/2002GL015611.
HACKER B. R., GNOS E., RATSCHBACHER L., GROVE M., Mc WILLIAMS M., SOBOLEV S. V., JIANG W. & WU Z. 2000. *Science*, **287**. 2463-2466.
HIRN A., LEPINE J.C., JOBERT G., SAPIN M., WITTLINGER G., XU Z.X., GAO E.Y., WANG X.J., TENG J.W., XIONG S. B., PANDEY M. R. & TATER J. M. 1984. *Nature*, **307**. 23-25.
JACKSON J. 2002. *GSA Today*, **12**(9). 4-9.
MOLNAR P. & CHEN W.-P. 1983. *J. Geophys. Res.*, **88**. 1180-1196.
SAPIN M. & HIRN A. 1997, *Tectonophys.*, **273**. 1-16.

LITHOSPHERIC STRUCTURE OF THE SONGPAN BLOCK IN THE NORTHEASTERN TIBETAN PLATEAU— REVELATION FROM INVESTIGATION OF THE DEEP SEISMIC PROFILE

GAO Rui (1) MA Yongsheng (2) ZHU Xuan (2) LI Qiusheng (1) LI Zhongyuan (2) ZENG Tianfa (2) LI Pengwu (1) WANG Haiyan (1) ZHU Haihua (1) ZENG Hongwei (1)

(1) Institute of Geology, Chinese Academy of Geological Sciences, Beijing 100037, China.
(2) Southern Exploration & Production Company, China Petroleum & Chemical Corporation, Kunming 650021, China.

Songpan block is located in the northeast of Tibetan plateau among the Qiangtang terrane, the East Kunlun-West Qinling orogen belts and Longmenshan orogen belts. Its outline is very like a reverse triangular tectonic element. It belongs to a part of the Songpan-Ganzi-Hoh Xil terrane (An Yin et al., 2000).

As the eastern part of Tibetan plateau, Songpan block lithosphere structures and changes record the dynamic information of plateau eastward (include northeast) evolution. The contact relationship with the margin orogen belt responses the plateau tectonic process of developing outward and turning to margin craton basin. P. Molnar£®1989£©ever considered that the northeast Tibet expanding outward through thicken crust is the important way of Tibetan uplift.

The average altitude of Songpan block is 3500 meter. Its surface is covered with Trias flysch sedimentary formation broadly, and makes it difficult to study the crust of basement and under basement. Because of its special geology structure and abominable environment, such as jokul, meadow, swamp, and so on, Songpan block's lithospere structure ,tectonic property ,and the role played in the continent evolution are always mysteries, and attract Chinese and foreign learner to research.

Huang (1962) and Ren (1980) presumed its basement is old lump. Sengör£®1984£©considered Songpan block lose continental basement, and flysch sedimentary formation deposited at subduct oceanic crust directly. Burchfield£®1995£©proposed Songpan basement is a part of the South China continent, Triassic strata conformably overlie Paleozoic shallow marine sequences of South China. An Yin£®2000£©supported Burchfield's opinion of continental basement, and pointed that Songpan is a remains oceanic basin directly overlay the crustal basin of South China continent. Summarizing, it is difficult to deduce Songpang block basin's property only by sporadic exposed geology body in the surface.

With together staked by National Natural Science Foundation of China (NSFC) and China Petrochemical Corporation (SINOPEC), we have surveyed a deep seismic profile across northern boundary of Songpan Terrane and the whole of Western Qinling orogen belts from autumn to winter 2004. The profile was 254 km long, from north and south, starting from Hezuo City Gansu Province located in the northern boundary of Western Qinling orogen belts, crossing the whole of the orogen belts, and then entering Ruoergai basin£¨ finally ending Tangke Country in Sichuan Province which locates in the southern boundary of the Basin. We call the profile as Hezuo-Tangke (HT) Profile in brief.

The HT deep seismic profile is a common-midpoint(CMP) stacked section acquired with explosive source using SN 388 24-places seismograph, 480 receiver-groups, 50 m receiver-group spacing, 30 s listening time and 2 millisecond samplings. In order to collect subface information of high resolution, we have taken three kinds of explosive energy. The first seismic source consisted of 16-kg seismic charges in boreholes 20 m deep and at intervals of 100 m and 120-fold.

The second source consisted of 48-kg charges, using the combined well with the depth of 20m and 400m intervals and 30-fold. With the first and second seismic source, we have used a middle-exploding array, 480-channel geophone group interval of 50 m and 175 m migration space. As the third 200-kilogram explosive, the single well in the depth of 50m, 3 well combined, and 5km interval, the maximum migrated space is 29175km. Two sets of seismic data processing systems, GRISYS and PROMAX, were used to monitor the collected data in the work-site. One explosive record map was done to monitor signal-to-noise ratio. After the preliminary processing of data collected every day, a preliminary stacked profile would be done to direct the collection work of the next day. Thus, good quality of data collection was ensured.

The preliminary processing deep seismic reflection time profile drawn at the large scale reveals the reflection wave image of the fine mantle top and crustal structure of the Songpan block and the whole of Western Qinling orogen belts. The mainly character of the seismic reflection time profile were obtained by multi-group strong and near level reflections. The most evident feature in the seismic profile is the multi-group strong reflections occur in 7.0s that divided the up and lower crust. Another most evident feature is a set of layer-like reflections with intensity, close multiphase, continuously traceable seismic reflections phase occur in 17s-18.5s, which indicated that the Moho depth of the northern West Qinling and Songpan block is about 51-56 km.

(References)

An Yin and T. Mark Harrison, *Annu. Rev. Earth Planet. Sci.,* 2000, 28, 211-80.
Burchfiel, BC, Chen Zhiliang, Liu Yuping Royden LH, *Int. Geol. Rev.*, 1995,37, 661-735.
Molnar P, Lyon-Caen H, *Geophys. J. Int.*, 1989,99,123-153.
Sengor AMC, *Geol. Soc. Am. Spedcial Paper* 195, 1984, 1-82.

FOCUSED EROSION AT HIMALAYAN SYNTAXES AS DOCUMENTED BY THE COMPOSITION OF INDUS AND BRAHMAPUTRA RIVER SANDS

Eduardo GARZANTI (1), Giovanni VEZZOLI (1), Sergio ANDÒ (1), Christian FRANCE-LANORD (2), Peter CLIFT (3), Gavin FOSTER (4), Paolo PAPARELLA (1), and Sunil SINGH (5)

(1) Dipartimento di Scienze Geologiche e Geotecnologie, Università di Milano-Bicocca, 20126 Milano, Italy.
(2) CENTRE DE RECHERCHE PÉTROLOGIQUE ET GÉOCHIMIQUE, CNRS, 54501 VANDOEUVRE-LES-NANCY, FRANCE.
(3) Department of Geology and Petroleum Geology, University of Aberdeen, AB24 3UE, UK.
(4) Department of Earth Sciences,University of Bristol, Queens Road, Bristol BS8 1RJ, UK.
(5) Physical Research Laboratory, Navrangpura, Ahmedabad 380 009, India.

Even in presence of uniform convergence and steady-state input of crustal material into the thrust belt, erosion rates are far from homogeneous over the Himalayan orogen (Galy and France-Lanord 2001; Finlayson et al. 2002). The focused spatial distribution of detrital production and the association between major-river drainage and crustal-scale folds, where rapid exhumation takes place within tectonic windows and half-windows, have suggested the existence of positive feedback between erosion and tectonic uplift in various parts of the Himalayas (Zeitler et al. 2001; Vannay et al. 2004). The most spectacular examples occur at the eastern and western Himalayan syntaxes, where the Tsangpo and Indus Rivers leave the elevated Tibetan Plateau in the rain shadow of the Himalaya, to turn sharply south and cut impressive gorges transverse to the structural grain of young metamorphic massifs. Here up to granulite- facies rocks or anatectic granites of Plio-Pleistocene age are exposed, indicating exhumation rates in excess of 3 mm/yr (Burg et al. 1998; Rolland et al. 2001)

The quartzofeldspathic bulk petrography and hornblende-dominated heavy-mineral-rich suites of modern Indus and Brahmaputra River sands (Garzanti et al. 2004; 2005), as well as their geochemical and isotopic features (Clift et al. 2002; Singh and France-Lanord 2002; Singh et al. 2003), chiefly reflect regional unroofing of amphibolite-facies mid-crustal rocks at the two Himalayan syntaxes, and only subordinately contributions from active-margin batholiths in the Mishmi Hills, South Tibet, and Kohistan. Such compositional fingerprints, unique with respect to all other Himalayan rivers, are the sedimentary expression of "tectonic aneurysm" (Zeitler et al. 2001).

From detrital modes to denudation rates

High-resolution bulk-petrography coupled with heavy-mineral analyses of modern sands represent an effective low-tech way to obtain a complete set of compositional information on the sediments of a river system. The relative contribution from each single source of detritus to the total sediment budget can next be quantified by forward mixing calculations. This simple mathematical tool allows us to partition the total sediment flux of one big river system and to obtain estimates of sediment yield and average denudation rate from various subcatchments. This method provides an independent key to trace and quantify patterns of erosion in mountain belts, to constrain denudation rates obtained from temperature-time histories of exposed bedrock, and to better understand the complex dynamic feedback between surface processes and crustal-scale tectonics.

Focused erosion around the Eastern Syntaxis

Sediment composition changes drastically around the eastern Himalayan syntaxis, from the lithic Tsangpo sand in South Tibet to the quartzofeldspathic Siang sand in Arunachal Pradesh, indicating overwhelming detrital supply from the Namche Barwa Massif. Instead, compositional changes of Brahmaputra River sand across Assam are minor, indicating only subordinate supply from several major Himalayan tributaries.

Unmixing calculations based on an integrated petrographic, mineralogical and geochemical data set consistently indicate that the syntaxis, representing only ~ 4% of total basin area, contributes 40 ± 5% to the total Brahmaputra sediment flux, and > 20% of total sediments reaching the Bay of Bengal.

Given a total Brahmaputra load of 780 ± 370 10^6 t /yr (Islam et al. 1999), our data imply that focused erosion of the eastern Himalayan syntaxis alone produces a sediment flux of 275 ± 130 10^6 t /yr, corresponding to a sediment yield of 10,200 ± 5000 t/km^2 yr, and denudation rates of 3.6±1.7 mm/yr. These figures are fully consistent with exhumation rates of 4 ± 1 mm/yr since 2.2 Ma for the Namche Barwa Massif, calculated from thermochronological data on exposed bedrock (Burg et al. 1998). Four-to-five-times-lower average sediment yields are calculated for Himalayan regions to the west, pointing to incomparably faster erosion in the syntaxis than in the rest of the range.

Focused erosion around the Western Syntaxis

Similar compositional trends are displayed along the Indus River. Indus sands in Ladakh have detrital modes and heavy mineral suites very similar to Tsangpo sands, but composition changes repeatedly and markedly across Baltistan, indicating overwhelming sediment flux from each successive tributary as the western syntaxis is approached.

Given a load of 250 ± 50 10^6 t/yr of sediments reaching the Tarbela reservoir (Rehman et al. 1997), unmixing calculations based on petrographic, mineralogical, and geochemical data indicate that focused erosion of the western Himalayan syntaxis produces a sediment flux of 140 ± 30 10^6 t /yr, corresponding to extreme yields and erosion rates for both the South Karakorum Belt (up to 12,500 ± 4700 t/km^2 yr and 4.5 ± 1.7 mm/yr for the Braldu catchment) and the Nanga Parbat Massif (8100 ± 3500 t/km^2 yr and 3.0 ± 1.3 mm/yr).

These figures match the lower end of the range of denudation rates calculated from temperature-time histories of bedrock exposed in the Nanga Parbat (3 - 5 mm/yr; Whittington 1996; Zeitler et al. 2001) and South Karakorum crustal-scale domes (5 - 6 mm/yr; Rolland et al. 2001). Estimated sediment yields and erosion rates decrease exponentially eastward, northward, and westward away from the sharp peak recorded in the syntaxis region. In the same directions fission-track ages show a parallel, exponential increase, reflecting exponentially decreasing exhumation rates (Zeitler 1985).

Summary

Integrated petrographical-mineralogical-geochemical data sets on modern Indus and Brahmaputra river sediments indicate that exhumation and erosion are much faster in the western and eastern syntaxes than anywhere else in the Himalayan range. Sediment yields estimated from unmixing calculations correspond remarkably well with exhumation rates calculated from thermochronological data of exposed bedrock..

The major impact of focused glacial and fluvial erosion of young metamorphic massifs on sediment budgets of big Himalayan rivers confirms that positive feedback between endogenetic tectonic forces and exogenetic erosional agents plays a critical role in shaping the evolution of collision orogens and associated sedimentary basins.

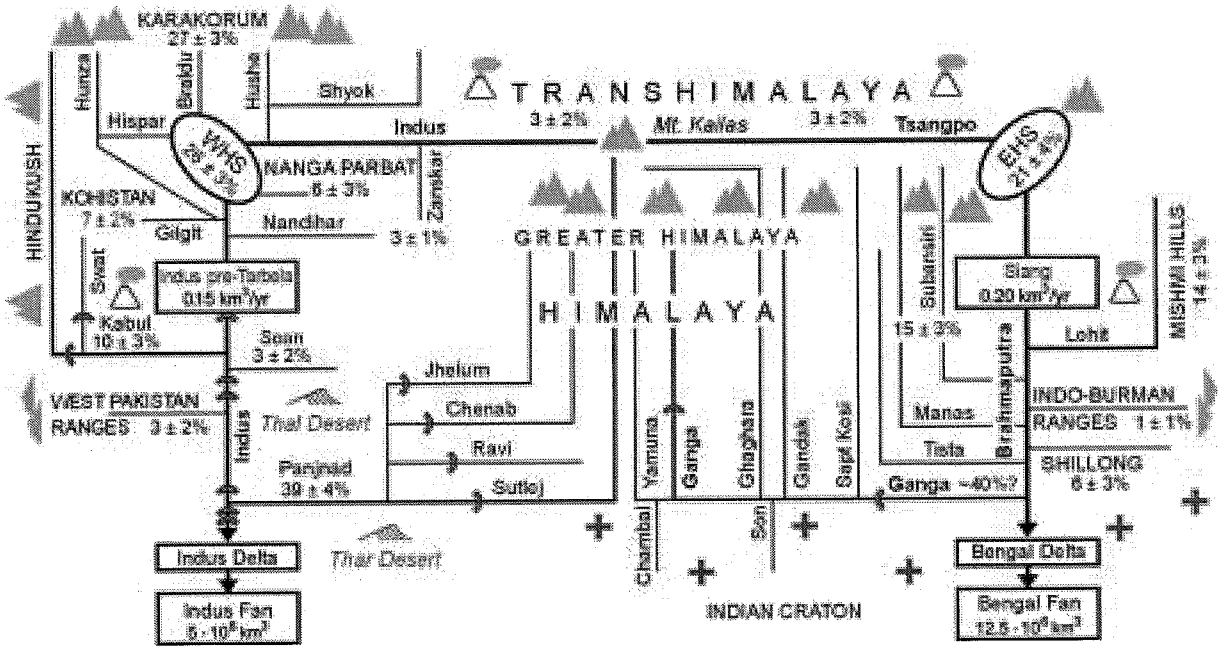

Fig. 1 – Quasi-symmetrical model and rough preliminary budget for Himalayan erosion and fluvial sediment transport. The incidence of the Ganga yield to the Bengal Fan is particularly poorly constrained.

Cited References

BURG J.-P., NIEVERGELT P., OBERLI F., SEWARD D., DAVY P., MAURIN J.-C., DIAO Z. & MEIER M. 1998. J. *Asian Earth Sci.*, **16**, 239-252.

CLIFT P.D., LEE J.I., HILDEBRAND P., SHIMIZU N., LAYNE G.D., BLUSZTAJN J., BLUM J.D., GARZANTI E. & KHAN A.A. 2002. *Earth Planet. Sci. Lett.*, **200**, 91-106.

FINLAYSON D.P., MONTGOMERY D.R. & HALLET B. 2002. *Geology,* **30**, 219-222.

GALY A. & FRANCE-LANORD C. 2001. *Geolog,* **29**, 23-26.

GARZANTI E., VEZZOLI G., ANDÒ S., FRANCE-LANORD C., SINGH S.K. & FOSTER G. 2004. *Earth Planet. Sci. Lett.*, **220**, 157-174.

GARZANTI E., VEZZOLI G., ANDÒ S., PAPARELLA P. & CLIFT P.D. 2005. *Earth Planet. Sci. Lett.*, **229**, 287-302.

ISLAM M.R., BEGUM S.F., YAMAGUCHI Y. & OGAWA K. 1999. *Hydrol. Proces.* 13, 2907-2923.

REHMAN S.S., SABIR M.A. & KHAN J. 1997. *Geol. Bull. Univ. Peshawar,* **30**, 325-336.

ROLLAND Y., MAHÉO G., GUILLOT S. & PÊCHER A. 2001. *J. Metam. Geol,.* **19**, 717-737.

SINGH S.K. & FRANCE-LANORD C. 2002. *Earth Planet. Sci. Lett,.* **202**, 645-662.

SINGH S., REISBERG L. & FRANCE-LANORD C. 2003. *Geochim. Cosmochim. Acta,* **67**, 4101-4111.

VANNAY J.C., GRASEMANN B., RAHN M., FRANK W., CARTER A., BAUDRAZ V. & COSCA M. 2004. *Tectonics,* **23**, TC1014, 10.1029/2002TC001429.

WHITTINGTON A. 1996. *Tectonopysics,* **206**, 215-226.

ZEITLER P.K., MELTZER A.S., KOONS P.O., CRAW D., HALLET B., CHAMBERLAIN C.P., KIDD W.S.F., PARK S.K., SEEBER L., BISHOP M. & SHRODER J. 2001. *GSA Today,* **11**, 4-9.

Note Page

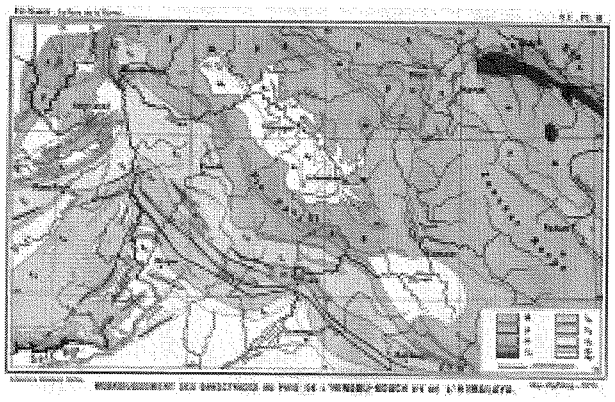

Suess, 1905

PRECISE TIMING OF HOLOCENE GLACIATION AND PALEOCLIMATIC EVOLUTION IN GANESH HIMAL (CENTRAL NEPAL) CONSTRAINED BY COSMOGENIC ^{3}HE DATING OF GARNETS.

E. GAYER[1], J. LAVÉ[2], R. PIK[1], C. FRANCE LANORD[1]

1- CRPG, Nancy, France
2- LGCA, Grenoble, France.

Glacial landforms indicate the existence of past glaciation and the limits of past glaciers extent may suggest paleoclimatic conditions. Glaciations in the Himalayan region are sensitive to the variations of the global climate but also to regional variables. In Himalaya, the monsoon precipitations above 5000-5500m are, for example, believed to play an important role in glacier accumulation and fluctuation. Detailed reconstructions of the chronology and extent of glaciations could then provide information on monsoon fluctuation in this region, and the respective sensitivity of the Himalayan glaciers to both global and regional changes. More generally they can provide new insights on the response of Himalayan region to Quaternary climatic cycles, and eventually some keys to understand potential evolution of this region (in terms of glaciers extent, GLOFF hazards, ...) in response to global warming.

In order to quantify the timing and extent of glaciations in central Himalaya we have conducted a detailed study in the upper valley of the Mailun Khola (Paldor region, Ganesh Himal) in central Nepal. We have mapped and dated glacier moraines and striated surfaces using cosmogenic ^{3}He in garnets [Gayer et al., 2004], ^{10}Be in quartz and ^{14}C in organic soils. The present Mailun Khola upper valley is occupied by a small slope-type glacier: its length and denivelation reaches 2-3 km and 1000m respectively. However, in the past it has built and left well preserved lateral dumped moraines down to 3600m and an unambiguous U-shape valley can be followed down to 3200m. Numerous striated rocks, *roches motonnées* and *whale backs* can be tracked all along this valley. The past glacier tongue has carved into highly deformed and metamorphosed Lesser Himalayan units in the vicinity of the Main Central Thrust. Garnet rich micaschists are the dominant lithologies of this area. The presence of these garnets offered us the opportunity to test and use a new dating method based on the exposure age provided by in situ cosmogenic He3 in garnets. This new method, independently calibrated with cosmogenic Be10 in quartz, and whose analytical procedure is described in detail in Gayer et al. [2004], provided numerous and high quality dating: for each sample 2 to 4 aliquots have been run and attest for the reproductibility of the results. If we except two dated blocks on the lowest and steepest moraine, which likely suffered from a more intense erosion, all the ages are in stratigraphic order whatever they correspond to striated rocks exposed after the glacier retreat or to blocks on tops of lateral moraines abandoned also after a glacier retreat.

More than 25 dates permitted to define the precise timing of the Mailun glacier retreat since the Last Glacial Maximum at ~22 kyr B.P., according to a C14 soil dating in the lowest part of the U-shape valley:

* The most significant Holocene retreat and bulk volume reduction for the glacier occurred at 10-9 kyr B.P., and is marked by the sudden exposure of striated rocks on the walls of the U-shape valley at any elevation and all along the valley.

* This massive ice volume reduction was followed by a relative stability of the glacier extent between 8.5 and 7.5 kyr B.P. as indicated by lateral and frontal dump moraines, and by intercalated striated surfaces. At that time, the glacier front was at 7 km from its present-location and at an elevation 1000m lower than today.

* A second phase of retreat started soon after. A suite of well-preserved striated surfaces and secondary moraines indicate a continuous retreat of the glacial tongue between 7 and 5 kyr B.P.. This phase could have been followed by an acceleration of this retreat perhaps to level higher than present tongues. However, a last phase of re-advance at 0-1 kyr B.P. (potentially during the little Ice Age)have obscured the exact timing of this retreat. During this later and very recent re-advance the glacier front was 500m below present one.

Since the LGM, those successive glacier extents if directly interpreted in terms of ELA (Equilibrium Line Altitude) would correspond to successive rise of the ELA from 4250m during the LGM to 4500m at 8.5 kyr BP, 4550m at 7.5 kyr, 4700m at 5kyr, 4900m during the Little Ice Age and 5150m today.

The early part of this chronology is in good agreement with the global paleo-climatic records. The major extent of the glacier and the major ice volume drop are in phase with the global Last Glacial Maximum (25-17 kyr B.P.) and with the major temperature increase following the Younger Dryas respectively. During the Holocene, the glacier chronology indicates, however, a rather different trend with the other regions of the Northern Hemisphere. During the climatic optimum (9-6 kyr) global temperatures were around 1°C higher than today. In South Asia, paleoclimatic proxies indicate similarly a warmer climate during this period than today [Gasse et al., 1996]. Taking a lapse rate of 6°C/1000m, the 550-650m ELA depression during the early Holocene would require a temperature drop larger than 3°C inconsistent with these plaeoclimatic indicators. Alternatively, this depression could have been maintained by much higher snow fall (an increase by almost 1000mm). This hypothesis would be consistent with the heavier precipitation observed during the early Holocene in all the region [Bryson, 1981; Gasse et al., 1996; Gu et al., 1993]. Higher snowfall would either result from increased precipitation during winter, or at least an increase of the summer monsoon duration, characterized by abundant snowfall above 5000m in May, September or October.
This study demonstrates that the Himalayan glaciers have responded in a different manner to the Holocene climatic changes than the rest of the northern Hemisphere, and confirms also, when compared to glacier chronology studies on other Himalayan glaciers [Phillips et al., 2000; Finkel et al., 2003; Tsukamoto et al., 2002], that sharp differences may exist from one area to another, probably in response to very contrasted Holocene changes of the precipitation rates.

References

Bryson, R.A. and A.M. Swain, Quaternary Research, 16, 135-145, 1981.
Finkel, R., L.A. Owen, P.L. Barnard and M.W. Caffee, Geology, 31, 561-564, 2003.
Gasse, F., J.C. Fontes, E.Van Campo, and K. Wei, Pal. Pal. Pal., 120, 79-92, 1996.
Gayer, E., R. Pik, J. Lavé, C. France Lanord, D. Bourlès, B. Marty, EPSL, 2004.
Gu, Z., L. Jiagi, Y. Baoyin, L. Tunsheng, L. Rongmo, L. Yu, and Z. Guangzu, Chinese Science Bull. 38, 61-64, 1993.
Phillips, W.M., V.F. Sloan, J.F. Shroder, P. Sharma, M.L. Clarck and H.M. Rencell, Geology, 28, 431-434, 2000.
Tsukamoto, S., K. Asahi, T. Watanabe and W.J. Rink, Quaternary International, 97/98, 57-67, 2002.

AN ACTIVE FAULT AT THE NORTHERN BORDER OF THE QAIDAM BASIN, CHINA: IMPLICATIONS FOR EXTRUSION MODELS

Johann GENSER (1), Franz NEUBAUER (1), Yongjiang LIU (2), Xiaohong GE (2), Gertrude FRIEDL (1) and Andrea RIESER (1)

(1) Dept. Geography, Geology and Mineralogy, University of Salzburg, Hellbrunner Str. 34, A-5020 Salzburg, Austria.
(2) Faculty of Earth Sciences, Jilin University, Changchun, China

Here we document evidence for recently detected, active faults at the northern margin of the Qaidam basin. Among these, we term the most interesting, newly detected one as Datonggou fault. Detailed analysis of SPOT satellite images show that the newly detected Datonggou fault, trends ca. N75E and can be traced over a distance of more than 10 kilometres to the north of the Hongsanhan anticline. The fault is particularly well exposed in the alluvial fan to the west of bedrock exposure northeast of the bend in the Hongsanhan anticline. To the west, the fault seemingly turns to a ENE trend, where the Hongsanhan anticline is displaced against the Altyn basement. Here, it merges with an important, already mapped fault at the northwestern margin if the Qaidam basin, which separates the Altyn basement block from the Qaidam basin block.

In the field, the most impressive sites with fault and fault rock exposure are two locations (sites A and B) to the north of the Hongsanhan anticline, which are ca. 2.6 km apart. The south-directed slope is draining the Altyn Mountains. In general, the southern margin of the fault is uplifted, opposite to the drainage direction. This results in easy recognition of the fault trace, dam effects and development of a draining system along the fault system. At site A (N 38° 41.571′, E 91° 55.257′; elevation: 3325 m), at the entrance to a dry channel, the apparent vertical offset is ca. 1.4 to 1.9 meters, varying from place to place. There, the average orientation of the fault is nearly E–W, and is composed of a several meters wide fault zone with numerous slickensides and subhorizontal striae. The fault gouge is mostly dark, comprising shear lenses with less altered high-grade metamorphic rocks like gneisses. The slickensides dip steeply towards N respectively NE, constituting together a conjugate set of strike-slip faults. NW-trending faults display mostly a sinistral sense of shear and E-trending faults both sinistral and dextral shear. Assessment with standard palaeostress techniques suggests ca. E–W maximum principal stress and N–S extension in a strike-slip regime.

Site B (N 38° 41.576′, E 91° 53.562′; elevation: 3315 m), several kilometres to the east of site A, is located at a ridge separating two major alluvial fans. There, the fault displaces gravels, and the apparent vertical offset of the fault reaches maximum 5 meters. The presence of a further terrace on the southern side suggest that there likely a higher cumulative apparent vertical offset of ca. 7 – 8 meters.

Inspection of SPOT satellite images indicates that more E-trending fault traces can be detected, from which we report those, which can reasonably well considered to as active faults. These include a segment to the west of Lapiquan (fault trace 1), a fault to the S of Lapiquan (fault trace 2) and a segment to the SE of mountains of Lapiquan (fault trace 3). Fault trace 1 is characterised by the offset of Holocene wadi and playa deposits. Fault trace 2 shows an impressive dam. Fault trace 3 also show dam effects and bending of wadis. All of these three traces trend ca. E–W and represent independent faults. On all three fault traces, geomorphic evidence suggests sinistral offset. None of these faults is considered as lateral extension of the Datonggou fault, and represent, therefore, independent faults, constituting together a wrench-type Northern Qaidam basin margin fault system. Further E-trending faults are numerous within basement rocks constituting the Altyn Mountains south of the Altyn fault. Nearly none of them, except extensions of fault traces 2 and 3, has an extension within the alluvial fans, so there is no evidence for present-day activity.

Recently published data on seismicity show nearly no earthquake along the Datongou fault at the northern margin of the Qaidam basin (Chen et al., 1999). In contrast, the Earthquake DataBase 1973–1994 of the U.S. Geological Survey shows a number of earthquakes in the region under consideration. Magnitude reaches MS=6 (event from December 26, 1987). No surface rupture was reported at that time, as the region is free of inhabitants, particularly during winter. However, all these earthquakes together show significant ongoing seismic activity along the northern Qaidam basin.

The newly detected faults from the northern margin of the Qaidam basin, together with recent seismicity, evidence present-day, neotectonic activity along this fault system. The offset is significant, particularly if the Datonggou fault is considered as the lateral extension of the fault displacing the northwestern margin of the Hongsanhan anticline. There, the minimum sinistral displacement is ca. seven kilometres, although the exact displacement cannot be specified due to missing markers and could be much larger. The bend at the northwestern edge of the Hongsanhan anticline is considered to represent a restraining bend, where the growth of the Hongsanhan anticline partly accommodated displacement along the WSW extension of the Datonggou fault through N-S shortening. This linkage also suggests that much of N–S convergence is consumed by folding and lateral displacement.

The Datonggou fault together with the three other newly detected fault traces constitutes a major fault system, which largely separate the Qaidam basin block from the Altyn Mountain block. Geomorphic evidence indicates ongoing activity. The age of the Datonggou fault trace is obviously recent, because the fault trace is nearly not modified by surface drainage. The northern margin of the Qaidam basin is a semiarid area with a very low precipitation, 50–150 mm per year. Consequently, the fault scarp can be preserved over a relatively long time without major modification. The Earthquake Data Base 1973–1994 and the few data reported by Chen et al. (1999) show recent seismicity, which can be linked to newly detected fault traces, although details are to be investigated.

We interpret the Datonggou fault and other fault as secondary, Riedel-type shears related to the Altyn fault system, constituting together a wrench corridor, although it only separates in part the Altyn basement block and the Qaidam basin block. The whole system can be considered as Northern Qaidam basin margin fault system. The offset seems to be a purely strike-slip motion along ca. E-trending faults, along which the Qaidam basin block is moving eastwards. This suggests that the decrease of displacement rates along the Altyn fault could be partly accommodated by the sinistral Northern Qaidam basin margin fault system. Fault distribution and palaeostress data are characteristic for an extrusional wedge, which moves out of the zone of maximum compression.

The finding of the sinistral, ca. E-trending Datonggou fault and the Northern Qaidam Basin Margin fault suggests that N–S shortening related to India-Asia collision resulted in more distributed shear as previously suggested. This may explain the missing motion and misfit between GPS measurements (e.g., Bendick et al., 2000) and palaeoseismological studies (Tapponnier et al., 2001). The data also show that detailed work may result in the detection of more faults in the area as previously considered.

Bendick, R., Bilham, R., Freymueller, J., Larson, K. & Yin, G., 2000. *Nature*, **404**, 69–72.
Chen, W.-P., Chen, C.-Y. & Nábelek, J.L., 1999. *Tectonophysics*, **305**, 165–181.
Tapponnier, P., Ryerson, F.J., Van der Woerd, J., Mériaux, A.-S. & Lasserre, C., 2001. *C.R. Acad. Sci. Paris, Sci. Terr. Planet.*, **333**, 483–494.

RECENT EVOLUTION OF THE LONGMEN SHAN, EASTERN TIBET: INSIGHTS FROM DENUDATION RATES AND NUMERICAL MODELING

Vincent GODARD (1), Jérôme LAVÉ (2) and Rodolphe CATTIN (1)

(1) Laboratoire de Géologie, École normale supérieure, Paris, France.
(2) Laboratoire de Géodynamique des Chaînes Alpines, Observatoire des Sciences de l'Univers de Grenoble, Grenoble University, France.

The Longmen Shan range, along the eastern margin of the Tibetan Plateau marks a sharp transition between the low elevated (~ 500m) Sichuan Basin to the Songpan Garze fold system (4000m in average). No recent important deformation stage (i.e. Quaternary or late Tertiary) has been identified so far, and GPS measurements do not show any significant shortening across the range (<5mm/an). In addition, the foreland basin, i.e. the Sichuan basin, is characterized by low Quaternary sedimentation rates. Understanding how such topographic step is maintained is of major interest for the understanding of the dynamics of the system.

Clark and Royden [2000] propose that the dynamics of this region is mainly controled by eastward propagation and blockage of a low viscosity channel flow in the lower crust. This channel flow could explain the maintain of a significant topographic gradient despite the absence of localized shortening in the upper crust. Another explanation is that the uplift is Tertiary and that shortening has ceased even more early. In this case topography would be residual and not balanced.

We address this issue through the use of a thermomechanical numerical model that includes surface denudation processes. We first calibrated the erosional parameters on the basis of experimental and field measurements of fluvial incision in the Longmen Shan. The consistency of the erosion model was then tested and compared to long term denudation rates as derived from published and new thermochronologic data (FT and (U,Th)/He in apatites). We then discuss different scenarios: in terms of denudation distribution, in terms of subsidence/uplift of the Sichuan basin and in terms of the characteristic time for a topographic scarp to retreat in absence or in presence of a ductile channel flow in the lower crust.

Clark M. K., & Royden L. H. 2000. *Geology*, 28. 703-706.

EXTRUDED DOMES IN THE GREATER HIMALAYAN SEQUENCE: MODEL PREDICTIONS AND POSSIBLE EXAMPLES

Djordje GRUJIC (1), Christopher BEAUMONT (2), Rebecca A. JAMIESON (1) and Mai H. NGUYEN (1, 2)

(1) Department of Earth Sciences, Dalhousie University, Halifax, N.S., Canada, B3H 3J5
(2) Department of Oceanography, Dalhousie University, Halifax, N.S., Canada, B3H 4J1

Along-strike variations in Himalayan tectonic style suggest that ductile extrusion of the Greater Himalayan Sequence (GHS) is more complicated than predicted by simple channel-flow models (e.g., Beaumont et al., 2001). For example, high-temperature (>800°C) and moderate- to low-pressure (4-7 kbar) assemblages characterise the upper tectonic level of the GHS in several regions of the central and eastern Himalaya. In these areas, out-of-sequence thrusts separate the upper GHS from a lower tectonic level with peak conditions of 700-800°C at pressures up to 12 kbar. Based on recent model results, we suggest that the two levels of the GHS may represent sequentially exhumed parts of a hot mid-crustal channel, with the upper tectonic level possibly corresponding to an extruded dome.

In central Bhutan, cordierite-sillimanite gneisses and migmatites are thrust over garnet-staurolite schist along the conspicuous, out-of-sequence, Kakhtang thrust. In the hanging wall, leucogranite in the roof of the Monlakarchung-Kula Kangri pluton has been dated at 12-13 Ma (Edwards & Harrison 1997), the youngest known in the Himalaya. Beneath the pluton, the Kakhtang thrust cuts the main foliation and metamorphic isograds in the GHS. Leucogranite dykes deformed by the thrust with ca. 14-15 Ma intrusion and cooling ages document rapid exhumation of the hanging wall associated with late Miocene shearing along the Kakhtang thrust. Quartz textures indicate syn-thrusting amphibolite facies (≥650°C) conditions in the hanging wall and greenschist facies conditions in the footwall. Garnet zoning in footwall schists suggests growth with increasing pressure (Davidson et al. 1997). These schists, which can be correlated with Neoproterozoic sediments found further south in klippen of the South Tibetan Detachment (Grujic et al. 2002), point to significant displacement that progressively diminishes to east and west along the trace of the Kakhtang thrust. In central Bhutan, the thrust and the foliation are steep and locally overturned, outlining a non-cylindrical, recumbent, south-facing antiform. In its frontal part, the steep foliation is overprinted by a sub-horizontal crenulation cleavage which is likely co-kinematic with north-directed shear bands in the detachment at the roof of the leucogranite pluton. Together, these textures are consistent with flattening of a hot structure (upper GHS) during southward thrusting beneath the Tethyan cover and over the previously exhumed lower GHS.

Recent models for the tectonic evolution of large hot, orogens (Beaumont et al. 2004) demonstrate that channel flows can be accompanied by the development of domes and hot fold nappes. These structures may be exposed by extension of the overlying upper crust, or may be extruded as part of the channel and exposed by erosion. Models with the latter type of development exhibit structures similar to those described above. In particular, overthrusting of the dome or nappe at high structural levels in the channel creates an out of sequence Kakhtang-like thrust with the dome/nappe arched above it. Such structures are produced without the need to appeal to low-viscosity or low-buoyancy enclaves; it therefore is uncertain whether the observed leucogranite sheets are an active or passive part of the system.

Comparisons between observations and model results suggest that the GHS is likely to be structurally and metamorphically more complex than predicted by the simple 'toothpaste-like' extrusion of a channel. Along-strike variability in GHS tectonic style may provide evidence of the types of processes seen in the numerical models. Moreover, the process of dome extrusion above a mid-crustal channel provides an additional mechanism for out-of sequence thrusts in the cores of hot collisional orogens.

BEAUMONT, C., JAMIESON, R. A., NGUYEN, M. H. & LEE, B. 2001. *Nature* **414**, 738-742.
BEAUMONT, C., JAMIESON, R. A., NGUYEN, M. H. & MEDVEDEV, S. 2004. *Journal of Geophysical Research* **109**, 10.1029/2003JB002809.
DAVIDSON, C., GRUJIC, D., HOLLISTER, L. S. & SCHMID, S. M. 1997. *Journal of Metamorphic Geology* **15**, 593-612.
EDWARDS, M. A. & HARRISON, T. M. 1997. *Geology* **25**, 543-546.
GRUJIC, D., HOLLISTER, L. & PARRISH, R. 2002. *Earth and Planetary Science Letters* **198**, 177-191.

CLIMATE LEADS – TECTONICS FOLLOWS: GEOLOGIC CONSEQUENCES OF ASYNCHRONOUS DENUDATION ALONG THE HIMALAYA

Djordje GRUJIC (1), Isabelle COUTAND (2), Bodo BOOKHAGEN (3), Ann BLYTHE (4), Stéphane BONNET (5) and Chris DUNCAN (6)

(1) Department of Earth Sciences, Dalhousie University, Halifax, Canada,
(2) UMR CNRS 8110, Processus et Bilans des Domaines Sédimentaires, Université des Sciences et technologies de Lille, 59655 Villeneuve d'Ascq Cedex, France,
(3) Institut für Geowissenschaften, Universität Potsdam, Potsdam 14415, Germany. Now at: Institute for Crustal Studies, 1140 Girvetz Hall, University of California, Santa Barbara, Santa Barbara, CA 93106-1100
(4) Department of Earth Sciences, University of Southern California, Los Angeles, California 90089, USA
(5) Géosciences Rennes, Université de Rennes 1, UMR CNRS 6118, Campus de Beaulieu, 35 042 Rennes Cedex
(6) Department of Geosciences, University of Massachusetts, Amherst, Massachusetts 01003, USA

Two adjacent areas within the eastern Himalayas with homogeneous geology but different climatic histories over the last 4-5 Myrs are used to evaluate the climatic influence on landscape and tectonics. We show that the changes in the spatial distribution of precipitation caused by the uplift of the Shillong Plateau at the Miocene-Pliocene transition and resulting changes in erosion in the lee of the plateau in the Bhutan Himalaya have triggered tectonic responses.

To assess the erosional history and by inference, the landscape evolution of the Bhutan Himalaya, we have obtained apatite fission-track analyses on 42 samples collected along a broad E-W trending transect through the Greater Himalayan Sequence. The study area covers two longitudinal regions with different climatic histories, one in the lee of the Shillong Plateau and one not. Samples were collected at elevations below < 4000 m, excluding areas that were glaciated recently or during the Last Glacial Maximum. With this sampling strategy lithological and structural influence on erosion are minimised, the tectonic rock uplift rate for all the samples is similar and the mixture of glacial and fluvial erosion processes avoided. Accordingly, any along-strike difference in exhumation rate, landscape and tectonics ought be climate-, or more specifically, precipitation-induced.

Using apatite fission-track data we document differences in Late Miocene to Pliocene denudation rates in eastern and western Bhutan. We propose that change in erosional efficiency (caused by decrease in precipitation) led to changes in the landscape, which in turn has resulted in a tectonic response that has further influenced both the rock and surface uplift rates. We demonstrate that the climatic and tectonically driven landscape in Bhutan follow in sequence because the new climate-driven landscape did not completely reset an earlier landscape. Although we suspect that the tectonic landscape will eventually dominate the recent landscape, we suggest that the climatic trigger is essential for the landscape changes, leading to changes in crustal load and those to tectonic responses which in turn influence landscape.

PETROLOGY, GEOCHEMISTRY AND GEOCHRONOLOGY OF HIGHLY FOLIATED AMPHIBOLITES UNDERLYING THE YARLUNG ZANGBO SUTURE ZONE OPHIOLITES, SOUTHERN TIBET ; GEODYNAMICAL IMPLICATIONS FOR THE DISMEMBERED DYNAMOTHERMAL SOLE

Carl GUILMETTE [a]*, Réjean HÉBERT [a], Céline DUPUIS [a], Viviane DUBOIS-COTÉ [a], WANG ChenShang [b], LI ZeJung [b]

[a]Département de géologie et de génie géologique, Université Laval, Sainte-Foy, Qc., Canada G1K 7P4.
[b]Institute of Sedimentary Geology, Chengdu University of Technology, Chengdu, Sichuan 610059, People's Republic of China.

*Corr author. Tel.: 1-418-656-2131 # 12710; Fax: 1-418-656-7339 E-mail address: carl.guilmette.1@ulaval.ca

Blocks of highly foliated amphibolites locally occur as clasts within a sheared serpentinite matrix mélange underlying the Xigaze ophiolites, Tibet. The Xigaze ophiolites belong to the central section of the Yarlung Zangbo Suture Zone (YZSZ), between the Indian and Eurasian plates. Units along this suture are interpreted as remnants of the Neo-Tethys oceanic domain, which separed the two continents prior to the Eocene collision. Obduction of the ophiolitic nappes over the Indian passive margin is thought to be responsible for the tectonic dismemberment of the base of the ophiolites and therefore for the creation of the ophiolitic mélange. Accordingly, blocks of highly foliated amphibolites found in the mélange, near Bainang and Buma localities, are interpreted as parts of a dismembered dynamothermal sole, as found beneath many ophiolites. Dynamothermal soles are thought to form at the initial stage of ophiolite emplacement, during inception of a subduction. Their study brings important constraints on the evolution and destruction of the obducted oceanic basin. This paper presents new geochemical, petrological and geochronological data from highly foliated amphibolite blocks underlying the YZSZ ophiolites.

Amphibolites can be divided in three groups : the garnet, banded and common amphibolites. Mid-grained garnet amphibolites contain assemblage A) Hbl+CPX+Grt+Pl+/-Rt and B) Grt+Hbl+Pl (corona assemblage). Fine to medium-grained banded amphibolites contain assemblage C) Hbl+CPX+Pl+Ep+/-Spn+Qtz+Ap. Fine-grained common amphibolites contain facies D) Hbl+Pl+/-Ep+Ap+Spn. In all samples, plagioclase is invariably pseudomorphised by an albite-prehnite simplectite. Retrograde cataclastic veins containing assemblage E) Ab+Prh+/-Chl+Ep are also common. Geochemistry of the garnet, banded and common amphibolites is very similar to geochemistry of other mafic blocks in the mélange and of mafic magmatites within the ophiolitic massifs. Light depletion of LREE (La/Yb = 0.65-0.97) and mild HFSE depletion (Ta/Th = 0.33-0.65) would suggest a mixing between the IAT and MORB sources, as seen in back-arc basins and nascent intra-oceanic arcs. Hot peak metamorphism conditions of 11.5-14.5 kbars and 800-875 ∞C were obtained using Fe-Mg garnet + amphibole or clinopyroxene thermometry, Al-Ti content of amphiboles and TWEEQU calculations. Presence of a metamorphic fluid is confirmed by oxygen stable isotopes geochemistry. Ar/Ar analysis of amphiboles revealed a metamorphic age of 121-130 Ma, which is synchron with ages obtained from the overlying ophiolites. A late metamorphic event caused heterogeneous coronitization of pyrope-rich (up to 35 %) garnet by Al-Tschermakites (Al_2O_3 up to 21 wt %) at high-pressures. After rapid exhumation, amphibolites were intruded by very fine-grained diabasic rocks of SSZ geochemical signature and were subject to percolation of a prehnite-crystallising fluid. Oxygen stable isotopes suggest fluid was of magmatic origin.

Magmatic and metamorphic history of the dynamothermal sole are in accord with inception of a subduction within an actively spreading SSZ domain from which originate the ophiolites. Such an event had not been recognized yet and reflects major changes in plate motion near 130 Ma. Further subduction of an incoming buoyant body could provide an explanation for the high-pressure retrograde event seen as coronitization of garnet. Injection of dikes at shallow depths associated with magmatic fluid percolation and prehnite metamorphism indicates subduction of a magmatic center prior to obduction and dismemberment of the sole. These new data, coupled with new data from other nearby units, would suggest that the subduction responsible for the generation of the dynamothermal sole, for the accretion of the Bainang subduction complex and for the obduction of the ophiolites is not the one responsible for the generation of the ophiolites, which had to be older.

3D STRAIN ANALYSIS AS A TESTER FOR NUMERICAL SIMULATION

Daigoro HAYASHI

Department of Physics and Earth Sciences, University of the Ryukyus, Nishihara, Okinawa, 903-0213, Japan

One of the important topics of numerical simulation is how to check its results. If we consider the underthrusting of Indian lithosphere beneath the Himalaya and Tibet, this will be done using the earthquake focal mechanisms, distribution of earthquake hypocenter, neotectonic morphology, stress measurement and strain measurement (Alam and Hayashi, 2003; Howladar and Hayashi, 2004).

3D strain was once calculated using the oriented samples collected from Annapurna Region though the result seemed not reasonable (Kawamitsu and Hayashi, 1991). Recently I have performed the calculation again using the same data by the least square method (Hayashi,1994) and have obtained reasonable strain. The strain shows us a remarkable feature that the foliation plane almost coincides with principal strain XY plane. This strongly suggests that the least square strain analysis method is correct and effective.

From the viewpoint of checking simulation, the benefit of this 3D strain analysis method is; (1) many kinds of rock which consists of grains, i.e. sandstone and metamorphic rocks derived from sandstone can be treated as marker rocks and (2) almost everywhere we can find such rocks in Himalayas.

Although there are some 3D strain analysis techniques, none of them are used to examine the simulation results so far. One the other hand, many simulations are examined by comparing with the stress measurements to test their reality.

References

ALAM,M.M. and HAYASHI,D. 2003. Japanese Journal of Structural Geology, **47**.37-48.

HAYASHI,D. 1994. Jour.Geol.Soc.Japan, **100**, 150-161.

HOWLADAR,M.F. and HAYASHI,D. 2004. Geoinformatics, **15**. 207-219.

KAWAMITSU,K. and HAYASHI,D. 1991. Bull.Coll.Sci.Univ.Ryukyus, 52. 37-52.

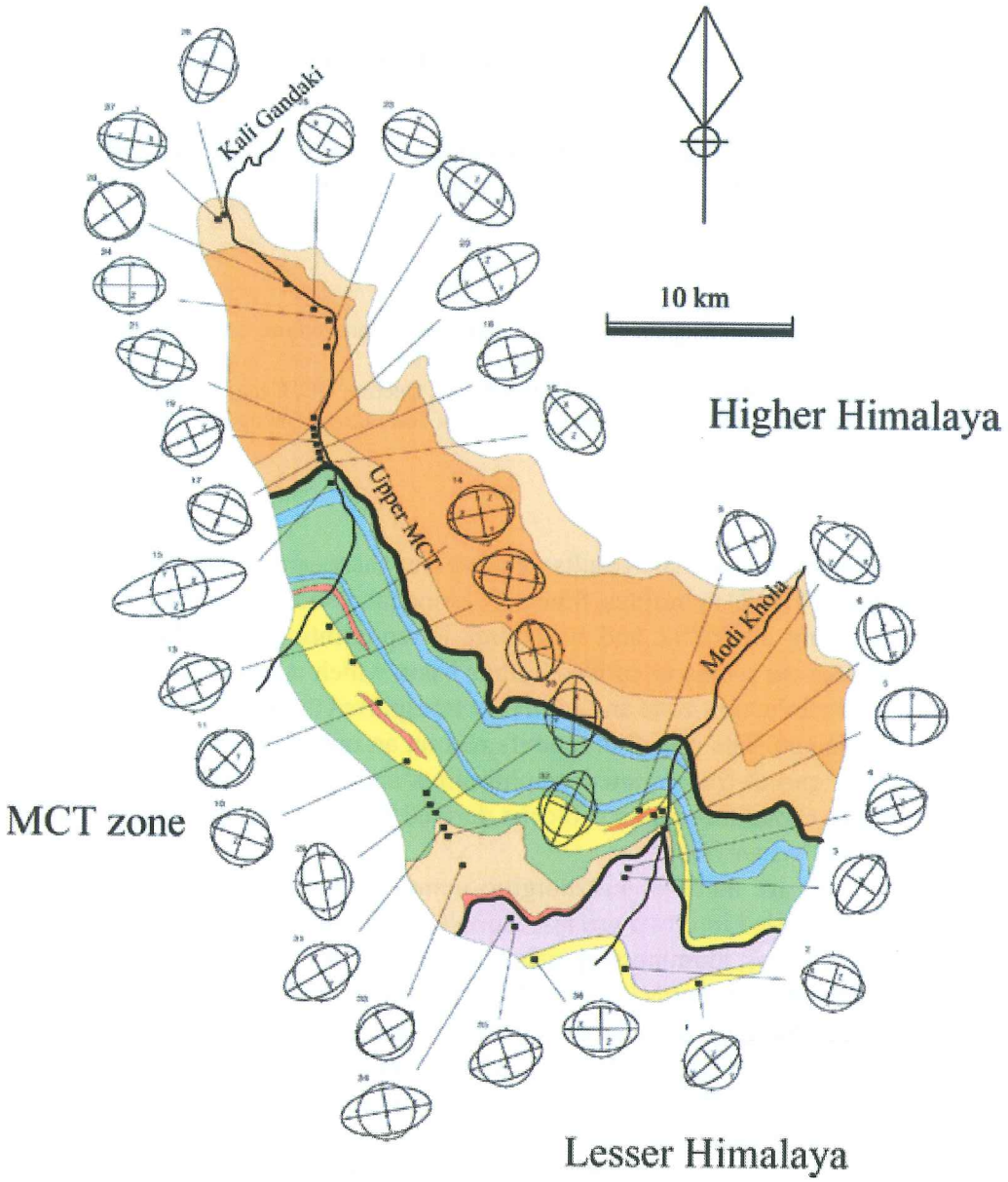

Fig. 1- 3D strain location in northwest Pokhara, central Nepal.
Circle shows Schmidt net where principal strain axes X, Y and Z are drawn.
Ellipse indicates XZ plane.

THE YARLUNG ZANGBO SUTURE ZONE OPHIOLITES, TIBET : A SYNTHESIS

Réjean HÉBERT (1), Carl GUILMETTE (1), Céline DUPUIS (1), Viviane DUBOIS-CÔTÉ (1), François HUOT (2), Chengshan WANG (3), Yalin LI (3)

(1) Département de géologie et de génie géologique, Pavillon Adrien-Pouliot, Université Laval, Québec, QC, Canada, G1K 7P4
(2) Géo-Conseils TB, 4174 D'Estrée Street, Québec, QC, Canada, G2A 3P2
(3) Institute of Sedimentary Geology, Chengdu University of Technology, Chengdu, Sichuan 610059, PR China

This paper presents the main results of a five-year assessment project focussed on Yarlung Zangbo Suture Zone (YZSZ) ophiolites. Since 1998 several ophiolitic sections have been revisited. They are located along the YZSZ and study area is representing a 300 km long segment. The Cretaceous ophiolites are remnants of Neo-Tethys basin which was almost totally consumed in a northward oriented subduction zone and southerly transported onto the Indian plate colliding with Eurasia circa 50 Ma ago. The ophiolite massifs rest on an ophiolitic mélange, locally containing garnet-bearing and garnet-free foliated amphibolites and further south on Triasic flysch and Cretaceous mélange containing igneous blocks derived from partial reworking of Indian passive margin and Tethysian ocean-floor.

The ophiolites are made of harzburgitic mantle and thin gabbro-lacking crust. Mantle harzburgites are subdivided into two groups. Samples from the western massifs are characterized by porphyroclastic textures, aluminous spinels (Cr/(Cr+Al) : 0.13-0.21), average low TiO_2 content (0.04 wt.%), depleted REE patterns (average La/Sm ratios 0.4) and derive from 7-12% melting of N-MORB-like source. Samples from the eastern massifs are granular peridotites with Cr-rich spinels (Cr/(Cr+Al) : 0.33-0.74), average very low TiO_2 content (0.008 wt. %), enriched REE patterns (average La/Sm 5.6) and could originate from 20-30 % partial melting of a depleted source further enriched by an episode of metasomatism. Crustal samples are basaltic flows and diabasic intrusions. They are subdivided into two groups. The western group is made pl-cpx-phyric basaltic rocks with depleted REE patterns (average La/Sm 0.6)and slight Ta-Nb negative anomalies. The eastern group is made up of pl-cpx-(am)-phyric basaltic rocks having fractionated REE patterns (average La/Sm 4.6) and strong Ta-Nb negative anomalies. These results are consistent with derivation of the ophiolites from dismemberment of back-arc (western portion) and intra-oceanic arc (eastern portion) sectors of the Neo-Tethys marginal basin.

Geochemical, thermobarometric and geochronological study of mélange-embedded amphibolite blocks confirm that they derive from a dismembered dynamothermal sole. Geochemical signature of the sole indicates genesis at the Neo-Tethys back-arc spreading center. Early Cretaceous metamorphic ages from the amphibolites (121-130 Ma) are synchronous with ophiolite genesis. Together with intense peak metamorphism conditions and geochemical signature of the sole, overlapping ages would indicate inception of a subduction within the Neo-Tethys back-arc basin. Such a setting illustrates the rapid dismemberment of the SSZ domain. Present-day architecture indicates that this subduction led to the final emplacement of the ophiolitic massifs over the Indian passive margin.

Note Page

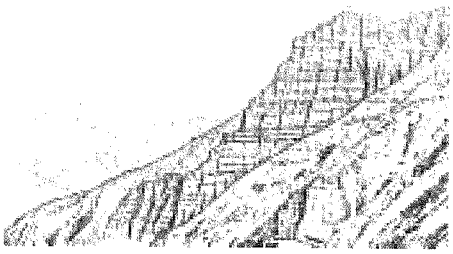

Spiti, Hayden, 1905

AN OVERVIEW OF CRUSTAL AND MANTLE ANISOTROPY IN TIBET

Georges HERQUEL
IPG, EOST, 5 rue René Descartes, Strasbourg, 67084, France

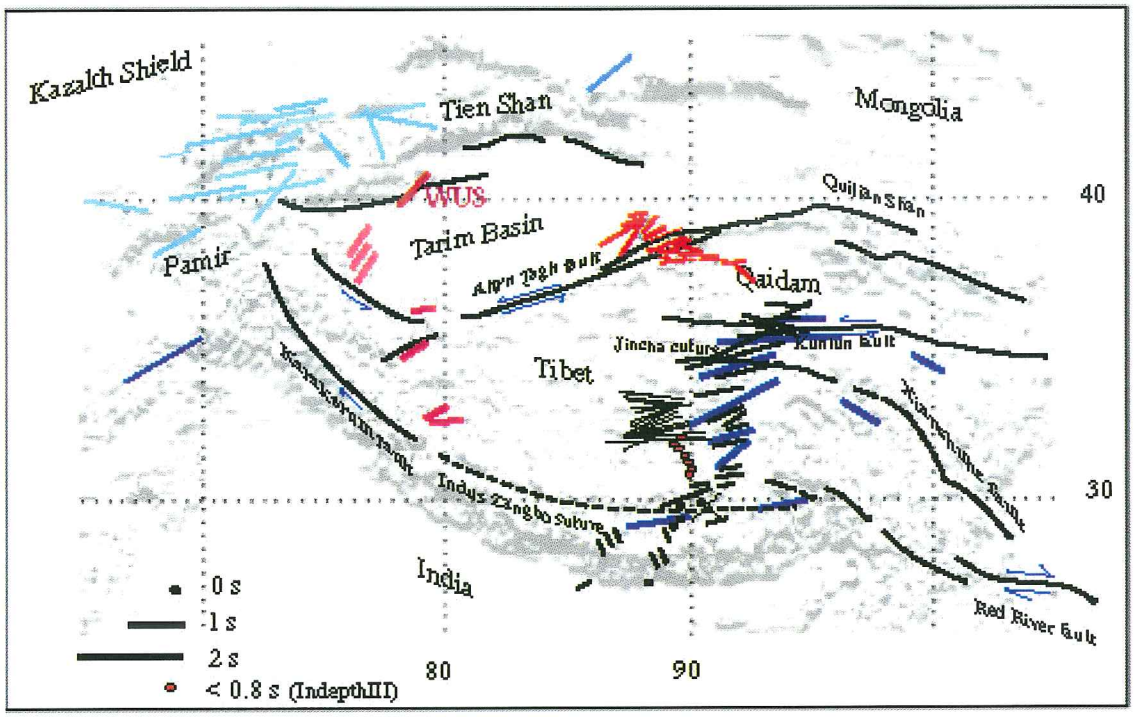

Map of SKS splitting anisotropy plotted on Mercator projection of India-Asia collision zone DEM. Results are from Makayeva et al (1992) in light blue lines, Guilbert et al (1996) in thick black line, Hirn et al (1995) in thick black line, McNamara et al (1994) in dark blue line, Herquel et al (1999) in orange line, Huang et al (2000) in thin black lines, and Herquel et al (2005) in pink lines.

If SKS splitting anisotropy mapping is now in Tibet at a good stage, contribution of crustal anisotropy to the total is still under debate.
Main questions are concerning the total crustal anisotropy contribution and the anisotropic structure of the crust.

Total crustal anisotropy contribution under-evaluated under Tibet ?

Moho P-to-S converted phases may be used to determine the complete crustal component of anisotropy
Previous results (Herquel et al, 1995) may be low estimates of this contribution in Northern Tibet (0.15-0.3s) since some very large mantellic delays have been observed in other areas of the plateau.

New measurements use data from stations with the largest mantellic delays _t observed in Tibet, at least 2 seconds (stations ST17, ST18 and ST19 from Indepth III and BUDO again).
At all 4 stations using 190 clear Ps a mean value of delay of 0.17s is retrieved with an uncertainty of 0.05s: no single value exceed 0.3s. Finally, we observe also a good correlation with the fast polarization direction obtained by teleseismic shear wave analysis (Herquel et Pedme, 2003).

This results are compatible with results from Ural Mountains, New Zealand and Basin and Range.

Anisotropic layering of the Tibetan crust.

When using receiver functions (RF) stacked by back-azimuth windows, amplitude variations of coherent phases observed on transverse RFs can be analyse to discriminate between dipping interfaces, anisotropy or diffracting heterogeneities (e.g., Levin et al., 2002).
Many results were published using the good data of Budo station (Vergne et al, 2003; Frederiksen et al, 2003; Sherrington et al, 2004).
Forward modeling can be used to match synthetic RFs computed for very simple models, including two layers in a stack of flat anisotropic layers with anisotropy as high as 15% related to highly deformed flyshs and schists in the first 25 km of the crust. Maximum delay time is 0.5s, and directions are compatible with SKS (Vergne et al, 2003).
Amplitude variations resolved by anisotropic receiver function inversion in a 20-30 parameters at constant Vp/Vs on the same data at Budo explained the same amplitudes variations by a sequence of two or three thick crustal anisotropic layers with varying anisotropic axis from 30 to 50° in different directions and anisotropy as high than 10%.
Sherrington et al (2004) using other data from Passcal experiment in 1992, Arda Ozacar et G. Zandt (2004) from stations of Indepth III in the Bangong-Nujiang area, define other crustal models where orientations of crustal anisotropy are significantly different from shear wave polarization directions, implying distinct deformation in the crust and mantle. The same range of high value of 4 to 14% anisotropy are used.

References:

Frederiksen, A.W., H. Folsom, and G. Zandt, Neighbourhood inversion of teleseismic Ps conversions for anisotropy and layer dip, *Geophys. J. Int.*, **155**, 200-212, 2003.
Herquel, G., G. Wittlinger and J. Guilbert, Anisotropy and crustal thickness of Northern Tibet. New constraints for tectonic modeling, *Geophys. Res. Lett.*, **22**, 1925-1928, 1995.
Herquel, G. and P. Edme, Crustal anisotropy contribution under-evaluated under Tibet ?, *EGU Nice*, 2003.
Levin, V., J. Park, M. Brandon, J. Lees, V. Peyton, E. Gordeev, and A. Ozerov, Crust and upper mantle of Kamchatka from teleseismic receiver functions, *Tectonophysics*, **358**, 233-265, 2002.
Arda Ozacar A. and G. Zandt, Crustal seismic anisotropy in central Tibet: Implications for deformational style and flow in the crust, *Geophys. Res. Lett.*, **31**, L23601, 2004
H. Sherrington, G. Zandt and A. Frederiksen, Crustal fabric in the Tibetan Plateau based on waveform inversions for seismic anisotropy parameters, *J. Geophy. Res.*, **109**, B02312, 2004
Vergne, J., G. Wittlinger, V. Farra, and Heping Su, Evidence for upper crustal anisotropy in the Songpan- Ganze (northeastern Tibet) terrane, *Geophys. Res. Lett.*, **30**, No.11, 1552-1556, 2003

SEISMIC–INSPIRED MODEL SECTION OF CRUST AND MANTLE WEDGES AND ITS BALANCING: TIME EVOLUTION OF LOCALIZATION OF DEFORMATION WITH DEPTH AND ACROSS HIMALAYA-TIBET

Alfred HIRN (1), Audrey GALVE (1), JIANG Mei (2), Mireille Laogle(1), Martine SAPIN (1), Béatrice DE VOOGD(4), Jordi DIAZ (3)

(1) Sismologie Expérimentale, UMR 7580 Dpt Sismologie, Institut de Physique du Globe de Paris, 4 place Jussieu 75252 Paris Cedex 05, France
(2) Chinese Academy of Geological Sciences, Baiwanzhuang road, 100037 Beijing, China
(3) Institute of Earth Sciences Jaume Almera, calle Lluis Sole I Sabaris, 08028 Barcelona, Spain
(4) Dept. Sciences de la Terre, Université de Pau, 64000 Pau, France

An early seismic section through Himalayas and South Tibet has imaged, by topside wide-angle reflections resolved on fan and in-line profiles, a seismic Moho that appeared to be made of segments, which relay, overlap and superpose each other. This suggested a model of indentation in vertical plane of a rheologically multilayered lithosphere (Hirn et al., 1984; Burg et al., 1994). This model of indentation differed from others as to the depth range to which tectonic growth of Tibet involves the lithosphere. Here in addition to an intracrustal rheological décollement level, another one is required in the upper mantle lithosphere. This may indeed be seen now by the interface below 100 km depth that could form its base and that can be followed in a receiver-function image through the Himalayas and into the Lhasa block, that documents also with a different and independent method the stack of Moho segments inferred from wide angle reflections (Galvé et al., 2002a). An approximate continuation of this section across the plateau can be based on wide-angle reflections in the Northeastern Tibet (Galvé et al., 2002b) and, receiver-functions for the crust (Vergne et al., 2002) and mantle (Kind et al., 2003).

Around the series of Moho segments and attached lower crust, jigsaw puzzle pieces can be cut along faults along which they would have been transported, assuming an earlier continuous single Moho. Balancing the lithospheric-scale section through time is then possible by restoring backwards the line-length of the Moho interface, which holds even if in places the imaged seismic Moho were now the top of an eclogitized lower crust (Sapin and Hirn, 1997, Galvé et al., 2005).

A minimum 1000 km of the shortening between India and the Gobi platform is thus inscribed in the present structure as the stack of resulting segments of the Moho. With a 40 mm/yr convergence rate and assuming the proportion of shortening of Replumaz and Tapponnier (2003), restoration of the Moho line-length along the section amounts to about 40 Ma, on the order of the time since collision. At least 500 km of shortening through the Himalayas is inscribed in the crustal material stored deeper than the shallowest of the seismic Moho segments and reaching north of the surface suture, and above the 100 km deep converter that can be considered as the interplate, the interface below which total subduction occurs as it dips northward to 180 km depth under the Lhasa block. The restoration of the section with time and its comparison to mantle tomographies at diverse scales (Van der Voo et al., 1999; Tilmann et al., 2003) illustrate disposal in section towards depth, of additional lengths of lower lithosphere that hence measure convergence, with respect to the shortening indicated by the Moho line-length contained in the section, with the imbricate wedges containing the Moho participating to the episodes of extrusion.

Principal stages of the shortening are given by the snapshots when new segments enter the stack seen at present, with a succession of different styles as shortly mentioned hereafter. Accumulation and backstop growth when Indian continental margin segments follow oceanic subduction, with slab break-off. Growing topographic head favoring sideway propagation of strike-slip faults for extrusion in the retrowedge. Foreland migration of a succession of intracontinental crustal thrusts from the suture to south of the Himalayas as step-up pro-shears, possibly with conjugate step-down pro-shears in the lower crust through shallow mantle. Step-up and -down retro-shears north of the suture to the Karakoram-Jiali Fault zone as an accretionary wedge and forearc involving units of the crust and its base, above the oblique subducting Indian lower lithosphere. Hinterland migration from the accumulating lithospheric wedge, of a succession of crustal scale thrusts or imbrications reactivating regions of the earlier sutures of Jinsha and Kun Lun and shoving the thickened crust imbricate above an Asian lower lithosphere that is thus brought to dip southward in subduction.

In this model only the deeper part of the mantle lithosphere undergoes total subduction, only the upper part of the crustal lithosphere collides and imbrication of crust-mantle wedges occurs in between. It is thus a partial collision and partial subduction of crustal material and partial collision and partial subduction of uppermost mantle material.

(REFERENCES)

BURG J. P., DAVY P. & MARTINOD J. 1994. *Tectonics*, **13**. 475-483.

GALVE A., SAPIN M., HIRN A., DIAZ J., LEPINE J.-C., LAIGLE M., GALLART J. & JIANG M., 2002a. *Geophys. Res. Lett.*, **29** (24). 2182. doi:10.1029/2002GL015611.

GALVE A., HIRN A., JIANG M., GALLART J., DE VOOGD B., LEPINE J.-C., DIAZ J., WANG Y. & QIAN H. 2002b. *Earth Planet. Sci. Lett.*, **203**. 35-43.

GALVE A., JIANG M., HIRN A., SAPIN M., LAIGLE M., DE VOOGD B., GALLART J. & QIAN H. 2005. *Tectonophys.*, in review.

HIRN A., LEPINE J.C., JOBERT G., SAPIN M., WITTLINGER G., XU Z.X., GAO E.Y., WANG X.J., TENG J.W., XIONG S. B., PANDEY M. R. & TATER J. M. 1984. *Nature*, **307**. 23-25.

KIND R., YUAN X., SAUL J., NELSON D., SOBOLEV S. V., MECHIE J., ZHAO W., KOSAREV G., NI J., ACHAUER U., & JIANG M. 2002. *Science*, **298**. 1219-1221.

REPLUMAZ A. & TAPPONNIER P. 2003. *J. Geophys. Res.*, **108**(B8). doi:10.1029/2001JB000661.

SAPIN M. & HIRN A. 1997, *Tectonophys.*, **273**. 1-16.

TILMANN F., NI J. & INDEPTH III SEISMIC TEAM. 2003. *Science*, **300**. 1424-1427.

VAN DER VOO R., SPAKMAN W. & BIJWAARD R. H. 1999. *Earth Planet. Sci. Lett.*, **171**. 7-20.

VERGNE J., WITTLINGER G., QIANG H., TAPPONNIER P., POUPINET G., JIANG M., HERQUEL G. & PAUL A., 2002. *Earth Planet. Sci. Lett.*, **203.** 25-33.

SEDIMENTOLOGICAL ANALYSIS OF THE KARNALI RIVER SECTION (SIWALIKS OF WESTERN NEPAL) : IMPLICATION FOR THE UPPER MIOCENE EVOLUTION OF THE HIMALAYAN BELT AND CLIMATE

Pascale HUYGHE [1], Ananta Prasad GAJUREL [1] [2], Jean-Louis MUGNIER [1], Matthias BERNET[1] and Peter VAN DER BEEK [1]

[1] Laboratoire de Géodynamique des Chaînes Alpines, Université de Grenoble - France
[2] Department of Geology, Tribhuvan University, Kathmandu - Nepal

A multi-disciplinar study has been conducted within the Siwalik series exposed along the 5000 m thick Karnali River section. Facies, clay mineralogy and neodymium isotope compositions analysis permitted to outline major changes and to discuss their tectonic or climatic origin.

From these analysis, 2 major changes within the sedimentary fill are discussed: the change from meandering to braided river system and the change from deep sandy braided to shallow sandy braided river system which occurred respectively at ~9.5 Ma and ~6.5 Ma along the Karnali section.

The 9.5 Ma event follows an abrupt decrease of $\varepsilon_{Nd}(0)$ values indicating local exhumation and erosion of Lesser Himalaya rocks within the Karnali catchment basin. The onset of Lesser Himalaya tectonics caused this local exhumation, and by changing the morphology, the proximity of relief and the surface slope, the tectonic forward propagation is responsible for the high gradient and sediment load shown by the development of braided river system. Around 6.5 Ma, the change from deep sandy braided to shallow sandy braided river system is contemporaneous with a change of clay mineralogy towards smectites/kaolinite dominant clay assemblages. As no source rock change, no exhumation pulse (as determined from zircon fission-track analysis) and no burial effect are detected by that time, the clay mineralogy change is interpreted as resulting from variations of environmental conditions. The facies analysis shows abrupt and frequent increasing discharges by that time. Both could be linked to an increase of seasonality induced by monsoon climate intensification. The major fluvial changes recognized along the Karnali section have been recognized from Central to Western Nepal (Nakayama & Ulak, 1999 ; Ulak & Nakayama, 2001) although they are diachronous (Fig. 1). Both the change of clay mineralogy towards smectites/kaolinite rich assemblages and the slight decrease of $\varepsilon_{Nd}(0)$ have also been detected in the Bengal Fan sedimentary record showing the extent and importance of the corresponding climatic and tectonic events.

References :

GAUTAM P. & FUJIWARA Y. 2000. Magnetic polarity stratigraphy of Siwalik Group of Karnali River section in western Nepal, *Geophysical Journal International* 142, 821-824.

GAUTAM P. & RÖSLER W. 1999. Depositional chronology and fabric of Siwalik group sediments in Central Nepal from magnetostratigraphy and magnetic anisotropy, *Journal of Asian Earth Sciences* 17, 659-682.

NAKAYAMA K. & ULAK P.D. 1999. Evolution of fluvial style in the Siwalik Group in the foothills of the Nepal Himalaya, *Sedimentary Geology* 125, 205-224.

ULAK P.D. & NAKAYAMA K. 2001. Neogene fluvial systems in the Siwalik Group along the Tinau Khola section, west central Nepal Himalaya, *Journal of Nepal Geological Society* 25, 111-122.

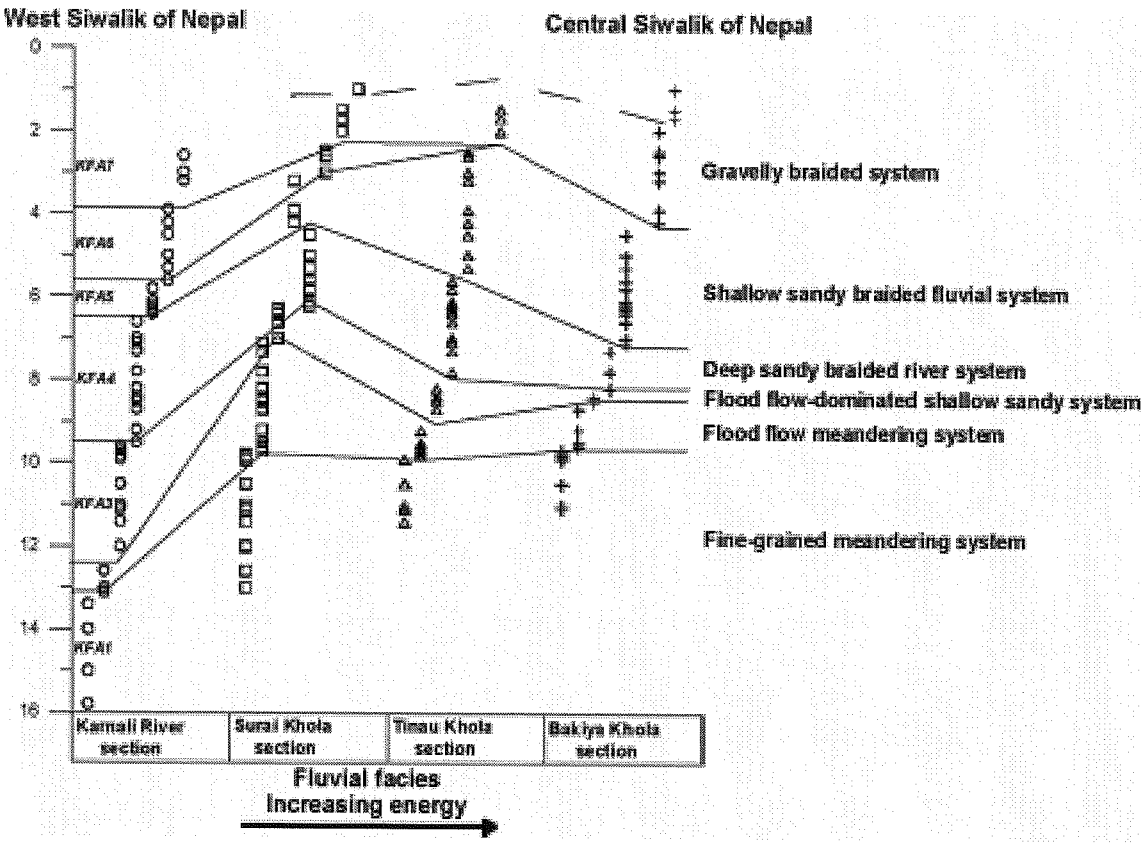

Figure 1 : Regional evolution of the neogene fluvial system in Central and Western Nepal from the comparison of the Siwalik sedimentary facies recognized along the Bakiya, Tinau, Surai and Karnali sections. Fluvial facies are shown along the horizontal axis. Magnetostratigraphic ages come from Gautam & Fujiwara (2000) and Gautam and Rösler (1999). For each section, increasing energy facies from fine-grained meandering system, flood flow meandering system, flood flow-dominated meandering system, deep sandy braided system, shallow sandy braided system to gravely braided system are found from left to right, respectively.

SR-ND ISOTOPIC STUDY OF MAIN CENTRAL THRUST ZONE IN NEPAL HIMALAYA

Takeshi IMAYAMA (1) and Kazunori ARITA (1)

(1) Department of Earth and Planetary Sciences, Graduate School of Science, Hokkaido University, Kita-10, Nishi-8, Sapporo, 060-0810, Japan.

The Higher Himalayan Crystalines (HHC) have been thrust over the Lesser Himalayan metasediments (LHS) along the Main Central Thrust (MCT) for a distance of 140km (Schelling and Arita, 1991). Althought the HHC has been considered to be equivalent to the Indian basement, recent U-Pb zircon and Sm-Nd isotopic studies suggest other origins of the HHC (Parrish and Hodges, 1996; DeCelles et al., 2000).

The metamorphic rocks of the MCT zone (between the Upper MCT or MCT and the Lower MCT; Arita, 1983) in the entire Nepal Himalaya can be distinguished from the HHC in terms of Nd isotopic ratio. Nd and Sr isotopic ratios provide complementary information on the discrimination among the metamorphic rocks of the HHC, the MCT and the LHS zones. We analyzed Nd and Sr isotopic ratios of the metamorphic rocks in Taplejuang -Ilam area (far-eastern Nepal; Fig. 1a), Pokhara-Kusma area and Maikot-Ila area (central-western Nepal; Fig. 1b). Samples from the HHC and MCT zones indicate ¶≈Nd (0) values of –10 to –18.5 and –19.5 to –26, respectively. The¶≈Nd (0) values of the MCT zone are similar to those (–19.5 to –26) of the LHS zone. The metamorphic rocks of the MCT and the LHS zones are distributed more widely in Sr isotopic ratio than those of the HHC zone. Considering our data in addition to the published data, the protoliths of the MCT zone are different from those of the HHC all over the Nepal (Fig. 2). In other words, the MCT is originally a material boundary between the LHS and the HHC.

Parrish and Hodges (1996) suggested that the MCT zone has been developed in a tectonic melange composed of units derived from both the HHC and the LHS after the protoliths of the HHC had been deposited unconformably on the protoliths of the LHS. According to them, the Mongol quartzite of the MCT zone in Langtang area (central Nepal) has Nd isotopic ratio plotted within the range of the HHC. However, the metamorphic rocks of the MCT zone in other areas mostly have similar Nd isotopic ratios to those of the LHS. If the MCT, which can be traced along the 2,000 km-long strike of Himalayan orogen, were formed on an unconformable contact, the units derived from the HHC and the LHS should be found ubiquitously in the MCT zone outside of the Langtang area. Above mentioned regional difference in isotopic ratios between the HHC and the MCT zone support that the MCT zone was activated in the Tertiary, taking advantage of the pre-Tertiary collision contact (DeCelles et al., 2000) rather than an unconformable contact (Parrish and Hodges, 1996).

References

SCHELLING, D. & ARITA K., 1991. *Tectonics*, **10**, 5, 851-862.
PARRISH R. R. & HODGES, K. V., 1996. *G. S. A. Bulletin*, **108**, 7, 904-911.
DECELLES P. G., GEHRELS G. E., QUADE J., LEREAU B. & SQURLIN M., 2000. *Science*, **288**, 497-499.
ARITA K., 1983. *Tectonophysics*, **95**, 43-60.
ROBINSON D. M., DECELLES P. G., PATCHETT P. J. & GARZION C. N., 2001. *E. P. S. L.*, **192**, 507-521.
AHMAD T., HARRIS N., BICKLE M., CHAPMAN H., BUNBURY J. & PRINCE C., 2000. *G.S.A. Bulletin*, **112**, 3, 467-477.

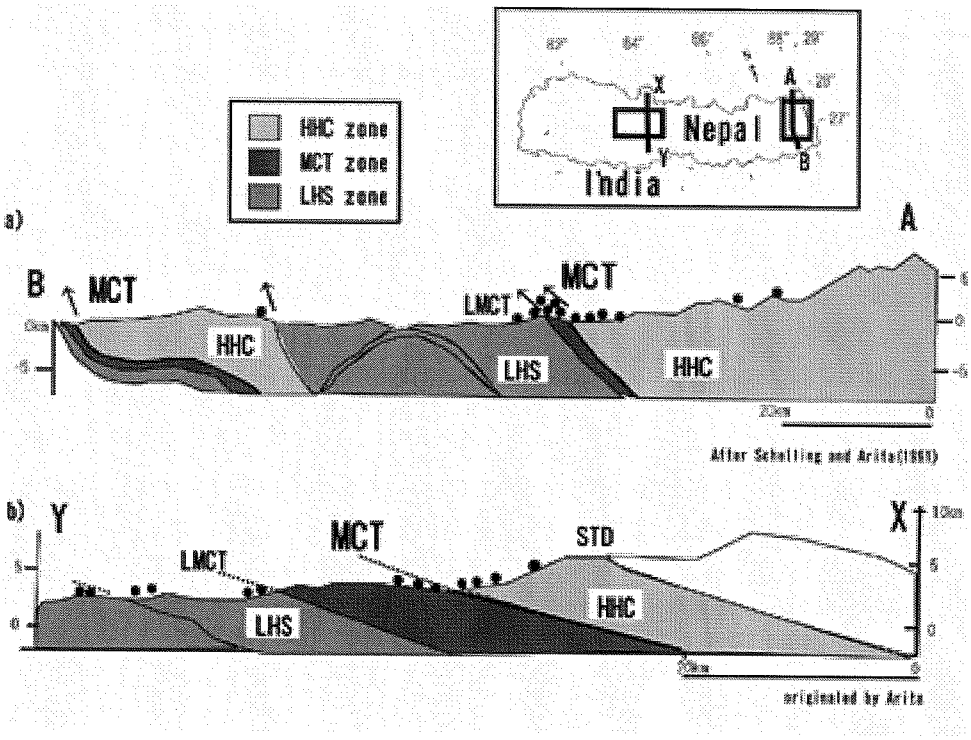

Fig. 1. Geological cross-section of a) far-eastern and b) central-western Nepal showing position of the samples.

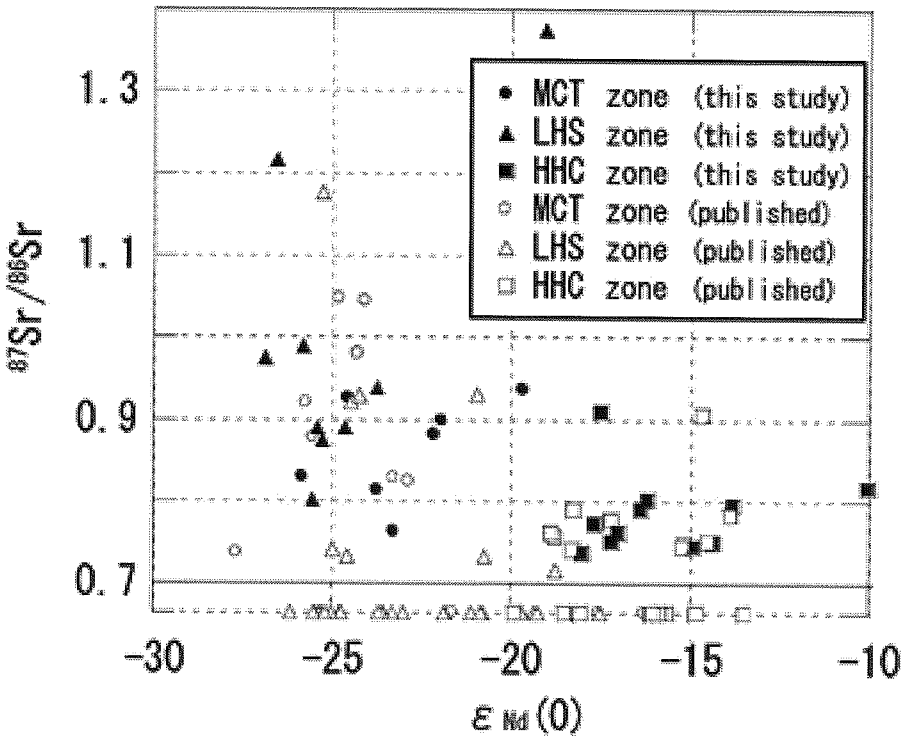

Fig. 2. $^{87}Sr/^{86}Sr$-É$\sqrt{}_{Nd}$ (0) from Nepal and Garhwal Himalayas
Data from Nepal (Parrish and Hodges, 1996; Robinson et al., 2001) and Garhwal (Ahmad et al., 2000, except for the Outer Lesser Himalaya).

THE PLUTONIC CRUST OF THE KOHISTAN ISLAND ARC (NW PAKISTAN): HISTORY FROM LA-ICPMS U-PB ZIRCON AGES OF INTRUSIVE UNITS.

O. JAGOUTZ[1], J.P. BURG[1], T. IIZUKA[2], T. HIRATA[2], S MARUYAMA[2], S. HUSSAIN[3], H. DAWOOD[3], N.M. CHAUDHRY[4]

[1] Department of Earth Sciences, ETH Zurich, Sonneggstr. 5, CH-8092 Zurich, Switzerland
[2] Department of Earth and Planetary Sciences, Tokyo Institute of Technology, Tokyo 152, Japan
[3] Pakistan Museum of Natural History, Garden Avenue, Shakarparian, 44 000 Islamabad, Pakistan
[4] University of the Punjab, Quaid-e-Azam Campus 54590 Lahore, Pakistan

Geological understanding of the evolution of the Kohistan arc is essential to infer and comprehend crust differentiation taking place in active island arcs. Based on Rb-Sr whole rock data, Ar-Ar hornblende dating and the presence or absence of a penetrative fabric within the plutonic units, the evolution of the Kohistan Batholith has been subdivided into three stages: The first stage (104-85 Ma) is composed of a bi-modal sequence of foliated gabbro-diorites and trondhjemites. Stage 2 consists of undeformed gabbros, diorites and granites that intruded between 85 and 40 Ma with a general basic to acid trend. Sr and Nd contents supportively indicate an increasing crustal component for the younger stage 2 plutons (Petterson et al., 1993; Petterson and Windley, 1991). Stage 3 refers to swarms of circa 30 Ma old leucogranitic dykes. Intra arc deformation features as in stage 1 plutons are attributed to the collision of the Kohistan arc to the Karakoram terrain to the north (Coward et al., 1986; Petterson and Windley, 1985; Treloar et al., 1996). Based on this hypothesis, suturing is inferred to have occurred between the age of deformed and undeformed plutons, between 104 and 85 Ma (Treloar et al., 1996). Accordingly, stage 1 plutons would have intruded during the intra-oceanic stage of the Kohistan arc and undeformed stage 2 plutons would have intruded after the Kohistan-Karakoram collision, in an Andean type margin. Plutons that have intruded the Dir-Utror volcanites have been attributed to stage 2 based on an ^{40}Ar-^{39}Ar hornblende age of 48 ± 1 Ma (Treloar et al., 1989), whereas foliated dioritic plutons to the south of the Barul Banda slates were attributed to stage 1 (Sullivan et al., 1993). Treloar et al. (1996) noted that the geochronological information contains a gap in magmatic activity within the Dir area. Therefore, above authors proposed time-depending and iterative extensional and compression within the Kohistan arc. Major magmatic hiatuses are due to compression around 104-85 Ma and between 75-55 Ma. Additional geochronological information is essential to clarify the geological evolution of the arc and the related arc building mechanisms.

We present 7 U-Pb zircons ages from dioritic to granitic plutonitic samples of the SW Kohistan paleo-island arc using laser ablation ICP-MS. Results indicate continuous magmatism from at least 78 Ma to approx 44 Ma. Relative dating of plutons according to the presence or the absence of a penetrative fabric is inconsistent with the U-Pb ages since undeformed rocks may be older than deformed ones. A ~72 Ma intrusion age of a granite intrusive into the Dir-Utror volcanites contradicts the assumed late Eocene age of these rocks. A comparism of whole rock geochemical data suggests that these metavolcanites could be, at least in part, the effusive equivalents of the Chilas gabbronorite. This information supports the conclusion that the Kohistan arc went through an arc wide rifting stage around 85 Ma. Accumulation of volcanite and sediments occurred in a related basin that possibly existed until collision of India with Kohistan.

COWARD, M.P., WINDLEY, B.F., BROUGHTON, R.D., LUFF, I.W., PETTERSON, M.G., PUDSEY, C.J., REX, D.C., AND ASIF, K.M., 1986, *Geol. Soc. Sp. Pub* **19**, p. 203-219.

PETTERSON, M.G., CRAWFORD, M.B., & WINDLEY, B.F., 1993, *J. Geol. Soc.London*, **150**, p. 125-129.

PETTERSON, M.G., & WINDLEY, B.F., 1985, *Earth and Planetary Science Letters*, v. **74**, p. 45-57.

—, 1991, *Earth and Planetary Science Letters*, **102**, p. 326-341.

SULLIVAN, M.A., WINDLEY, B.F., SAUNDERS, A.D., HAYNES, J.R., AND REX, D.C., 1993, *Geol. Soc. Sp. Pub*, **74**, 139-160.

TRELOAR, P.J., PETTERSON, M.G., JAN, M.Q., AND SULLIVAN, M.A., 1996, *J. Geol. Soc.London*, **153**, 681-693.

TRELOAR, P.J., REX, D.C., GUISE, P.G., COWARD, M.P., SEARLE, M.P., WINDLEY, B.F., PETTERSON, M.G., JAN, M.Q., AND LUFF, I.W., 1989, *Tectonics*, **8**, 881-909.

Note Page

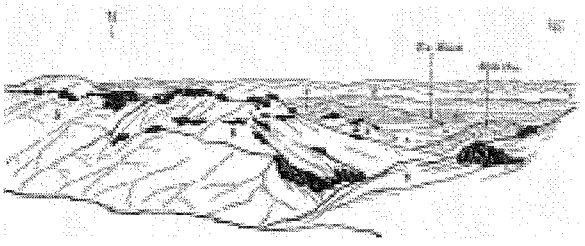

Kiogar, Gansser, 1939

THE ZONED ULTRAMAFIC BODIES OF THE CHILAS COMPLEX IN THE KOHISTAN ISLAND ARC (NW PAKISTAN)

O.JAGOUTZ[1], O.MÜNTENER[1], J-P.BURG[2], P.ULMER[2], E.JAGOUTZ[3], T.PETTKE[2]

[1] Institute of Geological Sciences, University of Bern, Baltzerstr. 1, CH-3012 Bern, Switzerland
[2] Department of Earth Sciences, ETH Zurich, Sonneggstr. 5, CH-8092 Zurich, Switzerland
[3]Max-Planck Institute für Kosmochemie, Saarstrase 23, Mainz, Germany

In this study we examined the zoned ultramafic bodies of the Chilas complex, one of the largest (250*40 km) intrusion in the Kohistan paleo-island-arc (Pakistan). The Chilas complex is a large mafic, lower-crustal intrusion dominantly composed of gabbronorite. Associated zoned ultramafic complexes (UMA) are concentrically but irregularly zoned with a massive dunitic core and subsequent shells of lherzolite, plagioclase-bearing lherzolite and plagioclase-bearing olivine-pyroxenite. Amphibole-bearing lherzolite with porphyroclastic clinopyroxene (hereafter called porphyroclastic lherzolite) appears as xenoliths within the dunitic core. Dunitic dykes cross-cut the porphyroclastic lherzolite. Larger tens-of-centimeters wide dykes have straight contacts but smaller centimeter-sized dykes display irregular contact relations with embayment of dunite into porphyroclastic lherzolite. Centimeter- to tens-of-centimeters-big xenoliths of the porphyroclastic lherzolite are found in increased quantity within the contact-zone between massive dunite and porphyroclastic lherzolite. Accordingly, at least in part the origin of the dunitic core is replacive and related to melt-rock reaction between the porphyroclastic lherzolite and an ascending melt.

The observed zoning of the ultramafic bodies is defined by a decrease in olivine content and increase of pyroxene content towards the surrounding gabbronorite. The increase of pyroxene content is irregular and within a single lherzolite outcrop, dyke-shaped pyroxene-richer domains can be identified. Reactive halos around gabbronoritic dykes and dunite blocks within lherzolite indicate lherzolite formation due to a second melt-rock reaction. The zoning is interpreted as the result of an irregular centimeter to meter-scale reaction front developed at the contact between ultramafite and surrounding gabbronorite.

Upwards shearing and bending of layered gabbronorite indicate a relative upwards movement of the ultramafite units in respect to the surrounding gabbronorite sequence. In summary the contact relations indicate intrusion of a dunitic unit under sub-solidus conditions into a partially consolidated gabbronorite mush, which in turn has intruded and reacted with the ultrabasic rock forming lherzolite and pyroxenite.

Based on the analytical gap in plagioclase mineral chemistry between the UMA sequence (An_{98-83}) and the main gabbronorite (An_{64-40}) the UMA were originally interpreted as being issued from a different, more mafic magma batch than the gabbronorite (Jan et al., 1984; Khan et al., 1989). Our above described field observations complemented by whole-rock and mineral major and trace elements and Sm-Nd isotopic data challenge the previously published interpretation of the origin of the Chilas complex and the associated ultramafite: The mineral major element chemistry and the Nd isotopic signature of the ultramafite and the surrounding gabbronorite sequence indicate fractionation of both from a common sequence. The anorthite (An) content of plagioclase indicates a continuous overlapping sequence from An_{91} to An_{41} for the gabbronorite sequence (including tonalite occasionally present within the gabbronorite) and An_{98}-An_{80} for plagioclase-bearing lherzolite. Additionally, the primitive mantle normalized trace element pattern of plagioclase from UMA and gabbronorite sequences are parallel. The absolute trace element concentration increases with decreasing anorthite number. The mineral major and trace element chemistry is consistent with differentiation of a common magma body for the entire Chilas complex.

Even so the mineral chemistry and the succession from dunite- lherzolite-pyroxenite is in accordance with the classical Bowen discontinuous differentiation sequence, the field observations are not in accordance with an ordinary cumulate origin in terms of crystal settling in a magma chamber. Based on the replacive origin of the dunitic core and the mutual intrusive relationship between gabbronorite sequence and ultramafic units the ultramafic bodies are interpreted as melt channels of the Chilas complex. Numerical simulation indicate that melt channels with a certain melt filled porosity can get mobilized due to buoyancy forces and intrude into overlying, less dense sequences, if the channels reaches down into denser rocks e.g. into the upper mantle. Accordingly, the Chilas ultramafite bodies could be surface exposure of melt channels which reach down into the upper mantle possibly down to the melting region. The high and low Mg# of olivine in the dunitic core of the ultramafic bodies indicate that melt evolved during its ascent in the melt channels. We estimate the composition of the flux in and out of those melt channels: Based on primitive olivine chemistry, the primary melt that entered the channels to form the Chilas complex was a high Mg# basaltic liquid in equilibrium with a high Mg# mantle assemblage. The bulk composition of the gabbronorite sequence essentially represents the melt composition of the melt getting out of the channels. Estimates indicate a basaltic-andesitic bulk composition of the Chilas gabbronorite, with a low Mg# bulk composition matching closely estimates of lower crustal compositions.

JAN, Q. M., M. U. K. KHATTAK, M. K. PARVEZ, & B. F. WINDLEY, 1984, *Geological Bulletin, University of Peshawar*, **17**, p. 163-169

KHAN, M. A., M. Q. JAN, B. F. WINDLEY, J. TARNEY & M. F. THIRLWALL, 1989, *Special Paper - Geological Society of America*, **232.** 75-94

EROSION VS. TECTONIC EXHUMATION: FT AND RB-SR MINERAL AGES FOR FOLD-CONTROLLED TECTONICS FROM NORTHWEST HIMALAYA

A. K. JAIN (1), Devender KUMAR (2), Nand LAL(3), R. M. MANICKAVASAGAM (4), A. K. CHOUDHARY (4), and Sandeep SINGH (4)

(1) Department of Earth Sciences, IIT Roorkee, Roorkee, India
(2) National Geophysical Research Institute, Hyderabad, India
(3) Department of Earth Sciences, Kurukshetra University, Kurukshetra, India
(4) Institute Instrumentation Center, IIT Roorkee, Roorkee, India

In the present-day context of uplift of convergent orogenic belts, exhumation processes for unroofing the deeply-buried sequences are linked with erosion, tectonics, or a combination of both, where one of the mechanism may dominate over the other. In highly mountainous and climatically-wet active convergence zones, surfacial erosional processes have recently gained significance, where concomitant removal of eroded detritus through denudation by an efficient fluvial drainage system has been recognized as an effective alternative to tectonic exhumation mechanism to modify structural and internal deformation patterns for achieving steady state. Tectonically-driven exhumation models essentially are either fault or density dependent in different geodynamic settings ranging from deeply subducted ultrahigh pressure (UHP) terrains to buoyant magma diapirism.

In the northwestern parts of the Himalaya, tectonic exhumation of the slab-like Himalayan Metamorphic Belt (HMB) has been constrained through low to medium temperature using fission track dating of apatite and zircon and Rb-Sr muscovite – biotite geochronology in this work. This folded belt is bounded by the Main Central Thrust (MCT) along the base and the South Tibetan Detachment System (STDS) at its top and thrust over the Lesser Himalayan Belt. Beneath the overthrust metamorphic pile, low temperature FT apatite – zircon geochronometers reveal that the Bandal Granite has exhumed @ 1.5 mm/a between 4.5 and 2.7 Ma and 1.1 mm/a since 2.7 Ma within the core of the Kulu – Rampur Window. When traced along the hinge zone of the KR Antiform towards Manali and Rohtang, the overthrust HHC has exhumed @ 1.0 mm/a since 2.9 Ma to Present and 0.8 mm/a between 6.5 and 2.9 Ma. In remarkable contrast to the exhumation pattern within the hinge zone, southwestern limb of the KR Antiform around Kulu region has exhumed slowly at rates accelerating from 0.4 to 0.6 mm/yr since ~ 13 Ma to Present, while its northeastern limb has experienced an exhumation of 0.6 mm/yr since 4.9 Ma. Very slow exhumation rates between 0.2 and 0.3 mm/a across this antiform at higher temperatures ~ 300 ± 50 and 500 ± 50°C, constrained by Rb-Sr biotite and muscovite geochronology, reveal that exhumation of this fold was initiated since ~ 6.5 Ma, only. In addition, exhumation patterns along hinge zones of the following domes and windows of the NW Himalaya provide undisputed evidences of fastest growing structures during Pliocene–Pleistocene as a very efficient mechanism for tectonic exhumation of deeply-buried sequences in the Himalaya: the Chandrabhaga Antiform (0.8 0.3 mm/a since 3.6 ± 0.6 Ma or 1.8 ± 0.8 mm/a since 2.2 ± 0.5 Ma), the Tso Morari Dome (0.5 ± 0.2 mm/a since 7.5 Ma), the Suru Antiform (0.8 ±0.3 mm/a since 3.8 ± 0.3 Ma), the Chisoti Dome (1.4 ± 0.4 mm/a since 2.1 ± 0.1 Ma), and the Kishtwar Window (3 mm/a since 1 Ma), and the Nanga Parbat (10 mm/a since 0.4 Ma)and Eastern Himalaya Syntaxes (10 mm/a since 0.5 Ma),. The Himalayan antiforms and windows appear to have started growing since 7.5 Ma from deep interior of the orogen and have migrated southward sequentially. Differential exhumation rates over very short distances indicate that these are not controlled by climatic factors like heavy monsoon precipitation and consequential accelerated erosion.

Note Page

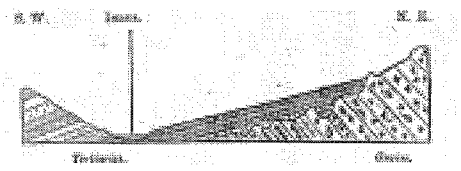

Indus valley, Lydekker, 1883

PETROLOGY OF THE ULTRAMAFIC-MAFIC TORA TIGGA COMPLEX, KOHISTAN MAGMATIC ARC, NORTHERN PAKISTAN

M. Qasim JAN (1) and Barry L. WEAVER (2)

(1) Department of Geology, University of Peshawar, Peshawar, NWFP, Pakistan.
(2) School of Geology &Geophysics, Univ. of Oklahoma, Norman, OK730911, USA.

Several mafic-ultramafic complexes occur in the southern fringe of the Kohistan magmatic arc in the hanging wall of the Indus suture. Of these, the Spat, Jijal, and Tora Tigga ones have particularly interesting rock associations. The Tora Tigga complex (TTC) is emplaced in garnetiferous amphiolites of the Kamila belt in southwestern Dir. The main mass covers some 6 sq. km, but there also are several small bodies in the area. The TTC comprises amphibolitized gabbronorites and a range of ultramafic rocks seemingly intruding them. These consist of: 1) olivine-rich ultramafites (dunite, peridotite, Hbl peridotite, serpentinite), 2) pyroxene-rich ultramafites (diopsidite, Ol diopsidite, Hbl diopsidite, Hbl orthopyroxenite, Hbl websterite, Hbl-Ol websterite), and 3) hornblendites (pure hornblendite, Pxn hornblendite, Pl hornblendite). Intruding these are trondhjemitic dykes (commonly < 3m across) and thin dolerite dykes.

The mutual relationships of the ultamafic rocks are complex, although in some places the hornblendites appear to be last in sequence of emplacement. Locally, the rocks are in zonal dispositions that differ in detail from those in Alaskan-type concentric complexes. The preponderance of hornblendites and hornblende in the ultramafic rocks is puzzling. There are over 2.0 km long and 0.5 km wide bodies of nearly pure, medium to course hornblendites, and small dykes of Pl hornblendites containing up to 25 cm long crystals. These may be magmatic in origin. Then there are veins, patches and pools of hornblende that may have developed during the amphibolite faciers hydration of the complex. But hornblende shows complicated textural relations in the rocks (Jan et al., 1983) which may have resulted from reactions between olivine/pyroxene and magma. Some textural features can be explained better by invoking deformation and annealing, even though there is no evidence of pervasive deformation in the ultramafic rocks. Tight isoclinal folding, and plastic and brittle dformation, including porphyroclastic fabric, in the trndhjemites suggest that the complex was deformed during Kohistan-India collision.

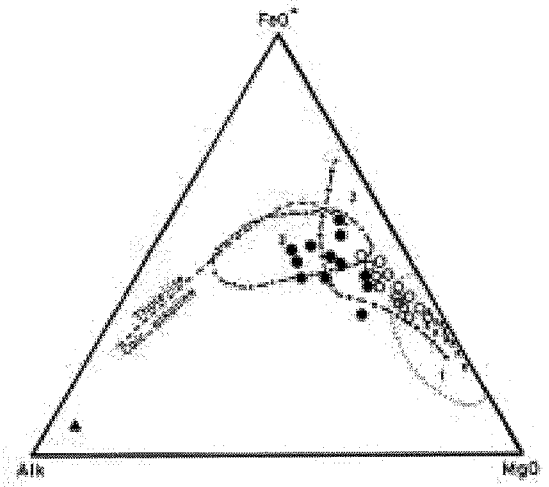

Fig. 1. MFA plot of Tora Tigga rock analyses. Crosses represent olivine/pyroxene ultramafites, open circles are hornblendites, closed circles are gabbronorites and triangle is trondhjemite-Tholeiite-calc-alkaline boundary is after Barker and Arth, 1976. Fields of ophiolite cumulates (1), and island arc cumulates (2) and non-cumulates (3) are after Coleman (1977) and Beard (1986), respectively.

In several aspects the TTC compares well with the Chilas complex. The main gabbronorites in the latter appear to extend through Swat towards southern Dir. So, it is likely that the TTC is the equivalent of the ulramafic-mafic-anorthosite association of the Chilas complex. Major and trace element XRF analyses were performed on representative rocks of the complex. Ti - Zr - Sr, MnO - TiO2 - P2O5, Cr - Y, Ni - FeO/MgO, Cr - FeO/MgO, and FeO/MgO - SiO2 relations suggest that the gabbronorites are calc-alkaline in nature and comparable with rocks of subduction-related magmas. On MgO - FeO* - Na2O+K2O diagram (Fig. 1), the analyses of ultamafic rocks, hornblendites and gabbronorites classify calc-alkaline and plot in the fields of island arc cumulates and non-cumulates.

Mantle-normalized multi-element spidergram for three hornblendites and a representative gabbronorite is shown in Fig. 2.

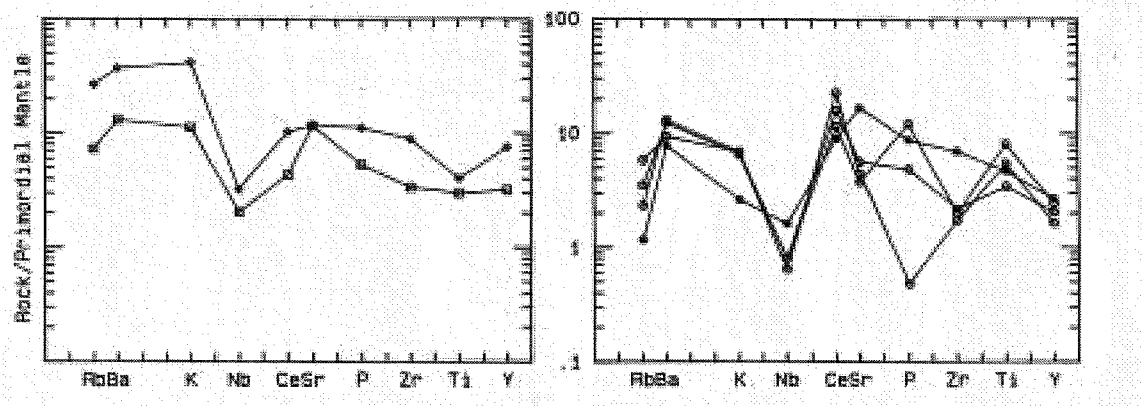

Fig. 2. Multi-element plots of Tora Tigga analyses normalized to primordial mantle values of Wood (1979). TTC gabbronorite (asterics) and hornblendites (circles) are shown in righ, and low-K tholeiite (squares, after Holm, 1985) and present day lavas from Mariana island (rhombs, after Hole et al., 1984) in left. Despite their plutonic nature and likely effects of cumulus minerals, the TTC rocks compare well with the island arc rocks.

The analyses are characterized by distinct Nb trough, positive anomalies for Ba and P, and rather high K/Rb ratios. The gabbronorite also shows a peak for Sr (because of mineralogical control, the hornblendites show negative Sr and positive Ti anomalies. These features, notably the Nb troughs, are commonly displayed by subduction-related magmas and are fasairly similar to the Chilas complex (Khan et al., 1989). A comparison of the present data with low-K thoileiite (Holm, 1985) and lavas of the active volcanoes of the Mariana arc (Hole et al., 1984) suggests that the TTC rocks were generated in an island arc -type setup.

(References)

BARKER E. & ARTH J.G. 1976. *Geology*, 4, 596-600.
BEARD J.S. 1986. *Geology*, 14, 848-851.
COLEMAN J.G. 1977. Ophiolites. Springer, Berlin.
HOLE M.J., SAUNDERS A.D., MARINER G.F. & TARNEY J. 1984. *Jour. Geol. Soc.*, 141, 453-472.
HOLM P.E. 1985. *Chem. Geol.*, 51, 303-323
JAN M.Q., BANARAS M., GHANI A. & ASIF M. 1983. *Geol. Bull, Univ. Peshawar*, 16, 11-29.
KHAN M.A., JAN M.Q., WINDLEY B.F., TARNEY J. & THIRWALL M.F. 1989. *Geol. Soc. Amer.,Spec. Paper*, 232, 75-94.
WOOD D.A. 1979. *Geology*, 7, 499-503.

MESOZOIC PHLOGOPITE-BEARING OLIVINE WEBSTERITE IN TETHYAN-HIMALAYA

JIANG Wan[1,2], YE Peisheng[1], HU Daogong[1], WU Zhenhan[1]

1, Institute of Geomechanics, CAGS, Beijing, PRC, 100081, namco@sina.cn
2, Institute of Geology Survey, Tibet, PRC, 850000

Phlogopite-bearing olivine websterite, which was not notified before, was found for the first time in Tethyan-Himalaya, just along the South Tibet Thrust. The rock intruded in undeformed gabbro diabase, which intruded in strongly deformed Triassic to Juassic strata. Combined with surrounded gabbro diabase, they could be thought as a mafic-ultramafic complex. The websterite and the gabbro diabase were thought to be Cenozoic products in 2003's field work, and after zircon SHRIMP dating work in 2004, It is now recognized that this complex formed at c. 147Ma. Both occur as cumulates and as non-cumulate dykes.

The olivine websterite carries olivine (Fo83–Fo80, 30Vol%), orthopyroxene (En:Fs:Wo= 81:15:4, 25Vol%), clinopyroxene (En:Fs:Wo=51:41:8, 25-30Vol%), phlogopite (10-15Vol%) and plagioclase (about 5Vol%), amphibole, opaque minerals. According to the mineral composition of the rock, it seems that this rock could be named after lherzerlite, but from the cumulated texture with some narrow clinopyroxene layers, the rock is thought to be olivine websterite, and from the compositions of the mineral a high Cr, Ti and K character should be imaged. And crystallization temperature was assessed by partitioning of Mg/Fe between orthopyroxene and clinopyroxene, which indicates the magma crystallized at 1350-1450°C.

Whole rock chemical composition was investigated by XRF and ICP-MS, the olivine websterite has Mg# ([100Mg/(Mg +Fe_{tot})] of 79 and 43wt% SiO_2, MgO (25.5wt%), average 6wt % Al_2O_3 and 4.1wt % CaO, TiO_2(1wt %), MnO (0.17wt %), Na_2O+K_2O >1wt% . Relatively high values for loss on ignition (>5%) show some alteration of the rocks. Chromium concentration is about 3000ppm, where Ni is about only 495ppm, the rock is lightly REE(LREE)-enriched [$(La/Sm)_N$=2, and $(La/Yb)_N$=5-7] and shows positive Eu anomalies, trace element has a flat pattern compared with primary mantle but P strongly deplete. Concentrations of PGE have also been determined.

Tethyan-Himalaya consists of late Precambrian to early Paleozoic sedimentary and metasedimentary rocks (Yin et al 1988, Burchfiel et al 1992) and thick Permian to Cretaceous continental margin sequences (Brookfield 1993). Basalt from Sangxiu Formation J_3-K_1s shows OIB character (Zhu Dicheng, 2004), does olivine websterite have any relation with these basalts? And concerning about the economic value of such mantle-derived rock, can we find olvine websterite in other site in Tethyan-Himalaya? How and why such rocks are exposed in this terra attract us to do some more research.

Note Page

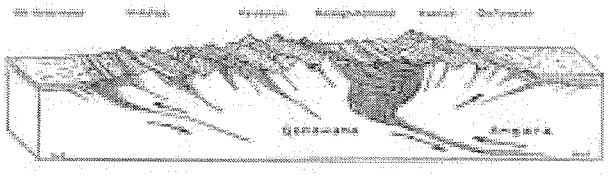

Wyss, 1931

CENOZOIC REACTIVATION OF THE EAST GOBI FAULT ZONE: EXTRUSION TECTONICS IN SOUTHEASTERN MONGOLIA

Cari L. JOHNSON (1) and Laura E. WEBB(2)

(1) Dept. of Geology and Geophysics, University of Utah, Salt Lake City, UT USA
(2) Dept. of Earth Sciences, Syracuse University, Syracuse, NY USA

Northeast-trending faults define a structural corridor traceable for more than 250 km along strike through the center of the East Gobi basin in southeastern Mongolia (Fig. 1). This corridor, the East Gobi Fault Zone (EGFZ), has occupied an intraplate position since late Paleozoic time (Badarch et al., 2002), and has experienced multiple phases of deformation in the Mesozoic and Cenozoic. The reactivation history of the EGFZ Late Triassic sinistral shear (Lamb et al., 1999), Early Cretaceous NW-SE extension (Graham et al., 2001), and mid-Cretaceous transpressional basin inversion (Johnson, 2004). New data document the most recent phase of movement along the EGFZ: sinistral strike-slip on northeast-trending faults during Cenozoic time (Fig. 1).

Cenozoic faults in the EGFZ generally do not have a clear surface expression (i.e., modern fault scarp) except where they cut extremely resistant units (e.g., Paleozoic basement rocks), or where they have been exposed through erosion in small gulleys. At Tavan Har (Fig. 1), fault gouge, breccia, and slivers of Paleozoic basement rocks are associated with fault strands that define a zone ranging from 10s to 100s of meters wide. Trenching along the southern fault strand reveals clay and powder-sized fault gouge and breccia, in multiple zones 1—10 m wide. Most significantly, trenches reveal that unconsolidated alluvium was caught up and deformed during faulting. A thin, undisturbed layer of unconsolidated sediment overlaps both the gouge and deformed sediment zones. Thus, as predicted by subsurface studies (Johnson, 2004), the most recent phase of movement along the EGFZ is post-Upper Cretaceous in age.

Fault slip data are dominated by northeast-trending sinistral faults that exploit the preexisting structural grain of the EGFZ. Field data and digital elevation models both suggest that conjugate, NW-trending dextral strike-slip faults play a more prominent role in the southwestern portion of the study area (Ulgay Khid and Tsagan Subarga blocks, Fig. 1). Results from inversion of Cenozoic fault slip data sets for each of the study localities all indicate that faulting accommodated NNW-SSE horizontal shortening and ENE-WSW horizontal extension (Fig. 1).

Palinspastic restorations of Cenozoic offset in the southeast Mongolia—China border zone are not currently available: various piercing points have been proposed, but are not yet tested. For example, Yue and Liou (1999) proposed some 400 km (± 50 km) of left-lateral offset beginning in the Late Oligocene (c.f. Yue et al., 2001). In contrast, Lamb et al. (1999) proposed 185-235 km of offset, and note that much of this deformation was likely associated with Late Triassic shear. Amount of offset along the EGFZ is critical for regional basin reconstructions. If the amount of Cenozoic offset was significant (i.e., > 100 km), this could have major economic implications for mining and petroleum interests (Johnson, 2004), which seek to exploit potential offset units. Both Yue and Liou (1999) and Lamb et al. (1999) propose offset of Paleozoic arc terranes, although they are not in agreement about specific piercing points or timing of movement. Given the evidence for left-lateral shearing in the Late Triassic, at least some of this offset must be Early Mesozoic.

Although the amount of offset and exact timing of Cenozoic fault activity awaits further study, these observations suggest that strike-slip faulting in southeastern Mongolia may have been kinematically linked with movement on the Altyn Tagh fault in China. This linkage would extend deformation associated with eastward extrusion of China relative to Mongolia, driven by the India-Asia collision, at least 500 km further to the northeast.

As observed in the East Gobi basin, inherited structural weaknesses play an important role in the evolution of intraplate sedimentary basins subject to multiple phases of deformation over long time periods (250 my), and associated with distinct tectonic phases including compression, extension, and wrench faulting. It is unlikely that the EGFZ is defined by one single terrane boundary along its full length, but rather that a series of arc systems together define the heterogeneous crust of Mongolia since the Paleozoic, reactivated during the Late Triassic, Early and middle Cretaceous, and again in the Cenozoic.

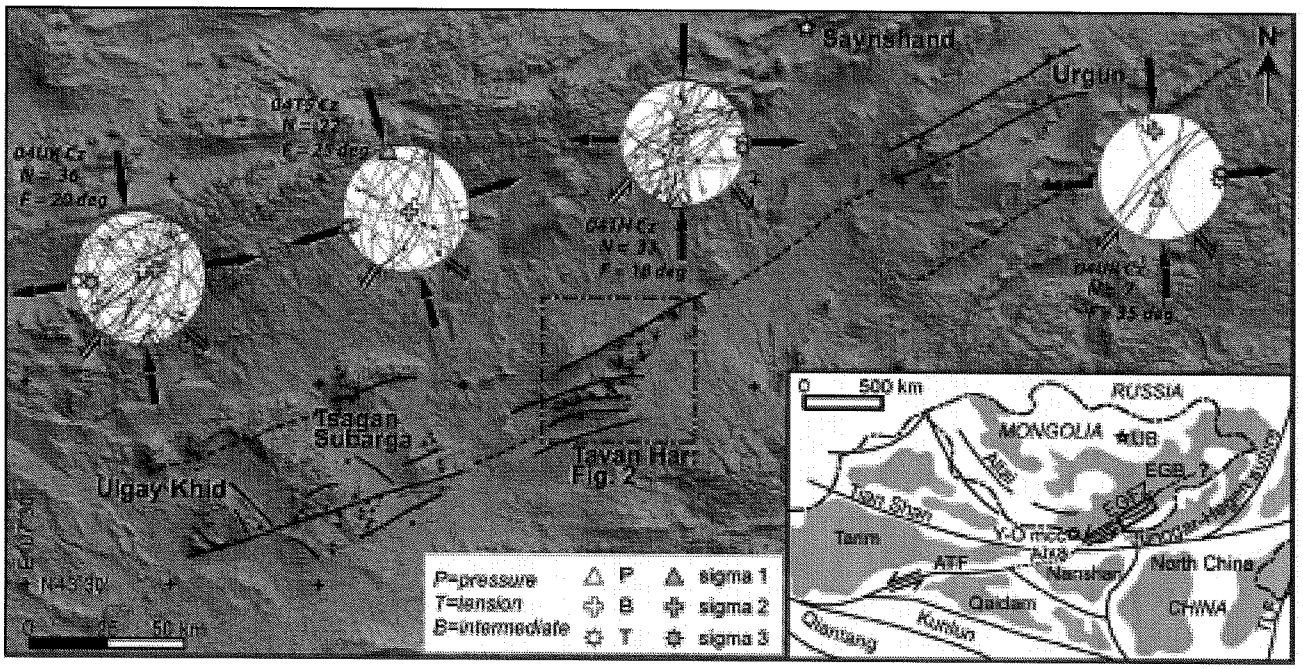

Figure 1. Inset: Regional map showing major tectonic elements of China and Mongolia. Shaded areas are Mesozoic-Recent sedimentary basins. ATF = Altyn Tagh fault, EGB = East Gobi basin, EGFZ = East Gobi Fault zone, TLF = Tan Lu fault, Y-O mcc = Yagan-Onch Harhan metamorphic core complex, UB = Ulaan Baatar. Main figure: Digital elevation model of the study area, showing main localities (small black dots mark selected 2004 field stops), and fault traces (dashed where inferred). Stereonets show Cenozoic fault slip data and principal stress orientations for each locality (see text for further explanation). UK = Ulgay Khid, TS = Tsagan Subarga, TH = Tavan Har; UR = Urgun. N = number of data; F = arithmetic mean of fluctuations between observed and calculated glide directions associated with stress axes determinations. Latitude-longitude grid (+ symbol) is shown in 30 minute intervals (reference point at lower left).

BADARCH, G., CUNNINGHAM, W.D., AND WINDLEY, B.F. 2002. A new terrane subdivision for Mongolia; implications for the Phanerozoic crustal growth of Central Asia. *J. Asian Earth Sci.*, **21**. 87-110.

GRAHAM, S.A., HENDRIX, M.S., JOHNSON, C.L., BADAMGARAV, D., BADARCH, G., AMORY, J., PORTER, M., BARSBOLD, R., WEBB, L.E., AND HACKER, B.R. 2001. Sedimentary record and tectonic implications of late Mesozoic rifting, southeast Mongolia. *Geol. Soc. Am. Bull.*, **113**. 1560-1579.

JOHNSON, C.L. 2004. Polyphase evolution of the East Gobi basin: sedimentary and structural records of Mesozoic-Cenozoic intraplate deformation in Mongolia. *Basin Res.*, **16**. 79-99.

LAMB, M.A., HANSON, A.D., GRAHAM, S.A., BADARCH, G., AND WEBB, L.E. 1999. Left-lateral sense offset of upper Proterozoic to Paleozoic features across the Gobi Onon, Tost, and Zuunbayan faults in southern Mongolia and implications for other Central Asian faults. *Earth and Planet. Sci. Lett.*, **173**. 183-194.

YUE, Y., LIOU, J.G., AND GRAHAM, S.A. 2001. Tectonic correlation of Beishan and Inner Mongolia orogens and its implications for the palinspastic reconstruction of North China. *Geol. Soc. Am. Mem.*, 194. 101-116.

YUE, Y., AND LIOU, J.G. 1999. Two-stage evolution model for the Altyn Tagh Fault, China: *Geol.*, **27**. 227-230.

CURRENT SHORTENING ACROSS THE HIMALAYAS OF NEPAL

F. JOUANNE (1), J. L. MUGNIER (2), J. F. GAMOND (3), P. LE FORT (2) M. R. PANDEY (5), L. BOLLINGER (4), M. FLOUZAT (4) AND J. P. AVOUAC (4).

(1) LGCA, UMR CNRS 5025, Universit´e de Savoie
(2) LGCA, UMR CNRS 5025, Universit´e J. Fourier
(3) LGIT, UMR CNRS 5559, Universit´e J. Fourier
(4) CEA, LDG, Bruyeres le Chatel, France
(5) Department of Mines and Geology, Lainchaur, Katmandu, Nepal

Underthrusting of the Indian lithosphere beneath the Himalayas occurs during the Quaternary period along a gently north-dipping main basal detachment (main Himalayan thrust: MHT), from which the southernmost emergent ramp (main frontal thrust: MFT) branches. Historical seismicity shows that slip on the MHT is frequently accommodated through M > 8 shallow earthquakes, but shows a seismic gap in western Nepal. This absence of major historical earthquakes in western Nepal can be explained either by an aseismic slip on the MHT or a long lived elastic strain accumulation. To test these hypotheses, the present-day displacement field has been measured for a GPS network formed of 35 sites. The updated solution presented in this contribution combines data from 1995, 1997, 1998 and 2000 measurements (Fig 1) (Jouanne et al., 2004). The lack of deformation (less than 3 · 10_8 yr_1) through the outer belt does not fit with a regional aseismic slip along the southern part of MHT. A less than 3 mm yr_1 aseismic slip could nonetheless affect restricted areas of the outer belt. In contrast, a strain accumulation of more than 30 · 10_8 yr_1 is measured south of the Higher Himalayas, in a zone where an intense microseismicity reflects a stress build-up. It is presumably generated by locking of the aseismic creep that occurs along the MHT beneath the Higher Himalayas and Tibet. The displacement field is simulated by a dual-dislocation model that takes into account the pattern of microseismicity, and particularly a segmentation between central and western Nepal. The best fit between the measured and simulated displacement fields is obtained with 19 mm yr_1 thrust and 0–1 mm yr_1 dextral strike-slip components along a 117_NE dislocation locked to a depth of 20–21 km beneath western Nepal, and 19–20 mm yr_1 thrust and 0–2 mm yr_1 dextral strike-slip components along a 108_NE dislocation locked to a depth of 17–21 km beneath central Nepal. The width of the locked zone between the main frontal thrust and the creeping zone is of the same order, but rather greater, in western Nepal than in central Nepal. Therefore it is expected that M > 8 earthquakes could occur in western Nepal.

Reference

JOUANNE F., MUGNIER J. L., GAMOND J. F., LE FORT P., PANDEY M. R., BOLLINGER L., FLOUZAT M. and AVOUAC J. P., *Geophys. J. Int.* (2004) **157,** 1–14

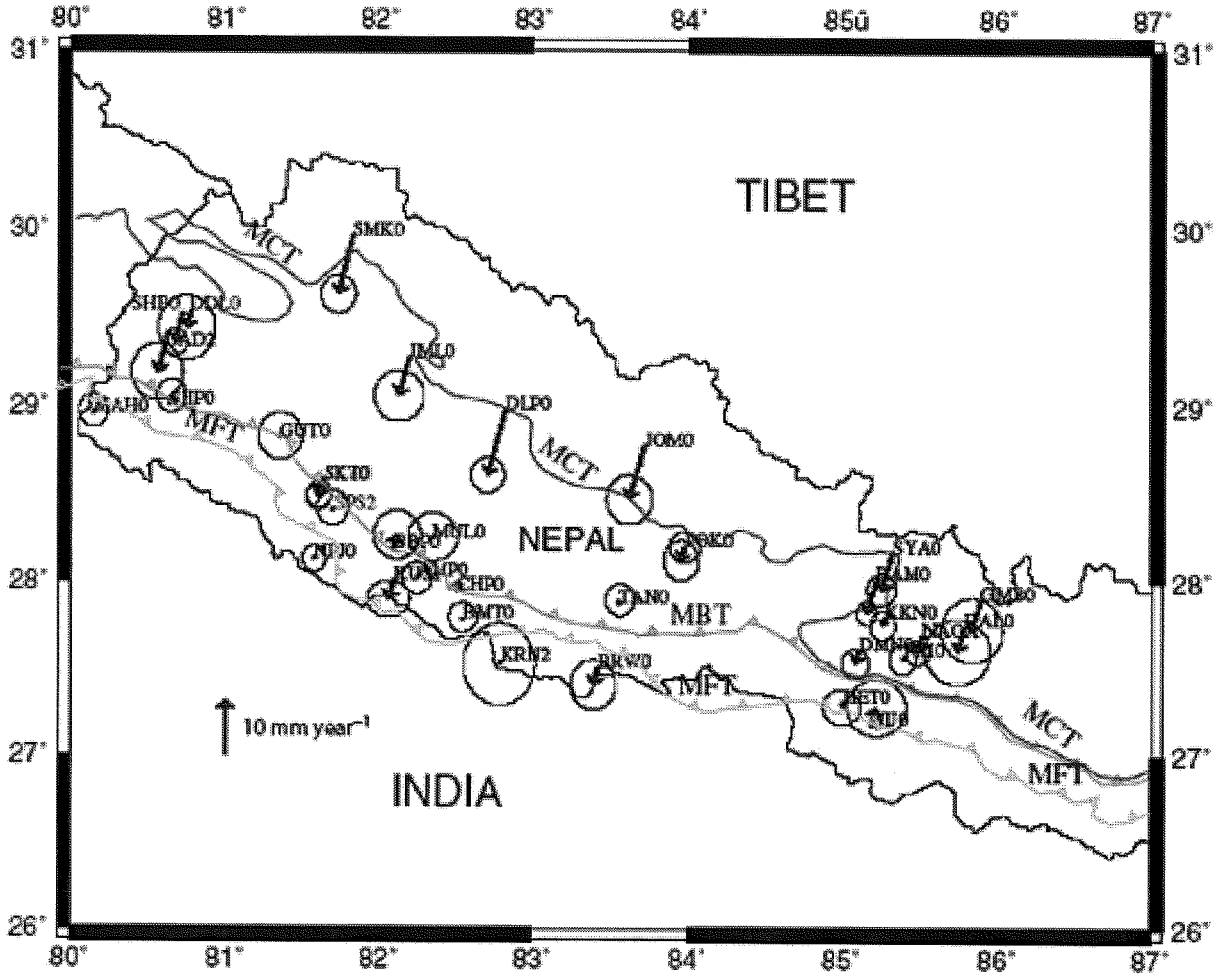

Figure 1. Velocities of the 34 sites of the LDG-IDYLHIM network in the India fixed reference frame. This reference frame, has been defined by the determination of the Eurasia/India rotation pole (latitude: 28.5_N, longitude: 22.1_E, rotation: 0.4_ Myr_1). It allows to account for the displacements of IISC (southern India), BRW0, KRN2, MAH0, NIJ0 and NPJ0 in the Ganga plain, Eurasia being considered fixed.

PETROGENETIC CHARACETERISTICS AND TECTONIC SETTING OF THAK GAH AND JIJAL ULTRAMAFIC-MAFIC COMPLEXES OF KOHISTAN ARC, PAKISTAN

Allah B. KAUSAR (1), Christian PICARD (2), Yutaka TAKAHASHI (3), Masumi U. MIKOSHIBA (3) Hiroshi YAMAMOTO (4), Said R. KHAN (5), Tahseenullah KHAN (5), and Hafeez U. REHMAN (4)

(1) Geological Survey of Pakistan, Sector H-8/1, Islamabad 44000, Pakistan
(2) Laboratorire de Geodynamique des Chaines Alpines, Observatoire des Sciences de l'Univers de Grenoble, Grenoble University, France.
(3) National Institute of Advanced Industrial Science and Technology, Geological Survey of Japan, Tsukuba 305-8567, Japan
(4) Department of Earth and Environmental Sciences, Faculty of Science, Kagoshima University, Kagoshima, Japan
(5)Geoscience Laboratory, Geological Survey of Pakistan, Shahzad Town, Islamabad 44000, Pakistan

The Kohistan block, consisting of (from north to south) Yasin Group, Kohistan Batholith, Chilas Complex, Kamila Amphibolites and Jijal Complex, is widely regarded as one of the most complete and best exposed section from ultramafic underpinnings, at the crust/mantle boundary, to surface volcanic rock through the crust of an oceanic island arc. This block has a number of ultramafic-mafic blocks and the most important ones are: 1) Thak Gah Ultramafic-Mafic Association (TUMA) and 2) the Jijal Ultramafic-Mafic Complex (JUMC).

The JUMC extends for more than 35 km E-W and is some 15 km wide in its central part. The complex is thought to have been uplifted in Miocene time along the Main Mantle Thrust, which separates Indian plate to the south from the JUMC to the north. To the north, the JUMC is separated from the Kamila Amphibolites by the Pattan fault. On the western side, a serpentinite body separates the JUMC from the Kamila Amphibolites. The JUMC contains a continuous sequence of ultramafic through mafic plutonic rocks. The ultramafic unit consists of cumulate dunite at the exposed structural base, which grade upward to purely cumulate pyroxenite rocks. Wehrlite and pyroxenite compositional bands increase in abundance upward until pyroxenite becomes the major lithologies. Pyroxenites vary from pure clinopyroxenite to clinipyroxene dominant websterite. Websterite grades upward into garnet websterite, which in turn grade into garnet gabbro.

The TUMA occurs mostly in eastern part of the Chilas village. It is composed mainly of olivine (with or without clinopyroxene) cumulate (dunite, wehrlite) and plagioclase-clinopyroxene-orthopyroxene cumulate (two pyroxene gabbro), with minor amount of clinopyroxene-orthopyroxene cumulate (pyroxenite). The layered structure of plagioclase-clinopyroxene-orthopyroxene cumulate often develops on the olivine cumulate, with sedimentary structure such as graded bedding and trough bedding etc. Within each gabbroic band, the eastern side is younger and grade into massive part from fine-layered bottom part.

MORB normalized trace element distribution patterns of garnet gabbro and gabbro from JUMC and TUMA respectively show moderate enrichment in Rb, Ba and K relative to other incompatible elements and with strong negative Ta and Nb anomalies, a feature characteristic of arc-related rocks. The chondrite normalized REE patterns of pyroxenites from Thak Gah and Jijal appear very similar. They are characterized by low REE (0.1 to 2 times chondrite), a strong LREE depletion and flat HREE patterns, a feature typical of mineral segregation.

The ferromagnesian minerals show large chemical variations in accordance with the lithological change in the series from dunite to garnet gabbro. The Mg-number of olivine and clinopyroxene decreases systematically through the rock series dunite through olivine clinopyroxenite, websterite, garnet websterite, to garnet gabbro (Fo94-Fo78). The most aluminous clinopyroxene occurs in the most differentiated, olivine- and orthopyroxene-poor garnet gabbro. The rocks from the Jijal Complex were crystallized from a melt at pressures between 10 and 12 kbar and equilibrated at temperatures of 800° to 1100° C based on the phase relationships in the cumulus assemblages, clinopyroxene-orthopyroxene, garnet-orthopyroxene and garner-amphibole thermometry and olivine-spinel thermometry.

In the TUMA, Chilas Complex, mineralogy and textural relationships are quite different from the JUMC. Pyroxene and spinel are more Fe-rich. As a result, chemical trends in minerals do not indicate the same high-pressure origin as Jijal cumulates. Based on phase relationships in the cumulate assemblages, pressure of formation for this association can be constrained within 5 to 6 kbar. They were crystallized from a melt at a temperature of 800° to 950° C, as deduced from geothermometry based on two pyroxene pairs. This lower pressure implies that TUMA probably represents a contemporary, shallower magma chamber in the same Kohistan arc.

GEOCHEMISTRY AND PETROLOGY OF TAXKORGAN ALKALINE COMPLEX, NW HIMALAYA

Shan KE, Zhaohua LUO, Xuanxue MO

Department of Geosciences and Land Resources China University of Geosciences, Beijing, China

A-type granitoids were divided into two chemical groups by their distinct geochemical characteristics (Eby, 1990, 1992). These two types have very different sources and tectonic settings. Group one (A_1) represents magmas derived from mantle but emplaced in continental rifts or during intra-plate magmatism. The second group (A_2) represents magmas derived from continental or underplated crust that has been through a cycle of continent-continent collision or island-arc magmatism,

Taxkorgan Cenozoic alkaline complex is A-type granitoids. This complex, distributed along the Karakorum fault, is the largest alkaline intrusive rocks (~ 200km^2) in the Karakorum Region and located in the middle east of the Pamirs syntaxis. The complex mainly consists of alkaline syenites and subalkaline granitoids with the rock types from aegirine syenite, quartz syenite, syenogranite, to biotite monzonitic granites. There are different dates about its age: 52.0±0.66Ma of augite syenite (Ar-Ar of Kf, Zhang et al., 2000), 18Ma of syenogranite (Ar-Ar of Kf, Jiang, 1992), 18.2Ma of syenite (K-Ar of Kf, Xu, 2000), and 11.058±0.76Ma of monzonitic granite (Ar-Ar of Kf, Xu, 2000). We use U-Pb zircon to obtain the more precise ages about the complex: 11.1±0.3 Ma, 11.3±0.4Ma.

The predominant minerals in the complex are K-feldspar, quartz, oligoclase, aegirine-augite and their crystallized sequence is K-feldspar—aegirine, oligoclase—quartz. K-feldspars commonly have perthitic texture. SiO_2 of the complex is wide from 50.71% to 72.32 %. The Cenozoic complex is rich in K_2O (6.47%, n=13), CaO (5.62%, n=13), and low in Na_2O (2.79%, n=13). It should be noted that K_2O doesn't show tendency with evolution of Na_2O and Si2O of the magma. This implied that this intrusive rock might have been affected by K-rich fluid. Average K_2O+Na_2O is 9.27£•£¨K_2O/ Na_2O ratio is about 1.00~3.90 and Al2O3°÷K2O+Na2O (molecule). These features show that the complex is a high-K, metaluminous, and alkaline pluton. According to its mineralogy, the syenite was a high-temperature magma without fractional crystallization process during its evolution.
The alkaline complex shows enrichment in LREE, Ba, Sr, and has high $^{87}Sr/^{86}Sr$ ratio (0.708 ~ 0.711) and very low εNd (-14.03 ~ -8.47). The pluton almost has no negative Eu anomaly (δEu: 0.83-0.92). Its $^{206}Pb/^{204}Pb$, $^{207}Pb/^{204}Pb$, $^{208}Pb/^{204}Pb$, $^{87}Sr/^{86}Sr$, $^{143}Nd/^{144}Nd$ ratios all show close relationship with Indian Oceanic sediments and enriched mantle source (EMII).

The tectonic setting of the alkaline complex suggests undoubtedly that the complex should belong to A_2-type, since the Pamirs syntaxis has been in the process of compression and orogeny at ~11Ma and even at present. Its geochemical characteristics and element ratios, however, display similar features to A_1-type. This A-type granitoids represents the low degreed partial melting of the lower thickened crustal material—eclogite and had been affected by K-rich fluid during its evolution. Besides, the partial melting lower crust had been assimilated with an enriched mantle source region(s) carrying a subduction component inherited from Indian oceanic crust that had probably subducted to the place beneath the Pamirs syntaxis. The Taxkorgan complex was the product during the magmatism resulted from the regional extension (e.g. slab break off or large scaled strike-slip movement) in the process of orogeny.

G. Nelson Eby, chemical subdivision of the A-type granitoids: petrogenetic and tectonic implications, Lithos, 1992 (20): 641-644.
Zhang Yuquan, Xu Ronghua, et al., Geochemistry of granitoids, In: Pan Yusheng ed. Geological Evolution of the Karakorum-Kunlun Mountains, Beijing, Sciences Publishing House (in Chinese), 2000: 209-258
Jiang Chunfa, Yang Jinshui, et al., Opening-closing tectonics of Kunlun Mountains (in Chinese). Beijing, Geological Publishing House, 1992.
Xu Ronghua, Zhang Yuquan, et al., Geochemistry of granitoids, In: Pan Yusheng ed. Geological Evolution of the Karakorum-Kunlun Mountains (in Chinese), Beijing, Sciences Publishing House, 2000: 209-258

RESOURCE ASSESSMENT AND HYDROCARBON POTENTIAL OF THE FORELAND BASIN PETROLEUM SYSTEM OF NEPAL

Dharma Raj KHADKA and Stephen J. LIPPARD
Department of Petroleum Engineering and Applied Geophysics NTNU, Trondheim, Norway

The kingdom of Nepal covers the central sector of the Himalaya. It is geologically subdivided into the Tethyan Himalaya , the Higher Himalaya, the Lesser Himalaya , the Sub- Himalaya (Siwaliks) and the Terai (northern part of the Indo–Gangatic basin) from north to south. The southern two geological proviences comprise the Himalayan foreland basin which has a potential for hydrocarbon generation, migration and entrapment The regional hydrocarbon occurrences in the Himalayan region such as Potwar basin of Pakistan in the west, Assam petroleum provience of NE India in the east and Ganga basin to the south of Nepal support the possibility of hydrocarbon occurrences in Nepal.

The resource assessment of the foreland basin petroleum system of Nepal has been carried out focusing on the following input parameters: 1. Area of closure has been estimated using a normal distribution considering same structural evolution of the foreland basin system of Potwar and Nepal and also aspected closure areas and their likeyhood of occurrences.2. Thickness of reservoir rock is considered using Melpani Formation of Nepal whose thickness varies from 100 to 230 m in the outer Lesser Himalaya of Nepal(outcrop analogue) and considered to be primary reservoir found below the Terai plain and Siwaliks of Nepal. 3. Geometrical factor, Net to Gross are assigned using uniform distribution considering minimum and maximum values in the range of 10%. 4. Porosity is considered based on the primary reservoir facies of the Melpani Formation. So the lower level of porosity of Melpani Formation is assigned as a normal distribution. 5. Trap fill and HC saturation range are assigned considering the min. to max. range of 20%. 6. Recovery rate of oil is considered world average value 35-40%, but a 10% range is assumed in this case. Each value is assigned signalling uncertainty. Oil formation volume factor (Bo) is 1.28m3/m3 mean, min-1.1 and max.-1.45. Gas-Oil Ratio (GOR) is 1.61 m3/m3, min- 11 and max- 33 (considering GOR in Potwar). Since Siwaliks foreland basin in Nepal has no proven hydrocarbon accumulation, all the marginal risk factors have been set. Hydrocarbon source is set to 1 because there are number of gas and oil seeps in Dailekh area of western Nepal. Timing is set to 0.5 since generation, migration and accumulation of hydrocarbon and trap formation are considered to be contemporaneous which could have an uncertainty. Migration is set to 1 because there are gas and oil seeps in Dailekh area. Similarly the potential reservoir facies is set to 0.98 considering the relatively clean sandstones of the Melpani Formation. No other Tertiary clastics are included in the analysis . There are three conditional risk factors: probability of adequate trapping, probability of reservoir quality and probability of hydrocarbon accumulation. The resource diagram (figure1) shows the frequency distribution of the recoverable oil resources in a singal prospect.

Figure 1 - Resources diagram

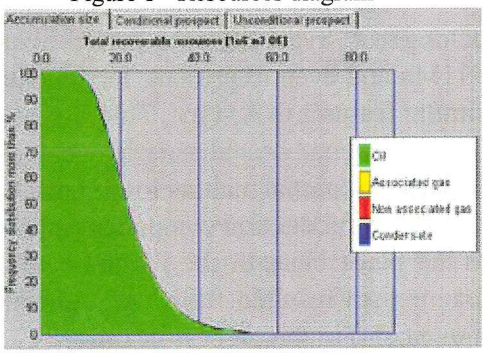

The conditions that favor the discovery of a potentially commercial volume of hydrocarbons in the basin are: i) the distribution of the source and reservoir rocks, and ii) the time relation between entrapment and the maturation, expulsion and migration of the hydrocarbon. The basin's hydrocarbon resource is estimated using the 'GeoX/Starter' software. The recoverable oil resources in a single prospect are estimated to be 22.5 MMBL.

Friedenreich O., Slind O,L, Pradhan U.M..S. and Shrestha R.B. 1994. Canad. J. Petreoleum Geophysics, 30, 103-114
Husson L., Mugnier J.L., Leturmy P. and Vidal G. 2004. AAPG Memoir Thrust Tectonics and Petroleum Systems.
PEPP DMG 1996. Petroleum Exploration Opportunities in Nepal : Brochure
Upreti B.N. 1999. J. Asian Earth Sciences, 17, 577-606.
Wandrey C.J, Law B.E. and Haider Ali Sha H. 2004 Patala-Nammal Composite Total Petroleum System, Kohat-Potwar Geologic Province, Pakistan, U.S. Geological Survey Bulletin 2208-B.
Wandrey C.J. 2004.Sylhet-Kopili/Barail-Tipam Composite Total Petroleum System, Assam Geologic Province, India U.S. Geological Survey Bulletin 2208-B.

Note Page

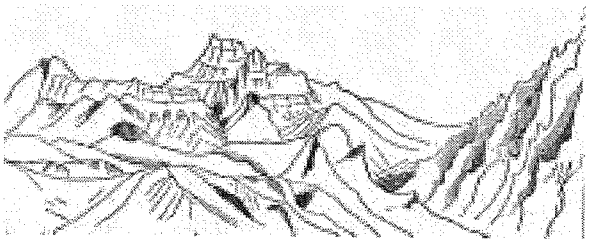

Shingo La, La Touche, 1888

IMPLICATIONS OF COMAGMATIC RELATIONSHIP BETWEEN GANITOIDS OF SOUTHEAST KOHISTAN, NW HIMALAYAS, PAKISTAN.

Muhammad Ahmed KHAN

The Kohistan island arc terrane in the northwestern Himalayas of N. Pakistan is sandwiched between the Indian and Karakoram plates (Tahirkheli et al. 1979; Coward et al. 1986). The base of the arc is occupied by a major stratiform ultramafic-gabbroic complex (the Sapat-Babusar complex), which overrides the crust of the Indian plate along the Indus suture (i.e., the Main Mantle Thrust; MMT) (Jan et al. 1993). It was intruded into the base of a thick pile of metavolcanics (the Kamila belt), which comprise a tectonic collage of MORB-type tholeiitic basalts, island-arc tholeiites and calc-alkaline andesites. The Chilas complex comprising ultramafic and gabbronorite rocks, is also intrusive into the Kamila belt, it is emplaced onto the top rather than the base of the Kamila belt (Khan et al. 1989).

A sizeable proportion of granitoid rocks are present in the south-eastern part of Kohistan, which are intruded the Kamila amphibolites (Khan M.A. 1997). These are predominantly a dioritic in composition, but include gabbros, granodiorites, granites and trondhjemites (Fig. 1). The granitoids occur in two types: 1) large sheet-like lenticular masses, and 2) minor intrusives in the form of veins, sills or dykes. Three large sheets like bodies are mapped. The body in the northern part is up to 5 km thick, and stretch east to west for a distance over 40 km in the mapped area. The constituent rocks are foliated but deformation is distinctly less intense than the other two southern bodies. All these bodies are composite, comprising gabbros, diorite/ tonalite, granodiorite and granite. Deformation has obscured contact relations between what would have been cross-cutting sequential phases. The minor intrusions of granitic and trondhjemitic composition are abundantly present in form of veins, sills and dykes; and are characterized by variance in distribution. The southern bodies are strongly foliated with the general trend of the host rock and the xenoliths mostly aligned to the foliation. Strong shearing transformed the rocks into balstomylonite gneisses. The mineral assemblage consists of quartz, plagioclase, amphibole, epidote, chlorite, biotite, muscovite, sphene, magnetite and apatite. The granitoids are classified into gabbro, gabbroic-diorite, diorite, granodiorite and granite.

The granitoids show a wide variation in SiO_2 content. TiO_2, Al_2O_3, Fe_2O_3, MgO, CaO and MnO show linear decreasing trends with increasing SiO_2 while P_2O_5 show inflection at SiO_2 60 wt%. Na_2O is increasing with SiO_2. Nb and Zr show a slight enrichment with respect to increasing SiO_2 whereas Y and Sr show scatter trend. Transitional elements like Ni, Co, Cr, V, Cu, Zn and Sc all show a general depletion with increasing SiO_2, suggesting their mutual compatibility. Spidergrams show three distinctive patterns; i) flat patterns showing small enrichment in HFSE with lack of Nb anomaly, ii) enrich in LILE sloping towards right with Nb anomaly and showing coherent trends with increasing LILE component from diorite through granodiorite to granite and iii) the highly spiked patterns sloping towards right with more depletion in Nb, P, Zr, Ti and Y (Fig. 2).

The HFSE enriched granitoids are comparable with the host metavolcanics of MORB type Kamila amphibolite belt. Both types of rocks sloping towards left and show a close similarity. This supports the petrogenetic link between this group of granitoids and the host Kamila amphibolites. The HFSE depleted granitoids include rock types gabbro, diorite, tonalite, granodiorite and granite, which show enrichments in LILE relative to HFSE and coherent behavior. Majority of the rocks have typical subduction-related chemistries, with characteristics such as low TiO_2 and high Al_2O_3 contents, high LIL/HFS element ratios, variable inter-alkali ratios and distinct Nb depletion anomalies, all consistent with magma derivation from a metasomatized mantle wedge above a subduction zone.

The trondhjemites characterized by enriched HFSE are in intimate association with Kamila amphibolite belt and the HFSE depleted trondhjemites with highly spiked patterns with very low incompatible trace element abundances are considered 1) to be unrelated with gabbro-diorite-tonalite-granodiorites-granite series, and 2) to have resulted from partial melting of Kamila amphibolites. The melt produced for these trondhjemites whether due to the process of subduction or due to the intrusion of 90-80 Ma Chilas Complex and crustal shortening accompanying the Jal shear zone of 80 Ma (Treloar et al., 1990) is not clear.

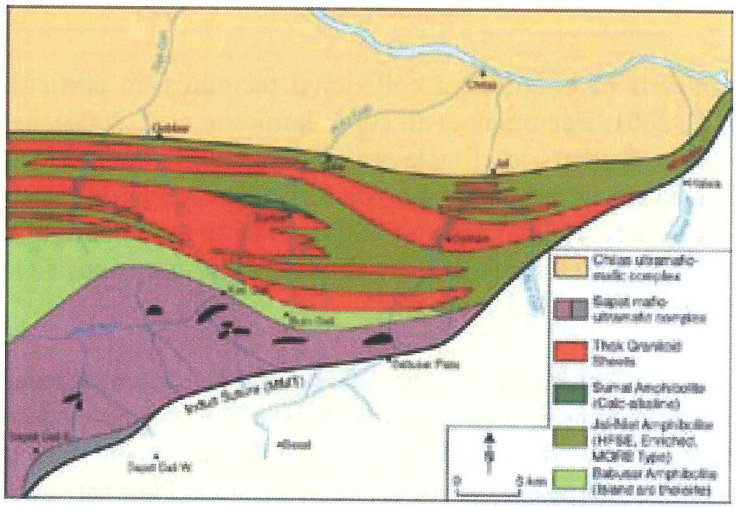

Figure 1: Geological map of south-eastern part of Kohistan, Pakistan, showing the Three varities of Amphibolites (Jal-Niat, Babusar & Sumal), Granitoids (Thak), Mafic-Ultramafic (Sapat), Main Mantle Thrust (MMT) and the Chilas Complex.

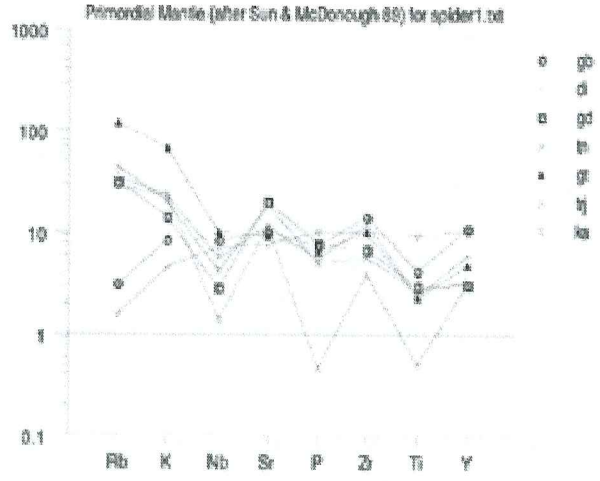

Figure 2: Spidergrams showing the contrasting and mutual behavior of the granitoids of the studied area: i) Gabbros(gb) showing similarity with the host Kamila amphibolites (ka), ii) diorites (di) through granodiorites (gd) to granites (gt) showing the same patterns and iii) the trondhjemites (trj) having the same trend but very distinctive with very low HFSE concentration.

References:

COWARD M.P., WINDLEY B.F., BROUGHTON R.D., LUFF D.C., PETTERSON M.G., PUDSEY C.J., REX D.C. & KHAN M.A. 1986. *Collision Tectonics. Geol. Soc. London.*, **19.** 203-219.

JAN M.Q., KHAN M.A. & QAZI M.S. 1993. *Himalayan Tectonics. Geol. Soc. London.*, **74.** 113-121.

KHAN M.A., JAN M.Q., WINDLEY B.F., TARNEY J., & THIRLWAL M.F. 1989. *Geol. Soc. America.*, **232.** 75-94.

KHAN M Ahmed., 1997. Ph.D. Thesis, Tectonic Evolution of SE Kohistan, NW Himalayas, Pakistan. Peshawar University.

TAHIRKHELI R.A.K. & JAN M.Q. 1979. *Geol. Bull. Uni. Peshawar.*, **11.** (map in pocket).

TRELOAR P.J., BRODIE K.H., COWARD M.P., JAN M.Q., KHAN M.A., KNIPE R.J., REX D.C. & WILLIAMS M.P. 1990. *Exposed Cross-Sections of the Continental Crust. Amsterdam.*, 175-214.

CONSTRAINTS ON TECTONIC MODELS FROM CRUSTAL MELT FORMATION IN SOUTHERN TIBET

Jessica KING (1), Nigel HARRIS (1), Tom ARGLES (1), Randy PARRISH (2)

(1) Department of Earth Sciences, CEPSAR, The Open University, Milton Keynes MK7 6AA, UK
(2) NERC Isotope Geosciences Laboratory, British Geological Survey, Keyworth, Notts NG12 5GG, UK

Numerical models of continental collisional tectonics, in particular that of 'Channel Flow'(Beaumont et al. 2001; Beaumont et al. 2004; Jamieson et al. 2004), have become the focus of much debate between workers in Himalayan orogenic evolution. Alternative models include crustal wedge extrusion or rapid exhumation of mid-crustal material pro-ward of the original suture zone (Grasemann & Vannay 1999; Lee et al 2003). The proposition that the High Himalayan Crystalline Series (HHCS) represents the gravity-driven ductile extrusion of a low-viscosity channel of mid-crustal material is a testable hypothesis.

Using a combined geochemical, geochronological and structural approach, field relationships within the North Himalayan gneiss domes may be unravelled by simple observation and dating of crosscutting relationships created by multiple post-collisional crustal melt emplacement events. Further to this, the isotopic characteristics of the HHCS (Indian Plate) are quite distinct from those of the Lhasa Terrane (Eurasian Plate). Hence, the sources and conditions of melt emplacement either side of the suture can now be traced, thus delineating the evolving crustal architecture beneath southern Tibet.

South of the Tsangpo suture, Tertiary granitic melts within the North Himalayan antiform (27.5 to 10 Ma) are sourced from the HHCS. The granites range in emplacement geometries from anatomising sheets and dykes (Kuday granite complex intruding gneisses and migmatites of the Sakya gneiss dome) to discrete plutons (Donggong, Kouwu, Gomdre, Mabja granites). North of the suture, there is no evidence for melts sourced from the HHCS being emplaced, as might be expected if melting of the boundaries of the underthrust HHCS sheet were to facilitate channel flow. Instead, mid-Miocene crustal melting (19-10 Ma) within the Lhasa Terrane is restricted to dacitic dykes and flows from a source that is isotopically identical to anatectic gneisses from Nyainqentanglha (exhumed from the mid-crust of the Lhasa Terrane).

In this study, structural relationships observed near Kuday village, at the northern contact of the Sakya Gneiss Dome and Tethyan Sedimentary Series (TSS) cover, show D1 top-to-south shear, penecontemporaneous with onset of Oligocene granitic melt emplacement. D1 is overprinted by D2 top-to-north relative reversal in shear motion, seen clearly as shear band development in the TSS cover, penecontemporaneous with later episodes of Kuday melt emplacement. This is consistent with southwards extrusion of a ductile channel. Preliminary data from a north-trending, mid-Miocene (~11.5 Ma) dyke swarm that intrudes the TSS (Indian Plate) at Kuday, suggest that these melts share the same Nyainqentanglha source as dykes from north of the suture, establishing that melting from this source extends *south* across the suture. These observations are consistent with the southwards propagation of anatectic material from the Lhasa Terrane, possibly by channel tunnelling. D2 deformation of the dykes is restricted to their margins, implying dyke emplacement occurred towards the end of D2.

Observations at the Mabja and Gomdre granites (Zhang et al. 2004) find that these plutons (14 -10 Ma), located to the west of the main Sakya gneiss dome, form prominent footwall scarps bounded to the west by young N-S striking normal faults. Observations of a similar nature have been made at the Kampa dome (Quigley et al 2004), east of the Sakya dome. Whilst sharing a similar D1 and D2 shear history with those seen in the Sakya dome at Kuday, a further D3 top-to-SSW shear (N-S compression) is well developed in the TSS near the southern contact of the Gomdre granite. The Gomdre granite is also pervasively foliated with top-to-south sense of shear. Tectonic contacts with these N-S normal faults are cataclastic at Mabja and Gomdre. These observations, therefore, are not consistent with ductile channel flow, and display a closer affinity to some form of 'core-complex' mechanism of exhumation for these mid-Miocene granite domes.

The presence of the dacite melts north of the suture have previously been ascribed to extension and crustal melting following 'slab-breakoff' or some form of convective removal of mantle lithosphere (Maheo et al 2002; Williams et al. 2004). The observed E-W extension and proposed 'core-complex' formation are consistent with this hypothesis. However, the presence of dacitic melts south of the suture still requires an explanation involving some form of southward material flow. So, while it may be fair to say that the youngest tectonic style of dome exhumation in evidence relates more to exhumation by pure shear extension, observations substantiate that mass balance and exhumation of mid crustal material earlier in the orogen may well have been governed by tectonic processes such as channel flow. The presence of the dacite melts may mark the transition of tectonic style from a mid-crustal channel flow process, to the dominance of deep crustal/mantle lithospheric processes (root instability). Melt analysis of a larger sample set will clarify the significance of both dacitic and granitic Miocene melts in this process.

References

Beaumont et al (2001). *Nature* 414: 738-742.
Beaumont et al (2004). *Journal of Geophysical Research* 109(B06406).
Grasemann & Vannay (1999). *Journal of Structural Geology* 21(7): 743-750.
Jamieson et al (2004). *Journal of Geophysical Research* 109(B06407).
Lee et al (2003). *Journal of Structural Geology.*
Maheo et al (2002). *Earth and Planetary Science Letters* 195: 45-58.
Quigley et al (2004). *Fourth International Symposium on the Tibetan Plateau - Abstracts* SS1.2-4.
Williams et al (2004). *Journal of Petrology* 45(3): 555-607.
Zhang et al (2004). *Earth and Planetary Science Letters* 228: 195-212.

GEOCHEMISTRY AND PETROGENESIS OF MICROGRANULAR ENCLAVES IN CAMBRO-ORDOVICIAN GRANITOIDS OF CHAMPAWAT REGION, KUMAUN LESSER HIMALAYA, INDIA

Santosh KUMAR[1] and Antonio CASTRO[2]

[1] Department of Geology, Kumaun University, Nainital 263 002, India Email: skyadavan@yahoo.com
[2] Department of Geology, University of Huelva, Campus del Carmen, 210071 Huelva, Spain, Email: dorado@uhu.es

Felsic magmatism in Champawat and adjoining regions, referred herewith as Champawat granitoids (CG), represents one of the significant Cambro-Ordovician (500±25 Ma) plutons equivalent to Pan-African magmatism occurring all along the Lesser Himalaya. The enclaves observed in CG (560±20Ma) can be broadly classfied into country-rock xenoliths, surmicaceous (biotite rich) enclaves (SE), and microgranular enclaves (ME), in addition to mafic aggregates composed of biotite. The CG bear the mixed (hybrid, H-type) characters. The ME in CG are commonly spheroidal to ellipsoidal (up to 0.5 meter across), fine- to medium grained, dark coloured typically showing hypidiomorphic textures with or without biotite and feldspar phenocryts. Occasionally light-coloured, fine grained spheroidal (1meter diameter) ME containing several small spotted SE, as identically noted in CG, can also be recognized, which likely represent cumulate or border facies of the granite. The aspect ratio of dark coloured ME varies from 1:1 to 1:5 commonly forming rounded to ellipsoidal shapes, having sharp contacts with felsic host and sometimes stretched, elongated and turned into having partly diffused margins more likely attained under partly crystalline conditions before solidified in isolated mixing region of CG i.e. region of ME mingling whereas several smaller ME (few cms across) more likely retained in active mixing region of CG pluton, i.e. the region of near homogenization. Mineral assemblages (Bt-Pl-Kfs-Qtz) of ME are identical to that of felsic host but K-feldspar is less common in ME, and their modal proportions and grain size differ. It is therefore less likely that dark coloured ME represent autolith, also because they lack cumulate-like texture. The ME, on the other hand, contain elongated biotite, accicular apatite, corroded mafic (biotite) and felsic (feldspar and quartz) xenocrysts, and patchy zoned plagioclase set into felsic interstitial groundmass. Field and prtographic features of ME indicate intrusion, disruption, mingling and undercooling of ME (hybrid) magma into relatively cooler felsic host CG. Modal compositions of ME largely correspond to tonalites, but most CG are granodiorites and few are granites. The ME are metaluminous to peraluminous (Molar $Al_2O_3/CaO+Na_2O+K_2O$=0.98-1.26) in the silica range of 58.39-68.27 wt% whereas CG are slightly to strogly peraluminous (Molar $Al_2O_3/CaO+Na_2O+K_2O$=1.04-1.37) in the silica range of 62.97-70.77 wt%, but both in terms of modified alkali-lime index are largely related to calc-alkaline series of aluminous association but a few ME are scattered and relate to alkali-calcic series. Major oxides (Al_2O_3, $Fe_2O_3^t$, MnO, MgO, CaO, to a certain extent TiO_2 and P_2O_5) and trace elements (V, Co, Ga, Rb) show fairly good linear variation trends with increasing silica for both ME and CG, which suggest the formation of ME by mixing of mafic (enclave) and felsic (CG) magmas in various proportions consistent with the variable contents of mafic-felsic xenocrysts observed in ME. Some of the data scatter noted for the elements Na_2O, K_2O, Pb, Ba, Cs, Sr, Y against silica may have resulted partly by difussion mechanism at varying rates during mixing and mingling events, and partly by modal variations of rock-forming and accessory phases as observed between ME and CG. Some geochemical variations ($Fe_2O_3^t$ vs MgO, Rb/Sr vs SiO_2 and Cs vs Rb) of the ME and CG suggest that enclave and CG magmas follow the evolutionary trends governed by the combined effects of fractional crystallization and magma mixing processes.

It is suggested that both enclave and felsic host magma have experienced some degree of fractionation prior to mixing event, and has therefore formed xenocrysts bearing ME. The ME are remarkably higher in Fe_2O_3, TiO_2, MgO, Nb, Y, Ga and transitional metals (V, Cr, Co, and Ni) compared to that of CG suggesting involvement of mantle-component in the generation of pristine mafic (enclave) magma and also in the generation of the granite. Except for alkalies most of the major elements of ME retain sufficient disequilibria with respect to felsic host CG as evident by tielines joining the ME-CG pairs on multicationic R_1-R_2 diagram, where syn-collisional tectonic regime for CG is clearly discernible. However, Rb and high field strength elements discriminate the tectonic affinity of ME and CG equivocally transitional between vaolcanic arc granite (VAG) and syn-collisional (syn-COLG), and in terms of Nb and Y contents slightly approaches to mildly alkaline (WPG) type. It is likely that magma mixing environment has blurred and overprinted the original tectonic features for these elements. Chondrite-normalized REE patterns of ME-CG pairs probably suggest partly to near equilibration between them. The ME mostly show moderate degree of negative Eu-anomalies whreas some bear positive Eu-anomalies but one ME clearly lacks Eu-anomaly. Overall features of REE patterns of ME suitably suggest a likely process of fractional crystallization of an andesite melt (SiO_2=58.39 wt%, MgO=2.46 wt%, $Fe_2O_3^t$=7.46 wt%, molar Mg# =0.57) as shown by one ME which lacks Eu-anomaly. The ME depleted in sum of REE showing positive Eu anomalies may actually represent fractionated cumulate of mafic (enclave) magma pooled below the felsic (CG) magma chamber or the ascent conduit, and the ME bearing high sum of REE and negative Eu-anomalies may represent evolved residual enclave magma with which felsic melt interacted, and therefore CG bear REE patterns and degree of negative Eu-anomalies as identically noted for evolved ME. It is more probable that felsic (CG) melt partially to nearly equilibrated with more evolved ME but the distribution and mingling of various ME in felsic magma is the result of whole body convective dynamic system, which is also capable to exacavate the base of the magma chamber. Once hybrid (ME) magma injected into cooler felsic melt, have started experiencing physical and chemical changes depending upon ME sizes and resident time in the felsic melt, before the ME-CG convecting magma system solidified, but these processes may have also occurred within the conduites during magma ascent.

EVIDENCE FOR A GREAT MEDIEVAL EARTHQUAKE (~A.D. 1100) IN CENTRAL HIMALAYA, NEPAL, AND SEISMOTECTONIC BEHAVIOR OF THE MAIN HIMALAYAN THRUST

J. LAVÉ[1], D. YULE[2], S. SAPKOTA[3], K. BASANT[3], C. MADDEN[4], M. ATTAL[1], AND R. PANDEY[3]

1- Laboratoire de Géodynamique des Chaînes Alpines, BP53, 38041 Grenoble, France.
2- California State University, Northridge, California, USA.
3- Seismolab, Department of Mines and Geology, Lainchaur, Kathmandu, Nepal.
4- Earth Consultants International, Orange, California, USA.

The primary features of the Himalayan orogen are now understood, but the details of its seismotectonic behavior and maximum earthquake magnitudes are mostly unknown, despite their important implications for seismic hazard facing densely populated regions. During the past century, the Himalayan arc has experienced three major thrust earthquakes of M_w>7.8. Growth folding and surface faulting have been reported in Holocene strata and terraces [Nakata, 1989; Lavé et Avouac, 2000 ; Upreti et al., 2000; Kumar et al., 2001; Wesnousky et al., 1999], and indicate that 50 to 100% of the shortening across the Himalaya is transferred toward the Main Frontal Fault (MFT). Paradoxically, none of these recent events reportedly produced coseismic surface ruptures, including the 1934 Bihar Nepal M_w8.1 earthquake [Ambraseys and Douglas, 2004], with high intensity shaking experienced throughout east Nepal and bordering regions of India. To confirm the absence of rupture associated with this event and determine which events have led to the tectonic scarps, we conducted a paleoseismic study across the Himalayan front in the Marha Khola region, southeast of Kathmandu, in an area close to the inferred 1934 rupture zone.

The study area is well suited to improve our understanding of the current seismotectonic behavior of the Himalayas: it is located west of the maximum intensity felt during this 1934 event, but within the hypothetical 200-300-km-wide rupture segment, and also across an active anticline where numerous folded fluvial Holocene terraces indicate a full transfer of the convergence to the frontal structure. Along the Mahra Khola, fluvial strath terraces have been uplifted 5 to 40 m above its present channel. A tectonic scarp marks the southern extent of these terraces (Fig. 1). Three trenches were excavated across this scarp, which consists of three main fault zones (F1, F2, and F3) and related folds. According to our observations, supported by a careful analysis of the stratigraphic relationships in the three trenches, we conclude that these three faults F1, F2, and F3 are coeval and the timing of their rupture is constrained by charcoal dating at ~A.D. 1100. The vertical separation of the faulted terrace reaches 7.5 m, and the seismic slip associated to this large medieval earthquake can be estimated to be 17 +5/-3 m.

According to the classical view on scaling between slip value, rupture area, and magnitude, we could expect that the ~A.D. 1100 earthquake ruptured a large segment of the Himalayan arc. Unfortunately, published scaling theories are inappropriate to estimate the extent and magnitude of large shallow thrust earthquakes [Scholz, 2002]. Consequently, the surface rupture observed at Marha Khola suggests at least two possible interpretations.

According to the classical view on scaling between slip value, rupture area, and magnitude, we could expect that the ~A.D. 1100 earthquake ruptured a large segment of the Himalayan arc. Unfortunately, published scaling theories are inappropriate to estimate the extent and magnitude of large shallow thrust earthquakes. Consequently, the surface rupture observed at Marha Khola suggests two possible end-member hypotheses:

* a large earthquake ($7.6 \leq M_w \leq 8.1$) with slip enhancement close to the surface, like the recent M_w7.6 Chi-Chi thrust earthquake in the western foothills of Central Taiwan which produced a surface slip of >10 m, but activated a relatively small rupture plane (30 km x 80 km) [Ma, 1999]. Here, a Chi-Chi-type earthquake would release tectonic loading accumulated elastically below the Siwaliks Hills or the southern part of the Lesser Himalaya.

* a great earthquake ($8.4 \leq M_w \leq 8.8$) activating a large fault plane with an average rupture slip similar to the value observed at Marha Khola. In this hypothesis, the ~A.D. 1100 earthquake may have nucleated below the High Himalaya and broke through to the surface trace of the MFT, a cross strike distance of about 100 km. Its lateral extent could have therefore reached or overcome the 200 to 300km length that has been ascribed to the M_w8.1 1934 Bihar Nepal earthquake.

A major conclusion of this study is the absence of surface rupture during the M_w8.1 1934 event, confirming previous reports. We suspect that earthquakes like the 1934 event therefore could break the locked segment of the Main Himalayan Thrust but die out before reaching the surface and deliver strain at the southern tip of their rupture to active folding in the Siwalik Hills. The absence of a surface rupture south of Kathmandu since the ~A.D. 1100 event requires that strain has been accumulating for ~830 years beneath the Siwaliks Hills. The uplift profiles of young Holocene terraces along the Marha Khola and Bagmati, across the frontal anticline, do not exhibit any component of elastic deformation. They rather suggest that the ruptures associated with blind M_w<8.2 events contribute by permanent post-seismic deformation (plastic or viscous deformation, aseismic slip on the frontal thrust) to the long-term folding of the most frontal Himalayan structures. This observation would favor the hypothesis of a great Himalayan earthquake at ~A.D. 1100. In contrast with M_w<8.2 events, its seismic energy would have been sufficient for its rupture to propagate up to the surface and break it at Marha Khola.

According to our trenches and terraces observations, we propose the following seismotectonic model for the Main Himalayan Thrust system: current deformation mostly accumulates elastically at the transition along the decollement from steady creep beneath southern Tibet to locked beneath the High Himalaya [Bilham et al., 1997], where today most of the microseismicity and intermediate earthquakes are located [Pandey et al., 1995]. This elastic deformation is released and transferred to the front during large 7.5<M_w<8.2 earthquakes every ~100-200 yrs possibly like the 1934 M_w8.1 and 1833 M_w7.6 events. However, every 500 to 3000 yrs, the Main Himalayan Thrust could generate a larger earthquake (8.4<M_w<8.9), like the ~A.D. 1100 event, which could accommodate 25% to 50% of the shortening across the Himalaya, and would help to bring the seismic moment summation to closure [Bilham et al., 2001]. Large and great Himalayan earthquakes would contribute to folding of the frontal Siwaliks Hills by mostly post-seismic and co-seismic deformation respectively.

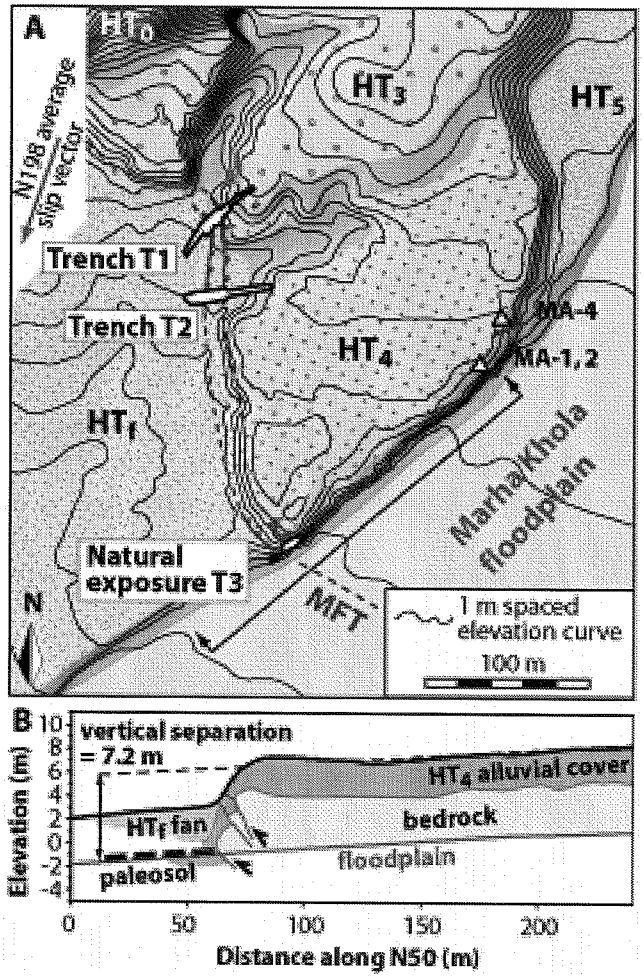

Figure 1: A. Topographic map of the trench site showing the location of trench exposures and the tectonic scarp of the Main Frontal Thrust fault (MFT) and uplifted terraces on the right bank of Marha Khola. B. Cross section shows vertical separation across the fault of the top of HT_4 alluvial cover (vertical exaggeration = 5:1). Since scarp formation, active sedimentation (HT_f fan deposition) has occurred on the footwall to the southwest of the fault.

Ambraseys N., Douglas J. *Geoph.. J. Int.*, **159**, 165 (2004).
R. Bilham, et al, *Nature* **386**, 61 (1997).
R. Bilham, etal, *Science* **293**, 1442 (2001).
S. Kumar et al., *Science* **294**, 2328 (2001).
J. Lavé, J.P. Avouac, *J. Geophys. Res.* **105**, 5735 (2000).
H.F. Ma, *Eos Trans. AGU* **80**, 605 (1999).
T. Nakata, *Spec. Pap. Geol. Soc. Am.* **232**, 243 (1989).
M.R. Pandey, R.P. Tandukar, J.P. Avouac, J. Lavé, J.P. Massot, *Geophys. Res. Let.* **22**, 751 (1995).
Scholz, C.H., *The Mechanics of Earthquakes and Faulting*, 2nd edition, Cambridge University press, pp. 471, 202.
B.N. Upreti, et al., Eds. (*Proc. of the Hokudan Intern. Symposium and School on Active Faulting*, pp. 533-536 (Letter Press Ltd., Hiroshima, Japan, 2000).
S.G. Wesnousky, S. Kumar, R. Mohindra, V.C. Thakur, *Tectonics* **18**, 967 (1999).

A DUCTILE THRUST ZONE WITHIN THE GANGDESE BATHOLITH (SOUTH TIBET).

P.H. LELOUP (1), N.A. ARNAUD (2), B. VUADELLE (2), R. LACASSIN (3), F. VALLI (3), G. MAHÉO (4), P. TAPPONNIER (3)

(1) Laboratoire de Dynamique de la Lithosphère (UCB-Lyon), CNRS UMR 5570 2 rue Raphaël Dubois, 69622 Villeurbanne Cedex, France.
(2) Lab. Dynamique de la Lithosphère, UMR 5573 CNRS, ISTEEM et Univ. Montpellier 2, Pl. Eu. Bataillon, cc.066, 34095 Montpellier, France.
(3) Laboratoire de Mécanique de la Lithosphère, IPG Paris et Univ. Paris 7, France.
(4) Division of Geological and Planetary Sciences, California Institute of Technology, 100-23 N-Mudd, 1200 E. California Bvd, 91125 California, USA,

In the frontal collision zone between the Indian and Asian continents, shortening of the northern part of the Indian plate has been taken up by a series of continental scale south-verging thrusts responsible for the building of the Himalayas. It has been proposed that, more to the north in south Tibet, another south-verging large-scale thrust brings the Gangdese plutonic rocks on top of the suture zone absorbing ~50km of N-S shortening (e.g., Yin et al, 1994, 1999 ; Harrison et al., 2000). However, there are few descriptions of small-scale structures and shear evidence associated with that major structure. Furthermore, its existence has been denied from field observations at its type locality near Zedong (Aitchison et al., 2003). In this context we present a micro-structural study along a N-S section across the Gangdese batholith south of Lhassa.

South of Lhassa, most of the granodiorites of the Gangdese batholith are not deformed and show magmatic textures. However, at 29°24'29.4"N 90°54'20.8"E outcrops a few tens of meter thick shear zone where these rocks are strongly deformed (Fig. 1). They exhibit a foliation, striking ENE-WSW and dipping ~40° to the North, that bears a N-S stretching lineation. Some of the shear planes correspond to quartz ribbons bearing a spectacular N-S lineation. C/S relationships indicate a top to the South thrusting. Immediately South (below) of that shear zone, the granodiorite is little deformed. A few km further to the South (29°23'19.5" N 90°53'01"E), the granodiorite is again deformed, exhibiting two distinct deformation phases: a mild foliation striking ~E-W on average deformed by steep, north-dipping, shear planes which are in turn later cut and offset by planar quartz ribbons. The shear planes bear slickenslides and C/S relationships indicating a normal motion. The quartz veins strike NE-SW and dip shallowly to the north. They bear N-NE striking lineations and the offsets indicate that they correspond to top to the South small-scale thrusts.

Our interpretation is that after cooling of the Gangdese batholith down to greenschist conditions, the area was affected by at least two deformation episodes. The first one is marked by a mild NNE-SSW stretching, while the second corresponds to a more intense N-S shortening. Our preliminary geochronological results do not allow us to constrain the timing of the second deformation episode more precisely than between 18 and 35 Ma. In the same area, Copeland et al. inferred several pulses of rapid cooling in that time interval from thermochronology, and related them to episodic thrusting above the Gangdese thrust (Copeland et al, 1987, 1995). More work is needed to precise the geometry and timing of thrusting within the Gangdese batholith south of Lhassa which appears more complicated that what has been proposed ~100km farther to the east near Zedong (e.g. Harrison et al., 2000).

Fig. 1

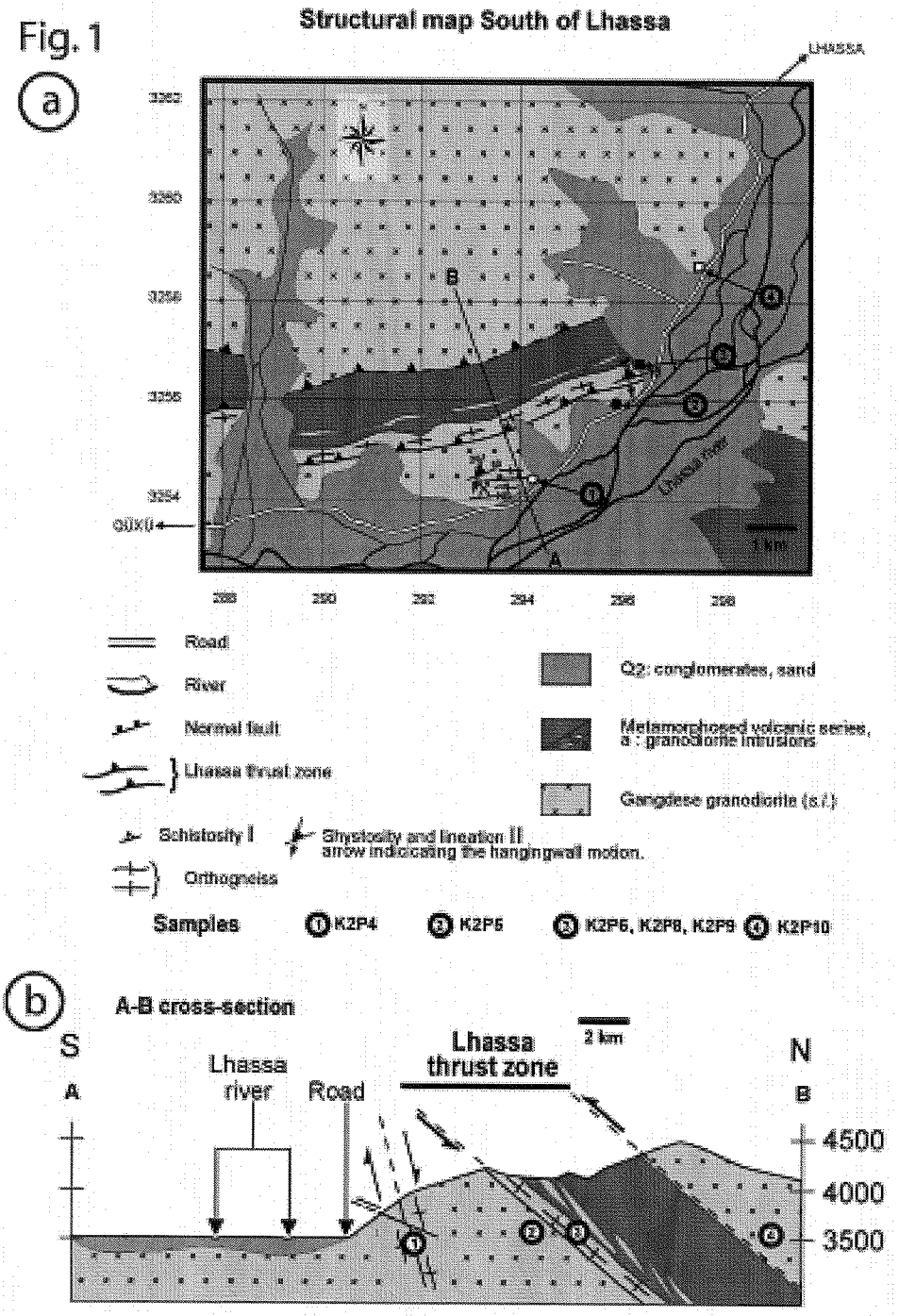

Aitchison, J.C., A.M. Davis, Badengzhu, and H. Luo. 2003. . *Terra nova, 15*, 155-162.
Copeland, P., T.M. Harrison, W.S.F. Kidd, X. Ronghua, and Z. Yuquan, 1987. *Earth Plan. Science Letter, 86*, 240-252.
Copeland, P., Y. Pan, T.M. Harrison, W.S.F. Kidd, M. Roden, and W. Chen. 1995. *Tectonics, 14*, 223-236.
Harrison, T.M., A. Yin, M. Grove, O.M. Lovera, F.J. Ryerson, and X. Zhou. 2000. *J. Geophys. Res., 105*, 19211-19230.
Yin, A., T.M. Harrison, M.A. Murphy, M. Grove, S. Nie, F.J. Ryerson, X.F. Wang, and Z.L. Chen. 1999. *Geol. Society America Bulletin, 111*, 1-21.
Yin, A., T.M. Harrison, F.J. Ryerson, C. Wenji, W.S.F. Kidd, and P. Copeland. 1994. *J. Geophys. Res., 99*, 18175-18201.

RIVERS GEOMORPHOLOGY OF THE YANGTZE RIVER SOURCE REGION AND NEOTECTONIC MOVEMENT OF NORTH TIBET

Yalin LI (1), Chengshan WANG (2), Mou WANG (1) and Haisheng YI (1)

(1) College of Earth Sciences, Chengdu University of Technology, Chengdu, 610059,China
(2) China University of Geosciences, Beijing, 100083, China

The northern piedmont of Tanggula mountain of north Tibet is the source region of the third longest River of the word—Yangtze River, 5 rivers are running in this area, they are Tuotuohe River, Ga'erqu River, Buqu River, Dongqu River, Dangqu River and distributed from west to east. Those rivers consist of the main river networks of the area. From 2000 to 2004, we have made a very careful field investigation on geomorphology and Neotectonic activities of the Yangtze source region.

From the geomorphic point of view, we can mark off seven basic geomorphic units of Yangtze River source region of north Tibet, they are extra high mountains, high mountains, low mountains, hill, alluvial-diluvial platform and plain. Rivers geomorphology of the Yangtze River source region appear difference with subsections. In the upriver regions, caused by glacier movement and rivers incision activities, canyons are the main landscape; the middle reaches of the rivers mainly controlled by faults and fault depression basin, and wide valleys are developed alternate with narrow valleys; in the lower reaches, wide valleys are the main landscape with developed river terraces. The formation and development of the Yangtze source region river system have close relationship with Neotectonic movement.

Strong Cenozoic tectonic activities with multiple deformation patterns can be found in the Yangtze river source region. Analysis on tectonic deformation indicate that tectonic deformation of Cenozoic can be divided into two stages, the first stage developed SN trend compression- shortening tectonic deformation, while the second stage develops EW trend extensional deformation. Tectonic patterns include fold-thrust deformation and strike-slip shear deformation of the earlier stage, and extensional normal fault of late. Unconformity of strata indicate that the fold-thrust deformation stage occurred in 31.0-17Ma, Strike-slip shear fault are of conjugate characters, and its age is 15-18Ma. The ages of normal faults are 9.3Ma, 6.6Ma, 6.3Ma and 3.7Ma and 2.6-2.8Ma . we also got the sedimentary age of those rivers, they are 1.1-0.03Ma.

Based on the researches of Geomorphology of the Yangtze river source region and river Geomorphology, we can get the following conclusions. Cenozoic tectonics not only control geomorphology of the rivers and caused river captures of the area, but also formed the drainage distribution pattern. The Yangtze River source region river system was forming from 1.1Ma ago by the river headward erosion movement along with the faults.

References

LIU Z, X ZHAO, C WANG, S LIU & H YI, 2003. *Geophysical Journal International*, 154: 233-252.
WANG C, Z LIU, H YI, S LIU & X ZHAO, 2002. *Journal of Asian Earth Sciences*, 20 (3): 211-223.
THE RESEARCH TEAM OF QINGHAI-TIBET. 1983. *Geomorphology of Xizang(Tibet)*,1-238

Note Page

Kailas, Hedin, 1917

SHRIMP U-PB ZIRCON AGE OF CENOZOIC ALKALI BASALTS IN THE TUYON BASIN, SW TIEN SHAN, AND ITS GEOLOGIC IMPLICATIONS

Tao LIANG, Zhaohua LUO

School of Earth and Mineral Resources, China university of Geoscience, Beijing, 100083, China

The Tuyon basin (TYB), NW China, is located near the crossing-site of the Tien Shan orogenic belt, the Western Kunlun fold systems and the Tarim-Alashan blocks. The Talas-Ferghana dextral strike-slip fault(TFF) cuts its SW margin, and the NE extended Wuqia strike-slip fault(WQF) is just at south margin of the TYB(Fig.1). The Mesozoic and Cenozoic strata are well exposed and the Paleozoic strata are very little in the TYB.

Tuyon volcanic rocks are well known since 1981, but it has not been paid sufficient attention in the past. Recently, many geoscientists all over the world have been attracted because of the discovery of the peridotite in the basalts and the attention about response of the India-Asia collision. The key problem is geochronology of the volcanic activities. According to previous researches, Tuyon volcanic rocks can be divided into two units: the lower basalts and the upper basalts, aged as 120~110Ma and 70.4~36.6Ma, respectively, by K-Ar and Ar-Ar. These isotopic data contradict the volcanic rocks age (E_1~E_2) in terms of the stratigraphy and fossils.

In order to get accurate age of the Tuyon basalts, the U-Pb dating of zircon by SHRIMP II has been used basing on the interpretation of remote sensing(RS) image of TYB and detailed field observations.

Fig.1 Tectonic map of Tuyon basin

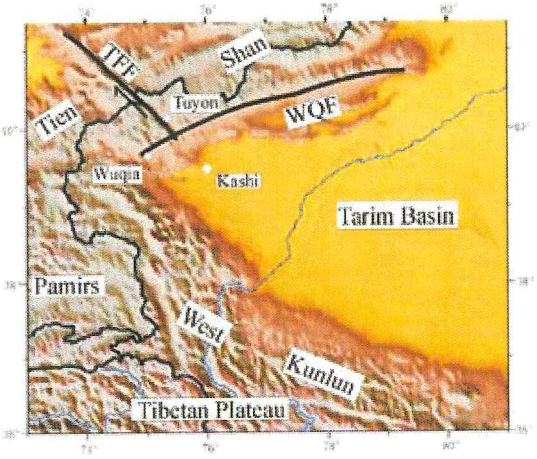

Tab.1 Features of zircons from the Tuyon volcanic rocks and their geochronology The analysis was performed in Beijing SHRIMP Center, Chinese Academy of Geological Sciences

Sample No	B014	AB15D	AB15E	A-D016
Sample weight	4.35 kg	3.78kg	4.38kg	4.24kg
position	the lowest layer in the cone sheets	Arbesaerdy caldera, the lower lava layer	Arbesaerdy caldera, the upper lava layer	Koketaspang volcanic neck
Petrographic description	Dark gray, massive structure and porphyritic texture, clinopyroxene, phlogopite and plagioclase are of phenocrysts, matrix-hialentic texture with clinopyroxene and plagioclase microlite, magnetite, volcanic glass	Dark gray, columnar joint structure, vesicular structure, porphyritic texture, olivine phenocrysts, edge altered into iddingsite, a little clinopyroxene phenocrysts, matrix - pilotaxitic texture, the void among long columnar plagioclase microlite filled by pyroxene grains	Dark gray, columnar joint structure, vesicular structure, porphyritic texture, olivine(iddingsite) clinopyroxene and plagioclase phenocrysts, matrix hialentic texture clinopyroxene and plagioclase microlite, magnetite,	Dark gray, massive structure and porphyritic texture, olivine and clinopyroxene phenocrysts, matrix hialentic texture clinopyroxene and plagioclase microlite, magnetite,
Feature of zircon	Most light yellow, transparent, allotriomorphic, angular, zircon chord, 100_200um	Most transparent, some crack and inclusion, allotriomorphic and idiomorphic, 50_100um	Most light yellow and transparent, allotriomorphic, obviously circled, 50_100um	Most transparent, some crack and inclusion, allotriomorphic and idiomorphic, 50_100um
SHRIMP age_Ma_	43.1±1.6	1538±13 2186±7	275.3_349.6 and 414.5_470.7	2166±27 435±16

The analysis was performed in Beijing SHRIMP Center, Chinese Academy of Geological Sciences

According to interpretation of RS image and field researches, TYB is of a complex basin with a volcano group rather than a monogenetic volcanic. Volcanic rocks are distributed mainly in the north and the northeast TYB, and occur as three types of facies: lava, volcanic neck and sub-volcanic facies. There are seven volcanic centers in the TYB, as well as a series of volcanic apparatus, such as calderas, volcanic necks and cone sheets. The approximately round Koketaipang volcanic neck, about 1.5km in diameter, is in northeast TYB and intruded the Paleocene. The elliptic Arhesaiordy caldera(about 10km°¡5km) is in southwest TYB and circled by the arc volcanic rocks and sub-volcanic rocks, which are formed at the same period when the volcano erupted. The underlying strata are lower Cretaceous, and the center of Arhesaiordy caldera covered discordantly and unconformably by Paleocene. The so-called lower basalts are in south TYB and preserved as a series of cone sheets, which emplaced in Jurassic sedimentary rocks. Many megacrysts have been found in the lowest cone sheets, such as augite, phlogopite, amphibole and anorthoclasite, and lots of deep-seated xenoliths, including peridotite, granulite, pyroxenite, gneiss, and so on. As mentioned above, Tuyon volcanic rocks are the response to a single igneous event. Four samples collected in differeent volcanic apparatus(Tab. 1) have been analysed by the SHRIMP II in order to date the accurate magma atctivities, because the cone sheets represent high pressure in central magma chamber and the beginning of valcano activity, but the volcanic neck indicates these conditions are completely contrary and represent the end time of magma activities.

According to the features and Cathodolum inescence(CL) images of zircons, these zircons are considered as two genetic types: magmatic zircons and metamorphic zircons. The zircons in B014 are magmatic zircons because of conspicuous crystallization zoning, and other zircons are metamorphic zircons in terms of crystal form and structure characters. It suggests that the SHRIMP age in cone sheets can reflect the age of Tuyon volcanic rocks, and the remainder fails. The reasons as follow: firstly, the primary magma, which has characteristic of enriching in alkaline and volatile component, formed the cone sheets. In high pressure condition the primary magma may locate in the first crystal area of zircon, and the zircons have been formed earlier. It is evidence that the zircons in the B014 are angular shard. Secondly, the deep-seated xenoliths suggest that the magma undergo hardly evolution and less fractional crystallization. So the zircons in the cone sheets can be regarded as a kind of megacrysts, and the SHRIMP age of B014 (48.1±1.6Ma, 13 spots, 95% conf., MSWD = 0.61) is the beginning time of magma atctivities.

The primary magma ascended more slowly after cone sheets and igneous rocks characteristic of primary magma were formed, the latter was not observed in field and had been denuded. In this condition, the basaltic magma trends polybaric crystallization and interacts with surrounding rocks, so that the previously formed zircons were resorption and metamorphic zircons came into being. The rest SHRIMP age suggests that there existed the Lower Proterozoic, Lower Paleozoic and Upper Paleozoic metamorphic strata beneath the TYB, it accords with the regional geologic setting of South Tien Shan.

As mentioned above, the age of Tuyon volcanic rocks not only has time significance to Toyon volcanic rocks, but also is chronologic limit to response of long distance transfer to the India-Asia collision.

CHARACTERISTICS AND SIGNIFICANCE OF THE ACCESSORY MINERALS FROM THE TIBET PERALUMINOUS GRANITES

LIAO Zhongli*[1], MO Xuanxue[2], PAN Guitang[1], ZHU Dicheng[1], WANG Liquan[1], LI Guangming[1], GENG Quanru[1], ZHAO Zhidan[2], LIU Bo[1]

[1] Chengdu Institute of Geology and Mineral Resources, 610082, Chengdu, CHINA

[2] China University of Geosciences, 100083, Beijing, CHINA

* Correspondence should be addressed to LIAO Zhongli (E-mail: cdlzhongli@cgs.gov.cn)

The behavior of accessory mineral can direct indicate geochemistry process of magma system[1-3]. Zircon is the important accessory mineral in Tibet peraluminous granites. In order to discuss petrogenesis of peraluminous granites, mineralogical, petrological, accessory mineral characteristics, zircon contentand crystal form and zircon groups' features of the Tibet peraluminous granites have been studied in detail. As a result, the rock rich contain muscovite, tourmalin and plagioclase. These rock types are belonging to muscovite-type of strongly peraluminous granites (MPG-type) according to Barbarin's classification[4].

26 accessory minerals have been appearing in Tibet peraluminous granites. It has 6 accessory mineral combinations include: (1)zircon + phosphorite + sphene + pyrite + ilmenite, (2)zircon + phosphorite + pyrite + ilmenite + garnet, (3)zircon + phosphorite + sphene + ilmenite, (4)phosphorite + tourmalin + anatase, (5)zircon + phosphorite + garnet, and (6)garnet + galenite + magnetite + sphalerite type, the main type is zircon + phosphorite.

The distributing feature of accessory minerals shows (1) accessory mineral has less variety and simple combinations, the main accessory mineral includes zircon, phosphorite, sphene, ilmenite, pyrite, tourmalin, garnet, and anatase. (2)low abundant value of accessory minerals content with narrow range except tourmalin and garnet, zircon and phosphorite exist in all samples, it is similar to regional granite's[5].

Zircon types distributing of Tibet peraluminous granites shows big scatter of zircon form after Pupin(1980). Zircon type includes 6 types or 9 subtypes (Table 1). Zircon types distributing of Tibet peraluminous granites and main types and subtypes of zircon and corresponding scale of geothermometry indicate 900°Ê original temperature and 600°Ê close temperature, with 800-900°Ê and 600-650°Ê crystal range. The result is similar to the result of Ab geothermometer. It indicates magma evolution from deep to shallow and the high to low temperature.

Crystalphase	(211)	(101)<<(211)	(101)<(211)	(101)_(211)	(101)>(211)	(101)>>(211)	(101)	(301)	Crystal temperature(_)±50	Index T
Prism	B	AB_1	AB_2	AB_3	AB_4	AB_5	A	C	500 550	100
(110)	H	L_1	L_2	L_3	L_4	L_5	$G_1G_2G_3$	I	600	200
(100)<<(110)	Q_1	S_1	S_2	S_3	S_4	S_5	P_1	R_1	650	300
(100)=(110)	Q_2	S_6	S_7	S_8	S_9	S_{10}	P_2	R_2	700	400
(100)<<(110)	Q_3	S_{11}	S_{12}	S_{13}	S_{14}	S_{15}	P_3	R_3	750	500
(100)>(110)	Q_4	S_{16}	S_{17}	S_{18}	S_{19}	S_{20}	P_4	R_4	800	600
(100)>>(110)	Q_5	S_{21}	S_{22}	S_{23}	S_{24}	S_{25}	P_5	R_5	850	700
(100)	E	J_1	J_2	J_3	J_4	J_5	D	F	900	800
Index A	100	200	300	400	500	600	700	800		

Table 1 °°Main types and subtypes of zircon and corresponding scale of geothermometry (Imitate Pupin,1980)

* It appears in this work with adding black frame.

Based on the calculate result, the average point $I.T = 447$, $I.A = 443$ of zircon type in Gangdise belt locate in calc-alkaline series granites of crustal + mantle origin (Fig. 1). It indicates peraluminous granites are added mantle composition except crustal origin in Gangdis belt. It can be explained that the original magma exists mantle souces material, and it is main composed by crustal origin material when the temperature is low. The average point $I.T = 239$, $I.A = 572$ of zircon type in Himalaya belt locate in intrusive aluminous monzogranites and granodiorites (Fig. 1). It indicates peraluminous granites are main crustal origin in Himalaya belt. These indicate the crystal temperature of Gandese belt is higher than Himalayan belts'.

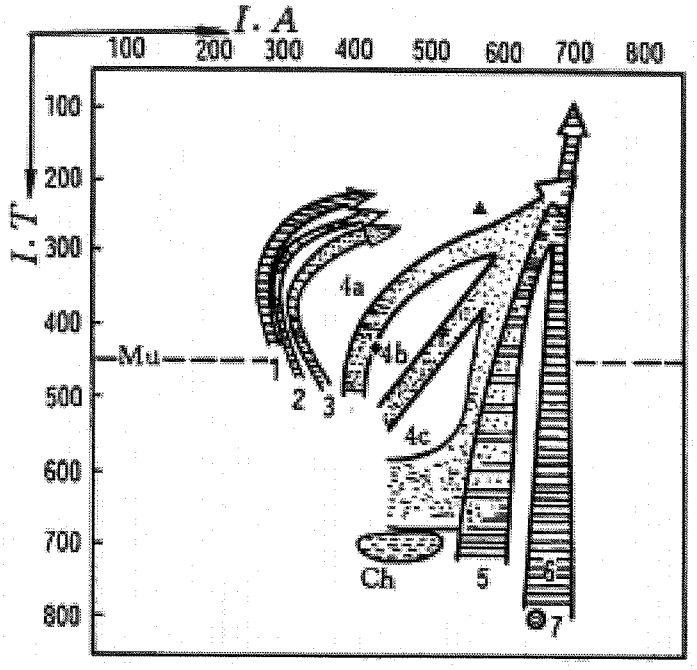

Fig. 1 Average points of zircon group versus evolution of different genetic types of rocks (Imitate Pupin,1980) °Ù- the average point of zircon type in Gangdis belt, °¯- Himalaya belt; 1- aluminous leucogranites; 2-(sub) autochthonous monzogranites and granodiorites; 3- intrusive aluminous monzogranites and granodiorites; 4a~4c- Granites of crustal+mantle origin, hybrid granites: calc- alkaline Series granites; 5- sub-alkaline series granites; 6- alkaline series granites - Granites of mantle or mainly mantle origin; 7- tholeiitic series granites. Mu - limit of the muscovite granites (I*T < 450); Ch - magmatic charnockites area.

General, Tibet peraluminous granites are formed in peraluminous setting condition and originated in low crystal temperature of magma, crystal range between 600-900°Ê. The crystal temperature of Gandese belt is higher than Himalayan belts'. Tibet peraluminous granites are magma petrogenesis. Magma is originated from part melt of the crust matter. The graph of accessory mineral show 3 petorgenesis types: high aluminum crust source, crust source and crust-mantle mix source. The crystal temperature of Gandese belt is higher than Himalayan belts'. The features of zircon groups in different tectonic belt show different information of petrogenesis. Himalayan belts is regarded as crust source petrogenesis, Gandese belt have added mantle source composition expect crust source petrogenesis. These difference show inhomogeneity of lithosphere compose and evolution in Tibet plateau.

Acknowledgments: This study is financially supported by the National Keystone Basic Research Program of China (Grant No.2002CB412609), and the Integrated Study of Basic Geology in the Blank Area of Southern Tibetan Plateau (Grant No. 200313000025).

References

[1]. Pupin J P. 1980. Zircon and Granite petrology. Contribution to Mineralogy and Petrology, 73(3): 207-220.
[2]. Hayashi M, Shinno I. 1990. Morphology of synthetic zircon crystals doped with various elements. Mineral J, 15:119-128.
[3]. Vavra G. 1990. On the kinematics of zircon growth and its petrogentic significance: a cathodoluminescence study. Contrib. Mineral. Petrol. , 106:90-99.
[4]. Barbarin B. 1990. Granitoids main petrogenetic classifications in relation to origin and tectonic setting. Geol. J. 25: 227-238.
[5]. Ding Xiaoshi. 1990. Character of accessory mineral in middle-southern Tibet. In: Liu Guohui et al. Metamorphic rock and igneous in Tibet. Beijing: Geological Publishing House (in Chinese).

PETROGENESIS AND CONTINENTAL DYNAMICS SIGNIFICANCE OF PERALUMINOUS GRANITE IN TIBET

LIAO Zhongli*[1], MO Xuanxue[2], PAN Guitang[1], ZHU Dicheng[1], WANG Liquan[1], LI Guangming[1], GENG Quanru[1], ZHAO Zhidan[2], LIU Bo[1]

[1] Chengdu Institute of Geology and Mineral Resources, 610082, Chengdu, CHINA

[2] China University of Geosciences, 100083, Beijing, CHINA

* Correspondence should be addressed to LIAO Zhongli (E-mail: cdlzhongli@cgs.gov.cn)

The peraluminous granites in Tibet, which are approximately distributed in E-W direction, are mostly occurred Gandise-Nyainqentanglha and Himalayan tectonic-magmatic provinces. There are 58 major peraluminous granitic intrusions in Southern Tibet, with an area of about 5000 km^2, which is distributed in seven belts [1]. The Himalayan and Gandise belts are the famous for research bases of peraluminous granites [2]. Peraluminous granites were attention because it associates with orogen evolution and uplift of Tibet plateau [3-5]. It considered that the peraluminous granite's petrogenesis is crust sources [4-7], and the result of intracontinental compression-orogeny in post-collision.

1 Petrology and Geochemistry

For lithology of the peraluminous granite, they include tourmaline granite, muscovite granite, and two-mica granite. In addition, andalusite two-mica granite can be seen in Pingdu pass, and garnet granite in Jianglin, Quzhen and Yelaxiangbo. All of these can be ascribed to a muscovite- type of strongly peraluminous granites (MPG-type) on the basis of Barbarin's classification [8].

The 169 analysed samples show a very narrow compositional range for all the major elements. They are granites (65.7%-79.52% SiO_2, average 73.25%) characterized by calc-alkaline chemistry, with low Al_2O_3 (10.42%-18.29%, average 14.53%) and moderate to high CaO (0.15-3.39%, average 1.05). The Na_2O/K_2O ratio is 0.26-3.6%, and there are about 66 percent is large than 1, shows $K_2O>Na_2O$ in major sample. These analyses also show the very low content in Fe, Mg and Mn that is in good agreement with the scarcity of ferromagnesian minerals. These samples have a very high A/CNK ratio (1.11-1.59). And the C-norm is larger than 1 with the range of 1.07-6.31. These are the typical characteristics of peraluminous granite. Petrochemistry shows a trend with gradually increase of TiO_2, CaO, MnO, FeO, and degression of Al_2O_3, Na_2O, K_2O from south to northern Tibet. And it shows the evolution trend that the rock is more and more acidic near south comparing to the same time period.

REE character shows obvious change contrast to a very narrow compositional range for the major elements. The total amount of REE ranges from $33.93*10^{-6}$ to $229.74*10^{-6}$(mean value $98.39*10^{-6}$). The samples shows $(La/Yb)_N$=2.14-64.77, $(La/Sm)_N$=3.05-7.89, $\sum LREE/\sum HREE$ =2.13-18.71, and ^{TM}Eu=0.05-0.99. It indicates that the rocks are rich in LREE and with remarkable Eu anomaly. According to the chondrite-normalized REE distributions, all of the patterns are similar to each other, the plots show totally right sloping pattern, belonging to LREE enrichment and with Eu depletion, implying that the continental collision belt medium-acid rock assemblage developed in Tibet had undergone a special generation process.

The chondrite-normalized trace elements distributions show the plots totally right sloping pattern. Some strong incompatible elements such as Sr, Ba and Ti are depletion in these rocks. It indicates the tectonic setting of continental collision. Petrochemistry shows high differentiation index and obvious Eu anomaly. These indicate the existence of crystal differentiation with the Ba, Sr, P, and Ti high depletion. Trace element spider diagram indicates the peraluminous granite is syn-collision granite. Compare to upper and lower crustal spider diagram [9], it indicates the upper crustal source of peraluminous granite. And then, the $‰^{18}O$ value =8.9-18.79‰, shows upper crustal source.

2 Petrogenesis and Continental Dynamics Significance

Based on the data of major and inactive incompatible trace elements, a tectonic setting of the peraluminous granites in Tibet has been discriminated. According to aluminum saturatuon index and QAP plots, these peraluminous granites were mostly plotted within CCG area, and on diagrams of R_1-R_2, Nb-Y, Rb-(Y+Nb) and Rb-Hf-Ta, its plots are fall within syn-collision granite area, indicating that the peralumious granites in Tibet were formed in a continental collision setting. Furthermore, Tibetan peraluminous granite has the character with high SiO_2, high Sr isotope ratio, and high O isotope ratio, aluminum supersaturation, $K_2O>Na_2O$, no paragenesis of intermediate-basic intrusive rock, and absence corresponding the same term volcanic, these features indicate the peraluminous granite is the result of pelite partial melting. The lack of spatial and temporal association with basalt magmatism suggests that the peraluminous granite of Tibet is the products of pure crustal melt.

The Rb-Sr-Ba ratio's change can distinguish sources composition [10], Tibetan peraluminous granite Rb/Sr ratio has linearity relation along with the increase of Rb/Ba ratio. Our analyses coupled with those of Ferrara et al. [11], clearly show such a trend and the Tibet peraluminous granite can thus be interpreted as resulting from muscovite dehydration reaction. According to Rb/Ba-Rb/Sr diagram, the sample plot form a linear array of increasing Rb/Sr with Rb/Ba, distributes in clay-rich sources area, and a few spots locate in clay-poor ones.

Detailed studies of element and isotopic geochemistry suggest that peraluminous granites in Tibet were originated from middle-upper crust source, characterized by mainly schists and gneisses (metamorphosed argillic rocks). Peraluminous granites in Tibet are represented by a muscovite-type of strongly peraluminous granite (MPG-type) and are magmatic in origin. Comprehensive studies of petrology and trace element and isotope geochemistry together with field investigation suggest that the peraluminous granites in Tibet are a S-type granite. The sources rock of Tibet peraluminous granite is formed in mature clay-rich sources (pelite), other or paracelsian of basement. The form of peraluminous granites is controlled by heat which continental collision lead crustal thickening. The material of lower crust is heated up after entering deeper position.

A magmatic activity of these peraluminous granites is controlled by plate mechanism. Since Eocene, it breaks collision between India Himalaya slab and Eurasia Gangdis slab. Along Gangdis slab move to south, the peraluminous magma of Himalayan area is mainly evolved from the local melt of mudy sediments on a top of subduting plate, therefore, lead to the incursion of peraluminous granites.

Acknowledgments: This study is financially supported by the National Keystone Basic Research Program of China (Grant No.2002CB412609; 1998040800), and the Integrated Study of Basic Geology in the Blank Area of Southern Tibetan Plateau (Grant No. 200313000025).

References

[1] Liao Zhongli, Mo Xuanxue, Pan Guitang et al. 2004. Temporal-spatial distribution and implications of peraluminous granites in Tibet. Himalayan Jjournal of Sciences, 2:292-293.

[2] Deng Jinfu, Zhao Hailing, Lai Shaocong et al. 1994. Generation of Muscovite/Two-Mica Granite and Intracontinental Subduction. Earth Science£≠Journal of China University of Geosciences, 19: 139-147 (in Chinese with English abstract) .

[3] An Yin ,T.M.Harrison 2000. Geologic Evolution of the Himalayan-Tibet Orogen Annu.Rev. Earth Planet Sci. 28:211-80.

[4] Tong Jinsong, Zhong Hua ming, Xia Jun et al. 2003. Geochemical features and tectonic setting of peraluminous granite in the Lhozag area, southern Tibet. Geological bulletin of China, 22: 308-318 (in Chinese with English abstract).

[5] Zhang Jinyang, Liao Qun'an. 2004. Leucogranites-geological proof of uplifting, decompressing and melting of the basemen t, Dingjie, South Tibet. Northwestern geology, 37: 7-12 (in Chinese with English abstract).

[6] Harrison TN McKeegan K D Le Fort P.1995. Detection of inherited monazite in the Manaslu leucogranite by $^{208}Pb/^{232}Th$ ion microprobe dating.Crystallization age and tectonic significance.Earth Planet. Sci. Lett. 133: 271-282.

[7] Guillot S, Le Fort P. 1995. Geochemical constrains on the bimodal origin of High Himalayan leucogranite. Lithos. 35: 221-234.

[8] Barbarin B. 1990. Granitoids main petrogenetic classifications in relation to origin and tectonic setting. Geol. J. 25: 227-238.

[9] Rollison H.R., 1993, Using geochemical Data: Evaluation, Presentation, Interpretation. Longman Scientifif and Technical Limited.

[10] Sylvester P J. 1998. Post-collision strongly peraluminous granites. Lithos. 45: 29-44.

[11] Ferrara G., Lombardo B., Tonarini S., B T. 1991. Sr, Nd and O isotopic characterization of the Gomphu La and Gumburanjon leucogranites (High Himalaya): Schweiz. Mineral. Petrogr. Mitt., 71: 35-51.

EIGHT-HUNDRED-YEAR RECURRENCE OF LARGE EARTHQUAKES ON THE HAIYUAN FAULT NEAR SONGSHAN, GANSU PROVINCE, CHINA

Jing LIU[1], Yann KLINGER[1], Xiwei XU[2], Cécile LASSERRE[3], Guihua CHEN[2], Wenbing CHEN[2], and Paul TAPPONNIER[1]

1. Laboratoire de Tectonique, Institut de Physique du Globe, 4 place Jussieu, 75005 Paris, France
2. Insitute of Geology, China Seismological Administration, Beijing 100029, China
3. Laboratoire de Géologie, Ecole Normale Supérieure, 24 Rue Lhomond 75231 Paris Cedex 05, France

The Haiyuan fault is a major active left-lateral fault that bounds the Tibetan Plateau to the north. Studying this fault has profound implications on the framework of deformation of the Tibetan Plateau, and themechanics of continental deformation in general. Previous studies have mainly focused on the slip rate of the fault. Late quaternary average rate does not seem to be compatible with GPS-derived rate. To understand this discrepancy, it is essential to study the earthquake history on the fault in the last several millenniums. Paleoseismic investigations on the fault are sparse and mainly in the reach of the 1920 earthquakerupture, or along the eastern half of the Haiyuan fault. To investigate the seismichistory of the western Haiyuan fault, we have opened two trenches in a small pull-apart basin near Songshan, Gansu Province. The excavation exposes layers of alternating colors: black organic-rich silty to clayey deposit and yellowish white layers of coarser-grained sandy deposit. The main fault zone is readily recognizable in trench exposures, by the disruption and tilting of the layers. Six events are identified. Charcoal is abundant yet generally tiny in the upper stratigraphy of exposures. Thirteen samples have been dated to constrain the age of paleoseismicevents. They occurred during the last 3,500-3,900 years. The youngest event sems to be a minor event, probably the 1900 Mw 5.8 earthquake. The second to fourth youngest events occurred, sometime during 1440-1460 A.D., 890-1000 A.D., and 80 $^{+220}_{-50}$ B.C., respectively. not considering the most recent event, the recurrence interval is on the order of eight hundred years. The offsts associated with these events are poorly known. If we assume geomorphic estimation of 8- to 10-m of slips for large events, 800-1000 years of recrrence time implies around 12 mm/yr average slip rate. However, a more realistic evaluation depends on more rigorous investigation of earthquake slips.

STRUCTURAL FEATURE OF YARLUNG ZANGBO OPHIOLITE ZONE AND ITS TECTONIC SIGNIFICANCE

Xiaohan LIU

Institute of Tibetan Plateau Research, Chinese Academy of Sciences, Beijing, China

The Yarlung Zangbo ophiolite zone is thought as a continental boundary between India and Eurasia formed during Cenozoic subduction and collision. Some new structural investigations reveal a feature contradicting with such tectonic limit in continental scale which has absorbed thousands km of shortening. Many cross sections show that this zone composed generally of completed members of "ophiolitie family", dunites, harzburgites (cumulates), dolerite sills, pillow lavas, radiolarites, etc. They crop out following the original tectonic-sedimentary sequences and show large antiform in almost all segments along this zone. Whole ophiolite zone suffered brittle to brittle-ductile deformation with low greenshist metamorphic facies. Symmetric, the Permian to Triassic flysch over lay disconformable on both northern and southern slopes of mafic-ultra mafic formations, displaying a dome shaped feature. The faults analyses reveal that the Paleozoic and Mesozoic flysch formations in both sides thrusted firstly face to face over the mafic-ultra mafic zone during compressional phases, followed by collapsed with regional uplifting.

No typical middle-high temperature shear zone in large scale has been made certain in north-south direction, even the mélange zones have been deformed in brittle-ductile mechanism. Several parallel mafic-ultra mafic zones, separated by brittle faults and narrow flysch belts, have been recognized, which are unlike the relic whole crust slab bequeathed from a large oceanic lithosphere.

Considering the comparability of Paleozoic paleo-ecosystem of both High Himalaya and Qiangtang formation, and the lack of affirmative geophysical proof of subducted India lithosphere under the Zangbo zone, we doubt that this ophiolite zone could represent a real continental boundary of subduction-collision between India and Eurasia.

Our explicating scenario is that the Yarlung Zangbo ophiolite zone could be a relic back-arc basin whith its juvenal narrow oceanic crusts between High Himalaya continental margin arc and synchronous Gangdise magmatic arc. This back-arc basin has been developed after Triassic, during the oceanic lithosphere subduction of India in southern of High Himalayan fore-arc region, beginning from 2 expanding centers at Bailang County and Gurla Mandata regions. Following its collapse during the collision epoch, this zone floated with the regional uplifting as a relatively intact oceanic crust in southern of Tibetan Plateau.

TECTONIC EVOLUTION OF THE CENTRAL HIGHER HIMALAYAN CRYSTALLINES IN THE KHARTA AREA, SOUTHERN TIBET: NEW CONSTRAINTS FROM PETROLOGIC AND GEOCHRONOLOGICAL DATA

Yan LIU (1), Wolfgang SIEBEL (2), Hans-Joachim MASSONNE (3), Xuchang XIAO (1)

1, Institute of Geology, Chinese Academy of Geological Sciences, Beijing 100037, China
2, Department of Geosciences, 72074 Tübingen, Germany
3, Institut für Mineralogie und Kristallchemie, 70174 Stuttgart, Germany

Within the Kharta area, east of Mt. Qomolangma (Everest), garnet sillimanite gneisses and granites including overprinted eclogite lenses were displaced beneath the North Col Formation by a ductile normal fault (STD1) and above the upper Lesser Himalayan Crystallines by a ductile thrust (MCT1). Zircons from the overprinted eclogite lenses which are interpreted as former dikes were dated by the TIMS method. All samples plot close to a discordia line with Neoproterozoic upper intercept ages of about 970 Ma, suggesting a late Proterozoic age for emplacement of the dikes. Zircon SHRIMP analyses show that the garnet sillimanite gneisses and granites were derived from Pan-African acidic rocks produced by partial melting of Neoproterozoic sediments. Monazites from two granite bodies beneath the STD1 give very similar crystallization ages between 12-13 Ma, whereas monazites from a sample of highly sheared sillimanite gneisses beneath the MCT1 give a lower-intercept age of 13.4°+/-1 Ma, suggesting that the MCT1 and the STD1 were active contemporaneously. Our data show that the Pan-African acidic rocks with Neoproterozoic mafic inclusions were subducted to form eclogite and HP metapelitic rocks first, and then experienced high-T and intermediate-P metamorphism to be converted into garnet sillimanite gneisses and overprinted eclogite lenses at about 33 Ma below south Tibet. At around 13 Ma, these rocks were exhumed southwards to shallow depth probably by ductile channel flow between the MCT1 and the STD1. Finally, they underwent N-S trending folding after 13 Ma.

LATE QUATERNARY CLIMATIC CONTROL ON EROSION AND WEATHERING IN THE EASTERN TIBETAN PLATEAU AND THE MEKONG BASIN

Zhifei LIU (1), Christophe COLIN (2), Alain TRENTESAUX (3), Giuseppe SIANI (2), Norbert FRANK (4), Dominique BLAMART (4), Segueni FARID (2)

(1) Laboratory of Marine Geology, Tongji University, Shanghai 200092, China; email: lzhifei@online.sh.cn; fax: +86-21-6598 4877.

(2) Laboratoire Orsayterre, FRE 2566, BAT. 504, Université de Paris XI, 91 405 Orsay, France.

(3) PBDS Laboratory, UMR 8110 CNRS, University of Lille 1, 59 655 Villeneuve d'Ascq, France.

(4) Laboratoire des Sciences du Climat et de l'Environnement, Laboratoire mixte CNRS-CEA, Avenue de la Terrasse, 91198 Gif-sur-Yvette Cedex, France.

Much of the sediment derived from erosion of the Himalayas is well preserved, especially in the Arabian Sea and the Bay of Bengal, providing an opportunity to examine how clastic sediments record erosion and weathering processes (Curray, 1994). Results from sediments stored in the Bay of Bengal indicate that the strength of summer monsoon rainfall is an important factor driving weathering and erosion of the Himalayas (Derry and France-Lanord, 1996). Over the last two glacial/interglacial cycles, smectite/(illite+chlorite) and kaolinite/quartz rations combined with a chemical index of alteration indicate that the weathering intensity of the Himalayan and Burman ranges is mainly controlled by the summer monsoon rainfall intensity based on the Andaman Sea and Bay of Bengal sediments (Colin et al., 1999). Therefore, the similar monsoon-controlled weathering and erosion would be expected to occur over the eastern Tibetan Plateau, where the erosion and climate relationship remains poorly understood (Schäfer et al., 2002).

This study reports high-resolution studies of oxygen isotope and carbonate stratigraphy, clay and bulk mineralogy, major element geochemistry, siliciclastic grain size, combined with rubidium, strontium, and neodymium isotopes, on high sedimentation rate cores, MD01-2393 (10°30.15'N, 110°03.68'E, 1230 m water depth) and MD97-2150 (10°11.76'N, 119°31.51'E, 292 m water depth), off the Mekong River in the southwestern South China Sea. The primary objective was to reveal the relationship between past changes in the erosion and chemical weathering and the East Asian monsoon rainfall during late Quaternary (over the past 190 kyr) in the eastern Tibetan Plateau and the Mekong Basin.

The ranges of isotopic composition from Core MD01-2393 are limited throughout sedimentary records: $^{87}Sr/^{86}Sr$ = 0.7206 to 0.7240 and $\varepsilon_{Nd}(0)$ = -11.1 to -12.1. These values match well to those of Mekong River sediments and suggest that the Mekong River has provided most of siliciclastic materials to the two cores, appearing to be ideally suited for the study of the interaction of climate change with erosion and weathering processes. Concerning clay minerals, illite and chlorite derived mainly from the eastern Tibetan Plateau, where physical erosion of metamorphic and granitic parent rocks is dominant; kaolinite derived mainly from active erosion of inherited clays from reworked sediments in the middle part of the Mekong Basin; smectites originated mainly through chemical weathering of parent aluminosilicates and ferromagnesian silicates under warm and humid conditions in the middle to lower reaches of the Mekong River (Liu et al., 2004).

Smectites/(illite+chlorite) and smectites/kaolinite ratios are used as indices of chemical weathering rates, whereas the bulk kaolinite/quartz ratio is used as an index of physical erosion rates in the eastern Tibetan Plateau and the Mekong Basin. Furthermore, siliciclastic grain size population 2.5-6.5 μm/15-55 μm and major element geochemical Al_2O_3/SiO_2 ratios present the intensity of sediment discharge of the Mekong River and, in turn, the East Asian summer monsoon intensity. Strengthened chemical weathering corresponds to increased sediment discharge and weakened physical erosion during interglacial periods. In contrast, weakened chemical weathering associated with reduced sediment discharge and intensified physical erosion during glacial periods. Such strong glacial-interglacial correlations between chemical weathering/erosion and sediment discharge imply the monsoon-controlled weathering and erosion history during the last 190,000 yr in the eastern Tibetan Plateau and the Mekong Basin.

COLIN, C., TURPIN, L., BERTAUX, J., DESPRAIRIES, A. & KISSEL, C., 1999. *E. P. S.. L.*, **171**. 647-660. CURRAY, J.R., 1994. *E. P. S.. L.*, **125**. 371-383. DERRY, L.A. & FRANCE-LANORD, C., 1996. *E. P. S.. L.*, **142**. 59-74. LIU, Z., COLIN, C., TRENTESAUX, A., BLAMART, D., BASSINOT, F., SIANI, G. & SICRE, M.-A., 2004. *Mar. Geol*, **209**. 1-18. SCHÄFER, J.M., TSCHUDI, S., ZHAO, Z., WU, X., IVY-OCHS, S., WIELER, R., BAUR, H., KUBIK, P.W. & SCHLÜCHTER, C., 2002. *E. P. S.. L.*, **194**. 287-297.

P-T EVOLUTION AND AGE OF THE BARROVIAN METAMORPHISM IN THE MCT ZONE OF THE ARUN VALLEY, E NEPAL

Bruno LOMBARDO (1), Daniela RUBATO (2), Franco ROLFO (3) & Piero PERTUSATI (4)

(1) CNR, Istituto di Geoscienze e Georisorse, Torino, Italy.
(2) Department of Earth and Marine Sciences, The Australian National University, Canberra, Australia.
(3) Dipartimento di Scienze Mineralogiche e Petrologiche, Torino University, Italy.
(4) Dipartimento di Scienze della Terra, Pisa University, Italy.

From Tumlingtar, in the core of the Arun tectonic window (ATW) northwards, the following lithotectonic units are exposed:

1) The Lesser Himalayan Tumlingtar Unit (*Nawakot nappes* of Hagen, 1969), a thick sequence of greenschist-facies metasediments, bounded to the north by a syn-metamorphic thrust zone (*Main Central Thrust 1* of Maruo & Kizaki, 1983; *Main Central Thrust Zone* of Meier & Hiltner, 1993).

2) The MCT zone (*Kathmandu nappes* of Hagen, 1969), staurolite to kyanite grade micaschists and granitic orthogneiss (*Num Orthogneiss* of Lombardo et al., 1993) lying on top of the Tumlingtar Unit.

3) The Higher Himalayan Crystalline nappe (HHC) bounded on both side of the ATW by thrust sheets defining a major syn-metamorphic thrust (*Main Central Thrust* of Bordet, 1961; *Main Central Thrust 2* of Maruo & Kizaki, 1983).

The Lesser Himalayan sequence and the MCT zone are characterized in the Arun valley (as elsewhere throughout the Himalaya) by an inverted metamorphism, such that metamorphic grade increases toward structurally higher levels. Mineral assemblages and geothermometric data indicate an up-structure increase in temperatures from 400°C in Tumlingtar Unit to 500°-650°C in the MCT zone and over 700°C in the HHC (Maruo & Kizaki, 1983; Brunel & Kienast, 1986; Pognante & Benna, 1993; Goscomb & Hand, 2000).

A polyphase metamorphic evolution has been documented in the HHC of the Arun valley (Brunel & Kienast, 1986; Pognante & Benna, 1993) and is best seen at the northern end of the ATW in the Kharta region of S Tibet. Here granulite-facies garnet-bearing metapelites, metabasics and calc-silicate rocks from the lower metamorphic complex (Kharta Gneiss) of the HHC preserve textural and chemical evidence for prograde equilibration in the sillimanite stability field at temperatures of at least 700-720°C and pressures close to 8 kbar during the main Himalayan metamorphic event. Post-deformational reaction textures indicate a decompressional pressure-temperature evolution which is confirmed by geothermobarometry of zoned and symplectite minerals, as well as by modeled phase equilibria. Decompression from 8 to *c.* 3 kbar occurred at temperatures of about 700°C, and was followed by static recrystallization at temperatures of *c.* 650°C and metamorphic pressures of *c.* 2.5 kbar (Borghi et al., 2003).

Petrological study of gneisses and amphibolites from upper structural levels of the MCT zone shows evidence for a clockwise P-T path similar to that followed by the HHC, but at significantly higher metamorphic P. Peak-P conditions retrieved from mineral cores are around 12.0 kbar at 720°C and the thermal peak is recorded from intermediate mineral zones at *c.* 9.0 kbar and 730°C, at the boundary between the kyanite and sillimanite stability fields. Compositions of mineral rims indicate later cooling to *c.* 620°C at 7.0 kbar. These estimates are consistent with data reported by Goscomb & Hand (2000), but extend the P range recorded by the highest-grade rocks (their metamorphic zone G) to slightly higher pressures. Earlier data by Brunel & Kienast (1986) and Pognante & Benna (1993) for kyanite gneisses and micaschists from the same section investigated by Goscomb & Hand (2000) and these authors appear to record mainly thermal-peak P-T conditions or the later cooling.

Zircon and monazite from an amphibolite facies Grt-Ky-Bt gneiss at the top of the MCT zone have been dated by SHRIMP. The zircon crystals show inherited detrital cores of various age, with a young component at *c.* 445 Ma. The cores are overgrown by a poorly zoned, U-rich rim with metamorphic characteristics, that yields a U-Pb age of 30.7±0.3 Ma (95% c.l.). Homogeneous monazite that contains metamorphic inclusions has been dated at 31.0±0.2 Ma (95% c.l.). Inclusion and trace element data have been gathered to link the Oligocene age to the metamorphic conditions of zircon and monazite formation.

BORGHI A., CASTELLI D., LOMBARDO B. & VISONÀ D. 2003. *Eur. J. Mineralogy*, **15**, 401-418. BORDET P. 1961. *Recherches géologiques dans l'Himalaya du Népal, région du Makalu.* Ed. CNRS, Paris, 275 pp. BRUNEL M. & KIENAST J.R. 1986. *Can. J. Earth Sc.*, **23**, 1117-1137. GOSCOMB B. & HAND M. 2000. *J.Petrology*, **41**, 1673-1719. HAGEN T. 1969. *Mém.Soc. Helv. Sc. Nat.*, **86/1**, 185 pp. LOMBARDO B., PERTUSATI P. & BORGHI S. 1993. In: P. J. Treloar & M. P. Searle (eds) - Himalayan Tectonics. *Geol. Soc. Sp.Pub.*, **74**, 341-355. MARUO Y. & KIZAKI K. 1983. In: Shams, F.A. (Ed.) *Granites of Himalayas, Karakorum and Hindu Kush.* Institute of Geology, Punjab University, Lahore, 271-286. MEIER K. & HILTNER E. 1993. In: P. J. Treloar & M. P. Searle (eds) - Himalayan Tectonics. *Geol. Soc. Sp.Pub.*, **74**,, **74**, 511-523. POGNANTE U. & BENNA P. 1993. *ibid.*, **74**, 323-340.

Note Page

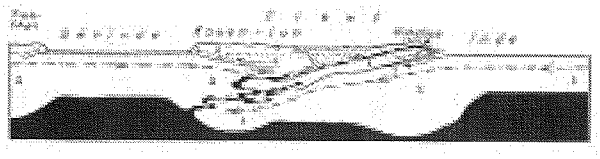

Argand, 1922

ON THE RELATIONSHIP OF THREE CENOZOIC GEODYNAMIC REGIMES IN TIBETAN PLATEAU: EVIDENCES FROM THE IGNEOUS ROCKS*

Zhaohua LUO, Xuanxue MO, Jinfu DENG, Zhongmin HUANG, Shan KE

(1) State Key Laboratory of Geo-Processes and Mineral Resources, China University of Geosciences, Beijing, 100083

To interpret the growth of Tibetan plateau have provided several tectonic models, among which the most famous are Tapponnier's extrusion model, Dewey's distribution shortening model and Argand's underthrust model. It is, however, difficult to explain the formation process of Tibetan plateau solely in one model. Recently, some geologists provided evidences that suggest the spatial and temporal inhomogeneity of the Plateau evolution. This means the Tibetan plateau undergone simultaneously different processes at different segments, determined by their dynamic conditions. Because the evolution of Tibetan plateau is generally controlled by the Indian-Asian collision regime, it is necessary to provide an integrated model for explanation of processes and their relationships.

The geophysical exploration suggests that the Tibetan lithosphere has heterogeneous structure and can be divided into three types. The lithosphere structures of Parmirs, Qiangtang and Nianqing Tanggula can be considered their typical representatives (Deng et al., 2001). Therefore, the Tibetan Plateau has an asymmetrically temporal and spatial evolution history. This feature can be accommodated by the geochronology of Cenozoic volcanic rocks.

The overview of dating results for the geological events shows a systematical diversity of age data obtained through various approaches. This is not only because of the difference of dating methods, but also the succession of events. We consider the lithosphere plate weakening is initiated by the heat energy injection from asthenosphere depths. As subsequent events, there will be occurred mantle-derived magmatism, crustal metamorphism, crust-derived magmatism, crustal shortening and thickening, regional rising and erosion. Therefore, the research of igneous rocks may be the key approach to achieve an integrated model.

The geochronology and stratigraphy of Linzhou volcanic rocks (at the southern Tibet) indicate that the collision of the two continents was onset at 65 Ma BP. The volcanic rocks show calc-alkaline trend and continental arc setting, and thus they are of lagged arc volcanism (Mo et al., 2003). The statistics of isotopic ages of the Cenozoic igneous rocks displays dubious cases and diversity of different segments. It is suggests that the magmatisms in different segments are controlled by tectonic factors. According to their linear distribution paralleled to the Yalung Zangbo suture, the volcanic rocks and their intrusive equivalent in the southern Tibet can be easily related to convergence processes. In the central Tibet, the Cenozoic igneous rocks are diffused and, therefore, the magmatism seems to be controlled by collapse of the thickened lithosphere. Igneous rocks contributed along large faults are the products of strike-slip movement and rotation of blocks. Therefore, it is reasonable to consider that there are three geodynamic regimes governed origin and evolution of the Cenozoic igneous rocks in the Tibetan Plateau: collision, strike-slip and collapse regimes.

Based on the progresses in petrology and geochemistry of Cenozoic igneous rocks, we show the relationships of the tree geodynamic regimes. The Indian-Asian continental collision is the primary power. The collision stress can be transport to a long distance when the lithosphere is cold and rigid. The collision process, therefore, presented not only between the Indian and the Asian continents, but also between large blocks, for example, between the Tibet plateau and the Tarim basin. At this time, strike-slip movement may take place along the old deep faults. The collision-synchronous volcanic activities at the adjacent region can be considered as the evidence that theIndian-Asian collision trigged the large-scale strike-slip motion. In this process, the northern Tibetan lithosphere can be heated by deep heat flow or weakened by fluid injection. As the lithosphere become hotter and plastic future, it will be deformed and thickened, following lithosphere collapse and extrusion.

The strike-slip movement, therefore, seems to immediately occur when the collision of India-Asia continents is onset. A good example is that the volcanic activities in Qilian Mountain and southwestern Tienshan synchronously occurred at about 60-70Ma when India-Asia collision is occurring.

The mantle-derived basaltic eruption and related intrusion can be found only at the ends or crossing parts of strike-slip faults. On the other hand, the volcanic activities radially migrate from the Central Tibet. These volcanic activity patterns can be explained only by delamination step by step. The most early mantle-derived magmatism in the main Tibetan plateau is present by the emplacement of lamprophyre magma in the central Qiangtang, northern Tibet. The event was dating at ca. 45 Ma. We believe this is the time when lithosphere is collapsing instead of India-Asia collision. Therefore, delamination is late than collision about 20Ma. This may be a necessary interval for that the lithosphere thickening obtains enough thickness to collapse. Then the delamination will occur around the central Qiangtang where the lithosphere instability is easy reached than other areas. So, the collapse process is radiative. At about 25~23Ma, for example, the delamination involved Bangong-Nujiang suture, and then touched Gangdes belt at 15-13Ma.

According to these, we consider the plateau formation as a successive process divided to several tectono-magmatic stages, which can be remarked by the mantle-derived magmatism. Although different segments have own characteristic event time scale decided by local dynamic condition, we can roughly provide a reference time scale for all the plateau: >65Ma, 65-45Ma, 45-25Ma, 25-15Ma, 15-4Ma and <4Ma.

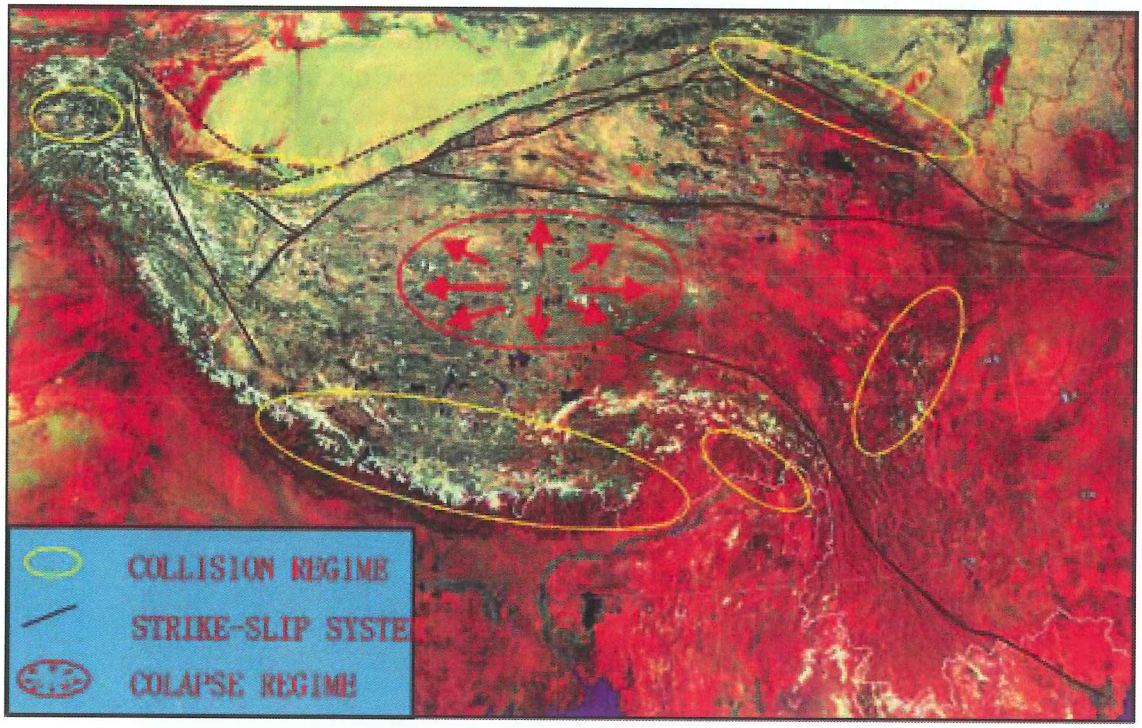

Fig. 1- A schematic map showing the distribution of different tectonic regimes (Luo et al., 2004).

* Supported by NSFC Project (40472038): The Cenozoic igneous rocks at the margins of Tarim Basin and their relation to the Indian - Asian continental collision.

THE CENOZOIC BASALTS FROM KANGXIWAR (WESTERN KUNLUN) AND THEIR IMPLICATIONS TO THE UPLIFTING OF THE TIBETAN PLATEAU

Zhaohua LUO (1), Yusheng WANG (2), Xuanxue MO (1), Jinfu DENG (1), Zhongmin HUANG (1)

(1) State Key Laboratory of Geo-Processes and Mineral Resources, China University of Geosciences, Beijing, 100083
(2) Beijing SHRIMP Center, Beijing, 100037

The Tibetan plateau has significant roles in the formation of the Asian monsoon circulation due to its high elevation. Many evidences suggest that the formation process of Tibet plateau has inhomogeneous features in spatial and temporal dimensions. These increase the interests of geologists in the phases and local differences of the plateau development. Deng et al. (2001) indicate that there are three main lithospheric types, showing evolutional relations. The representative types are named as Parmirs-type with cool lithosphere roots, Nianqing Tanggula-type with thinned lithosphere roots and Qiangtang-type with "warm" lithosphere roots. The lithosphere structure characteristics have been related to the tectonic development of the Tibetan plateau. Therefore, the initiation of Tibetan uplifting is related to the lithosphere – asthenosphere interactions induced by Indian-Asian collisions. According to this aspect, the mantle-derived primary volcanic rocks should record the foremost magmatism event in a tectono-magmatism cycle, and recognition of primary magma is very important.

The Kangxiwar Cenozoic volcanic rocks are located at about 9 km southeast far from Kangxiwar village, south of the river Kalakash (Fig. 1). The outcrop area is about 2 km^2. The Cenozoic volcanic (basaltic) rocks are covered by fine-grained sand transported from Tarim basin. The volcanic stratum consists of hypermelanic compact massive olivine basalt, aubergine volcanic agglomerate, vesiculation slag basalt, welding volcanic agglomerate, compact massive olivine basalt, aubergine volcanic agglomerate, secondary pyroclastic rock and welding cinder. The lava is dark grayness, porphyritic texture and vesicular structure with phenocrysts about 10 percent. The essential phenocryst minerals are clinopyroxene and plagioclase and the characterized minor biotite and olivine. The groundmass minerals are mainly microcrystalline plagioclase, clinopyroxene and a little olivine and glass. Apatite, titanomagnetite and zircon are the common accessory minerals. In addition, there are many xenoliths and xenocrysts. The volcanic rocks have higher contents of Ni and Cr, MgO/(MgO + FeO) ratio and lower SiO_2. These reveal their primary magma features.

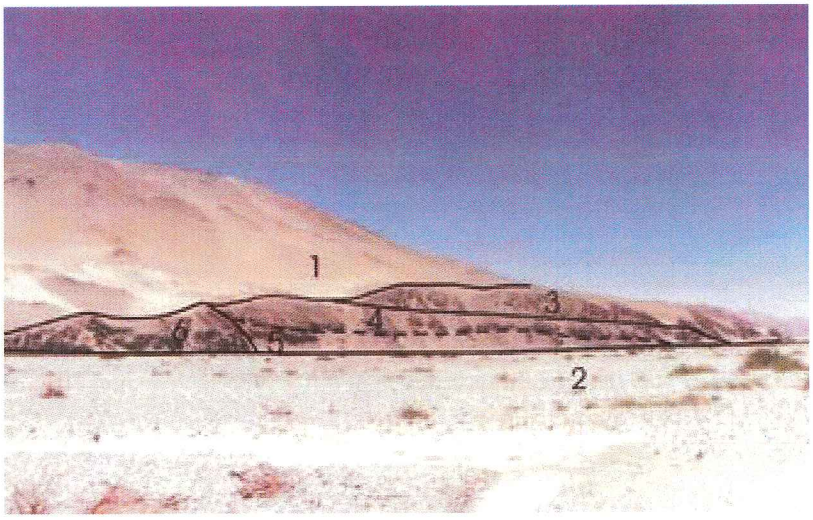

Fig. 1 The Kangxiwar basaltic stratum
1- eolian sand, 2-river bed, 3- massive basalt, 4- slag basalt, 5- welded agglomerate, 6-country rocks

Mantle-derived peridotite xenoliths firstly discovered in these basaltic rocks. They are mainly spinel-bearing lherzolite and harzburgite. Peridotite xenoliths are yellow-green, blocky structure and fine-grained blastic texture with essential olivine and minor orthopyroxene and clinopyroxene. The minor mineral spinel belongs to Cr-spinel with the ratio of 100 _Cr/ (Cr + Al) =20.30 ±. Correspondingly, olivine and orthopyroxene are also characterized by the low value of Mg#. The composition of olivine is Fo = 86.05 and Fa = 13.95 and orthopyroxene belongs to bronzite with composition of $Fs_{11}En_{88}Wo_1$. Peridotite xenoliths mainly have equilibrium granoblastic texture. Porphyroclast minerals can be seen once in a while. And a little minerals remain kink band. It is indicate that the peridotites have experienced a structure adjustment period equaling to the stable stage after it diapirs before the mantle rocks enter the basalt magma. Partial melting bubbles also present in peridotite xenoliths and their compositions vary greatly. It is indicated that the mantle underwent partial melting during its upwelling. The high modal olivine, low Mg# of olivine and orthopyroxene and presence of phlogopite (Fig. 2) show that the lithosphere effected by deep fluid metasomatism. This is coincident with the unusual characteristics of host rocks.

Due to the xenoliths and xenocrysts, it is very difficult to select an effective geochronology method. Fortunately, there are abundant zircon crystals. The U-Pb dating of zircon by SHRIMP II is used for obtaining an accurate age of 3.8 Ma (Fig. 3). This is the youngest zircon age obtained in China until now, and the youngest age of primary igneous rocks.

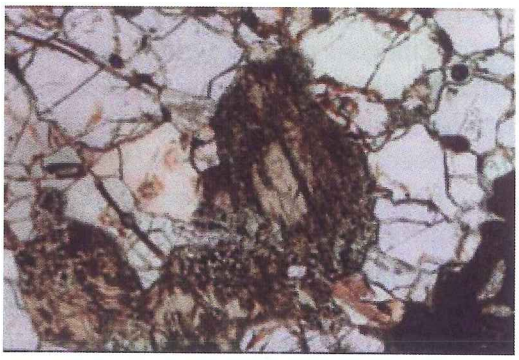

Fig. 2 Phlogopite crystals and their dissolution

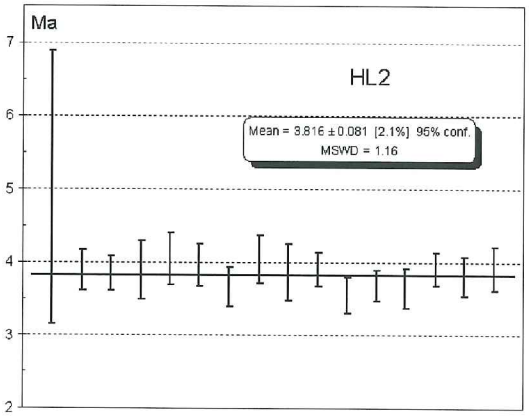

Fig. 3 Zircon $^{206}Pb/^{238}U$ age variation of Neogene basalt (HL2) in the Tibetan Plateau
Data point with high error and departure is 1.1. Error bar is 1σ. Weighted mean age is calculated for 16 data points (2σ, 95% confidence)

As we know, the surface rising depends on the crust buoyancy, which is induced mainly by the lower crust flowing. The lower crust only flows when heating significantly reduces its viscosity, either from igneous intrusions or by the addition of water (McKenzie, 2002). In the conditions without water input such as in the northern Tibet, convective heating is the only approach to induce crust flow and thickening. Therefore, the injection of mantle-derived magmas is necessary for heating of the lower crust. As a consequence, there will be appeared a time-event spectrum: mantle-derived magmatism, crust-derived magmatism and lower crust flowing, crust thickening, plateau uplifting, erosion of surface rocks and sedimentation of incompact sediments in basin. Based on this understanding of the geological processes, we propose the age of 3.8 Ma is the initial time of last plateau uplifting event.

References

Deng J, Mo X, Luo et al., 2001, Science in China (D), 44, 56-63
Dan McKenzie & James Jackson, 2002, *Tectonics,* 21, 1394-1401

NEOGENE EXHUMATION OF THE PALUNG GRANITE (LESSER HIMALAYA, NEPAL) FROM (U-TH)/HE THERMOCHRONOLOGY

Gweltaz MAHÉO (1), Jean Philippe AVOUAC (1), Aron MELTZNER (1), Laurent BOLLINGER (2) and Ken FARLEY (1)

(1) Division of Geological and Planetary Sciences, California Institute of Technology, 100-23 N-Mudd, 1200 E. California Bvd, 91125 California, USA. maheo@gps.caltech.edu
(2) Laboratoire Détection et Géophysique, Commissariat à l'Energie Atomique, Bruyère le Châtel, France.

The Himalaya is a particularly appropriate case study to analyze how topography evolves in response to tectonic and climatic forcing. The structure of the range is reasonably well constrained as well as the kinematics of present deformation, and the pattern of modern erosion. In complement recent thermometric and thermochronologic measurements have provided constraints on the thermal structure and the structural evolution of the range over the Miocene. So far most available data and observations can be explained by a simple model in which the topography is assumed to be in steady-state due to some balance between erosion and tectonic uplift. Although such an asymptotic balance is expected to result form the interplay between surface processes and crustal deformation, the system should always be out of equilibrium due to the varying climate and episodicity of tectonic adjustment. This problem might be best addressed from thermochronologic investigations using systems with low closure temperature (fission track or (U-Th)/He). So far such studies have been performed in the northern part of the Lesser Himalaya and in the High Crystalline Himalaya, the high elevation, high relief part of the range. To complement recent investigations which have focused on the High Himalaya, we have started a preliminary study of the Neogene exhumation of Lesser Himalaya. As a field target we have selected the Palung granite, a Paleozoic granite body which crops out south of Kathmandu basin. We collected 6 samples along a ~700m vertical cross section, for both apatite and zircon (U-Th)/He dating. These data will be compared with synthetic ages obtained from a given time-temperature path computed with the He production-diffusion equation following the method developed by Wolf et al. (1998). The time-temperature paths will be predicted from thermo-kinematic modeling. These thermochronological data will allow us to compare how exhumation rates in the Lesser Himalaya have varied with time over the last about 8Myr.

WOLF, R.A., FARLEY, K.A. & KASS, D.M. 1998. *Chem. Geol.*, **148**. 105-114.

Note Page

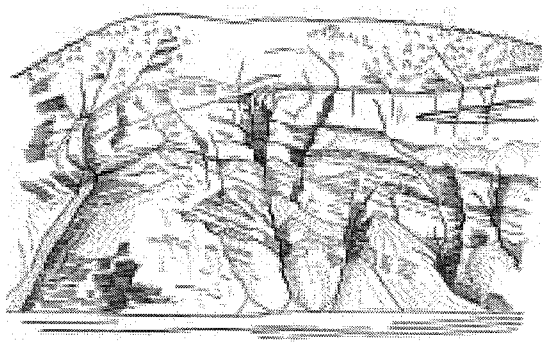

Marpha, Bordet, 1954

TIMING CONSTRAINTS ON THE KUNG CO PLUTON AND NORMAL FAULT (SOUTH TIBET, P.R.CHINA) BASED ON AR/AR AND (U-TH)/HE THERMOCHRONOLOGY

Gweltaz MAHÉO (1), Franck VALLI (2), Philippe Hervé LELOUP (3), Robin LACASSIN (2), Nicolas ARNAUD (4), Jean-Louis PAQUETTE (5), Alain FERANDEZ (3), Li HAIBING (2, 6), Ken FARLEY (1), and Paul TAPPONNIER (2)

(1) Division of Geological and Planetary Sciences, California Institute of Technology, 100-23 N-Mudd, 1200 E. California Bvd, 91125 California, USA (maheo@gps.caltech.edu)
(2) Laboratoire de Tectonique, Mécanique de la Lithosphère, UMR7578 CNRS, Institut de Physique du Globe de Paris, 75252 Paris CX05, France.
(3) Laboratoire de Dynamique de la Lithosphère, UMR5570 CNRS, UCB et ENS Lyon, 2 rue Dubois, 69622 Villeurbanne, France.
(4) Laboratoire de Dynamique de la Lithosphère, UMR5573 CNRS, ISTEEM – USTL, Place Eugène Bataillon, 34095 Montpellier, France.
(5) Laboratoire Magmas et Volcans, UMR6524 CNRS, Université Blaise Pascal, Rue Kessler, 63038 Clermont Ferrand CX, France.
(6) Institute of Geology, Chinese Academy of Geological Sciences, 26 Baiwanzhuang Road, Beijing 100037, PR China.

Estimation of the timing of extension in the Tibetan plateau has been widely used to constrain the geodynamic evolution of the India-Asia convergence zone and test different proposed models. However, very few reliable data on the initiation age of the normal faults are yet available. Armijo et al. (1986), the first to describe active normal faulting in south Tibet, estimated that they initiated after 2.5 Ma ago from stratigraphic and morphologic consideration. In this work we focus on one of these potentially Late Pliocene faults, the Kung Co half graben (Southern Tibet, China), bounded by an active normal fault with a minimum vertical offset of about 1600 m (Armijo et al., 1986). In order to constrain the opening age of this half graben we combined high and medium temperature (U-Pb, Ar/Ar) and low temperature ((U-Th)/He) thermochronometry. Ages have been obtained for 6 samples of the Kung Co pluton, collected along a vertical profile located in the hanging wall at elevations between 4560 and 5055 m.

The Kung Co pluton is a two mica granite formed at about 21 Ma (U/Pb zircon), that belongs to the northern Himalayan granitic belt. Biotite and muscovite Ar/Ar ages are similar, ranging from ~16 Ma (Ms) to ~ 15 Ma (Bt). The zircon (U-Th)/He ages are between 10.5 and 9.5 Ma and the apatite (U-Th)/He ages between 9.5 and 3.5 Ma. Both zircon and apatite (U-Th)/He ages increase with elevation.

Thermobarometric study of the contact aureole of the pluton indicates that the granite intrusion stopped at 2-3 kbar (~10km) and ~520-545°C. At such a depth the equilibrium temperature is between 200 and 400°C depending of the geothermal gradient. Thus muscovite and possibly biotite Ar/Ar ages are related to this thermal re-equilibration. The biotite and muscovite Ar/Ar ages imply a relatively fast cooling rate of 70 ± 30°C/Ma from 16 to 15 Ma. Coupling of biotite Ar/Ar and zircon (U-Th)/He ages indicates that the cooling rate significantly decreases after 15 Ma, to less than 30 °C/Ma. Considering the depth and temperature of emplacement of the pluton, the fast cooling period is associated with post-intrusion thermal re-equilibration occurring around 15-16 Ma. After the thermal-re-equilibration, modeling of the zircon and apatite (U-Th)/He ages indicates that the pluton was exhumed at 1 to 1.5 mm/yr between at least 10.5 and 8 Ma. Our modeling also suggests that this exhumation event might have start around 15 Ma. The two samples from the base of the fault scarp give apatite He ages of 3.5-4.5 Ma, too young to be compatible with the prolongation of that first exhumation event. These young ages may indicate a drop in the exhumation rate from 1-1.5 mm/yr between 15 and 8 Ma to ~ 0.02-0.03 mm/yr between 8 and 4 Ma. However, they can also result from resetting either by fluid circulation or by shear heating along the fault plane.

The first exhumation event, between 15 Ma and 8 Ma, is probably related to southward thrusting and doming along the Gyirong-Kangmar thrust and the formation of the northern Himalayan antiform. The Gyirong-Kangmar thrust is located just south of the Kung Co pluton and is controlling the formation and exhumation of the Kangmar dome between ~15 and 11 Ma (Lee et al., 2000). Since the thrust is crosscut by the normal fault, this implies that the extension started after 8 Ma ago.

If the ages from the two lowest samples have not been reset and are significant for the pluton cooling history, they provide another constraint on the timing of extension in the Kung-Co half graben. Actually, the slow apparent exhumation rate calculated between 8 Ma and ~ 4 Ma (0.02 – 0.03 mm/yr) cannot account for the formation of the Kung-Co half graben as extrapolation of such rate to the present would only produce between 120 and 75 m of exhumation compared with the ~1600 m of vertical offset along the active normal fault. We conclude that the graben probably initiated after 4 Ma ago. This maximum age is consistent with the initiation age of about 2.5 Ma proposed by Armijo et al. (1986).

ARMIJO R., TAPPONNIER P., MERCIER J.L., & HAN T. 1986. *J. Geophys. Res.*, **91**, 13803-13872.
LEE J., HACKER B.R., DINKLAGE W., WANG Y., GANS P., CALVERT A., WAN J.L., CHEN W., BLYTHE A.E. & MCLELLAND W. 2000. *Tectonics,* **19**. 872-895.

RE-ORGANISATION OF THE HIMALAYAN FORELAND BASIN GEOMETRY AS A RESULT OF A BREAK-OFF OF THE INDIAN SLAB

Jean-Louis MUGNIER, Pascale HUYGHE

LGCA, CNRS, Maison des Géosciences, BP 53, 38041, Grenoble Cedex

The Tertiary continental series of the Himalayan foreland basin are classically subdivided in Siwalik and pre-Siwalik groups with a boundary dated at ~13 Ma in Western Himalaya and ~15.5 Ma in Central Himalaya. From the analysis of 24 drills-holes of the foreland basin and seismic lines, we find that the southward migration rate of the pinch-out of the Siwalik sediment is 20 ± 6 mm/yr and equals the Himalayan shortening rate estimated by others tectonic methods. This equality confirm the previous assumption that the foreland basin development is linked to the flexure of the lithosphere ahead of the southward moving Himalayan thrust belt. For the Tertiary pre-Siwalik sediments, the pinch-out migration rate was smaller whereas the Himalayan shortening rate remained nearly constant. Furthermore erosion surfaces at the boundary between the two groups develop locally above Indian shield lineaments that were reactivated beneath the basin during the end of the deposit of the pre-Siwalik group.

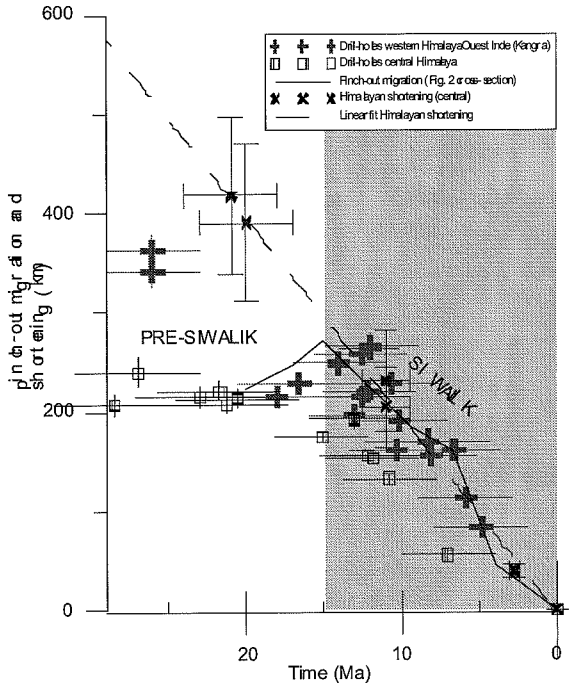

Fig. 1: Comparison between Himalayan shortening and migration of the pinch-out of the foreland basin. The thick crosses, the squares and the thin continuous line refers to a plot of inferred age of the base of the Tertiary sediment vs. distance from the edge of the Ganga basin.fore deep, respectively for drill-holes east of E78°, for drill-holes west of E78° and for a median cross-section. The thick x and the hached line refer to a plot of time vs. Himalayan shortening.

We suggest that this change in the development of the basin before 15 Ma is linked to the detachment of a subducted continental mantle at the trailing edge of the Indian lithosphere, because: A) a detached mantle body is presently imaged beneath India by tomographic studies; B) the detachment decreased the slab pull induced by the subducted lithospheric mantle; C) an increase of the compressive stress within the plate was needed to maintain the constant convergence of the Indian plate and D) this increase favoured fault reactivation within the Indian crust; E) detachment of the heavy roots of the Himalayan belt changed the forces at the trailing edge of the flexed lithosphere and decreases its curvature; F) this isostatic lithospheric rebound reduced the regional southward migration of the foreland basin and induced a regional increase of the Himalayan topography.

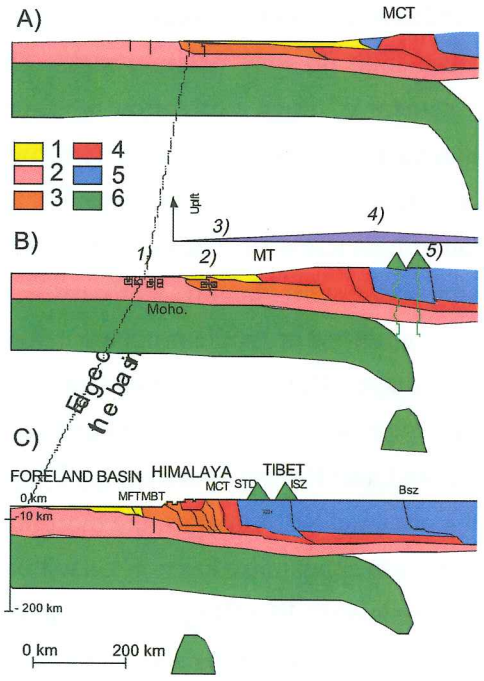

Fig. 2: A sketch of the evolution at lithospheric scale of the Ganga basin-Himalaya-Tibet. The vertical scale is magnified by 5, for the uppermost crust (above a depth of 10 km) to see the foreland basin and the Himalayan relief. The lithospheric structures are not vertically magnified.

1- Tertiary foreland basin; 2- Crust of the Indian shield; 3- Lesser Himalaya; 4- Higher Himalaya; 5- Tibetan Himalan Zone; 6- Indian lithospheric mantle.

MFT: Main Himalayan Thrust; Main Frontal Thrust; MBT: Main Boundary Thrust; MCT: Main Central Thrust. MT: Mahabarat Thrust; STD: South Tibetan detachment; ISZ: Indus-Yalu suture zone

a) Geometry at ~20Ma. The Indian continental lithospheric mantle subducted in the lithosphere.

b) Geometry at ~ 15 Ma. The inferred uplift pattern for a lithospheric mantle slab break-off is indicated above. Lithospheric mantle break-off induced an increase of the stresses and fault reactivation in the Indian shield *(1)* and in the future Lesser Himalaya *(2)*, local erosion of the foreland basin *(3)*, amplification of the altitude of the Himalaya *(4)* and thermal event and volcanism in south Tibet *(5)*.

c) Present day state (adapted from De Celles et al., 2002).

A NEW OCCURRENCE OF MICRODIAMOND FROM INDUS SUTURE ZONE, HIMALAYA: POSSIBLE ORIGIN

Barun MUKHERJEE (1,2), Himanshu SACHAN (1) and Talat AHMAD (3)

(1) Wadia Institute of Himalayan Geology, 33, G.M.S. Road, Dehra Dun-248 001, India
(2) Presently **at** Department of Earth and Planetary Sciences, Tokyo Institute of Technology, 2-12-1, Ookayama, Meguro, Tokyo 152-8551, Japan
(3) Department of Geology, Delhi University, Delhi- 110011, India
Corresponding author's e-mail barun@geo.titech.ac.jp & mukherjeebarun@yahoo.co.in

A new occurrence of microdiamond crystals in the Himalaya, were recovered from Tso-Morari Crystalline Complex, Indus Suture Zone, Ladakh. The microdiamond present as inclusions in garnet and zircon within ultra–high pressure eclogite rock[1]. The TMC is a metamorphic core complex comprises lower basement of Puga Formation overlain by Taglangla Formation and relatively undeformed Polokangla and Rupshu granitoid. The Puga consisting of ortho and para gneisses way up to green schist facies rock, hosting eclogite[2,3] boudins of 0.5 – 28 m dimension, running parallel to the foliation of host gneisses. The core of large boudins are fresh and unaltered, it has principally garnet and omphacite with phengite, carbonates, glaucophane, epidote, coesite ± kyanite, ± staurolite etc. The two grains of microdiamond inclusion has noticed, ranging from ~12-18 micron in size with varying shape. The microdiamond of multiple star shaped - intergrowth structure were found in the newly grown or recrystallized zircon devoid of any specific zoning, which is further confirmed by using Laser Raman Spectroscopy by typical and characteristic diamond peak at 1332.4 cm^{-1}. While the obtained SEM images, the morphology of microdiamond showing crystalline aggregate, feebly fibrous in appearance has noticed within sharply zoned garnet porphyry.

The record of polyphase inclusions like CO_2, CH_4, N_2 and ± H_2O along with preservation of microdiamond inclusion within UHP eclogite under static condition at T > 750°C and P > 39 kbar[4], showing equilibration relation. The trapping and influx of supercritical fluids at peak metamorphism are may giving rise the valid explanation for its origin, this might be explain due to CO_2 -H_2O (carbonic fluids) fluid influx in to the system or behavior of C (Carbon) in the solid carbonates (magnesite and dolomite).

Moreover the leading factor responsible for the origin and crystallisation of microdiamond soon after the peak metamorphism at the initiation of exhumation, possibly driven due to the interference of fluid activity during the leading edge of Indian subducting plate underneath the Eurasian plate, touching at the depth of >120 km (i.e. mantle depth).

References:

1. MUKHERJEE, B.K. & SACHAN, H.K. 2001. *Current Science* **81**, 1358-1361.
2. GUILLOT, S., SIGOYER, J.DE. LARDEAUX, J.M. & MASCLE, G. 1997. *Contrib. Mineral. Petrol.* **128**, 197-212.
3. SACHAN, H.K. BODNAR, R.J., ISLAM, R., SZABO, CS. & LAW, R.D. 1999. *Jour. Geol. Soc. Ind.*, **53**,181-190.
4. MUKHERJEE,B.K., SACHAN, H.K, OGASAWARA,Y., MUKO,A.,& YOSHIKA, N. 2003. *Internat. Geol. Rev.* **45**, 49-69.

PROVENANCE OF EARLY FORELAND BASIN SEDIMENTS, NEPAL: CONSTRAINTS TO THE TIMING AND DIACHRONEITY OF EARLY HIMALAYAN OROGENESIS.

Y. NAJMAN[1], P. DECELLES[2], G. GEHRELS[2], A. CARTER[3], A. MARTIN[2], G. OLIVER[4], E. GARZANTI[5].

[1]: Dept of Environmental Science, Lancaster University, Bailrigg, Lancaster, LA1 4YQ, UK.
[2]: Dept of Geosciences, University of Arizona, Tucson, AZ85721, USA
[3]: School of Earth Sciences, University and Birkbeck College, Gower St., London, WC1E 6BT.
[4]: Crustal Geodynamics Group, School of Geography and Geosciences, The University, St Andrews, Fife, KY16 9AL, UK.
[5]: Dip di Scienze della Terra, University Milan-Bicocca, Via Mangiagalli 34, 2013 Milan, Italy.

In contrast to Eocene Himalayan foreland basin sediments in India and Pakistan, co-eval sediments of the Bhainskati Formation in Nepal contain no petrographic evidence for orogenic input. Such data have been used as evidence to promote models of diachroneity of India-Asia collision. In this paper we provide evidence of orogenic input into the Eocene foreland basin sediments of Nepal, from U-Pb and fission track analyses of detrital zircons. Our data removes the evidence for diachroneity of collision as pertains to provenance information from the sediment record in Nepal, and brings the sediment record into better agreement with ages of early thrusting and metamorphism in the orogen. We also use our detrital fission track data to bolster previous age determinations of the overlying Dumri Formation, confirming the basin-wide occurrence of a major unconformity. Comparison of our fission-track dataset with that from the co-eval Dagshai Formation more than 500 kms along strike sediments in India suggests that there is no evidence of diachroneity in early stages of exhumation of the orogen.

ECOLOGICAL SIGNATURE OF SLOPE INSTABILITY AND ITS IMPLICATION IN LANDSLIDE HAZARD MITIGATION (LHM) - A CASE STUDY ALONG MCT ZONE IN HIMALAYAN MOUNTAINS

P.S. NEGI

Wadia Institute of Himalayan Geology
33, Gen. Mahadeo Singh Road, Dehra Dun - 248 001. INDIA

Ecological signal of area of potential hill slope movement deciphered through bioengineering in present research endeavor. Study reveals that Alnus nepalensis manifest as a phytological precursor for slope instability in Himalayan Mountains and area of potential landslides can be delineated by its floral dynamics. Laboratory investigation and microclimatic field studies suggest that obtrapezoid-winged nuts morphology, radiative balance at different aspects of micro-watersheds and interwoven air and wind dynamics create holistic system for viable mechanism of seed dissemination to new habitats of potential landslide.

Inherent nitrogen fixing, fast growth and multi-pedological adaptation characteristics of identified precursor taxa investigated as main factors for invasion, establishment and sustaining in unfertile soil or rocky strata of unstable slopes or exposed slip surface. Wide-spread occurrence in ravines, stream banks and along newly constructed roads is also attributed to unstable slopes habitat of Alnus nepalensis.

Intensive study conducted along geo-dynamically active and most fragile Main Central Thrust (MCT) zone of Himalaya while extensive coverage includes other geographical regions of Uttaranchal and Himachal state. It is established that the process of initiation, development and accumulation of shear stress towards effective level or periodic decrease in shear strength up to the threshold value is signaled qualitatively by invasion and growth pattern of indicator tree species. The ecological dynamics of species found simultaneously corroborated with decreasing value of factor of safety of slopes. The habitat ecology data is recorded from pre-slope failure phase by visual reconnaissance, ground studies and laboratory analysis. Phytogeographical range in study area explored between 1000-2600 m.s.l. and which is coinciding with Lesser Himalayan range (800-3000 m.s.l.).This range has turned very sensitive to landslide hazards due to active geological formations and intense anthropogenic pressure.

The proposed bioengineering technique is eco-friendly, cost effective, socially acceptable and involves local resource and traditional wisdom as a scientific tools and technical excellence. It will play significant role in landslides hazard mitigation for Hindu Kush-Himalayan range and similar geographical region of the world. Where landslides has become major devastating natural hazards and eventually acquired the tendency of natural calamity or annual catastrophe.

CENOZOIC SHORTENING AND LATERAL EXTRUSION OF THE QAIDAM BLOCK AT THE NORTHEASTERN MARGIN OF THE TIBET PLATEAU: CONSTRAINTS FROM STRUCTURAL ANALYSIS AND BASIN EVOLUTION

Franz NEUBAUER (1), Yongjiang LIU (1, 2), Johann GENSER (1), Andrea RIESER (1) and Xiaohong GE (2)

(1) Div. General Geology and Geodynamics, University of Salzburg, A-5020 Salzburg, Austria, franz.neubauer@sbg.ac.at
(2) Faculty of Earth Sciences, Jilin University, Changchun, China

The Tertiary tectonic evolution of the Qaidam block with its 8–16 km thick sedimentary cover has been investigated in order to constrain the eastward lateral extrusion between the sinistral Kunlun and Altyn wrench corridors. Extrusion is driven by N–S compression due to subduction and collision of the Indian subcontinent. These faults initiated as Oligocene low-angle ductile shear zones which were overprinted by brittle strike-slip faults. Folded Neogene and Quaternary sediments with unusual structural characteristics (e.g., extensional gashes with halite, gypsum and coelestine), the geometry of strata and angular unconformities allow monitor growing folds and erosion of anticlines. Together with the sinistral Kunlun and Altyn wrench corridors, they characterize the stepwise Pliocene and Quaternary shortening and extension due to transpression along the northeastern edge of the Tibetan plateau. Field relationships suggest the following preliminary succession of palaeostress orientation tensors: (1) Deformation stage D_1 is characterized by N- respectively S-dipping normal faults which bear quartz and/or chlorite fibres forming slickenlines. This suggests that they formed at elevated temperatures under circulation of hydrothermal fluids, therefore under higher temperatures than later faults and striae. Overprint criteria corroborate an early formation. Palaeostress patterns suggest ca. N–S extension. (2) Deformation stage D_2 comprises gently NW- and SE-dipping normal faults, but without any quartz- and chlorite fibres. These faults and striae indicate NW–SE extension. (3) Normal faults of the D_2 deformation stage are overprinted by N–S and ca. E–W trending D_3 strike faults and by thrust faults which together indicate NNW–SSW to NW–SE compression. The overprint of the Pliocene Qigequan Formation demonstrates the Plio-/Pleistocene age of deformation. (4) D_4 N- and S-dipping thrust faults and WSW-trending sinistral and N- to NNE-trending dextral strike-slip faults suggest ca. N–S to NE–SW compression. This stage indicates clockwise rotation of the maximum principal stress $_1$ in accordance with results of palaeomagnetic investigations.

A system of active, ca. E-trending sinistral strike-slip faults has been recognized at the northern boundary of the Qaidam basin, the most prominent one is the Datongou fault. These represent en echelon-arranged Riedel-type faults of the ENE-trending sinistral Altyn fault, which decouples the Qaidam basin fill from the Altyn Mountains and which is responsible for eastward lateral extrusion of the Qaidam block.

The Qaidam basin fill is folded during Pliocene to Recent, active folding as internal angular unconformities testify along ca. NW-trending fold axes. Ongoing Quaternary to present-day folding results in tilting of ca. four pediment terraces and indicate blind thrusting at depth and core of anticlines, decoupling of the Qaidam basin fill from a rheologically strong basement and ca. 25–30 percent NE–SW shortening for much of the western part of the Qaidam basin.

Together, the palaeostress and other structural data are characteristic for an extrusional wedge which moves out of the zone of maximum compression close the western termination of the Qaidam basin. Shortening structures suggest that much strain within the Qaidam block was accommodated by decoupling of the Qaidam basement from Cenozoic cover sequences.

$^{40}AR/^{39}AR$ DETRITAL WHITE MICA AGES OF PALAEOZOIC AND MESOZOIC SANDSTONES FROM QILIAN AND ALTYN MOUNTAINS, CHINA: CONSTRAINTS

Franz NEUBAUER (1), Yongjiang LIU (1, 2), Johann GENSER (1), Andrea RIESER (1)
Robert HANDLER (1), Gertrude FRIEDL (1) and Xiaohong GE (2)

(1) Div. General Geology and Geodynamics, University of Salzburg, A-5020 Salzburg, Austria, franz.neubauer@sbg.ac.at
(2) Faculty of Earth Sciences, Jilin University, Changchun, China

$^{40}Ar/^{39}Ar$ dating of detrital white mica of Early Palaeozoic (Ordovician?) to Cretaceous sandstones from the Qilian and Altyn Mountains allows monitor large-scale palaeogeographic relationships and the tectonothermal evolution of the poorly constrained Inner Asian orogens. In both pre- and post-orogenic sandstones of the Qilian Mountains we found a single grain of Sinian age (869 ± 6 Ma) but many grains with ages between 523 ± 4 and 591 ± 5 Ma (Late Neoproterozoic to Middle Cambrian, 'Panafrican' age). The majority of ages are between 504 ± 5 and 385 ± 3 Ma, reflecting the dominant 'Caledonian' orogenic source areas as exposed in Qilian, Altyn and Northern Kunlun Mountains. Jurassic-Cretaceous successions of Altyn Mountains also contain grains with ages of 371 ± 3 Ma – 322 ± 2 Ma (Late Devonian-Carboniferous) and 208 ± 2 – 202 ± 2 Ma (Late Triassic), reflecting 'Variscan' and Indosinian tectonic events, the latter found in Kunlun Mountains. Basement exposure of "Panafrican" age is apparently not known in Eastern Asia, however, except a small piece in Northern Altyn Mts. with an age of ca. 500 Ma. Because of the close relationships of "Panafrican", "Caledonian" and " early Variscan" ages, we consider close palaeogeogeographic relationships between these segments of Inner Asia, which are tentatively considered to have shifted during post-Carboniferous events from the Laurussian margin to its present position in Inner Asia. We interpret the Indosinian ages from Jurassic to Cretaceous successions of Altyn Mountains to record molasse-type sedimentation at the northern front of the Kunlun orogen. As a whole, the new $^{40}Ar/^{39}Ar$ ages of detrital white mica indicate a long-lasting accretion history at the southern margin of the Palaeozoic Siberian, respectively late Palaeozoic Eurasian continents, compatible with a long-lasting subduction history and formation of accretion-type orogens during "Caledonian", a sort of "early Variscan" and Indosinian tectonic events.

Recently, U-Pb zircon ages were published from detrital sediments from a similar region (Gehrels et al., 2003). Compared with these mainly early Proterozoic U-Pb zircon ages, the $^{40}Ar/^{39}Ar$ ages show systematically younger age clusters, which we interpret to record the main steps of tectonothermal overprint within respective source orogens and the age of microplate accretion towards the Eurasian continent. Using all available geochronological and tectonically relevant data from the Beishan to Kunlun mountain ranges, a model is developed displaying the stepwise subordinate "Panafrican", and predominant "Caledonian" to Indosinian accretion of island arc systems as well as Early-Middle Proterozoic continental microplates.

Reference

Gehrels, G. E., Yin, A., Wang, X.-F.,, 2003. *Geol. Soc. Amer. Bull.*, **115**, 881-896.

Note Page

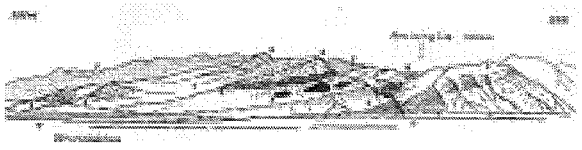

Amlang La, Gansser, 1964

HIMALAYAN ECLOGITE FORMATION: A CRITICAL PRECURSOR TO CHANNEL FLOW?

Patrick O'BRIEN

Institut für Geowissenschaften, Universität Potsdam, Potsfach 601553, D-14471 Potsdam, Germany.

Our understanding of the metamorphic evolution of the Himalaya has advanced considerably in recent years. This is a result of intensive field studies combined with detailed mineralogical, geothermobarometric and isotopic investigations of samples from key sections. Reliable pressure-temperature paths exist for numerous samples and in some cases these are complemented by temperature-time and depth-time paths thus allowing definition of a true pressure-temperature-time (P-T-t) path for the unit in question. Such complete P-T-t-paths are extremely important for the understanding of the geodynamic processes as they allow a direct comparison with the results of thermal-mechanical models. There are distinct differences in the style of metamorphism recorded by metamorphic rocks in the Himalaya. This is a result of the change from oceanic subduction (reflected in early low-T high-P blueschists in the accretionary prism along the southern boundary of the Kohistan arc) via continental subduction (recorded by coesite-eclogites in Indian-margin crust now exposed in Ladakh and NW Pakistan) to continent-continent collision (shown as Barrovian-type assemblages in metapelites resulting from crustal stacking which are overprinted by later lower pressure-higher temperature sillimanite-bearing assemblages as the thickened crust overheats). The sequential change in thermal regime, controlled as it is by the change from subduction to collision processes, is not really surprising as it is a pattern repeated in several orogens. A long-recognised phenomenon in the metamorphic rocks of the Himalaya is the presence of an inverted metamorphic profile from the Lesser to Higher Himalayan sequences. Several models have been developed to explain this – hot iron effect, frictional heating, thrusting, folded isograds, wedge extrusion – but one of the more recent models, channel flow (Beaumont et al., 2004; Jamieson et al., 2004), seems to provide a plausible explanation for some of these features. The timing of metamorphism, the grade of metamorphism, the inverted nature of isograds and the pattern of isotopic ages across the exposed Higher Himalayan sequence does seem to fit nicely with the predictions of the models. In addition, the separation of upper crustal levels from lower crust is consistent with reality and the advance of the subduction zone from its original position to a location below the continental margin of Asia is also consistent with some interpretations of geophysical data for southern Tibet (e.g. Owens & Zandt 1997). One major difficulty with the models at present is the inability to incorporate the eclogite facies stage. As the models require a shallow angle of subduction, and the crust does not thicken to that amount required for coesite formation (90-100km), there is no possibility to produce the eclogites in the present models. However, as already pointed out with the discovery of coesite-eclogite by O'Brien et al., (1989, 2001), and repeated by Kohn & Parkinson (2002), there is by necessity a change from a steep subduction angle to a shallow subduction angle between the earliest ultrahigh-pressure metamorphic stage and the subsequent crustal stacking episode. Looking at the timing of metamorphism and exhumation in the coesite-eclogites of Kaghan Valley (Pakistan) and Tso Morari (Ladakh) it is clear that the subduction and exhumation took place at rates of cm/a i.e. those of normal plate movements (e.g. Massonne & O'Brien 2003). This resulted in the deeply subducted leading margin of the Indian plate being already exhumed to sub-greenschist levels before 40 Ma i.e. well before the onset of Barrovian metamorphism in the central part of the Himalaya.

It is likely that the rapid exhumation of the coesite-bearing sequences was aided by crustal delamination and/or slab detachment. As collision was then further driven by continued oceanic subduction elsewhere along the plate margin, the lower crust and mantle lithosphere of the Indian plate renewed their subduction at a shallow angle. This is nicely illustrated in the model of Chemenda et al., (2002). In other words, in order to have the low angle of subduction required for the initiation of the channel flow models it is necessary to have a precursor deep crustal subduction/exhumation stage to block the subduction channel and detach the cold lithosphere of the oceanic margin.

In summary, metamorphism in the High Himalaya involves two stages: an initial UHP stage related to deep crustal subduction and rapid exhumation and a subsequent Barrovian (Ky) grade with a lower P sillimanite overprint. Early subduction is steep and rapid exhumation requires detachment of upper Indian plate crust from its lower crust and mantle. If the subducting oceanic slab is also locally detached, further collision will be of continental crust at a low angle. The models from Beaumont et al. (2004) for channel flow and extrusion require a low angle of subduction to drive them but this must start later than modelled (at around 40 Ma) as deep continental subduction is younger than 50 Ma. The thermal evolution of the modelled crust is an important factor in the reproducibility of natural phenomena by the models but, if slab detachment provides an extra mantle heat input, the later start to the crustal stacking could still yield the same result. Thus UHP metamorphism and detachment is most likely a necessary initiation mechanism for a channel flow regime and not just a novelty, identifiable only by a few petrologists, that doesn't appear to fit the pattern.

(References)

BEAUMONT, C., JAMIESON, R.A., NGUYEN, M.H., MEDVEDEV, S. 2004. *JGR*, **109**, B06406
CHEMENDA, A., BURG, J.-P., MATTAUER, M. 2000. *EPSL*, **174**, 397-409
JAMIESON, R.A., BEAUMONT, C., MEDVEDEV, S., NGUYEN, M.H., 2004. *JGR*, **109**, B06407
KOHN, M.J., PARKINSON, C.D. 2002. *Geology*, **30**, 591-594.
MASSONNE, H.J. & O'BRIEN, P.J. 2003. ***EMU Notes in Mineralogy***, 5, 145-187.
O'BRIEN, P.J., ZOTOV, N., LAW, R., KHAN, M.A. & JAN, M.Q. 1999. *Terra Nostra*, **99/2,** 109-111.
O'BRIEN, P.J., ZOTOV, N., LAW, R., KHAN, M.A. & JAN, M.Q. 2001. *Geology*, **29,** 435-438.
OWEN, T.J., ZANDT, G. 1997. *Nature*, **387**, 37-43.

DIVISION OF TECTONIC UNITS OF THE MAIN COLLISIONAL BELT BETWEEN INDIAN AND ASIAN CONTINENT AND ITS GEODYNAMIC SETTING

PAN Guitang, WANG Liquan, LI Guangming, ZHU Dicheng*, GENG Quanru

Chengdu Institute of Geology and Mineral Resources, 610082, Chengdu, China
*Correspondence should be addressed to Zhu Dicheng (email: cdzdc@cgs.gov.cn)

The collisional process between Indian and Asian continent, which is defined as a series of collisional events between Indian lithospheric plate and Asian lithospheric plate occurred at middle-late Cretaceous and Cenozoic time, can be divided into three stages including initial collision, climax of collision and post-collision, every stages could continues for a long period that is restricted at 120-65Ma, 55-50Ma and 45-35Ma, respectively. The main collisional belt of Indian / Asian continent is placed on the Gangdise archipelagic arc-basin tectonic realm between Bangong Co ophiolitic mélange zone to the north and Yarlung Zangbo ophiolitic mélange zone to the south.

All of the regional geological mappings at a scale of 1: 250, 000 in this main collisional belt have been completed up to now. Many important geological records including a series of ophiolitic mélange zones, important faults, regional discontinuities, new stratigraphical and paleontological data, volcanic rock-bearing strata and high precise ages of magmatic rocks, which are founded and confirmed in the process of geological mapping (China Geological Survey, 2004), providing an unparalleled opportunity to study the material composition and geodynamic setting related to tectonic evolution of Tethys and Tibetan Plateau.

Based on integrated analysis of the newly obtained geological data, the main collisional belt are divided into eight main tectonic units including Himalayan Tethys fold-thrust belt, Yarlung Zangbo ophiolitic mélange zone, Xigaze forearc basin, Gangdise- Nyainqentanglha magmatic arc, Shiquanhe-Yunzhug-Jiali-Bomi ophiolitic mélange zone, Anglonggangri – Baingoin - Boshulaling magmatic arc, Bangong Co-Nujiang ophiolitic mélange zone and southern Qiangtang-Zogang foreland basin from south to north according to the tectonic nature and spatial-temporal structures of different units in the process of archipelagic arc-basin evolution and arc-arc, arc-continent collision since Late Paleozoic time. Every main tectonic unit can be subdivided into many secondary tectonic units on the basis of the differences from stratigraphy, types of magmatic origin, tectonic nature and evolution history. The main and secondary tectonic units of the main collisional belt are listed following and illustrated on Fig.1.

We suggest that geodynamic setting of the main collisional belt between Indian and Asian continent is constrained by double-direction subduction including the subducted southward Tethyan oceanic crust initiated at Late Paleozoic time (Pan et al., 2004) and the subducted northward of Yarlung Zangbo oceanic crust began at Late Jurassic according to the characteristics of material compositions and spatial-temporal structures in this complex collisional belt (Fig.2).

Acknowledgments: This study is financially supported by the National Keystone Basic Research Program of China (Grant No.2002CB412609), the Integrated Study of Basic Geology in the Blank Area of Southern Tibetan Plateau (Grant No. 200313000025).

References

[1]. China Geological Survey, Results and progress of regional geological survey: the Gangdise belt. Geological Bulletin of China (in Chinese), 2004, vol.23, no.1, 45-60

[2]. Pan G. T., Zhu D. C., Wang L. Q., Liao Z. L. 2004. Bangong Lake-Nu River suture zone – the northern boundary of Gondwanaland: evidence from geology and geophysics. Earth Science Frontiers (China University of Geosciences, Beijing), vol.11, no.4, 371-382 (in Chinese with English abstract)

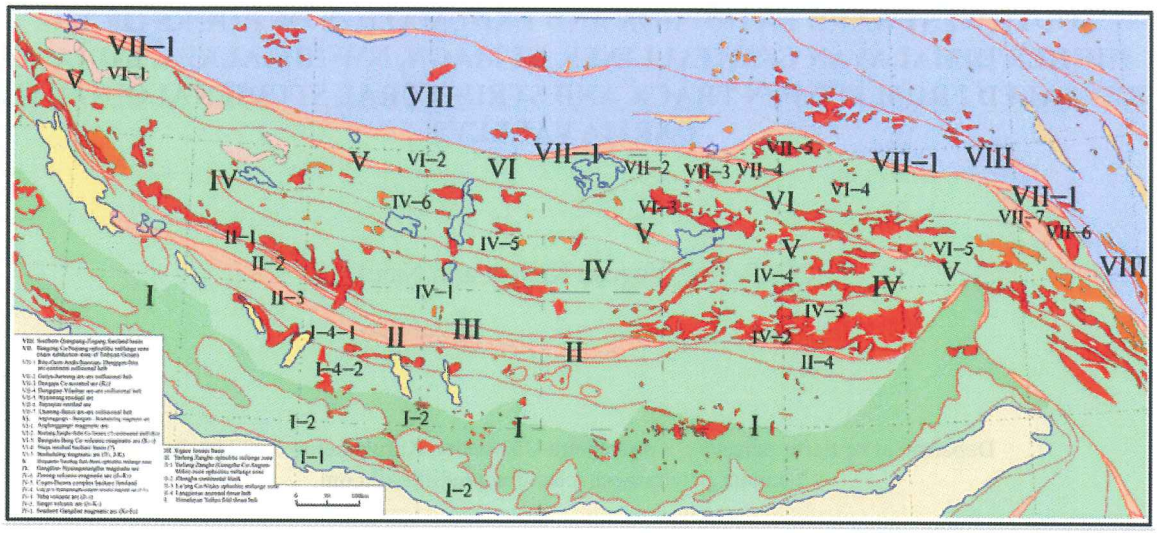

Fig.1 Tectonic units of the main collisional belt between Indian and Asian continent

I. Himalayan Tethys fold-thrust belt
II. Yarlung Zangbo ophiolitic mélange zone II-1. Yarlung Zangbo (Gongzhu Co – Angren – Milin) main ophiolitic mélange zone; II-2. Zhongba continental block; II-3. La'ang Co-Niuku ophiolitic mélange zone; II-4. Langjiexue accreted thrust belt
III. Xigaze forearc basin
IV. Gangdise- Nyainqentanglha magmatic arc IV-1. Southern Gangdise magmatic arc (K_2-E_2); IV-2. Sangri volcanic arc (J_3-K_1); IV-3. Yeba volcanic arc (J_{1-2}); IV-4. Long'ge'er-Nyainqentanglha complex volcanic-magmatic arc (P-T_3); IV-5. Coqen-Duowa complex backarc foreland; IV-6. Zenong volcanic-magmatic arc (J_3-K_1)
V. Shiquanhe-Yunzhug-Jiali-Bomi ophiolitic mélange zone
VI. Anglonggangri – Baingoin - Boshulaling magmatic arc VI-1. Anglonggangri magmatic arc; VI-2. Bochang Zangbo-Selin Co forearc (?) continental shelf (K_1); VI-3. Baingoin-Beng Co volcanic-magmatic arc (K_{1-2}); VI-4. Naqu residual backarc basin (?); VI-5. Boshulaling magmatic arc (T_3, J-K)
VII. Bangong Co-Nujiang ophiolitic mélange zone (main subduction zone of Tethyan Ocean) VII-1. Ritu-Geze-Ando-Suoxian- Dengqen-Bitu arc-continent collisional belt; VII-2. Guiya-Jueweng arc-arc collisional belt; VII-3. Dongqia Co accreted arc (K_2); VII-4. Dongqiao-Yilashan arc-arc collisional belt; VII-5. Nyainrong residual arc; VII-6. Jiayuqiao residual arc; VII-7. Lhorong-Baxoi arc-arc collisional belt
VIII. Southern Qiangtang-Zogang foreland basin.

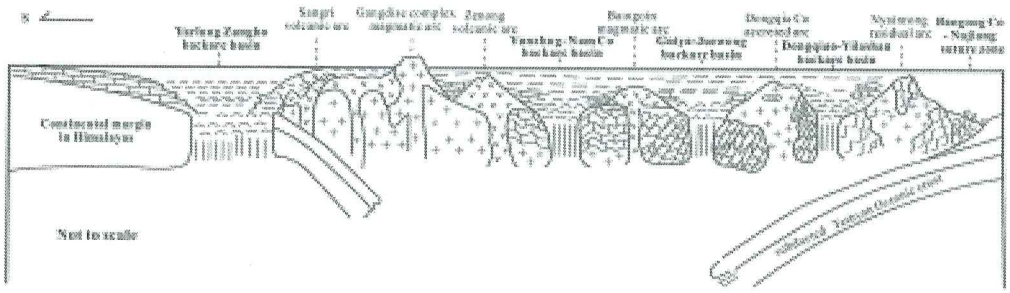

Fig.2 Schematically tectonic section of the main collisional belt between Indian and Asian continent at Late Jurassic time

SOUTHWESTWARD EXTRUSION AND EXHUMATION OF ROCKS OF THE HIGHER HIMALAYAN CRYSTALLINES, KUMAON, NW-HIMALAYA, INDIA: AS REVEALED FROM FISSION TRACK AND STRUCTURAL STUDIES ALONG KALI-DARMA VALLEYS

R.C. PATEL*, Yogesh KUMAR and Nand LAL

Department of Earth Sciences, Kurukshetra University, Kurukshetra- 136 119, India
* e.mail: patelramesh_chandra@rediffmail.com

Himalayan Proterozoic basement of the Higher Himalayan Crystallines (HHC) and cover rocks of the Tethyan Sedimentary Zone (TSZ) are exposed through tectonic zones within the hinterland of Kumaon Himalaya. The basement records history of pre-Himalayan (HD_1) to Himalayan crustal thickening ($HF_2/HF_3/HF_4$) related to southwestward emplacement of the HHC and northeastward detachment of the TSZ. The HHC then formed a crustal wedge that was extruded towards the foreland from the overthickened hinterland. Finally, the crystalline basement was exhumed by ductile and brittle extensional deformation (HD_5). The rocks of the HHC in Kumaon Himalaya are thoroughly transposed by HD_2 deformation into HS_m (HS_1+HS_2). The extent of transposition and a well-developed NE-plunging HL_2 lineation indicate intense strain during HD_2 throughout the studied portion of the HHC. Ductile flow continued, resulting in rotation of HF_1 and HF_2 folds due NE-direction and NW-SE plunging HF_3 folds within the HHC. A shear zone records significant reactivated slip on HS_m during HD_5. Rapid exhumation of the HHC is attributed to ductile flow during extrusion and extensional deformation. This ductile flow is correlated with foreland thrusting along the Main Central Thrust (MCT) and hinterland normal faulting along the Trans-Himadri Fault (T-HF).

The apatite fission track dating of the HHC shows differential but rapid exhumation history. Very young apatite fission track ages are located along a zone in the middle of the HHC while relatively older ages are located towards the boundaries. This pattern of age can be described by a combined ductile shear zone and channel flow as a plausible tectonic model for the exhumation of the HHC during Cenozoic Himalayan collision.

Note Page

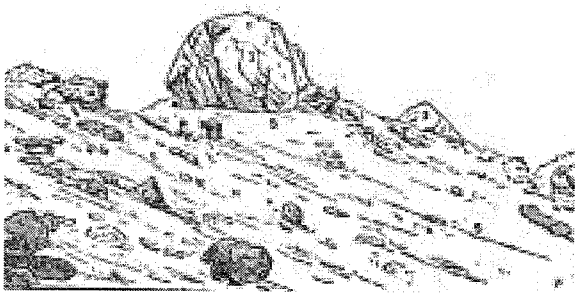

Malla Johar, von Kraft, 1902

METAMORPHIC HISTORY OF THE LESSER HIMALAYA IN CENTRAL NEPAL RECORDED BY METABASIC ROCKS: NEW CONSTAINTS FROM AMPHIBOLE CHEMISTRY AND THERMOBAROMETRY

Lalu Prasad PAUDEL(1, 2), Takeshi IMAYAMA (1) and Kazunori ARITA (1)

(1) Department of Earth and Planetary Sciences, Graduate School of Science, Hokkaido University, Kita-10, Nishi-8, Sapporo, 060-0810, Japan.
(2) Central Department of Geology, Tribhuvan University, Kirtipur, Kathmandu, Nepal.

The Lesser Himalaya in central Nepal consists of low- to medium-grade metasedimentary rocks with frequent intercalations of metabasites. The metamorphic evolution of the Lesser Himalaya has been extensively investigated in the past through studies of metapelites and metapsammites. However, studies on metabasites are extremely rare despite the fact that metabasites are mineralogically more sensitive to variations in pressure and temperature. In the present study, petrographic, mineral chemistry and thermobarometric analyses were carried out on metabasites taken along the Modi Khola section to constrain the metamorphic history of the Lesser Himalaya (Fig. 1).

In the field the metabasites occur as sheet-like bodies of a meter to tens of meters thickness. They are medium- to coarse-grained, with well-developed shear foliation. Almost all the samples contain the mineral assemblage Amp+Ab+Ep+Chl+Qtz+Titanite±Magnetite. Amphiboles occur as (i) sheared and elongated porphyroclasts with asymmetric pressure shadows and overgrown rims, and (ii) acicular and bladed aggregates parallel to the foliation and as inclusions in plagioclase.

Whole-rock chemical analysis shows that all the samples have similar major element compositions without any systematic compositional variation among samples. The amphiboles in all the samples belong to the calcic-amphibole group. Porphyroclasts in relatively less sheared sample (No. 163) have actinolitic composition without zoning. Porphyroclasts in mylonitic samples (Sample Nos. 623, 625 and 180) show very good prograde chemical zoning with actinolite cores and magnesio-hornblende or Tshermakite rims. Both the NaM4 and Al^{iv} contents increase from core to rim and slightly decrease at the outer margin of the grains (Fig. 2A). As NaM4 increases with pressure and Al^{iv} increases with temperature (Brown, 1976), the zoning pattern indicates a prograde/retrograde P-T path for the metabasic rocks.

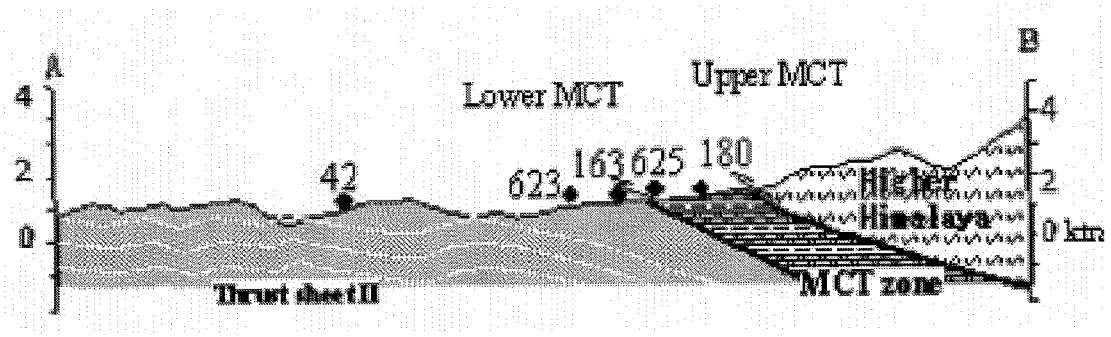

Fig. 1. Geological cross-section or the Pokhara area showing position of the samples.

Amphiboles occurring as fine recrystallized aggregates vary in composition from actinolite (No. 42) to magnesio-hornblende (No. 623) and Tschermakite/ferro-Tschermakite (Nos. 163, 625 and 180). The NaM4 and Al^{iv} contents in the recrystallized aggregates increase gradually from south to north up to the Lower MCT indicating northward increase of pressure and temperature (Fig. 2B). However, sample No. 180 from the upper part of the MCT zone has lower NaM4 content than in the sample from the lower part (No. 625).

Pressure increases from 2 kbar in the southernmost part of Thrust Sheet II to 4 kbar at the MCT zone as estimated from NaM4 semi-quantitative geobarometer (Brown, 1977). Temperature estimated using hornblende-plagioclase thermometer (Holland and Blundy, 1994) vary from 520 to 570°C for the cores of porphyroclasts. The rims have been re-equilibrated at about 540°C, 620°C, 640°C and 610°C in sample Nos. 623, 163, 625 and 180, respectively.

The above observations indicate a polyphase metamorphic history for the Lesser Himalaya in accordance with the results of illite crystallinity and white mica compositional studies in metapelites (Paudel and Arita, 2000). A pre-MCT greenschist facies metamorphism (Eohimalayan? or pre-Himalayan?) was followed by syn-MCT lower amphibolite facies metamorphism (Neohimalayan) and a late stage retrogression. Both pressure and temperature during the Neohimalayan metamorphism increased from south to north up to the level of the Lower MCT confirming a previously reported inverted metamorphism in the area (Le Fort, 1975; Arita, 1983). However, decrease in P and T shown by the sample No. 180 lying to the north of the Lower MCT raises question over continuous metamorphic inversion up to the level of the Upper MCT.

The zoning and heterogeneity of amphibole compositions argue for an overall lack of equilibration within and among amphibole grains. It has an important implication to the geochronometry using amphiboles.

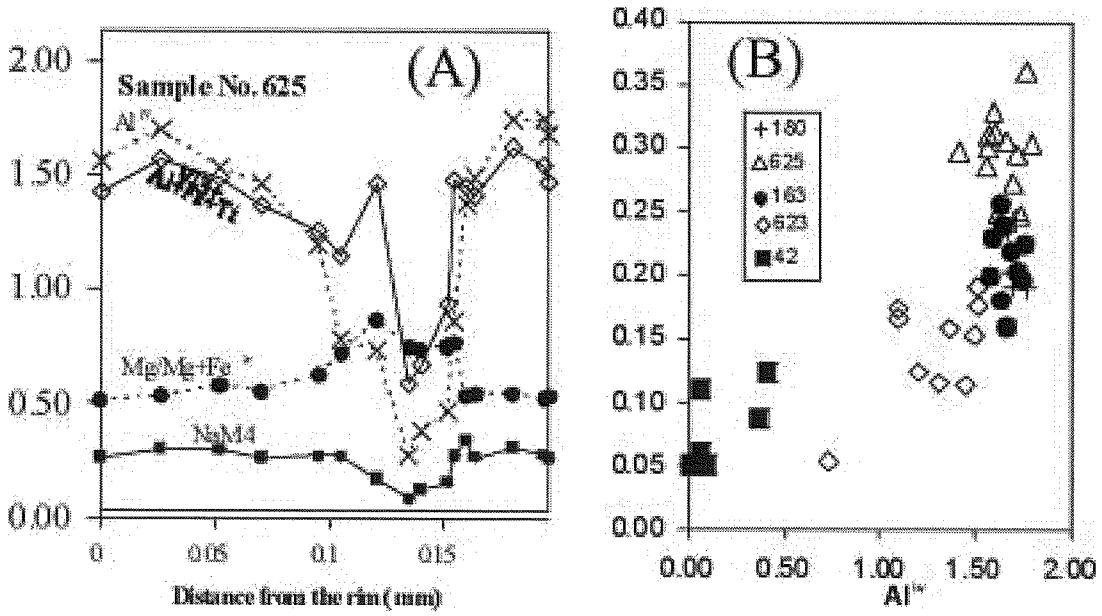

Fig. 2.(A) Compositional profile of a porphyroclast in sample No. 625.
2 (B) Al^{iv}-NaM4 plot of recrystallized aggregates from all the samples.

References

ARITA K., 1983. *Tectonophysics*, **95**, 43-60.
BROWN H., 1977. *J. Petrol.*, **18**, 53-72.
HOLLAND T. & BLUNDY J., 1994. *Contrib. Mineral.Petrol.*, **116**, 433-447.
LE FORT P., 1975. *Am. J. Sci.*, **275A**, 1-44.
PAUDEL L.P. & ARITA K., 2000. *J. Asian Earth Sci.*, **18**, 561-584.

EXTREME UPLIFT AND EROSION RATES IN EASTERN HIMALAYAS (SIANG-BRAHMAPUTRA BASIN) REVEALED BY DETRITAL (U-TH)/HE THERMOCHRONOLOGY

R. PIK, C. FRANCE-LANORD AND J. CARIGNAN

CRPG-CNRS, France, rpik@crpg.cnrs-nancy.fr

The distribution of erosion intensity in a major mountain range such as the Himalaya is a fundamental clue to investigate the interaction between climatic, tectonic and erosion processes that govern the morphology and evolution of an orogen. At the first order, the sediment flux measured on the two major rivers - Ganga and Brahmaputra - suggest higher mean denudation rates for the Eastern Himalaya than Western Himalaya (Galy and France-Lanord, 2001). However, the distribution of erosion in the Brahmaputra basin is not uniform and the Namche Barwa area, drained by the Siang-Tsangpo, appears to supply up to 50% of the total sediment flux of the Brahmaputra (Singh and France-Lanord, 2002).

In order to further constrain the relationships between such localized erosion and the associated exhumation rate of basement, we measured (U-Th)/He ages in detrital zircons from river sediments in the Brahmaputra basin. This thermochronological system (Z-He) is particularly interesting for detrital material because: (i) zircon is preserved during weathering and erosion processes, (ii) its closure temperature (150-180°C, Reiners et al., 2004) corresponds to a depth which is close to the surface but deep enough to avoid perturbations by topography variations, and (iii) the error associated to single grain measurement (8-10 %) allows a good definition of population ages.

Z-He ages from the Brahmaputra river in Bangladesh range from 0.4 to 77 Ma. 40% of the zircon population exhibit Z-He ages between 0.4 and 1 Ma defining the major distribution peak centred at 0.5 Ma. These very young ages correspond to extreme denudation rates of 5 to 7 mm/yr. Dispersed Z-He ages from 12 to 77 Ma do not define any population groups, whereas the remaining 40% of the zircons have ages distributed between 2.5 and 7 Ma, which correspond to the pool of ages recorded by preliminary Z-He ages on the other Himalayan rivers of the basin. Therefore, such very high denudation rates (5-7 mm/yr) seems to characterize the Brahmaputra itself. This result is in complete agreement with the isotopic geochemical budget of the rivers, and indicate that the 50 % of the detrital flux supplied by the Siang-Tsangpo system is characterized by very young Z-He ages originating from a very high-denudation rate area. These results are also in agreement with the Fission track data measured upstream in the Namche Barwa syntaxis which exhibit the same type of very young zircon ages (Stewart et al., 2004). These complementary results confirm that sediments originating from this part of eastern Himalaya, associated with extreme erosion rates, dominate the sedimentary budget of the Brahmaputra basin.

Galy and France-Lanord, 2001, Geology, 29, 23-26
Singh and France-Lanord, 2002, EPSL, 252, 645-662
Reiners et al., 2004, GCA, 68, 1857-1887
Stewart et al., 2004, Fall AGU abst. , T53A-0471

Note Page

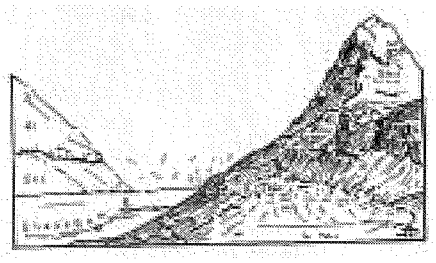

Bdongo peak,Desio, 1980

IMPACTS OF CLIMATE CHANGE ON SURFACE PROCESSES, NEPAL HIMALAYA

Beth PRATT-SITAULA (1), Douglas BURBANK(1), Arjun HEILSATH (2), Emmanuel GABET (3)

(1) Department of Geological Sciences, University of California Santa Barbara, USA
(2) Department of Earth Sciences, Dartmouth College, USA
(3) Department of Geology, University of Montana, USA

This study demonstrates how climate change can cause complex responses in surface processes. It includes quantitative results of climate-associated changes in river, hillslope, and glacial systems in the Annapurna region, Nepal (Figure 1). Periods of higher monsoon precipitation are linked to temporary river aggradation, followed by rapid incision during both the early Holocene monsoon maximum (~10-7 ka: e.g. BURNS et al., 2001; GASSE et al., 1996) and the Late Pleistocene strengthened monsoons (~50-30 ka: e.g. CLEMENS et al., 1991; SCHULZ et al., 1998). Perched fluvial deposits and cosmogenic dating of fluvial straths indicate that the Marsyandi River's bedrock gorge was filled with >100 m of sediment at ~8 ka and the alluvium was rapidly removed in the follow 1-2 ky (PRATT et al., 2002). ^{14}C dates and stratigraphy of the 150-m high alluvial fill terraces south of the Greater Himalaya show that rapid alluviation was completed by 35-30 ka (PRATT-SITAULA et al., 2004). Presumably, increased precipitation causes a rise in rock pore pressure and thus higher slope failure and sediment flux.

Though it is not possible to measure past hillslopes to see how they vary with changing climate, the modern precipitation gradient can be used in a space-for-time substitution. Hillslope angles derived from a 3-arc second DEM and precipitation data from a weather station network (BARROS et al., 2000) show average slopes decreasing from 35° to 25° as rainfall increased from <2 m/yr to >4 m/yr (GABET et al., 2004) (Figure 2). Glacierized regions and river channels were excluded; the trend cannot be explained by differences in lithology or rock uplift rates. Instead, slopes steepen and lengthen in drier conditions.

Cosmogenic exposure ages from moraine boulders reveal that glacial advances are intimately dependant on both climate and altitude. This region had two periods of significant recent glacial advances: early Holocene (10-6 ka) and late Glacial (15-13 ka) (Figure 3). Climate proxies suggest that both these periods had elevated precipitation, but that the early Holocene was warmer and wetter (e.g. ALTABET et al., 2002; BURNS et al., 2001; KUDRASS et al., 2001; NSIDC, 1997). Glacial catchments with lower altitude source areas advanced during the colder late Glacial, but not during the warmer Holocene. Glaciers in high-altitude catchments continued to flourish and advance despite the warmer Holocene temperatures because of additional precipitation. To achieve meaningful glacial chronology results, one must consider the altitude range of the glacial catchment and take multiple samples per moraine (≥4) in order to reduce uncertainties.

Increased precipitation clearly affects surface processes significantly, but the responses in the river, hillslope, and glacial systems are complex and dependant on feedbacks and altitude. Understanding the details of these processes is not possible without sensitive dating tools.

Figure 1. Regional map with field area indicated by white circle.

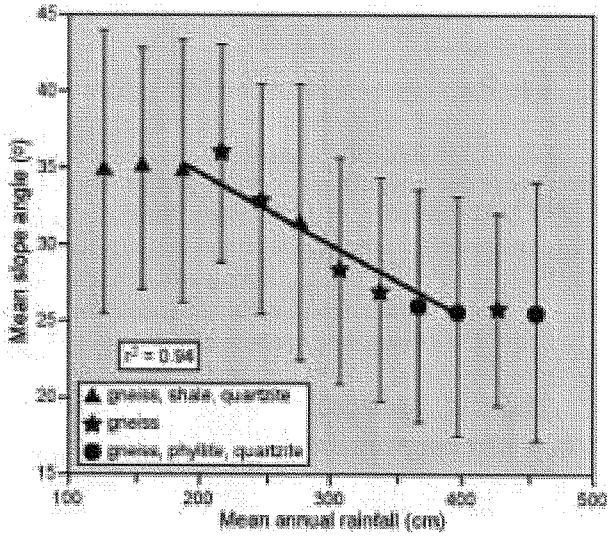

Figure 2. Mean annual rainfall vs. mean slope angle. Increase in mean annual rainfall between 180 and 400 cm is matched by decrease in mean hillslope angles. Error bars represent 1σ. Best-fit linear regression applies only to rainfall data between 180 and 400 cm. (adapted from GABET, PRATT-SITAULA, BURBANK, 2004)

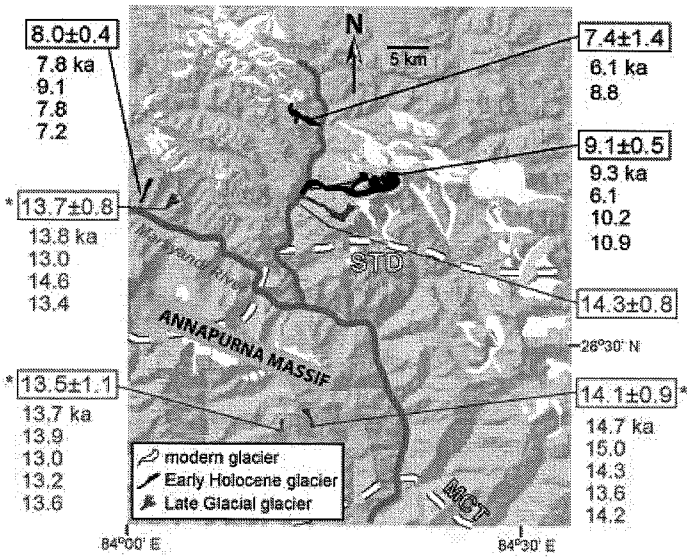

Figure 3. Cosmogenic exposure ages from moraine boulders and locations of modern and sampled paleo glaciers in the Marsyandi River catchment, Annapurna region, Nepal. Dates are remarkably consistent within each moraine set. Individual boulder exposure ages are in smaller text and moraine-set averaged ages are boxed. Ages fall into two main populations: Early Holocene and Late Glacial.

* denotes catchments with upper altitude bounds below 5000 m. All other dated glacial catchments extend to ≥6000 m.

(REFERENCES)

ALTABET M. A., HIGGINSON M. J. & MURRAY D. W. 2002. *Nature*, **415**, 159-162.

BARROS A. P., JOSHI M., PUTKONEN J. & BURBANK D. W. 2000. *Geophysical Research Letters*, **27**, 3683-3686.

BURNS S. J., FLEITMANN D., MATTER A., NEFF U. & MANGINI A. 2001. *Geology*, **29**, 623-626.

CLEMENS S., PRELL W. L., MURRAY D., SHIMMIELD G. B. & WEEDON G. P. 1991. *Nature*, **353**, 720-725.

GABET E. J., PRATT-SITAULA B. A. & BURBANK D. W. 2004. *Geology*, **32**, 629-632.

GASSE F., FONTES J. C., VAN CAMPO E. & WEI K. 1996. *Palaeogeography, Palaeoclimatology, Palaeoecology*, **120**, 79-92.

HARPER J. T. & HUMPHREY N. F. 2003. *Geophysical Research Letters*, **30**,

KUDRASS H. R., HOFMANN A., DOOSE H., EMEIS K. & ERLENKEUSER H. 2001. *Geology*, **29**, 63-66.

NSIDC. 1997. *Greenland Summit Ice Cores CD-ROM*, National Snow and Ice Data Center.

PRATT B. A., BURBANK D. W., HEIMSATH A. M. & OJHA T. P. 2002. *Geology*, **30**, 911-914.

PRATT-SITAULA B., BURBANK D. W., HEIMSATH A. & OJHA T. 2004. *Geomorphology*, **58**, 223-241.

SCHULZ H., VON ROD U. & ERLENKEUSER H. 1998. *Nature*, **393**, 54-57.

DISCUSSION ON THE BASEMENT OF QINGHAI-TIBETAN PLATEAU, CHINA: EVIDENCES FROM THE ND ISOTOPE OF IGNEOUS ROCKS

QIU Ruizhao (1), ZHOU Su (2,3), XIAO Qinghui (4), DENG Jinfu (2), CAIZhiyong (5) and ZHAO Guochun (2)

(1) Institute of geology, Chinese Academy of geological Sciences, Baiwanzhuang Road 26, Beijing 100037, China;
(2) China University of geosciences, Xueyuan Road 29, Beijing city, P R China, Beijing 100083, China;
(3) Key laboratory of lithospheric tectonics, deep-level process and exploration Ministry of education, China University of geosciences, Beijing 100083, China;
(4) Information Center of Ministry of Land and Resources, Beijing 1008122, China;
(5) Guangzhou institute of geochemistry, Guangzhou, P R China, Guangzhou 510640

There is a scientific issue has aroused debate for a long term, that is whether there is a boundary of Gongwanaland and Laurentia extending in Qinghai-Tibetan plateau. Based on the study Nd Isotopes of Granites in Qinghai-Tibetan plateau, the basement of Qinghai-Tibetan plateau has been discussed in this paper.

According to the develop process of orogenic belt, two kinds of orogenic belt can be divided in Qinghai-Tibetan plateau: one is continental collision orogenic belt which has undergone the process of Tethyan ocean developing, including Kunlun and Gangdese orogenic belt; the other is intra-continental collision orogenic belt, such as Himalaya. The former include the two kinds of igneous assemblages related to subduction and post-collision respectively. The study of Nd isotopic indicate that the granites in igneous assemblages related to oceanic subduction, Kunlun(+1.33~+3.65) and Gangdese (+2.5 ~ +5.7) both has positive$\varepsilon_{Nd}(t)$, but the former has the older Nd model ages(906~817Ma) than the latter(312~562Ma). In igneous assemblages related to collision and post-collision, the granites of Caledonian, Hercynian-early Yanshanian in west Kunlun has negative$\varepsilon_{Nd}(t)$ of –2.4 ~-11.9 and T_{DM} age of 1214 ~1981Ma with a 1568Ma average age, in east Kunlun has negative$\varepsilon_{Nd}(t)$ of –1.5~-9.2 and T_{DM} age of 1190 ~1856Ma with a 1400Ma average age; while the granites of late Yanshan and Himalayan Period which distributing on the Gandese block, have negative$\varepsilon_{Nd}(t)$ of -5.3 ~ -13.7 and T_{DM} age of 1329 ~ 1995Ma with a 1542Ma average age in west, and have negative$\varepsilon_{Nd}(t)$ of -5.35~ -8.28 and T_{DM} age of 1323 ~ 1496Ma with a 1395Ma average age in east. We notice those granites are formed in different periods(Caledonian, Hercynian-early Yanshanian, late Yanshanian and Himilayan period) and distributed in different areas(Kunlun and Gangdese), but they have similar Nd isotopic compositions, their max Nd model ages and negative$\varepsilon_{Nd}(t)$ are close to the granites in Himalayan block which there is not oceanic material to join in melting and to cause of intra-continental subduction($\varepsilon_{Nd}(t)$= -10.3 ~ -16.3, T_{DM} age =1792 ~ 2206Ma with a average age 1870Ma) and basement rocks($\varepsilon_{Nd}(t)$ = -3.29 ~ -13.32, T_{DM} age =1475 ~ 2419Ma with a average age 1894Ma). The average Nd model ages of granites in Kunlun ang Gangdese orogenic belts all with a mid-Proterozoic is similar to the Yanshanian granites in South China and quite different with the granite in Xinjiang. It is concluded Qinghai-Tibet plateau minght has the same basement of Proterozoic, and the boundary of Gongwanaland and Laurentia are located at least on the south margin of Tarimu plate.

*Acknowledgments: our research is supported by National Fund of Nature Science of China(No. NSFC 402344048), the special program of the Ministry of Land and Resources of China(No.200010202) and research projects of deep-level substance's model of china lithosphere, Key laboratory fund of Ministry of education in China(No.2003009 & 2003010), China Geology Survey (No. 200113900018) and international cooperating IGCP project of ministry of Science and technology of China(2001cb711002).

References

QIU Ruizhao, DENG Jinfu & ZHOU Su. 2003. Study on Sr-Nd isotopes of mesozoic-cenozoic granites in qinghai-tibetan plateau. *Acta Geoscientica Sinica*, 24(6): 611–617.

GUO Fieying, LIANG Dingyu & ZHANG Yuzhi. 1991. Geology of ngari tibet(xizang). china university of geosciences press, wuhan, 1991.

OBSERVATION OF DEFORMATION AND METAMORPHISM IN THE EVEREST AREA, EASTERN NEPAL HIMALAYA

Santa Man RAI[1*], Masaru YOSHIDA[1,2], Prakash Das ULAK[1] and Bishal Nath UPRETI[1]

[1]Department of Geology, Tribhuvan University, Tri-Chandra Campus, Ghantaghar, Kathmandu, Nepal
[2]Gondwana Institute for Geology and Environment, Hashimoto, Japan
(* Corresponding e-mail: santamanrai@yahoo.com)

Our recent field study in the Everest area of eastern Nepal Himalaya along the Dudh Koshi valley between Lukla and Lobche provided the following observations of deformation and metamorphism in the Higher Himalayan Crystalline Sequence (HHCS).

The study area covers only the Higher Himalayan Crystalline Sequence zone and is occupied by well -foliated, amphibolite grade metamorphic and granitic rocks. The metamorphic rocks include medium to fine grained sillimanite-garnet-biotite-muscovite-quartz-feldspar gneiss, diopside- hornblende calcic gneiss, garnet-biotite-muscovite-quartz-feldspar migmatitic gneiss, garnet-biotite-muscovite-quartz-feldspar (± hornblende) schist and calcite-diopside-hornblende marble. These rocks are intruded by coarse-grained quartz-feldspar-biotite-muscovite-tourmaline granitic pegmatite. The latest Tertiary granitic pegmatite of different times of generation can be found in this area. The earlier generation pegmatite is affected by late stage deformation.

The host rocks are folded with the development of major foliation during the syn-MCT deformation prior to the intrusion of the granitic pegmatite. Sometimes, pegmatite carries cleavage, which could be due to late deformation. Some foliated pegmatite is considered to be partially re-melted foliated granite of earlier generation.

The early granitic pegmatite is also folded with host rocks. Feldspar porphyroblasts of the host gneiss are remarkable figures found in this gneiss with the pegmatite. The relationship of folded pegmatite with host rocks, the development of cleavage in pegmatite and porphyroblasts developed along the foliation plane of gneiss show that the major foliation was first intruded by two mica-tourmaline pegmatite (Mu - rich) and then both of them were folded together, resulting in the development of the cleavage as well as flattening of the porphyroblasts. This deformation could be post-MCT.

Pegmatite locally shows contact effect along with shearing; e.g., coarsening of biotite clot is observed in some biotite schist near the contact with a pegmatite intrusion. This phenomenon is considered to reflect the late stage activity of the MCT activity associated with the pegmatite intrusion. Thus, in some places coarse-grained biotite schist occurs intruded by tourmaline-biotite pegmatite dyke, while in other places fine-grained biotite schist is seen apart from the intrusion.

The highly foliated ductile area shows the different metamorphic episodes. The grade of metamorphism in this area increases towards the upper section of the zone of the HHCS from the MCT as pointed out by Hubbard (1989). The P-T conditions below and above the MCT in this region show the inverse metamorphism in the rocks of the Lesser Himalayan zone. The development of the MCT, the inverse metamorphism and Miocene granitic intrusion in the higher section are genetically related (e.g., Le Fort 1975). From the field observation of the middle section of the HHCS zone, garnet crystals are transformed to chlorite, indicating the effect of retrograde metamorphism. It could be related either or both to the late-stage activity of MCT and/or to the normal faulting (South Tibetan Detachment Fault) event between the HHCS and Tibetan-Tethys Sedimentary Sequence.

The lower section of the HHCS consists mainly of coarse-grained sillimanite-garnet-biotite-muscovite-quartz-feldspar gneiss with migmatite and calcic gneiss. These rocks can be correlated with the rocks of the Formation I of the HHCS in central Nepal (Le Fort 1975) and Gosainkund Crystalline Nappe (Rai 2003). The middle section containing garnet-biotite-muscovite-quartz-feldspar (± hornblende) schist and calcite-diopside-hornblende marble can be correlated with the Formation II of the HHCS in central Nepal. Different phases of post-MCT deformation occurred after the main syn-MCT deformation resulting in the folding and development of cleavages along the marginal part of pegmatite and porphyroblasts in gneiss.

Hubbard, M. (1989). –. J. Met. Geol., 7, 19-30.
Le Fort, P. (1975). - Amer. J. Sci., 275-A, 1-44.
Rai, S. M. (2003). – J. Nepal. Geol. Soc. Special Pub, 25, 135-155.

ROCK GLACIERS AND THE LOWER LIMIT OF DISCONTINUOUS MOUNTAIN PERMAFROST IN THE LANGTANG VALLEY, NEPAL HIMALAYA

Dhananjay REGMI[1*] Tanaka SHUNSUKE[1] and Teiji WATANABE[1]

[1]Graduate School of Environmental Earth Science, Hokkaido University, Sapporo 060-0810, Japan
regumi@ees.hokudai.ac.jp, twata@spa.att.ne.jp

Introduction

Rockglaciers are important and fascinating landforms in alpine (high mountain) environments. Rockglaciers have been described in all major high mountain system of the world. Their existence indicates permafrost, since they contain a frozen body. Brasch (1978) first described the importance of rock glaciers as indicators for the lower limits of discontinuous alpine permafrost. Rockglaciers are classified into three types: active, inactive and fossil in terms of the activity status and the presence of permafrost (Barsch, 1996). The distribution of rockglaciers, including those presently lacking ice, indicates the distribution of permafrost at present as well as in the past.

The total amount of annual precipitation plays an important role in determining the mountain permafrost zone (King 1986; Haeberli *et al.,* 1993). The annual precipitation substantially decreases from east to west in the Himalayan regions. Therefore, previous studies (Owen and England 1998; Jakob 1992; Ishikawa *et al.,* 2001) showed significant difference in the estimated lower limit of discontinuous mountain permafrost in Himalaya.

In Langtang valley the rockglacier have not been studied quantitatively. Only Watanabe *et al.,* (1989) measured ground temperature at two sites and estimated that the distribution of discontinuous mountain permafrost is extremely limited. However the existence of discontinuous mountain permafrost and its lower limit has not been conformed in this valley. Therefore, this study attempt to: identify the lower limit of discontinuous mountain permafrost in north-facing slope (Ganja La area) and south-facing slope (Dakpatsen area) in Langtang Valley of Nepal Himalaya. The location of study area is shown in Figure 1.

Methods

Distribution and the morphology of rockglacier were identified from aerial photographs and field observation. The active, inactive and fossil rockglaciers were distinguished following (Barsh, 1996). For this, longitudinal profiles and front angles of the rockglaciers were measured and the vegetation cover was observed. The existence of permafrost was conformed from ground temperature (at the depths of 10, 50, 100 and 150 cm), and BTS (the bottom temperature of the winter snow cover) measurements. Thermo Recorder TR-52 and TR-51, manufactured by T&D Corporation, Japan was used to measured Ground temperatures and BTS, respectively.

Subsurface information (the active layer and the uppermost parts of permafrost) was obtained using seismic refraction method. For this, McSEIS-3 seismograph, manufactured by OYO (Corporation, Japan), was used. The survey was carried out at profiles of 30 to 50 m in length. A total of 36 sledge-hammer seismic traverses survey was carried out in this valley. These data were interpreted following Barsch (1996), who gives P-wave velocities (V1) for the active layer in the range of 300-800 m/s; and the P-wave velocities (V2) for upper permafrost in the range of 2,800 and 4,000 m/s.

Results and Conclusion

Examination of aerial photographs shows existence of ten rockglaciers in this valley. Four of them were exist on the south-facing slope (right side of the valley) at altitude between 4600 m and 4800 m and the rest exist on the north-facing slope (left side of the valley) at altitude between 4300 m and 4600 m.

Morphology and vegetation cover on front slopes of rockglaciers indicate that the upper part of each rockglacier is active. From the extrapolation of the measured ground temperature data, the permafrost table is estimated at the depth of 280–290 cm from the ground surface. BTS measured at debris slope shows BTS value slightly higher than -3°C. This datum indicates that debris slopes are in the marginal condition for permafrost. BTS values on rockglacier were well below –3 °C. This datum supports the existence of permafrost at this site. The seismic velocity profile in the north-facing slope (Gangja La area) supports the existence of permafrost at or above 4810 m in altitude. In the south-facing slope the altitude of permafrost was conformed to be exist at altitude above 4850 m in rockglaciers and above 5105 m in debris covered areas.

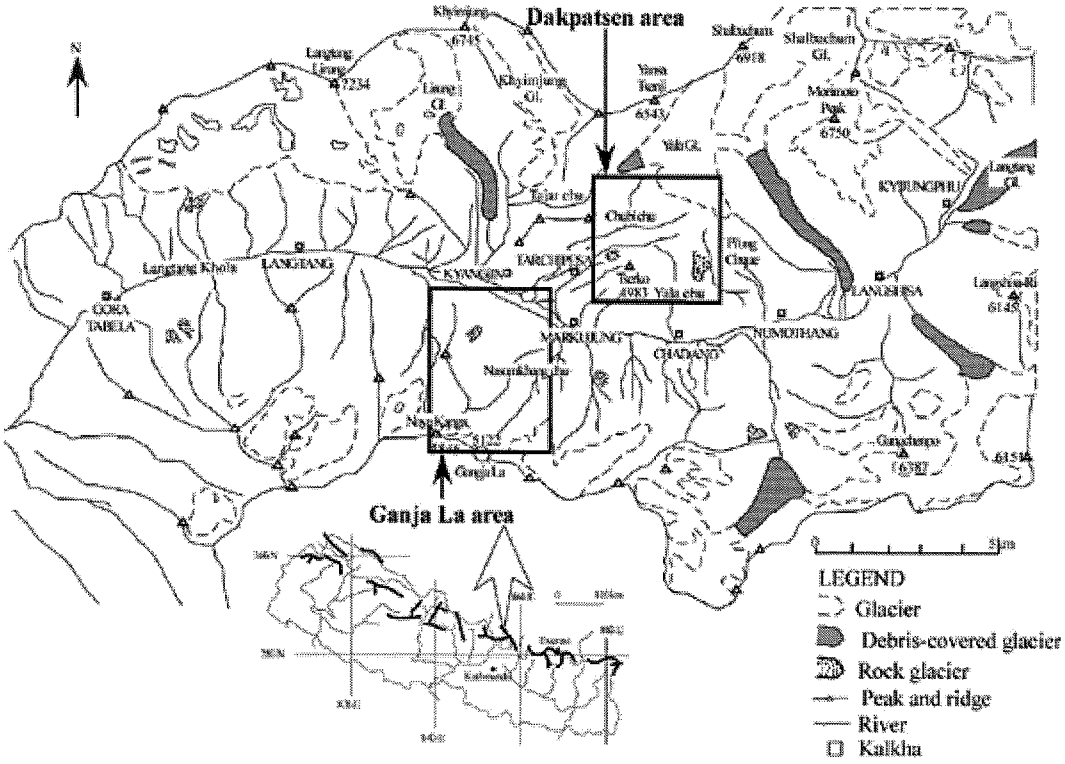

Fig . 1- Situation of the studied areas

References

Brasch D. 1978. In *proceedings, Third International Conference on Permafrost,* National research council, Ottawa, pp.349-352.

Barsch D. 1996. *Rock glaciers. Indicators for the Permafrost and Former Geoecology in High Mountain Environments.* Springer, Berlin, 331pp.

Haeberli W, Guodong C, Gorbunov AP and Harris SA. 1993. *Permafrost and Periglacial Processes,* 4, 165-174.

Ishikawa M, Watanabe T and Nakamura N. 2001. *Permafrost and Periglacial Processes,* 12, 13-25.

Jakob M. 1992. *Permafrost and Periglacial Processes,* 3, 253-256.

King L. 1986. *Geografiska Annaler,* 68A. 131-139.

Owen LA, England J. 1998. *Geomorphology* 26: 199-213.

Watanabe T, Shiraiwa T and Ono Y 1989. *Bulletin of Glacier Research,* 7, 209-220.

MINERALOGICAL AND TEXTURAL PATTERNS IN HP-UHP ECLOGITES AND SURROUNDING FELSIC/PELITIC ROCKS IN KAGHAN-NARAN VALLEY, PAKISTAN HIMALAYA

Hafiz UR REHMAN (1*) and Hiroshi YAMAMOTO (1)

(1) Department of Earth and Environmental Sciences, Kagoshima University, Kagoshima 890-0065, Japan
Email: gsehafez@moon.sci.kagoshima-u.ac.jp (*Corresponding Author: Rehman)

HP-UHP eclogites exposed in the structurally intermediate tectonic part (Unit II) of Kaghan_Naran Valley, Pakistan and the surrounding rocks have been investigated in detail for identifying the mineralogical and textural patterns. The metamorphic grade decreases towards upper tectonic part (Unit III) and lower tectonic part (Unit I) of the of Higher Himalayan crystalline sequence (Rehman et al., 2004). The eclogites of Unit II, exposed in a number of localities, are diverse both in mineralogy and textural features. Mineralogically HP and UHP eclogites are composed of garnet + omphacite + sodic augite + rutile ± epidote ± zoisite ± calcite ± quartz and garnet + omphacite + epidote ± zoisite + quartz ± coesite (as relics in omphacite) + rutile ± phengite ± glaucophane ± paragonite ± barroisite respectively (Fig 1. a, b). In UHP eclogite facies rocks garnet, omphacite, phengite, rutile and some of zircons (having inclusions of omphacite, garnet and phengite ± kyanite) are presumably in metamorphic equilibrium with a peak P-T condition of coesite phase stable field, while HP eclogites show garnet, omphacite, zoicite/epidote, rutile ± zircon respectively. Textural patterns indicate that these eclogites were probably hydrated under eclogite through epidote-amphibolite-facies conditions. The decompression and recrystalization is clearly preserved in the form of quartz-albite-amphibole symplectites. Garnet in the eclogites is mostly homogeneous with inclusions of quartz + omphacite + zircon and rutile. X-ray map of garnet shows a homogenous distribution of Mg, Fe, Ca and Mn with partial zoning at rims (Fig.2).

The rocks surrounding the eclogites are felsic/pelitic rocks. These are composed of garnet + epidote ± zoicite + feldspar + quartz ± phengite + biotite + kyanite ± coesite (as inclusions in zircon) + rutile ± ilmenite ± apatite. These are metamorphosed to kyanite-sillimanite grade (Rehman et al., 2004) and the felsic/pelitic gneisses close to the UHP eclogitic bodies preserve coesite inclusions in zircon (Kaneko et al., 2003) indicating a peak PÅ[T conditions of coesite stable field, suggesting a depth of about ~100km. Garnet porphyroblasts are fairly large and show well developed zoning pattern (Fig. 3). Fe is evenly distributed among the rims and cores, showing no peculiar zoning but Mg is rich at rims while Ca is in reverse order that is rich at core and poor at rims. Mn shows very little concentration. The retrogressive phases are evidenced by chlorite engulfing garnet and biotite at rims.

These mineralogical and textural patterns indicate the metamorphic history in HP-UHP eclogites and surrounding rocks in Himalayan metamorphic belt of the Kaghan_Naran valley. The presence and absence of metamorphic index minerals in the area indicate that prograde metamorphism took place while the subduction was in progress. The peak P-T conditions were attained when the rocks of Unit II reached at maximum depth (~110km) where probably slab break-off occurred during the India-Asia collision and the metamorphic history is preserved in the form of mineralogical and textural patterns. The mafic rocks turned to eclogites while the surrounding rocks turned into felsic/pelitic gneisses under a specific thermal gradient at depths in the subduction zone.

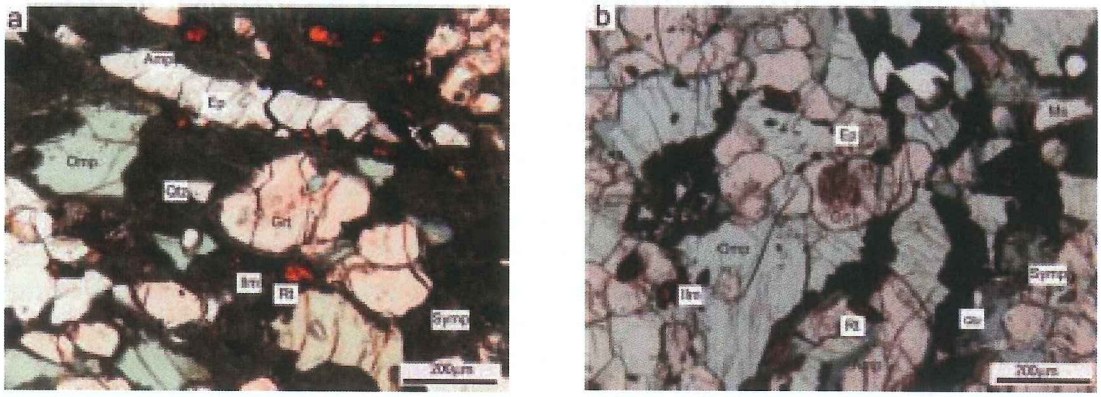

Fig. 1. (a) Photomicrograph of HP eclogite with main mineral assemblages. Garnet porphyroblast in the center show inclusions of quartz and omphacite while at rims recrystalization and decompression is very obvious. (b) Photomicrograph of UHP eclogite with main mineral assemblages. Rounded garnet porphyroblast in the center is rich of inclusions while omphacite is rather fresh. Mineral abbreviations are after Kretz (1983) except Amp: Amphibole, Sympl: Symplectites.

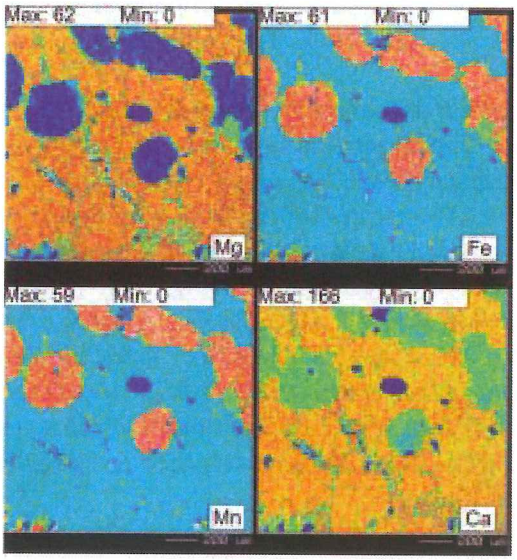

Fig. 2. X-ray map of garnet from UHP eclogites showing Mg, Fe, Mn and Ca concentration. The concentration of above elements is almost homogeneous with minor zoning at rims.

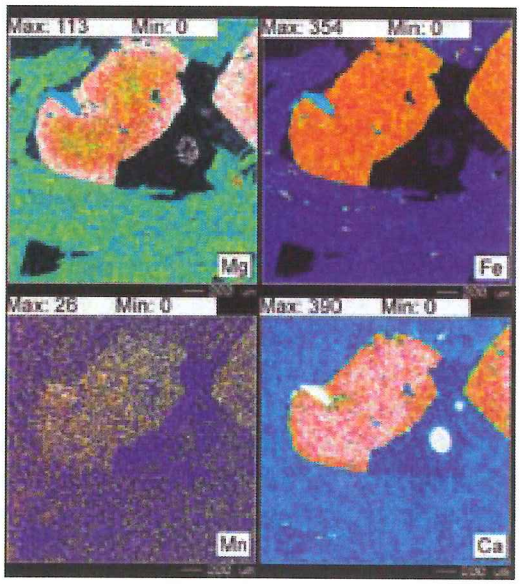

Fig. 3. X-ray map of garnet from Felsic/ Pelitic gneisses close to eclogites, showing Mg, Fe, Mn and Ca concentration. The zoning pattern is very clear in Mg and Ca but poorly zooned in Fe and Mn.

References:

Kaneko, Y., I. Katayama, H. Yamamoto, K. Misawa, M. Ishikawa, H. U. Rehman, A. B. Kausar and K. Shiraishi, 2003. Jou. Met. Geol. **21**, 589-599.

Kretz, R., 1983. Am. Min. **68**, 277-279.

Rehman, H. U., Yamamoto, H., Kaneko, Y., and Kausar, A. B., 2004. Him. Jou. Sci. **2**, 229-230

AN IMPORTANT GEOLOGICAL EVENT IN NORTHERN TIBETAN PLATEAU: EVIDENCES OF ^{36}CL DATING FROM WESTERN QAIDAM BASIN

Shoumai REN (1)(2)*, Yongjiang LIU (3), Dewu QIAO (1), Xiaohong GE (3), Zhenyu YANG (2), Andrea RIESER (4)

(1) Strategic Research Center for Oil & gas Resources, Ministry of Land & Resources, Beijing, China.
(2) Institute of Geomechanics, Chinese Academy of Geological Sciences, Beijing, China
(3) College of Earth Sciences, Jilin University, Changchun, China.
(4) Division General Geology and Geodynamics, University of Salzburg, Austria
* To whom Correspondence should be addressed. E-mail:realshaw@vip.sina.com

In the past decade, more and more researchers noticed that the uplift of Tibetan plateau were stepwise from south to north and unbalanced between eastern and western parts (Li et al., 1996; Chung et al., 1998; Tapponnier et al., 2001; An et al., 2001; Shi et al., 1999; Zheng et al., 2000; Ge et al., 2004), also, this behavior are responded by the multi-phased slip and uplift along the Altyn Tagh sinistral strike-slipping fault (Ren et al., 2004). The northwest part of the Qaidam basin, which locates on the northeast of Tibetan plateau, has been displaced by Altyn Tagh faults since the Late Mesozoic period (Liu et al., 2000). Therefore, it has been involved in several regional tectonic events, especially in the Cenozoic. In 1950's, some geologists mentioned that the youngest strata involved in the lastest folding were the Early Quaternary, named as Balongmahai Formation originally (Sun et al., 1958) and as the Early-Middle Pleistocene Qigequan Formation later by the workers from the Qinghai Oil-Gas sub-company of China. The conglomerate over the unconformity plane was called the Old Proluvial Conglomerate anteriorly (Zhu et al., 1994) and the Late Pleistocene Qaidam Formation subsequently. Based on the field work, some researchers suggest that two uncomfortable planes, one is appeared between Qaidam Formation and Qigequan Formation, the other between Qigequan Formation and the Pliocene Shizigou Formation, represent two important geological events (Yang et al., 1992). Unfortunately, a set of sandstones and conglomerates was developed at the upside and downside of the unconformity plane, so it is hardly to get the accurate age data for lack of the available fossils and dating minerals.

According to the field work, we found that a high-angular unconformity is well developed at the south side of the Altyn Mountain in the western Qaidam basin. The Pleistocene strata with slight dip have good outcrop at the north side of the Altyn Mountain in the Dunhuang basin. Two group ^{36}Cl dating samples were collected from the mudstone lens of the fluvial deposit on the upside and downside of the unconformity plane in Goukogou in the western Qaidam basin, and from slight incline mudstone layer in the Dunhuang basin. A couple of age is dated an age of 1.535Ma at the downside and 0.277Ma at the upside of the unconformity in the Goukogou, the other two samples from the Duanhuang basin at 1.142Ma and 0.837Ma (see Table 1). Considered with the recent report related to the this tectonic event from Tarim basin (Fang et al., 2002), western Jiuquan basin (Zhao et al., 2001) and Qaidam basin (Sun et al., 2000), we believed that a significant geological event was happened in the northwest China at the Early Pleistocene which representes evidently the latest rapid uplift of the northern Tibetan Plateau. Thus, it is necessary to re-understanding the tectonic evolution and regional framework in northwest China.

An Zhisheng, et al. 2001. *Nature*, **411**. 62-66. Chung Sunlin et al. 1998. *Nature*, **394**. 769-773. Fang Xiaomin et al. 2002. *Science in China (Series D)*, **45(4)**. 289-299. Ge Xiaohong et al. 2004. *Quaternary Sciences*, **24(1)**. 67-73. Li Tingdong. 1996. *Tectonophysics*, **260 (1-3)**. 45-53. Ren Shoumai et al. 2004. *Geol Bul.f China*, **23(9-10)**. 926. Sun Jimin, Liu Tungsheng. 2000. *Quaternary Research*, **54**. 309-320. Sun Tienching, et al. 1958. In: Li Szekuang, Sun Tienching, Wu Leibo edit, Vortical and other torsional structures and problems of syntaxis of tectonic systems. Science Publisher. 13-35 (In Chinese). Tapponnier P et al. 2001. *Science*, **294(23)**. 1670-1677. Yang Fan et al. 1992. *Actapetrolei Sinica*, **13(2)**. 97-101. Zhao Zhijun et al. 2001. *Chinese Science Bulletin*, **46(23)**. 2001-2005. Zheng Hongbo et al. 2000. *Geology*, **28(8)**. 715-718. Zhu Yunzhu et al.. 1994. Beijing: Geological Press. 57-72

Note Page

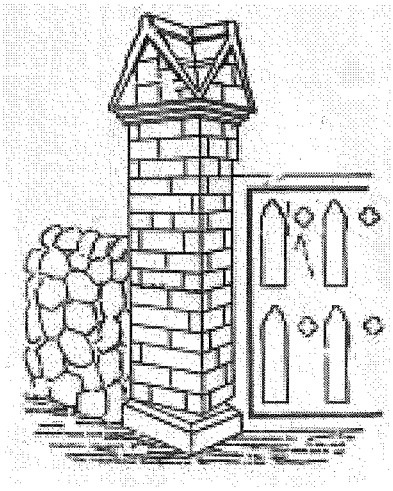

Kangra earthquake, Middlemiss, 1905

HIMALAYA ULTRAHIGH PRESSURE EVOLUTION AND WARPED INDIAN SUBDUCTION PLANE

Anne REPLUMAZ, Stéphane GUILLOT, Pierre STRZERZYNSKI

Laboratoire de Sciences de la Terre, CNRS UMR 5570, Ecole Normale Supérieure de Lyon et Université Claude Bernard, 2 rue Dubois 69622 Villeurbanne France. Anne.Replumaz@univ-lyon1.fr

On both sides of the Western Himalayan Syntaxis, P-T-t data on ultrahigh-pressure metamorphic rocks suggest that the western Kaghan unit was metamorphosed under UHP conditions significantly later (~ 46 Ma) than the Tso Morari unit (~ 54 Ma). This suggests that the Kaghan unit was originally located in a more internal part of the Indian plate, compared with the Tso Morari. By using the amount of Indian plate subduction from 55 Ma to 40 Ma in conjonction with the P-t evolution of the UHP units, we calculate the dip of subduction. We estimate that during burial of both units, the dip of the subduction plane was relatively high (30-40°), on both sides of the Western Syntaxis, indeed much higher than previously estimated. During their exhumation, the dip of the subduction plane in the Kaghan region remained high whereas, in the eastern part, it decreased to about 9° as observed today. The evolution of the subduction angles allows to constraint the evolution of the initial geometry of the continental collision zone. The Tso Morari unit, on the eastern side of the Western Syntaxis, recorded a flattening of the subduction dip between 55Ma and 47Ma, which probably corresponds to flattening of the buoyant continental Indian plate beneath Southern Tibet. On the western side, the Kaghan unit recorded a constantly steep angle of subduction. The Kaghan unit recorded the initiation of the formation of the Western Syntaxis, around 50Ma, pinched towards the west along the proto-Chaman fault, as present-day observed. The current difference in continental subduction on both sides of the Western Syntaxis seems inherited from the early continental subduction period. Using tomographic images, it is possible to image the subduction slab during its burial. Correlation of tomography and tectonic reconstructions allow to estimated the ages of the tomographic

Kaghan unit					
Facies	Pressure	Temperature	Age	Velocity	Dip angle
HP	~ 13 Kbar	~ 550 °C	50 ± 1 Ma		
				⇒ 12 cm/yr	⇒ 35 ± 10°
UHP	30 ± 2 Kbar	770 ± 30 °C	46 ± 0.7 Ma		
				⇒ 20 cm/yr	⇒ 45 ± 15°
Amph.	11 ± 1 Kbar	630 ± 30°C	40 ± 1 Ma		
				⇒ 7 cm/yr	⇒ 19 ± 9°
Greenschist	~ 4 Kbar	~ 500 °C	~ 40 Ma		
Tso Morari unit					
Facies	Pressure	Temperature	Age	Velocity	Dip angle
HP	10 ± 1 Kbar	470 ± 10°C	> 53 Ma		
					⇒ >40°
UHP	~ 28 Kbar	~ 630 °C	53-54 Ma		
				⇒ 3 cm/yr	⇒ 9 ± 4°
Amph.	9 ± 3 Kbar	630 ± 30°C	47 ± 2 Ma		
				⇒ 3 cm/yr	⇒ 9 ± 3°
Greenschist	~ 3 Kbar	530 ± 30°C	40 ± 2 Ma		

Table 1: Pressure temperature time path evolution of the UHP Kaghan and Tso Morari unit with the velocity and dip estimates.

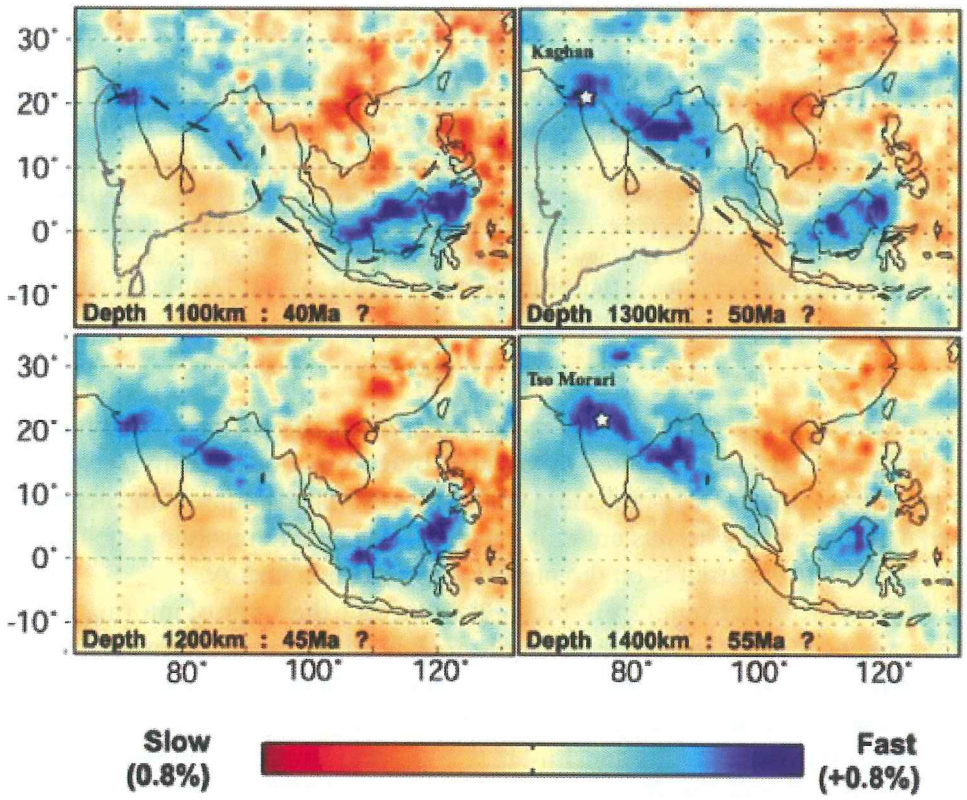

Figure 1: Horizontal, tomographic sections of mantle velocity structure beneath India-Asia at depths of 1100, to 1400 km (from Kárason, 2002). Seismically fast zones are interpreted as the remnant of subducted indian oceanic and continental lithosphere. Superimposed by 2 tentative correlations matching with contours of reconstructed Asian plate boundary position (Replumaz et al, 2004), 40 Ma at 1100 km and ~50 Ma at 1300 km.

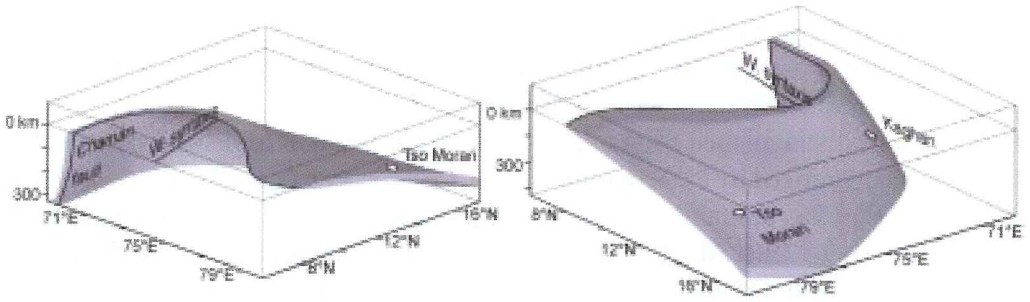

Figure 2: 3D Geometry of the Northwest Himalaya showing the warped geometry of the Indian subduction plane after 55 Ma. The initial India-Asia contact is located at ~10°N (Patriat and Achache, 1984). At this time, the Tso Morari unit reached a depth of about 100 km while the Kaghan unit was not still involved in the subduction zone. Notice that the intersection of the two parts of the subduction plane corresponds to a north-dipping axis, defining the future Nanga Parbat spur.

HIMALAYAN ARCHITECTURE CONSTRAINED BY ISOTOPIC TRACERS FROM CLASTIC SEDIMENTS

Andy RICHARDS (1), Tom ARGLES (1), Nigel HARRIS (1), Randy PARRISH (2), Talat AHMAD (3), Fiona DARBYSHIRE (2) and Erich DRAGANITS (4)

(1) Department of Earth Sciences, The Open University, Milton Keynes MK7 6AA, UK
(2) NERC Isotope Geosciences Laboratory, British Geological Survey, Keyworth, Notts NG12 5GG, UK
(3) Department. of Geology, University of Delhi, Delhi-110007, India.
(4) Institute for Engineering Geology, Vienna University of Technology, Karlsplatz 13/203, A-1040 Vienna, Austria.

Unified tectonic models for orogenesis require accurate information about the architecture of a mountain belt, which may be obscured by vagaries of deformation intensity, metamorphism, or uncertain stratigraphic correlation. Combining whole-rock isotopic studies with zircon provenance data (e.g. Parrish & Hodges 1996) has not only proved invaluable in resolving such problems, but has also provided critical constraints on the pre-orogenic tectonic history.

We present data from the Sutlej valley, NW India, that illustrate the range of information obtainable from four different geochemical techniques. Whole-rock Nd data provide information on the mean age of source areas contributing detritus to the sedimentary units in the mountain belt, regardless of their current metamorphic grade. U-Pb ages of detrital zircons from the same units identify the age of melt formation in the source rocks and Lu-Hf isotope data from zircons resolve discrete crust formation ages in the multiple eroding terrains. In contrast, whole-rock Sr behaviour provides insights into the extent of pre-Himalayan thermal events.

Isotopic data for whole rock samples show a bimodal distribution: Palaeoproterozoic metasediments of the Jutogh Group and Rampur Formation have $\varepsilon_{Nd}(500)$ values below −17, whereas Neoproterozoic and younger metasediments have $\varepsilon_{Nd}(500)$ above −13. The latter group encompasses the Vaikrita Group gneisses (High Himalayan Crystalline Series, HHCS) and the overlying Haimanta Group and Tethyan Sedimentary Series (TSS), but also includes a number of units in thrust sheets north of the Main Boundary Thrust in the Lesser Himalayan Zone. Following Ahmad *et al.* (2000), we designate these units as the 'Outer Lesser Himalaya' (OLH), to distinguish them from the 'Inner Lesser Himalaya' (ILH; i.e. the Jutogh Gp and Rampur Fm). Many ILH samples lie close to a 1800 Ma reference line on a plot of $^{87}Sr/^{86}Sr$ against $^{87}Rb/^{86}Sr$, whereas data from other units scatters around a 500 Ma reference line (or younger for some TSS samples).

The ILH can also be distinguished from other units using U-Pb ages of detrital zircons. ILH zircon populations are characterised by Palaeoproterozoic-Late Archaean ages (2.6-1.8 Ga), whereas other units (HHCS, OLH, TSS) contain populations both of this age, and a younger period (Meso- to Neo-proterozoic; 1.1-0.8 Ga). Along with corresponding Nd model ages, these data suggest that, whereas the ILH sediment detritus was dominated by Palaeoproterozoic-Archaean source regions, sediments of the HHCS, OLH, Haimanta Group and TSS comprised a mixture of detritus from a similar ancient source to that of the ILH, and a younger, mainly Neoproterozoic, source. Lu-Hf isotopes further confirm that the ILH and HHCS/OLH sediments shared a common source region, with zircon grains derived from melting of crust formed during Archaean times (3.4-2.6 Ga). Most of the younger zircons in the HHCS were derived from melting of Palaeoproterozoic crust formed around 2.1-1.7 Ga. In addition, ca. 1.8 Ga granitoid bodies (e.g. the Wangtu gneiss in the Sutlej valley) formed by anatexis of Archaean crust, and are exclusively associated with ILH units, while 500 Ma granitoids are apparently confined to Neoproterozoic units such as the HHCS and Haimanta Group.

These data allow us to place constraints on the palaeogeographical and tectonic histories of these diverse units. The Rampur Formation (ILH), deposited around 1.8 Ga in a restricted, probably intracontinental, rift basin, was fed almost exclusively with detritus from granitoids identical to the Wangtu gneiss. Provenance characteristics of the Jutogh metasediments are similar to those of the Bundelkhand Complex of the Aravalli craton, north-west India (zircon ages between 1.9-3.2 Ga, with similar Nd model ages). This may indicate either a direct correlation between the two units, or that the Jutogh Group was derived from erosion of the Bundelkhand. The Bundelkhand may also have fed detritus into the Meso- to Neo-proterozoic basin(s) in which the HHCS, Haimanta Group, OLH and TSS sediments were deposited, mixed with material from an unidentified, younger source.

This rapid influx of juvenile detritus coincided with the collapse of the Upper Riphean Shali-Deoban carbonate platform at around 850 Ma, coincident with a period of granite magmatism in the Himalayan zone (e.g. Chor granite), the Indian craton, and southern China. Most palaeogeographical schemes imply that southern China was separated from Greater India by no more than a narrow gulf from Neoproterozoic through to Palaeozoic time, and the widespread magmatism implies that this margin of Rodinia was far from stable at this time. Processes along this margin are the most likely source of juvenile material for the HHCS, OLH and Haimanta sediments.

Sr data provide some evidence that, whereas the HHCS, OLH and Haimanta units were partially reset at ca. 500 Ma, ILH formations escaped tectonism at both ca. 850 and ca. 500 Ma, but experienced partial resetting at ca. 1.8 Ga, coeval with rift-related mafic and granitic magmatism (e.g Wangtu gneiss). This implies that the HHCS/OLH and the ILH experienced contrasting geological histories, at least until the Mesozoic era, precluding the possibility that the HHCS was deposited on a LHS basement. If they represent proximal and distal sections of a single passive margin, as has been proposed by Myrow et al. (2002), then their lateral separation during both the Late Proterozoic and Early Palaeozoic must have exceeded the extent of the thermal resetting event in each case.

References

Ahmad, T., Harris, N., Bickle, M., Chapman, H., Bunbury J. & Prince, C. 2000 *Geol. Soc. Am. Bull.* **112**(3), 467-477.

Myrow, P.M., Hughes, N.C., Paulsen, T.S., Williams, I.S., Parcha, S.K., Thompson, K.R., Bowring, S.A., Peng S.-C., & Ahluwalia, A.D. 2003 *EPSL* **212**(3-4), 433-441.

Parrish, R.R., & Hodges, K.V. 1996 *Geol. Soc. Am. Bull.* **108**(7), 904-911.

SEDIMENTS OF THE CENOZOIC QAIDAM BASIN IN WESTERN CHINA: LINKING BASIN FILL WITH MOUNTAINS BY ISOTOPICAL AND COMPOSITIONAL CONSTRAINTS

Andrea B. RIESER (1), Franz NEUBAUER (1), Yongjiang LIU (2), Johann GENSER (1), Gertrude FRIEDL (1), Robert HANDLER (1) and Xiaohong GE (2)

(1) Division General Geology and Geodynamics, University of Salzburg, Hellbrunnerstr. 34, 5020 Salzburg, Austria
(2) College of Earth Sciences, Jilin University, Jianshe Str. 2199, 130061 Changchun, China

The ca. 120'000 km^2 large, rhomb-shaped Qaidam Basin is an intracontinental sedimentary basin that is considered to be part of the convergent systems at the northernmost margin of the Tibetan plateau (Meyer et al., 1998). Being a closed system since early Oligocene (Huo, 1990), its unusually thick Mesozoic to Cenozoic sedimentary sequence contains much information regarding tectonic and climatic history, which is the subject-matter of a recently finished PhD-study (Rieser, 2004). A summarizing overview shall be given herein.

Palaeogeographic relationships can be monitored by $^{40}Ar/^{39}Ar$ dating of detrital white mica. The new data allow discussion of linkages and tectonic relationships of the western Qaidam Basin. New $^{40}Ar/^{39}Ar$ detrital white mica ages from the north-western basin part yield four different age groups: (1) ca. 350–450 Ma, (2) 220–280 Ma, and less abundant clusters with (3) 122–140 Ma and (4) a group around 500 Ma. Late Miocene to Quaternary surface samples basically include grains belonging to the 350–450 Ma group. Samples from the eastern basin margin display a completely different, uniform age distribution from Eocene to Pliocene. All grains have ages ranging from 250 to 280 Ma. In most cases, the ages can be attributed to some known basement rocks in the surrounding mountains. The dominating group of 350–450 Ma ages has its origin mainly in the Altyn Mountains, where ages of this range are well known, while the 122–140 Ma old grains basically come from the Kunlun Mountains. The eastern basin is exclusively fed from the Qilian Mountains.

Not only the age-distribution of detrital mica helps to identify probable provenance areas for the sediments but also classical point-count analysis. Based on the moderate sorting of the sandstones and the subangular grains, one can conclude on relatively short transport distances. This observation is further supported by immaturity of the sandstones, indicated by a high proportion of feldspars and lithic fragments. Additionally sandstone composition can give insight into climatic evolution as well. Despite variable climatic conditions during the Cenozoic no significant changes can be observed in framework constituents within sandstones. The slight decrease in quartz content when regarding Cenozoic formation average values remains insignificant. Alone mica contents are increasing with time and proven higher aridity towards recent times. White mica increases from 1.0 to 3.7 percent and the biotite content from 0.1 to 1.6 percent, respectively. Muscovite is generally much better preserved than biotite, which is chemically less stable (e.g., Nagy, 1995). Thus, the high biotite content reflects well increasing aridity.

Even better climatic constraints are expected from carbon and oxygen isotope analysis of lake carbonates. There existed a palaeo-lake in Qaidam, which evolved from the western part of the basin to the east (Liu et al., 1998). This lake reached its maximum extension during a semiarid interval in the Miocene (Wang et al., 1999). The driest climatic conditions occurred in Pliocene and Pleistocene times (Wang et al., 1999), similar to today's climate, when abundant evaporates are formed. This aridity is well highlighted by isotopic records of both $d^{13}C$ and $d^{18}O$, that show a first order trend towards arid and highly evaporative conditions. Distinct sections show shorter cycles of various length from several thousands to three million years duration.

HUO, G.M. 1990. *Chinese Petroleum Industry Press*, 483 p. LIU, Z., WANG, Y., YE, C., LI, X., LI, Q. 1998. *Pal. Pal. Pal.*, **140**, 459-473. MEYER, B., TAPPONNIER, P., BOURJOT, L., MÉTIVIER, F., GAUDEMER, Y., PELTZER, G., SHUNMIN, G., AND ZHITAI, C. 1998. *Geoph. J. Int*, **135**, 1-47. NAGY, K.L. 1995. Min. Soc. America. p. 173-233. RIESER, A.B. 2004. The Cenozoic Qaidam basin in Western China: Linking basin fill with mountains by isotopical and compositional constraints [PhD thesis]: Austria, University of Salzburg, 165 p. WANG, J., WANG, J.Y., LIU, Z.C., LI, J.Q., XI, P. 1999. *Pal. Pal. Pal.*, **152**, 37-47.

Note Page

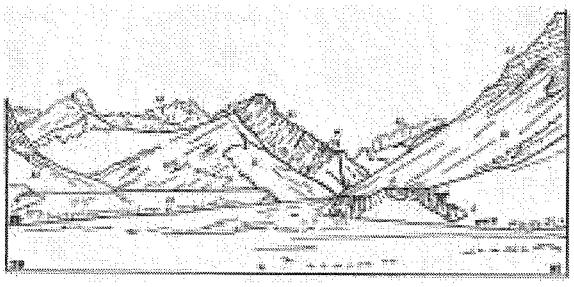

Skam Lungpa, Desio, 1980

TERTIARY SLIP RATES OF THE ALTYN TAGH FAULT AND MAGNITUDE AND TIMING OF SHORTENING AND STRIKE-SLIP IN NORTHEAST TIBET

Bradley RITTS (1), Yongjun YUE (2) and Stephan GRAHAM (2)

(1) Dept. of Geological Sciences, Indiana University, Bloomington, IN, USA; britts@indiana.edu
(2) Dept. of Geological and Environmental Sciences, Stanford University, Stanford, CA, USA

Recent studies of geological piercing points across the Altyn Tagh fault (ATF) have resulted in a well-constrained slip history for the fault which provides quantitative testable predictions about the timing and magnitude of slip on other structures on and adjacent to the northern Tibetan Plateau. It is essential that these new geological constraints be considered in studies that require knowledge of the ATF, traditionally viewed as an essentially unconstrained structure.

The total magnitude of displacement on the eastern-central Altyn Tagh fault is constrained by numerous pre-Tertiary piercing points, including Paleozoic and Precambrian basement features (Chu, 1998; Yang et al., 2001; Zhang et al., 2001; Gehrels et al., 2003) and Mesozoic structures and basins (Ritts and Biffi, 2000; Sobel et al., 2001). All of the pre-Cenozoic piercing points that have not been disproved by subsequent studies (Ritts and Biffi, 2000; Ritts et al., 2004) overlap within uncertainty between 350 and 400 km of left-lateral separation (Yue et al., 2003). Yue et al. (in review) demonstrated 360±40 km of displacement between Oligocene strata of the Xorkol basin and the northern Qilian Shan using detrital zircon geochronology, suggesting that the magnitude of slip on the ATF is high very near its presumed NE termination near Yumen. Together, these studies demonstrate 375±25 km is the total amount of Cenozoic left-lateral strike-slip on the central-eastern segment of the ATF (east of about 086°E).

The total magnitude of displacement on the western ATF is defined by a single published geological piercing point that is based on ages of granites in the western Kunlun Shan (Cowgill et al., 2003). This piercing point suggests an offset on the western segment of the ATF of 475±70 km. If this conclusion is supported by other piercing points, the western segment of the ATF (west of about 086°E) has ~100 km more left-lateral separation than the eastern-central segment.

Although previous workers have suggested large amounts of strike-slip on the Northern Altyn Tagh fault (Cowgill et al., 2000; Yin et al., 2002), piercing point studies (Yue et al., 2001) across the fault preclude large (>30 km) amounts of strike-slip on this oblique reverse fault (Yue et al., 2004). Thus, although it may reflect strain partitioning within the Altyn Tagh system, it is not a strike-slip fault.

The age of initiation of the ATF is defined to be late Oligocene or earliest Miocene based on piercing points (Yue et al., 2001). Oligocene strata of the Xorkol basin are offset from sediment sources in the Qilian Shan by the same amount as pre-Tertiary features, within uncertainty. Overlying Lower Miocene conglomerates show less offset from their sources in the Qilian Shan, indicating ~60 km of strike-slip by the time of deposition. These results are consistent with previous basin studies that proposed uplift (and by inference strike-slip) in the Altun Shan beginning in the Oligocene (Bally et al., 1986; Rumelhart, 1999; Hanson, 1999). Because Oligocene piercing points overlap with pre-Tertiary piercing points within uncertainty, these studies argue against a pre-Tertiary ancestral ATF. However, given large uncertainties, up to 100 km of post-Jurassic, pre-Oligocene strike-slip cannot be disproved.

Tertiary syn-slip piercing points are based on offset basins and sediment sources in the Altun Shan and Qilian Shan; there are no Tertiary piercing points from the western segment of the ATF. Piercing points are documented in the Xorkol basin (Yue et al., 2001, 2003, in review) and Aksay basin (Ritts et al., 2004) and demonstrate large offsets between Oligocene and Lower Miocene conglomerates and their source terranes (360±40 and 320±20 km, respectively), and small offsets between mid-Miocene and younger conglomerates and their source terranes (~65 km for mid-Miocene piercing points).

These results indicate that most of the displacement on the eastern-central ATF (~310 km) accumulated in the Late Oligocene and Early Miocene, and that only a small amount of slip (~65 km) accumulated after the Early Miocene. These results indicate two phases of slip on the ATF: an early phase of fast slip (>20 mm/y) in the late Oligocene-Early Miocene and a later phase of slow slip (<10 mm/y) mid-Miocene-Recent. These two phases of slip reconcile evidence for large total offsets with evidence for present slow slip rates based on geodetic methods (5.6±1.6 mm/y; Zhang et al., 2004).

We propose that the early phase of fast slip on the ATF corresponded to plate-like behavior of NE Tibet and lateral extrusion eastward of the present Tibetan Plateau. The slower slip after the Early Miocene corresponded to a phase of distributed crustal shortening within the Tibetan Plateau, when the ATF acted as a tear fault between Tarim and Tibet. *Thus, we suggest that the mechanisms that accommodated India-Eurasia convergence in Tibet changed in the mid-Miocene from plate-like lateral extrusion to distributed shortening, thickening and uplift.*

This model makes multiple quantitative predictions about the timing and magnitude of offset on other major structures in the NE Tibetan Plateau and beyond, which can be used to test this hypothesis. Of the ~375 km of slip on the eastern-central ATF, ~310 km was related to plate-like extrusion, thus 310 km of the ~475 km on the western Altyn Tagh fault is also predicted to be the result of plate-like lateral extrusion in the Late Oligocene and Early Miocene. The remaining, younger, slip on each segment of the fault (~65 km on the eastern-central ATF and ~165 km on the western ATF) was related to post-Early Miocene distributed shortening and thickening within Tibet. Thus, the post-Miocene long-term slip rate on the western ATF is likely more than 2 times as fast as that on the eastern ATF. Because the Oligocene-Early Miocene phase of deformation allowed extrusion beyond the present NE end of the ATF, structures beyond the Tibetan Plateau are required to accommodate the 310 km of slip prior to mid-Miocene; left-lateral faults that may accomplish this have been identified in the Alxa block (Darby et al., this meeting). Third, post-Early Miocene slip on the ATF, during the phase of distributed shortening, must be balance by shortening within the Tibetan Plateau. Thus, we predict ~65 km of mid-Miocene-Recent shortening in the Qilian Shan and northern Qaidam basin and ~100 km of shortening in the Kunlun Shan and western Qaidam basin. The magnitude of shortening in both belts is unconstrained, but thermochronology and sedimentary records suggest episodes of major shortening, uplift and exhumation in the mid-Miocene (e.g., George et al., 2001), consistent with our prediction.

BALLY, A.W., CHOU, I., CLAYTON, R., EUGSTER, H.P., KIDWELL, S., MECKEL, L.D., RYDER, R T., WATTS, A.B., AND WILSON, A.A. 1986. *U.S. Geol. Surv. Open-File Report.* **0196-1497**.
BURCHFIEL, B. C., DENG, Q., MOLNAR, P., ROYDEN, L., WANG Y., ZHANG P., AND ZHANG W. 1989. *Geology,* **17**. 748-752.
CHU, C. 1998. *Stanford University M.S. thesis*, 78 p.
COWGILL, E., YIN, A., WANG, X.F., & ZHANG, Q. 2000. *Geology.* **28**. 255-258.
COWGILL, E., YIN, A., HARRISON, T.M., & WANG, X.F. 2003, *J. Geophys. Res.* **108**. 2346.
GEHRELS, G.E., YIN, A., & WANG, X. 2003. *Geol. Soc. Am. Bull.* **115**. 881-896.
GEORGE, A. D., MARCHALLSEA, S. J., WYRWOLL, K. H., CHEN, J., & LU, Y. 2001. *Geology.* **29**. 939-942.
RITTS, B.D. & BIFFI, U. 2000. *Geol. Soc. Am. Bull.* **112**. 61-74.
RITTS, B.D., YUE, Y., & GRAHAM, S.A. 2004. *J. Geol.* **112**. 207-230.
RUMELHART, P. E. 1999. *University of California, Los Angeles Ph.D. dissertation*, 268 p.
SOBEL, E.R., ARNAUD, N., JOLIVET, M., RITTS, B.D., & BRUNEL, M. 2001. *Geol.Soc. Am. Mem.* **194**. 247-268.
YANG, J., XU, Z., ZHANG, J., CHU, C., ZHANG, R., & LIOU, J. G. 2001. *Geol.Soc. Am. Mem.* **194**. 151-170.
YIN, A., RUMELHART, P.E., BUTLER, R., COWGILL, E., HARRISON, T.M., FOSTER, D.A., INGERSOLL, R.V., ZHANG, Q., ZHOU, X., WANG, X., HANSON, A., & RAZA, A. 2002. *Geol. Soc. Am. Bull.* **114**. 1257-1295.
YUE, Y., RITTS, B.D., & GRAHAM, S. 2001. *Int. Geol. Rev.* **43**. 1087-1093.
YUE, Y., RITTS, B.D., GRAHAM, S., WOODEN, J., GEHRELS, G., & ZHANG, Z. 2003. *Earth Planetary Sci. Lett.* **217**. 111-122.
YUE, Y., RITTS, B.D., HANSON, A.D., & GRAHAM, S.A. 2004. *Earth Planetary Sci. Lett.* **228**. 311-323.
YUE, Y., GRAHAM, S.A., RITTS, B.D., & WOODEN, J.L. in review. *Tectonophysics.*
ZHANG, J., ZHANG, Z., XU, Z., YANG, J. & CUI, J. 2001. *Lithos.* **56**. 187-206.
ZHANG, P.Z., SHEN, Z., WANG, M., GAN, W., BURGMANN, R., MOLNAR, P., WANG, Q., NIU, Z., SUN, J., WU, J., HANRONG, S., & XINZHAO, Y. 2004, *Geology.* **32**. 809-812.

GEOCHRONOLOGICAL CONSTRAINTS ON THE AGE OF THE ECLOGITE-FACIES METAMORPHISM IN THE EASTERN HIMALAYA

Franco ROLFO (1), William MCCLELLAND (2) & Bruno LOMBARDO (3)

(1) Dipartimento di Scienze Mineralogiche e Petrologiche, University of Torino, Italy.
(2) Department of Geological Sciences, University of Idaho, USA.
(3) CNR, Istituto di Geoscienze e Georisorse, Torino, Italy.

The recent discovery of granulitized eclogites in the E Himalaya (Lombardo & Rolfo, 2000) opened the possibility of a Himalaya-wide eclogitic metamorphism of Early Tertiary age.

The E Himalaya eclogites occur at the top of the MCT zone in the Kharta region (Arun - Phung Chu valley). They record two superposed metamorphic events: a first eclogitic event (T = 600°-650°C ?; P = 1.2-1.4 Gpa ?) and a second granulitic event (T = 750°-770°C; P = 0.55-0.65 GPa). The granulitic event has also been recorded in country rocks which, however, only rarely preserve relics of HP mineral assemblages.

In order to place the Kharta eclogites in the tectonometamorphic frame of the whole Himalayan chain, it is of paramount importance to date them. The timing of the eclogitic event in the Kharta region is difficult to constrain by radiometric ages, because of the widespread high-temperature overprint and the poor preservation of high-pressure assemblages. The eclogitic event was considered by Lombardo & Rolfo (2000) to be older than the granulitic metamorphism and the generation of the Miocene leucogranites. The eclogitic event must also be older than 25 Ma, the age estimated for the Eohimalayan metamorphism from $^{40}Ar/^{39}Ar$ data on hornblende from amphibolites occurring at the top of the HHC in the Dinggyë area, 40 km E of the Kharta region (Hodges et al., 1994). On the other hand, no evidence was ever found in the Nepal Himalaya for a metamorphic event between the Tertiary Himalayan orogeny and the Early Paleozoic metamorphism and plutonism (Le Fort et al., 1986); consequently, the Kharta eclogites must be Precambrian if they are not Himalayan in age.

In order to get more precise constraints for the age of the Kharta eclogites, zircons were separated from one sample (EV02-45) and analysed by the U-Pb SHRIMP method. The zircons display complex systematics. Two analyses from low-U rim domains with low Th/U ratios (0.02-0.03) yield young $^{206}Pb/^{238}U$ ages of 13.9±0.9 and 13.4±0.8 Ma. Ages ranging from 88 to 110 Ma are interpreted to represent a Cretaceous protolith age of the mafic rock, while Proterozoic ages (1.8 Ga) are attributed to inherited components.

Even if the age of eclogitization apparently was not recorded by the zircons, from a regional viewpoint this seems to be the first indication ever in the Himalayan basement nappes for the widespread Cretaceous Rajmahal Trap basalt volcanism of NE India. Cretaceous basalt volcanism is already known in the Gondwana sequence overlying the Lesser Himalayan sequence of central Nepal (Aulis Volcanics: Sakai, 1983) and is also documented in the Tethyan sedimentary sequence of the Himalaya by volcaniclastic detritus in the Albian horizons of the Cretaceous Giumal Group (Garzanti, 1993).

A Cretaceous protolith age for the Kharta eclogites definitely rules out the possibility that the age of eclogitization is Early Paleozoic or Precambrian, and corroborates the hypothesis put forward by Lombardo & Rolfo (2000) that the Kharta eclogites are of Tertiary age. The metamorphic ages of 13-14 Ma could record the end of the post-granulite fluid circulation and thus be linked to the final stages of extrusion along the MCT.

GARZANTI E. 1993. *Geological Society Special Publ.*, **74**, 277-298.
HODGES K.V., HAMES W.E., OLSZEWSKI W., BURCHFIEL B.C., ROYDEN L.H. & CHEN Z. 1994. *Contribution to Mineralogy and Petrology*, **117**, 151-163.
LE FORT P., DEBON. F., PECHER A., SONET J. & VIDAL P. 1986. *Mem. Sci. de la Terre, Nancy*, **47**, 191-209.
LOMBARDO B. & ROLFO F. 2000. *Journal of Geodynamics*, **30**, 37-60.
SAKAI H. 1983. *Memoirs Faculty of Science Kyushu Univ.*, **25**, 27-74.

TETHYS: FROM THE MEDITERRANEAN TO TIBET. COMPARISONS OF OPHIOLITES FROM ARMENIA AND KOHISTAN-LADAKH, AND THEIR SIGNIFICANCE FOR THE RECONSTRUCTION OF TETHYS HISTORY.

Yann ROLLAND (1), Marc SOSSON (1), Michel CORSINI (1), Taniel DANELIAN (2), Ara AVAGAYAN (3), Gazhar GALOIAN (3), Raphael MELKONIAN (3) and Ruben JRBASHYAN (3).

(1) Université de Nice - Sophia Antipolis, UMR Géosciences Azur, 28 Av. de Valrose, BP 2135, 06103 Nice, France.
(2) Univ. Pierre & Marie Curie, Paris VI. 4, place Jussieu, 75252 Paris Cedex 05, France.
(3) Armenian National Academy of Sciences, Institute of Geological Sciences and Georisk, Baghramian Ave, 24a, 375019, Yerevan, Armenia

Himalayan Neo-Tethyan ophiolites are distinct from their Mediterranean equivalents. Though emplaced at the same period (Jurassic-Lower Cretaceous), they feature distinct geodynamic settings. The Mediterranean ones are produced at slow spreading centers and are amongst the Lherzolite Ophiolite Type (LOT); while the Himalayan ones are emplaced at fast spreading centers, Harzburgite Ophiolite Type (HOT). These two ophiolite types reflect that the Mediterranean Tethys has never been very large in comparison to its Himalayan equivalent. Subsequently, in the West, the amount of subducted ocean and the associated volume of arc magmatism were far smaller than in the East. The geodynamic implications of the amount of subduction on the very contrasted post-collisional evolutions of the Alps and Himalaya are probable and certainly underestimated. In this concern, Armenia is a key area where the transition between the two regimes can be analysed (Fig. 1).

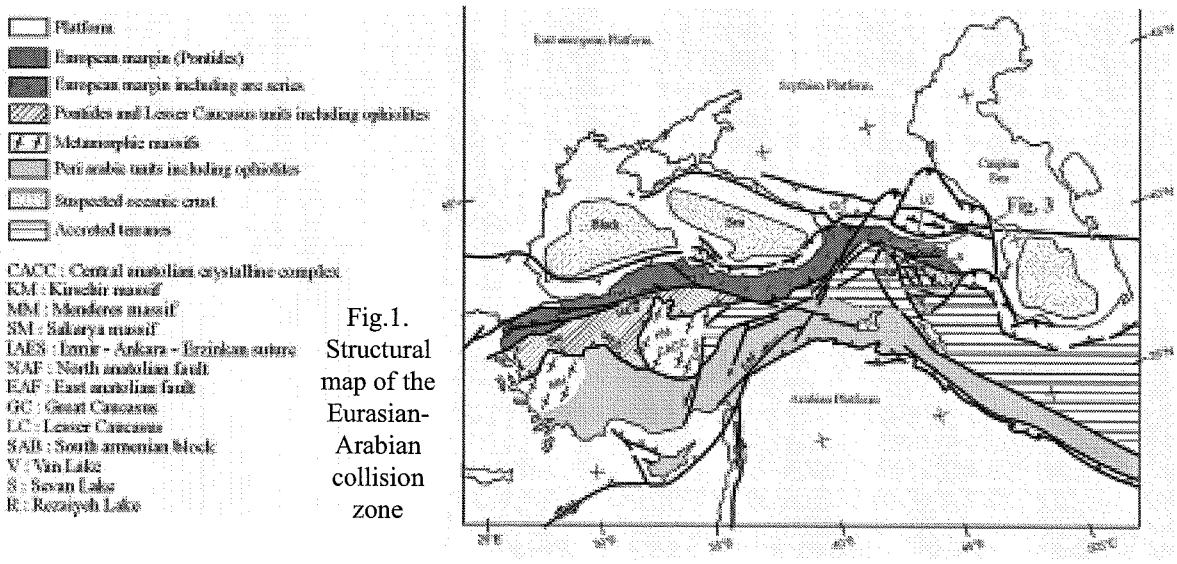

Fig.1. Structural map of the Eurasian-Arabian collision zone

LOT ophiolites are still present, but the amount of arc magmatism is comparable to Kohistan-Ladakh areas. The Ar-Ar age of subduction of the Stepanavan Blueschists in the North is very close (90-95 Ma) to that of blueschists from Kohistan-Ladakh. The very tightly dated Turonian Vedi obduction is within the range estimated for obduction of the Spontang ophiolite (Fig. 2). Timing of the collision to the Eurasian margin is also very similar to that estimated in the Kohistan-Ladakh arc. Finally, a preliminary proposition is made for lateral correlations between blocks and units. These will also help constrain the age and extent of lateral offset along post-collisional faults of the Western Himalayan-Lesser Caucasus region.

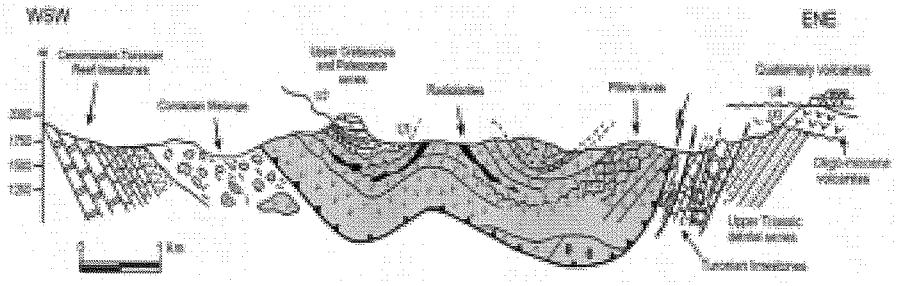

Fig. 2. Cross-section of the Vedi ophiolite obducted ophiolite sequence

THE CORRELATION OF THE FUSULINIDS (FORAMINIFERA) FOUND IN THE PERMIAN ROCKS OF SALT RANGE AND THE PERMIAN ROCKS OF KARAKORAM RANGE, PAKISTAN.

Ghazala ROOHI and S.R.H. BAQRI

Earth Sciences Division, Pakistan Museum of Natural History (Pakistan Science Foundation) Garden Avenue, Shakarparian, Islamabad 44000, Pakistan.

The fusulinds (Foraminifera) fossils found in the Amb Formation of Permian age and exposed in central and western Salt Range were studied in details to understand morphological variations and the environmental changes during the deposition of the Amb Formation in Katha area, central Salt Range. The representative samples of the sandy limestones to cross bedded calcareous sandstones were collected from Katha and fifty-two axial and tangential sections were prepared to study the fusulind fossils. The fossils were identified as *Monodiexodina kattaensis*. The fossils appear to represent the Late Artinskian to Early Murgabian age.

A comparative study between the lithostratigraphic units of the Katha beds of the Amb Formation exposed in Salt Range and fine grained calcareous hybrid arenites laterally grading into silt stones and calcarenites in the middle part of the Punjshah carbonates exposed in the Chapursan Valley of Karakoram Range, indicate some similar features. The common characters are the presence of calcareous sandstones to sandy limestones/dolomites/calcarenites, cross bedded sandstones, shaly carbonates, presence of fusulinds (abundant *Monodiexodina*), *Reichelina* etc. and high energy shallow marine conditions.

These studies indicate that the Tethys Sea during Permian times was full of different species of the fusulinds living in shallow water conditions, which survived and developed according to the local environments and available food materials. The influx of continental detritus during Late Artinskian to Early Murgabian times in Salt Range and Karakoram Range provide evidence of a general regression of Tethys Sea.

(References)
Gaetani M. et al. 1990. *Geo. Soc. Am. Bull.*, **102**. 54-62.
Reichel, M. 1938. *VISSER. Karakorum III.*, 89-118.
Sameeni S. J. & Mirza K. 1997. *Jour. Nepal Geol. Soc. (Sp. Issue).*, **16.** 56-58.

NEOTECTONIC FAULTING ALONG THE CENTRAL BANGONG-NUJIANG SUTURE ZONE, CENTRAL TIBET

Smriti SAFAYA, Jonathan AITCHISON and Jason ALI

Tibet Research Group, Dept. Earth Sciences, University of Hong Kong

The Karakoram-Jiali Fault Zone (KJFZ), along the E-W striking Bangong-Nujiang Suture Zone in central Tibet, and internal deformation of the plateau accommodates about 30% of the strain ensuing from the continuing India-Asia collision. The manifestation of the strain transferred between the fast dextral Karakoram (26mm/yr; to the west) and Jiali (32mm/yr; to the east) faults is vague due to limited neotectonic fault mapping and calculated slip rates in the region. This study involves the investigation of two faults in the northern vicinity of Dong Tso (32.40°N/84.65°E), within the central KJFZ: the dextral E-W striking North Dong Tso-Zhaxi Tso fault and the sinistral NE-SW striking Mi Ba Zang Mu fault. On ASTER, Corona and SRTM Radar DEM imagery, the fault zones exhibit apparent evidence for normal faulting, with cumulative scarps rising up to 23m and 45m, respectively. These high vertical offsets suggest multiple events, which usually vary between 0.5 – 1m. The relative gentle curvature (average scarp profile dips vary between 12° and 15°, maximum dips vary between 21° and 24°) of the 16 fault scarp profiles carried out along both faults suggests that little, if any, most recent activity has taken place. Sediment samples, taken from the hanging walls for optically stimulated luminescence dating, show preliminary sediment age of ~25,000 years. The subsequent minimum oblique slip rates for the North Dong Tso-Zhaxi Tso and Mi Ba Zang Mu faults are 1.7 mm/yr and 2.4 mm/yr, respectively. These minimum slip rates differ greatly when compared with previously calculated slip rates of ~10 mm/yr for faults in central Tibet. The results of this investigation present more refined data for the complex current internal deformation of central Tibet.

ARMIJO, R., TAPPONNIER, P., HAN, T.-L., 1989. Late Cenozoic right-lateral faulting in Southern Tibet, J. *Geophys. Res.* **94**, 2787 - 2838

BENDICK, R., BILHAM, R., FREYMUELLER, J., LARSON, K. AND YIN, G., Geodetic evidence or a low slip rate in the AltynTagh fault system, *Nature*, **404**, 69 – 72, 2000

FIELD ASPECTS OF THE GEMS AND GEM-BEARING PEGMATITES OF THE SHIGAR VALLEY, SKARDU, NORTHERN AREAS OF PAKISTAN

Mohammad Tahir SHAH and Hassan AGHEEM

National Centre of Excellence in Geology, University of Peshawar, Pakistan

Shigar valley is famous for the occurrence of various gemstones and for its spectacular Karakorum mountain chain and the highest peaks including K2 (8611m), the second highest peak in the world. The valley is characterized by the rocks of both the Karakorum plate and the Kohistan-Ladakh island arc with the intervening northern or Shyok Suture Zone. These rocks are mainly metasediments or metaigneous which are intruded by pegmatitic dikes. These belong to the Karakorum Metamorphic Complex and are considered as part of the Karakorum Axial Batholith. The gem-bearing pegmatite dikes and veins are exposed at different localities along the Shigar and Baraldu rivers in the study area. The dikes and veins vary both in length and in width and are generally zoned. The gemstones are present within the cavities or pockets in the wall or intermediate zones of these dikes and veins.

Beryl (aquamarine) and tourmaline (schorl) are the ubiquitous gemstones of pegmatites in Shigar valley but some gemstones (e.g., epidote, sphene, colorless to yellow apatite, green fluorite, quartz, diopside, goshenite, manganotantalite etc.) are confined to certain localities. This can be attributed to the involvement of various geochemical processes, involving the host rock chemistry, in the formation of gemstones in the pegmatites of the area. The contact metasomatism could be one of these processes. However, it is certain that the studied pegmatites were enriched in certain volatiles and elements such as beryllium, chlorine, fluorine and boron, which have facilitated the formation of aquamarine, topaz, tourmaline, fluorite etc.

These gem-bearing pegmatites are being mined by the local people for the above-mentioned gemstones and are generally exported either as polished or as a raw (rough) material. In this paper gems and gem-bearing pegmatites of the Shigar valley are described on the basis of field data.

CHARACTERISTICS OF ACTIVITY OF MAQU FAULT IN THE EAST SEGMENT OF KUNLUN FAULT

Wei SHI (1,2) Yinsheng MA (2) Yueqiao ZHANG (2) Chunshan ZHANG (2)
Huiping ZHANG (1)
(1) School of Earth Science and resource, China University of Geosciences, Beijing 100083 China
(2) Institute of Geomechanics, Chinese Academy of Geological Sciences, Beijing 100081 China

Maqu Fault as the east Segment of Kunlun Fault which is a very important NWW fault in the northeastern margin of Qinghai-Tibetan Plateau(Fig.1)(Van Der Woerd J. et al., 2002;Ren J.W., et al,1999; Seismological Bureau of Qinghai Province,1999; Avouac, J.P. et al.,1993; Peltzer, G. et al.,1988; Tapponnier, P. et al.,1977,1982), is a strongly active fault. Remote Sensing image interpretation show Maqu fault is mainly distributed in the Yellow River valley (Fig.1).

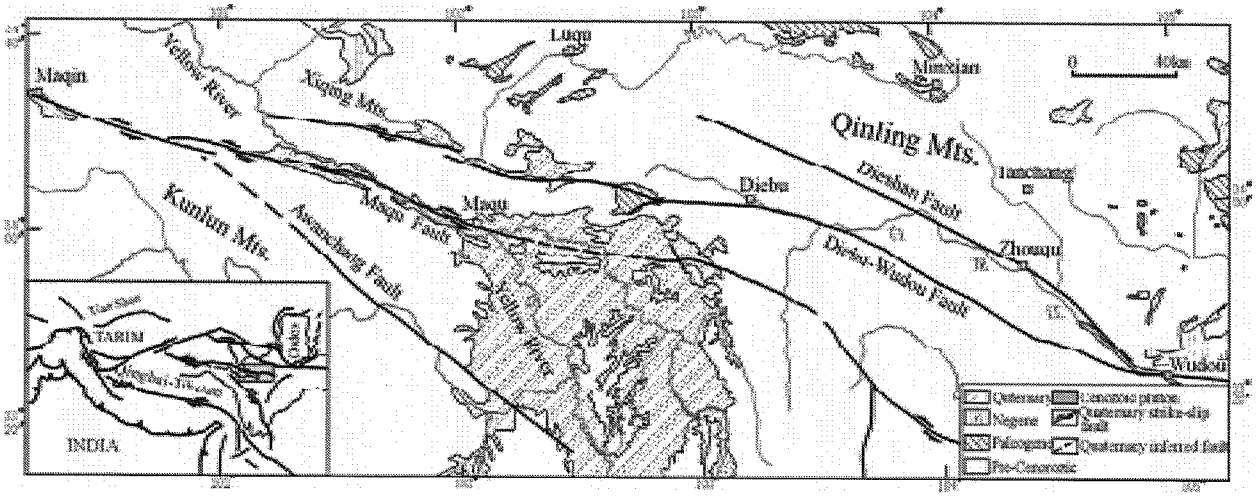

Fig.1 Distribution characteristics of Kunlun Mountain active fault and study area. Resulting from interpretation of 1/ 250000 Remote Sensing image.

Based on field observations and ETM image interpretation, we present in this paper Maqu fault is a left strike-slip and normal-slip fault since Quaternary. Combined with dating ages of Yellow River terrace,we present Maqu fault slip strikingly at the rate of about 10.15±0.34mm/a by the end of Late Pleistocene, at the same time, slip normally at the rate of about 0.25mm/a by the end of Late Pleistocene, and 0.01mm/a during the end of Early Pleistocene to end of Late Pleistocene.In addition,the Maqu fault still spreads eastward along the south margin of Qinling Orogen, and is subdivided into 4 active faults, including Awanchang fault,Maqu-Moxi fault, Diebu-Wudou fault and Dieshan fault from south to north, among which Maqu-Moxi fault and Diebu-Wudou fault are the main faults, which result in that the slip rate of the east Segment of Kunlun fault dwindle greatly.

Jerome Van Der Woerd, Paul Tapponnier, Frederick J. Ryerson *et al*.. . 2002,*Geoph. J.Int.*, 148. 356-388.
Avouac, J.P., and P. Tapponnier. 1993.*Geophys. Res. Lett.*, 20. 895-898.
Seismological Bureau of Qinghai Province, Institute of Crustal Deformation, China Seismological Bureau. Beijing: Seismological Press. 1999. 1-186.
Ren J.W.,Wang Y.P.,Wu Z.M. *et al. Research on Active Fault*(7), Beijing: Seismological Press.1999.147-163.
Tapponnier, P., and P. Molnar. *J. Geophys. Res.*,82(20). 2905-2930.
Tapponnier, P., G. Peltzer, A.Y. Le Dain *et al*.. 1982. *Geology*.,10. 611-616.
Peltzer, G., and P. Tapponnier. 1988.*J. Geophys. Res.*, 93. 15095-15117.

PRELIMINARIES PETROLOGICAL RESULTS ON THE UPLIFT OF THE LONGMEN SHAN MOUNTAIN RANGE (SICHUAN, CHINA)

Julia DE SIGOYER, Manuel PUBELLIER, Vincent GODARD, Wu XIAWEI

Laboratoire de Géologie, Ecole Normale Supérieure, 24 rue Lhomond, 75231 Paris cedex 05 (France)

Located in between the eastern border of the Tibetan plateau and the Yang Tse craton, the Longmen Shan range presents many similarities with the Himalayan belt, with summits approaching 7000m, and a topographic gradient of 4000m over 100 Km. The range is controlled by thrusts and wrench faults underlined by important seismicity. However, there is no evidence for strong Quaternary deformation, and GPS velocities across the range are moderate (<5mm.year-1), (Chen et al., 2000) compared to those of the Himalayas.

Understanding how such topography is sustained is a major interest in the comprehension of the dynamics of the lithosphere. To explain this Burchfiel (2004) has proposed that a low viscosity channel located within the lower crust accommodates shortening and that the high elevation topography is not recent. Another explanation is that uplift is Tertiary and that convergent rates have recently decreased across the belt. In this case, topography would not have reached a steady state. In order to resolve this problematic it is necessary to evaluate the contribution of each orogenic cycle in the building of the Longmen Shan range. The present formation of the range is polycyclic with an Indonesian orogeny (Triassic), a Yanshanian orogeny (Cretaceous) and an Himalayan orogeny (Cenozoic). Our work will be mainly focused on the Cenozoic to Quaternary deformation.

Preliminary results of the tectono-metamorphic studies carried out in the Longmen Shan range suggest an intense shortening across the belt, implying that deformation is controlled by one or more detachment levels. The belt is composed of crustal and sedimentary slices. Some faults around the Penguan crystalline massif may represent ancient (pre-Triassic) normal faults of the South Chinese passive margin.

Metamorphic rocks are always associated with these major contacts. The Longmen Shan is composed of large volumes of accreted sediments lacking metamorphic minerals suitable for conventional petrologic investigations. However, these units are rich in carbonaceous material, making it possible to determine thermal metamorphism through Raman spectroscopy of carbonaceous material. The graphitization of carbonaceous material is function of the temperature peak recorded by the metamorphic rocks, between 300-650°C (Beyssac et al., 2002).

Carbonaceous material sampled across the Longmen Shan belt is analyzed. First results reveal that the Longmen Shan has undergone a large-scale thermal metamorphism, with temperature decreasing from about 500°C close to the major contact to less than 330 °C far from the contact. The petrological study allows us to quantify the amount of vertical exhumation across the belt.

References

Beyssac, O., Goffé, B., Chopin, C. & Rouzaud, J.N. 2002, Raman spectra of carbonaceous material in metasediments: a new geothemometer, *J. metamorphic Geol.*, 20, 859-871.

Burchfiel, B.C. 2004, New technology; new geological challenges, *GSA Today*, 14, 4-10.

Chen, Z., Burchfiel, B.C., Liu, Y., King, R.W., Royden, L.H., Tang, W., Wang, E., Zhao, J. & Zhang, X. 2000 Global positioning system measurements from eastern Tibet and their implications for India/Eurasia intercontinental deformation, *Journal of Geophysical Research*, 105, 16.215-16.227.

GEOLOGY AND EVALUATION OF HYDROCARBON PROSPECTS OF TETHYAN SEDIMENTS IN SPITI VALLY, SPITI AND ZANSKAR, HIMACHAL PRADESH

Jagmohan SINGH*, S. MAHANTI & Kamla SINGH

Keshava Deva Malaviya Institute of Petroleum Exploration,
Oil and Natural Gas Corporation Limited, Dehra Dun-248001, INDIA
*Present address: RGL, WO, ONGC, Baroda-390007, (Gujrat), INDIA
E-Mail: jagmohansingh@hotmail.com

The Tethyan sediments in the Spiti Basin stretch from Pir Panjal in the south to the Zanskar Range in the north. The Tethyan sediments lie within the Higher Himalayan Physiographic Zone. Since such huge thicknesses of sediments are deposited in this area, it is anticipated by the geologists that favourable conditions might have prevailed for the generation and accumulation of hydrocarbon in the Tethyan sediments. It has been continuous endeavour of ONGC to explore and enhance hydrocarbon reserves from all Indian sedimentary basins including the category IV and frontier basins. Seismic data acquisition and geological modelling have been carried out for Lesser Himalayas and even parametric, structural, or wild cat wells have been drilled and one such well is under drilling at Sundernagar. The Tethyan part being inaccessible has not been subjected to detailed geological modelling.

Mesozoic sequences from Kibber?Gate?Tashegang and Lidang?Domal traverses have been subjected to sedimentological, Palaeontological, Palynological and source rock investigations to reconstruct microfacies, biochronostratigraphy, depositional environment, and organic matter maturation. The petrographic study of the Mesozoic Tethyan sediments exposed along the selected traverses shows occurrence of Kioto Limestone, Spiti Shale, Giumal Sandstone, Tashegang Limestone and Chikkim Limestone formations. The Kioto Limestone is highly sparitised and has poor porosity. The Giumal Sandstone consists of Glauconitic sands which are well indurated and have very poor intergranular porosity. The porosity is further reduced by calcite cementation. Similarly, the Tashegang Limestone is also highly sparitised and has poor porosity. Spiti shale is dark grey, black, carbonaceous, occasionally oxidised in nature.

Brachiopod fauna supportive of Lower Carboniferous age has been recorded from Lipak Formation and Ordovician - Silurian fauna from Takche Formation. Cephalopods supportive of Oxfordian - Callovian age have been recovered from Spiti Shale. Lilang Group has yielded rare Cephalopods of Triassic - Jurassic age. On the basis of FAD of Riguadella filamentosa and Egmontodinium torynum Late Bathonian to Late Tithonian age has been suggested to Spiti Formation. On the basis of FAD of E. cinctum and Batioladinium micropodum, Late Tithonian to Early Valanginian age has been suggested to Tashegang Formation. On the basis of FAD of B. micropodum the base of Giumal Formation is dated as Early Valanginian. The absolute pollen frequency (APF) value of the palynofloral assemblage from Spiti Formation suggests inner neritic to marginal marine environment of deposition, while palynoflora from Tashegang Formation indicate marginal marine to lagoonal environment and Giumal Formation was laid under marginal marine conditions. The Organic matter recorded from the studied samples shows Humic-Wood (H-W) to Humic-Sapropelic-Wood (HS-W) to Humic-Sapropelic-Charcoal (HS-C) facies.

The organic matter studies have indicated TAI value from 3 to 3.5 which is suggestive of thermally matured sediments. In general geochemical studies on all the samples have indicated poor hydrocarbon generation potential with very low TOC except for carbonaceous shales having indicated >1% TOC. S2 is very low in many organic rich samples probably due to weathering affects. So an entirely different picture can be anticipated in the subsurface. T max data is not reliable as S2 is low hence no maturity estimate could be made.

HIMALAYAN MIGMATITE AND ITS RELATION WITH COLLISION TECTONICS

Sandeep SINGH (1), A.K. JAIN (1), A.K.CHOUDHARY (2), Th. Nikunja Bihari SINGHA (1)

(1) Department of Earth Sciences, Indian Institute of Technology Roorkee, Roorkee-247 667, INDIA
(2) Institute Instrumentation Centre, Indian Institute of Technology Roorkee, Roorkee-247 667, INDIA

The Tertiary Leucogranite known as the Higher Himalayan Leucogranite (HHL) Belt occurs at the northern margin of the Himalayan Metamorphic Belt (HMB). It represents either: (i) crustal anatectic melting due to fluid migration during intracontinental thrusting along the Main Central Thrust (MCT), (ii) decompressional-controlled dehydration melting due to slip along the South Tibetan Detachement Zone (STDZ) along which the leucogranite plutons occur or (iii) vapour-absent muscovite dehydration melting of metamorphic rocks due to shear heating along a continous active decollement. Nevertheless, the leucogranite belt has been emplaced in a very short time span between 24 and 19 Ma from the western sector in Zanskar to Nepal and Bhutan.

In contrast to the Tertiary leucogranite, migmatite occurs within the middle to upper parts of the Higher Himalayan Metamorphic Belt (HHMB) also known as the Higher Himalayan Crystalline (HHC) along the Parbati, Sutlej and Baspa Valleys (all in Himalchal Pradesh), and the Bhagirathi, Alaknanda and Dhauliganga Valleys (all in Uttranchal). These migmatite occurrences are often related to local mesoscopic differentiation during anatexis. These bodies have also been attributed to the crustal dehydration melting reactions, which involves hydrous reactant giving rise to anhydrous melanosome and hydrous silicate melt as leucosome. The melting generally occurs/collects in low – pressure sites, synchronously with deformation.

The migmatites are stromatic – and diatexites – type (Parbati, Bhagirathi, Alakhnanda and Dhauliganga Valleys) with melt fraction ranging from 10% to more than 50% with clear production of *in situ* melt having tourmaline along with few garnets and relicts of kyanite, sillimanite. In melanosome, biotite has segregated and often intergrown with sillimanite, garnet and kyanite. Metatexite – type (Sutlej and Baspa Valley) migmatites show migmatization layer, which survived partial melting. The melt fraction ranges from 10% to 40% with production of *in situ* melt in higher reaches cross – cutting the main foliation. Various shear indicators, such as σ-shaped asymmetrical augen and S-C fabric in migmatite reveal consistent top-to-SW verging tectonic movements. The presence structures such as the extensional crenulation foliation, shear bands and foliation boudinage reveal superposed layer-parallel extension within the migmatites. The *in situ* melt are developed at places along these late stage extensional fabrics with discrete melt – enhanced deformation.

These migmatites are wider along Sutlej Valley with a vary narrow zone of *in situ* melt development, along Baspa Valley no *in situ* melt generation has been observed. Along Bhagirathi Valley the migmatites are exposed within about 50 m wide zone, however, the migmatite zone along Alakhnanda is narrower and along Dhauliganga it is wider but with less generation of *in situ* melt may be due to presence of calcsilicate band.

The samples normalised to C1 Chondrite plot of *in situ* melt and main Gangotri Leucogranite indicate higher fractionation pattern of the LREE with lower fractionation pattern in HREE with negative Eu anomaly in all the samples. These similar patterns indicate that both *insitu* melt and main body could have be generated from the same source. The $^{87}Sr/^{86}Sr$ ratios as calculated and measured from the ICP-MS geochemical data on Rb and Sr and present – day $^{87}Sr/^{86}Sr$ ratios indicate that these migmatites are related to Himalayan orogeny at around 46 Ma (SHRIMP U-Pb zircon rim age data) and not related to Pan-African orogeny (SHRIMP U-Pb zircon core age data). Because when calculated with Pan-African age the initial $^{87}Sr/^{86}Sr$ is around 0.65 which is much lower than BABI. Therefore, the age of migmatization was assigned to 46 Ma instead of Pan-African as indicated by the Swiss group from the Sutlej Valley and the zircon population from the same samples.

The field occurrences of these migmatites indicate that these all lie to the south of leucogranite plutons within the core of the HHC Belt marking the fastest exhumed middle- to lower-crust as indicated by fission-track ages. The migmatite extend over several kilometres within the core of the metamorphic complex, although the intensity of the migmatization remains generally small all along the Himalaya. It appears that the migmatite zone has acted as a source region with a dipping magma chamber and may represent fossilized geological processes which might still be active in the Great Himalayan Channel Flow with the present – day partial molten crust through dyke, a feeder dyke to the main body.

GLOBAL CLIMATE CHANGE – THE CONTRIBUTION OF HIGH ALTITUDE SOILS FROM THE HIMALAYA

Bla STRES (1), Ivan MAHNE (1), Teiji WATANABE (2) and Ines MANDI-MULEC (1)

(1) University of Ljubljana, Biotechnical Faculty, Ve_na pot 111, 1000 Ljubljana, Slovenia
(2) Hokkaido University, Graduate School of Environmental Earth Science, Sapporo 060-0810, Japan

Soil production of the greenhouse gases methane, carbon dioxide and nitrous oxide has received increasing attention over the past two decades, because these gases have significant adverse environmental effects (Conrad, 1996). Most of currently used models incorporate analyses of gas fluxes from temperate soils of northern hemisphere. These soils are mainly characterized by higher carbon content (2-40%), positive mean annual temperature and precipitations in form of rain. On the other hand, the mountain chains of Tian Shan, Hindukush, Karakorum and Himalaya contain soils with lower carbon content (< 2%), experience low temperatures and frequent freeze-thaw cycles. Despite harsher conditions, microorganisms were shown to be active and proliferate in such environments (Ley et al., 2004). In order to characterize the potential of these soils to emit carbon dioxide and nitrous oxide, representative soil samples were taken in 200 m height increments from 5000 m glacier up a south-facing slope of a 6000 m peak in Nepal, Kanchenjunga region, representing a successional gradient. Portions of soil samples were characterized for water-holding capacity, soil moisture, carbon and nitrogen content, chemical identity of carbonaceous functional groups by Fourier transformed infrared spectroscopy and particle analysis. The ambiental and soil temperatures were monitored nearby at 6012m and 5433 m (four different depths), respectively. Measurements of microbial basal respiration and biomass were performed by the use of substrate induced respiration technique with glucose amendment at actual water content and in slurry with glucose at two different temperatures, 4°C and 22°C (Anderson and Domsch, 1989). The emissions of nitrous oxide were determined in separate experiments. All gas analyses were performed on gas chromatograph equipped with thermal conductivity detector for carbon dioxide and electron capture detector for nitrous oxide. The analysis of chemical identity of carbonaceous functional groups and particle analysis showed that major components were similar among the vegetated and non-vegetated soil samples. The similarity of particle sizes in windblown patches of soil (6000 m) and alpine meadow soils (5200 m) pointed to eolian deposition as a source of fine inorganic and organic particles. The resources driving microbial processes especially nitrate and various carbonaceous compounds were shown to precipitate in the Himalaya during monsoon seasons and/or by local valley wind system, respectively (Marinoni et al., 2001; Caricco et al., 2003). All soil samples analyzed contained measurable microbial biomass that was active at all conditions measured. The lowest emissions of nitrous oxide and carbon dioxide were observed in recently uncovered glacial till, whereas the highest were found in alpine meadow at 5200 m and unexpectedly, in windblown soil particles from 6000 m. These results clearly show that soils in Himalayan environments just below permanent snow cover are capable of emitting significant amounts of greenhouse gasses that contribute to global warming and should therefore be included in current models. In the future, *in-situ* measurements of gas emissions should be performed to enable estimation of seasonal dynamics. The conservative estimation of greenhouse gas emitting soils in the Himalaya could also be obtained through computer aided high-resolution satellite image analysis to further refine the models.

References:

Anderson TH, Domsch KH (1989) Ratios of microbial biomass carbon and total organic carbon in arable soils. *Soil Biol. Biochem.* 21:471-479

Carrico C.M.; Bergin M.H.; Shrestha A.B.; Dibb J.E.; Gomes L.; Harris J.M. 2003. The importance of carbon and mineral dust to seasonal aerosol properties in the Nepal Himalaya. *Athmosph. Environ.* 37:2811-2824.

FATE OF THE LITHOSPHERIC MANTLE BENEATH TIBET : HIDDEN PLATE TECTONICS ?

Paul TAPPONNIER *, Anne REPLUMAZ °, R. D. VAN DER HILST #, Gérard WITTLINGER §, Jérome VERGNE +

* Institut de Physique du Globe, 4 Place Jussieu, 75252 Paris Cedex 05, France
° Université Claude Bernard, Lyon 1, France
Massachussets Institue of Technology, MA, USA
§ Institut de Physique du Globe de Strasbourg, France
+ Laboratoire de Géophysique Interne et de Tectonophysique, Grenoble, France

Relating crustal deformation to processes deeper in the mantle is a key to understand the evolution of the India/Asia collision zone. A comparison of geological reconstructions of block motions within Asia since ≈ 50 Ma ago with the tomographically imaged morphology of subducted Indian lithosphere yields insight into this evolution. Past positions of the convergent Asian margin correlate with high P-wave velocity anomalies at specific depths. The change in slab geometry, from a linear structure beneath 1100 km to an increasingly contorted shape at depths of less than 700 km, mirrors that of the collision zone. The slab contours match the progressive deformation of Asia's margin, including India's indentation and Sundaland's extrusion. Ever since the onset of collision, the Indian plate appears to have overridden its own sinking mantle. That such sinking mantle does not underthrust Tibet much north of the Zangbo suture argues against models of plateau build-up involving Indian lithosphere. Upper mantle velocity contrasts observed across the Bangong suture are thus likely of Asian rather than Indian origin. The tomograms below India confirm that Asian deformation has absorbed at least ≈ 1500 km of convergence since collision began. Beneath NW-Tibet, teleseismic tomography implies that the Tarim lithospheric mantle plunges 45°southwards, down to ~300 km. The Neogene tectonics of the W-Kunlun are thus simply accounted for by oblique subduction of continental mantle and upwards extrusion of a thrust-wedge of Tarim crust. The thickening crust in Asia appears to hide motions of lithospheric mantle blocks that are similar to those seen at oblique convergent margins. The upper crust appears to have thickened while the mantle, decoupled underneath gently-dipping decollements in the weak lower crust, did not. Even in the heart of the collision zone, the continental lithospheric mantle retained enough strength to behave " plate-like ", with deep deformation localizing along inherited weak zones such as ancient sutures. The great strike slip faults of Tibet result from slip partitioning, extrusion being coupled with oblique subduction of mantle slabs down to a few hundred km. In short, processes operating beneath the largest plateau on Earth may be little more than " hidden Plate Tectonics ".

ENVIRONMENTAL GEOCHEMISTRY OF THE SOILS OF PESHAWAR BASIN, LESSER HIMALAYAS, PAKISTAN

Shahina TARIQ (1), Syed HAMIDULLAH (2) and Mohammad Tahir SHAH (2)

(1) Institute of Earth & Environmental Sciences, Bahria University, Islamabad, Pakistan
(2) National Centre of Excellence in Geology, University of Peshawar

Peshawar basin is a huge basin (>5500Km^2) in the southwestern part of the Himalayan Crystalline Nappe and Thrust Belt of the lesser Himalayas in Pakistan. It has quaternary fanglomerates along the margins of the basin while the central part of the basin is generally covered with fluvial micaceous sand, gravels and lacustrine deposits. The soils of the basin have been divided in to Khyber piedmont soil, Peshawar floodplain soil, Peshawar lacustrine soil and Attock-Cherat piedmont soil. Representative samples from these soils of the basin have been evaluated for major, trace and heavy metals in order to (a) identify the sources of contamination in the soils of the basin, which affect and control the chemical composition of water in various aquifers of the basin and (b) to identify the character of these soils for the growth of the plants and environmental problems related to plants and human health in the area.

The chemical analyses of these soils show that major oxides concentration SiO_2, Al_2O_3, Fe_2O_3 stand normal in these soils. MgO, CaO, Na_2O, K_2O and P_2O_5 and the heavy metals such as Cu, Ni and Cr are, however, higher than the limits given for normal soils reported by the United States Department of Agriculture. The high concentrations of CaO, NaO, K_2O in these soils can be attributed to the water logging and salinity in the area while high Cu, Ni and Cr can be correlated with the ultramafic to mafic rocks of the Dargai area exposed along the north-western portion of the Peshawar basin. The high concentration of P_2O_5 could be either contributed by the carbonatites of the Selai Patai area or could be due to the overuse of phosphate-bearing fertilizers in the agricultural practices. The presence of high concentration of heavy metals in the soils at various places in the basin may cause hydro and biochemical contaminations which can cause serious environmental and health problems in the living organism of the area.

LATE QUATERNARY LANDSCAPE EVOLUTION IN FAULT-BEND FOLD SYSTEM, PINJOR DUN, PANJAB SUBHIMALAYA, INDIA

V.C. THAKUR, N. SURESH AND G. PERUMAL

Wadia Institute of Himalayan Geology Dehra Dun-248001, India

The Pinjor Dun, an intermontane flat-floored valley, is located between Pinjor and Nalagarh-Kiratpur area in SubHimalaya of Panjab and Himachal states in NW Himalaya. The NW-SE trending Pinjor Dun extends 50 km in length and average 5 km in width. It is bounded to south by the Frontal Siwlik range comprising of sandstone; mudstone and clays of middle and upper Siwaliks, and to north it is bordered by purple siltstone, clay and sandstone of Dharamsala Formation of lower Tertiary along the Nalagarh Thrust (NT). The Dun is filled by post-Siwalik alluvial fan deposits, referred to Pinjor Dun formation. The long axes of the fans, 8-10 km, trend NE-SW across the regional strike of Dun. The proximal part of fans is gently sloping to south, covering the most part of Dun. Two levels of fan surfaces recognized are the Primary fan surface and the Principal fan surface. The Principal fan surface in its proximal part is made predominantly of gravels with subordinate mudstone, whereas its distal part is comprised of mudstone-sandstone with intercalations of gravel beds. The Quartz OSL (optically simulated) dating assign ages of 84 + 16 Ka to the bottom part, 41 + 5.4 Ka to the middle part and 24.5 + 4.5 Ka to the top part of the Pinjor Dun formation. The Primary fan surface represents the alluvial fans deposited over the eroded Siwaliks lying immediately south of Nalagarh Thrust (NF). The Primary fans, lying at a higher level than the Principal fans, were uplifted and tilted NE as a result of displacement on an imbricate fault of the NT.

The major topographic structural features, south to north, in Pinjor Dun area are Piedmont zone, Himalayan Frontal Thrust (HFT), the Frontal Siwalik antiform, Dun synform and Nalagarh Thrust. The HFT, trending NW-SE, is marked by a sharp topographic break between the southern margin of Frontal Siwalik range and the Piedmont zone of Panjab alluvial plain. South of HFT, 10-15 km wide Piedmont zone is characterized by undulating badland topography. The hinterland primary streams originating from southern slope of Frontal Siwalik range show incision of 1-3 m and flowing NE-SW take knee-bend turn to NW joining river Satluj. The secondary streams originating within the Piedmont zone and showing gully erosion are characteristic features of the Piedmont zone. The characteristic topographic and drainage features of the Piedmont zone, distinct from the Panjab alluvial plain to south, indicative of fold growth and uplift resulted due to displacement on the Piedmont fault, a step out thrust from the HFT. In the Frontal Siwalik range, the Siwalik strata are folded into a broad, open and asymmetric antiform whose northern and southern limbs dip NE and SW respectively at low angles (15°-6°-28°). The geometry and growth of antiformal structure controls the morphology of landform and drainage pattern. The Frontal Siwalik antiform is interpreted as representing an early stage fault-bend fold of the hangingwall Siwaliks over the flat decollement of the footwall. The intermontane valley of Pinjor Dun, a down-wrapped structutre, is occupied by the synformal depression on the hanging wall, and it is filled by alluvial fans predominantly having provenance from north. The OSL dating of Pinjor Dun formation indicates the Dun was formed during late Quaternary (100-200 Ka). The uplift of Frontal Siwalik range is related to growth of antiformal structure generated due to displacement over the HFT, initiating during ~100 Ka. In Pinjor Dun the SW flowing rivers, originating from hinterland lower Tertiaries, join NW flowing trunk river Sirsa at steep angles. This drainage pattern was evolved in a NW-propagating antiform of the Frontal Siwalik range. South of HFT, undulating topography and uplift of Piedmont zone, post dating 5 Ka, resulted due to southward propagating step-out thrust. The landform and drainage pattern in Piedmont zone represents a modern analogue in early stage evolution of the Dun.

FROM TECTONICALLY 'TO EROSIONALLY' CONTROLLED DEVELOPMENT OF THE HIMALAYAN FOLD-AND-TRUST BELT

Rasmus C. THIEDE(1), Rámon ARROWSMITH (2), Bodo BOOKHAGEN (1,3), Michael O. MCWILLIAMS (4), Edward R. SOBEL (1) and Manfred R. STRECKER (1)

(1) Institut fuer Geowissenschaften, Universitaet Potsdam, Potsdam, Germany (thiede@geo.uni-potsdam.de)
(2) Department of Geological Sciences, Arizona State University, Tempe, Arizona, USA.
(3) now in Department of Geological Sciences, University of California, Santa Barbara, California, US
(4) Geological & Environmental Sciences, Stanford University, Stanford, California, USA

The role of coupling between erosion and tectonics during the development of the Himalayan orogen remains controversial. Whether variations in the spatial distribution of erosion can influence the location, style and magnitude of deformation within an orogen is a matter of debate. We report new $^{40}Ar/^{39}Ar$ white mica and apatite fission track (AFT) ages which constrain exhumation paths along an approximately 120-km-wide NE-SW transect spanning the greater Sutlej region of the northwest-Himalaya, India. The $^{40}Ar/^{39}Ar$ data indicates that the High Himalayan Crystalline units were exhumed in early to middle Miocene. Subsequently, southward propagating Lesser Himalayan Crystalline nappes were rapidly exhumed during late Miocene to Pliocene time. The AFT data, in contrast, imply synchronous exhumation of an elliptically shaped, NE-SW-oriented ~80 x 40 km region spanning both crystalline nappes during the Pliocene to Quaternary time. The locus of pronounced exhumation defined by the AFT data correlates with a region of high precipitation, discharge, and sediment flux rates during the Holocene. This correlation suggests that, while tectonic processes exerted the dominant control on the pattern of denudation before and until the middle Miocene, surface processes have been the most important factor controlling both pattern of denudation and deformation since the Pliocene time.

MID MIOCENE TO RECENT E-W EXTENSION IN THE TETHYAN HIMALAYA, LEO PARGIL DOME, NW-INDIA

Rasmus C. THIEDE(1), Rámon ARROWSMITH (2), Bodo BOOKHAGEN (1,3), Michael O. MCWILLIAMS (4), Edward R. SOBEL (1) and Manfred R. STRECKER (1)

(1) Institut fuer Geowissenschaften, Universitaet Potsdam, Potsdam, Germany (thiede@geo.uni-potsdam.de)
(2) Department of Geological Sciences, Arizona State University, Tempe, Arizona, USA.
(3) now in Department of Geological Sciences, University of California, Santa Barbara, California, US
(4) Geological & Environmental Sciences, Stanford University, Stanford, California, USA

Despite an overall convergent tectonic setting, synorogenic extensional processes play an important role in the extrusion of major gneiss domes during the evolution of orogenic belts. Since the Indian-Eurasian collision ~50 Ma ago several metamorphic-igneous gneiss dome complexes continuously developed in the collision zone, though the origin of these processes is remaining controversial.

In NW-India the Leo Pargil metamorphic-igneous gneiss dome (31-34° N/77-78° E) is located in the Tethyan Himalaya. Here we present new field mapping, structural, and geochronologic data document that the western flank of the Leo Pargil dome was formed by extensional deformation along linked normal faults system. Along a Leo Pargil detachment zone (LPDZ) this has led to the juxtaposition of low-grade metamorphic, sedimentary rocks in the hangingwall and high-grade metamorphic gneisses in the footwall. However, the distributions of new $^{40}Ar/^{39}Ar$ data are less dependant by local structures but rather indicate a regional cooling during the mid Miocene. New apatite fission track (AFT) data demonstrate that much of the footwall was extruded along the LPDZ in a brittle stage between 10 and 2 Ma with a minimum displacement of ~9 km. Additionally, since ~4 Ma AFT-data indicate a regional accelerated cooling and exhumation episode

DEFORMATION ALONG THE KARAKORUM FAULT, WESTERN TIBET: AR-AR, FISSION TRACKS, AND U-TH-HE GEOCHRONOLOGICAL CONSTRAINTS

Franck VALLI (1), Nicolas ARNAUD (2), Haibing LI (1-3), Robin LACASSIN (1), Edward SOBEL (4), Gweltaz MAHÉO (5), Paul TAPPONNIER (1), Philippe Hervé LELOUP (6), Stéphane GUILLOT (6), Zhiqin XU (3)

(1) UMR 7578, CNRS Institut de Physique du Globe de Paris, (2) UMR 5573, CNRS LDL-ISTEEM – Montpellier, (3) Ministry of Land Res.- Beijing China, (4) Univ. Potsdam, Institut für Geowissenschaften Postfach 60 15 53 14415 Potsdam, (5) California Institute of Technology, 1200 E Colorado Bvd, Pasadena, ca 91125 United States, (6) UMR 5570, CNRS UCLB Lyon1 - ENS Lyon. valli@ipgp.jussieu.fr/Fax:(0033) 144272440

The geodynamic importance of the Karakorum fault zone (KFZ) is debated. Published estimates about the slip-rate and the onset of deformation, range between 1 - 30 mm/yr and < 13 - 50 Ma, respectively. Together with U-Pb and Th-Pb results (Valli et al. this workshop), new structural and thermochronological data help better resolve these issues.

South of 33°N, oblique faulting along SW edge of Gar pull-apart basin, exhume the metamorphic and magmatic rocks of the Ayilari range. Most minerals have recorded a continuum of deformation from temperature higher than 500 °C down to very low-grade conditions (<250°C). The temperature conditions for the onset of dextral shearing of K-feldspars and micas were thus higher than their Argon closure temperatures. The 40Ar/39Ar ages, the oldest being 20.8 ± 0.2 Ma, yield minimum estimates for the initiation the KFZ. These ages corroborate U-Pb and Th-Pb dating results on syn-kinematic granitoids and hydrothermal zircons and monazites, which indicate that high–grade strike-slip shear (>500°C) occurred since at least 23-25 Ma. The exceptional flatness of micas 40Ar/39Ar plateaus is uncommon in gneisses or granitoids, since it is usually associated to very rapid cooling or quenching. This, together with the very narrow age difference between muscovites and biotites strongly suggest the onset of a rapid cooling period at ~14-16 Ma in the northernmost section (Lat ~32°30'N), and at ~12-13 Ma in other sections (Lat ~32°-32°25'N).

This rapid cooling is further constrained by Fission track and U-Th-He on apatites, which, together with the 40Ar/39Ar ages, suggest fast cooling rates of 27-67°C/Ma in the north and 30-47°C/Ma in the south. The High Temperature part of the K-feldspar plateaus spread in age from ~12 to 21 Ma and thus indicate that, before ~12 Ma, the cooling rate was less than 13°C/Ma. Microstructures and shear criteria in mylonites formed in the greenschist facies partially overprint the high-grade deformation (>500°C). They mark a clear kinematic change from purely dextral to dextral normal motion. The inception of a normal component of slip most likely produced the increase of the cooling rate at ~14-16 Ma (N section), and at ~12-13 Ma (other sections). It is this oblique motion, still ongoing today, that exhumed the Ayilari metamorphic rocks. It also resulted in the development and deepening of the Gar and Baer pull-apart basins, concurrently with the rise of adjacent ranges and the correlative incision and entrenchment of major river courses, most notably of the Indus. Therefore, our thermochronological data near Zhaxigang suggest that the Indus river might have become captive of the surrounding relief only after the onset of rapid uplift south of the fault at 12-16 Ma. At that time, the Indus River would have started to incise deeply across the newly formed Ayilari-Ladakh Range. The 120 km offset of the Indus River course thus represents only part of the total finite motion along the KFZ. This implies dextral motion at a minimum long-term average rate of 8.5 ± 1.5 mm/yr, compatible with the long-term rate deduced from U-Pb, Th-Pb ages, and the upper Quaternary rate deduced from cosmogenic dating (Chevalier et al., this workshop). Reconstruction and balancing of the Gar-Baer pull-apart basins in map view suggests that pure strike-slip fault strands cross the Gar-Baer pull-aparts and/or that the blocks surrounding the KFZ deform internally.

HIGH TEMPERATURE DEFORMATION ALONG THE KARAKORUM FAULT, WESTERN TIBET: U-TH-PB GEOCHRONOLOGICAL CONSTRAINTS

Franck VALLI (1), Jean Louis PAQUETTE (2), Haibing LI (1-3), Philippe Hervé LELOUP (4), Nicolas ARNAUD (5), Stéphane GUILLOT (4), Robin LACASSIN (1), Paul TAPPONNIER (1), Dunyi LIU (3), Zhiqin XU (3), Etienne DELOULE (6), Gweltaz MAHÉO (4).

(1) UMR 7578, CNRS Institut de Physique du Globe de Paris,
(2) Univ. Blaise Pascal de Clermont-Ferrand, (
3) Ministry of Land Res.- Beijing China,
(4) UMR 5570, CNRS UCLB Lyon1 - ENS Lyon,
(5) UMR 5573, CNRS LDL-ISTEEM - Montpellier, (6)
CNRS CRPG - Nancy.
valli@ipgp.jussieu.fr/Fax:(0033) 144272440

South of 33°N, along SW edge of Tashikang-Gar basin, active right-lateral normal fault strands, belonging to the Karakorum fault zone (KFZ), exhume metamorphic and magmatic rocks that form the Ayilari range, southeastern prong of the Ladakh range. Samples with evidence of ductile right-lateral shear systematically record ages around 23-25 Ma, corresponding to the neocrystallization, or resetting, of zircon and/or monazite. Three independent sets of observations demonstrate the syn-deformational character of this major event.

(1) Several generations of dykes, with crosscutting relationships, exist on the same outcrops. The oldest dykes are transposed into the strike-slip foliation and strongly sheared, while later generations are oblique and less deformed. These variously deformed veins, connected to a larger leucogranite intrusion (sample C32) indicate that melting and crystallization occurred during deformation. A concordant fraction of needle-like zircon grains yield the crystallization age of this syn-kinematic leucogranite at ~23 Ma.

(2) Petro-structural observations indicate continuous deformation from temperatures close to the rock solidus down to very low-grade conditions and suggest syn-kynematic crystallization of deformed migmatite (L89) and orthogneisses (P18, P20). Chemistry and inner structures of zircon grains are typically magmatic and insure that the $^{206}Pb/^{238}U$ mean ages ranging between 23.5 ± 1.8 Ma and 21.7 ± 3.0 Ma date the syn-kinematic crystallization of the rocks. Monazites armored into the major mineral phases of sample P18 give an independent $^{232}Th/^{208}Pb$ age estimate of the syn-kinematic crystallization of the orthogneiss at ~25.4 ± 3.8 Ma.

(3) Chemical data imply the crystallization of metamorphic and/or hydrothermal zircons (samples C32, C43, P18, P34, L89), revealing heat and fluid advection as typically recognized along (recent) strike-slip faults (San Andreas or Red River for examples), and along the KFZ itself, where hot spring (T>100°C) surge at places (Nubra Valley and Kailas area). These imply deformation and coeval fluid circulation along the KFZ during at least the 13-25 Ma period. Monazites located in the matrix systematically record this event (samples P18, L89, C32, C43). They most likely provide evidence of dissolution-recrystallization of monazite crystals below their closure temperature during fluid activity as already documented by laboratory experiments.

Thus, zircon and monazite grains record motion on the KFZ since at least 25 Ma to at least ~13 Ma. Interestingly, Ar/Ar dating, together with fission tracks and U-Th-Pb on apatites, reveal rapid cooling in the Ayilari Range at ~16-12 Ma, interpreted as the initiation of the right-lateral normal faults which bound the Gar pull apart basin (Valli et al., this HKT workshop). Owing to this rapid cooling event, the temperature conditions became too low to allow even hydrothermal zircon or monazite.

Several measurements made on different samples (C32, P18, L89), with different techniques (SIMS and ID-TIMS), show the existence of a ~ 34 Ma magmatic episode on the northeastern border of the Ayilari range. This magmatic event is difficult to relate to deformation as the ~25-23 Ma magmatism overprinted most previous structures. Regional field observations help constrain the mechanism(s) triggering such magmatism, and its possible relationship with deformation along the KFZ.

RATES OF CRUSTAL UPLIFT AND SHORTENING ALONG THE NORTHERN MARGIN OF TIBET BASED ON PLEISTOCENE-HOLOCENE COSMOGENIC DATING OF FOLDED ALLUVIAL FANS AND TERRACES

Jérôme VAN DER WOERD (1), Frederick J. RYERSON (2), Paul TAPPONNIER (3), Anne-Sophie MERIAUX (2), XU Xiwei (4), B. MEYER (5), and Robert C. FINKEL (2)

(1) Institut de Physique du Globe de Strasbourg, Ecole et Observatoire de Strasbourg, CNRS/ULP-UMR7516, Strasbourg, France (e-mail: jeromev@eost.u-strasbg.fr).
(2) Institute of Geophysics and Planetary Physics, Lawrence Livermore National Laboratory, Livermore, California, USA.
(3) Laboratoire de Tectonique, Mécanique de la Lithosphère, Institut de Physique du Globe de Paris, Paris, France.
(4) Institute of Geology, China Earthquake Administration, Beijing, China.
(5) Laboratoire de Tectonique, Université Paris VI - Pierre et Marie Curie, Paris, France.

North of the Eastern Kunlun shortening occurs across many large thrust faults. This process is particularly spectacular in the Plio-Quaternary piedmont of the Tanghenan Shan. Thrust faults along the front and in the foreland of this hundred kilometers long NW-SE trending range cut and offset most recent alluvial fans. The historical seismicity of that desertic region does not reflect its degree of tectonic activity. Fieldwork has led to the discovery of seismic breaks, some of them continuous over tens of kilometers.

The rising foothills force the rivers to abandon and incise uplifted and folded strath terraces. Precise topographic leveling in the field and on topographic maps permits identification of different terrace surfaces that we can correlate along and between the ranges. In the foothills of the Tanghenan Shan several terraces are folded and uplifted several meters to tens of meters above the present day active streams. Cosmogenic Be^{10} and C^{14} dating of quartz pebbles and charcoal, respectively, helps constrain the rates of uplift and the timing of depositional processes. The Be^{10} ages of theses terraces range from 2-3 kyrs to 250 kyrs.

Because cosmic-ray exposure ages may be biased towards younger or older ages, mostly due to erosion or pre-exposure, respectively, we performed several tests to quantify these effects in the geomorphic setting of our study. For example, at one site, in order to estimate the amount of cosmogenic nuclide accumulation before deposition we sampled shielded samples from about 10 m below the surface of a terrace from which the surface samples yield and average of 68 kyr. The low nuclide content ($<2.10^5$at/g of quartz of ^{10}Be) of the shielded samples indicates negligible pre-exposure during transport in the small catchment upstream. At another site, we measured the nuclide content of rock ships of different sizes and of rounded pebbles from the surface to estimate the effect of erosion. Consistent results from the different samples indicate that the diffusion and smoothing processes of terraces and fans are fast relative to the lifetime of these surfaces.

By taking the surface ages as the time of abandonment of the fans by the active stream, it is possible to calculate minimum uplift rates of 0.2 to 0.5 mm/yr along each of the two main thrusts that reach the surface along the Tanghenan Shan piedmont. The map geometry of these shallow thrusts and geological cross sections in the piedmont indicate that the thrusts root on a main crustal ramp under the 5500 m high range. They thus appear to form folds of crustal size growing at rates of several mm/yrs. Balanced sections and the topography permit to estimate total vertical offsets, hence amounts of shortening and growth times for the range. Comparing the shortening rate of the Tanghenan Shan to the other similar ranges of the Qilian Shan, allows to precise the kinematics of northern Tibet consistent with cm/yr slip transfer between the eastern Altyn Tagh Fault to the northwest and the Haiyuan Fault to the southeast.

LATE MIOCENE – RECENT DENUDATION OF THE HIMALAYAS AND RECYCLING IN THE FORELAND BASIN FROM DETRITAL APATITE FISSION-TRACK ANALYSES OF SIWALIK SEDIMENTS, NEPAL

Peter VAN DER BEEK, Jean-Louis MUGNIER, Pascale HUYGHE,
Erika LABRIN and Matthias BERNET

Laboratoire de Géodynamique des Chaînes Alpines, Université Joseph Fourier, Grenoble, France

Foreland basin sediments contain a record of denudation rates in the source area that may be recovered by thermochronological studies of detrital apatite, zircon and mica. Here, we report new detrital apatite fission-track (AFT) data from Miocene to Pliocene Siwalik Group sediments in central and western Nepal, which were collected in conjunction with detrital zircon fission-track data presented by Bernet et al. (this issue). 30 detrital samples were analysed from modern river sediments as well as from magneto-stratigraphically dated sections along the Karnali, Surai and Tinau rivers. All samples were dated using the external detector method, with ~30-60 individual grains dated per sample. Binomial peak fitting was employed to decompose the observed single-grain age distributions into major age components or peaks (Brandon 1996).

Whereas the high temperature zircon fission-track or mica Ar-Ar systems are best suited to monitor long-term variations in exhumation rate of the source area, the lower temperature AFT system allows testing for shorter-term variations in exhumation rates. Because of the relatively low closure temperature (110±10°C; e.g. Brandon et al., 1998), AFT thermochronology is also sensitive to the thermal evolution of the foreland basin itself. Typically, stratigraphically higher samples that have not been buried deep enough for partial annealing to occur will retain a source signal whereas deeper samples will record the burial and exhumation history within the basin (e.g., Rohrman et al., 1996).

Within the three stratigraphic sections studied, the samples from the Surai section (800 – 2400 m stratigraphic depth) are unannealed and preserve a source signal, whereas those from the Tinau section (2800 – 4000 m depth) are all partially annealed. The most complete sample recovery was attained in the Karnali section (Figure 1), where both unannealed to annealed samples were observed. The transition (i.e., the top of the pre-exhumation Partial Annealing Zone) occurs at ~2500 m, indicating a pre-exhumational geothermal gradient of 15-20°C within the basin, in accord with vitrinite reflectance data and heat flow measurements in Ganges basin wells. The annealed AFT samples from the lower part of the Karnali section have a consistent minimum age (i.e., youngest age population) peak of 2 Ma and therefore permit dating the exhumation of this part of the Siwaliks along the Main Frontal Thrust at this time. Above this level, the minimum AFT age has a constant lag time of ~2 My since ~7.5 Ma, indicative of maximum source region exhumation rates of ~1.5 km/My (Brandon et al., 1998), similar to the longer-term rates measured by Bernet et al. (this issue). The unannealed Surai samples are consistently younger than, and therefore inconsistent with, the magnetostratigraphic ages reported for this section by Appel et al. (1991; as recalculated by Gautam and Rösler, 1999). When using the unpublished magnetostratigraphic data of T.P. Ojha (pers. commun.), these data indicate lag times of ~1 My. These lag times are similar to those found in modern river sands from the Marsyandi and Trisuli rivers, as well as to *in-situ* AFT ages from the Marsyandi catchment (e.g., Burbank et al., 2003). They indicate higher source exhumation rates (~2.5 km/My) for this central Nepal section as compared to the western Karnali section.

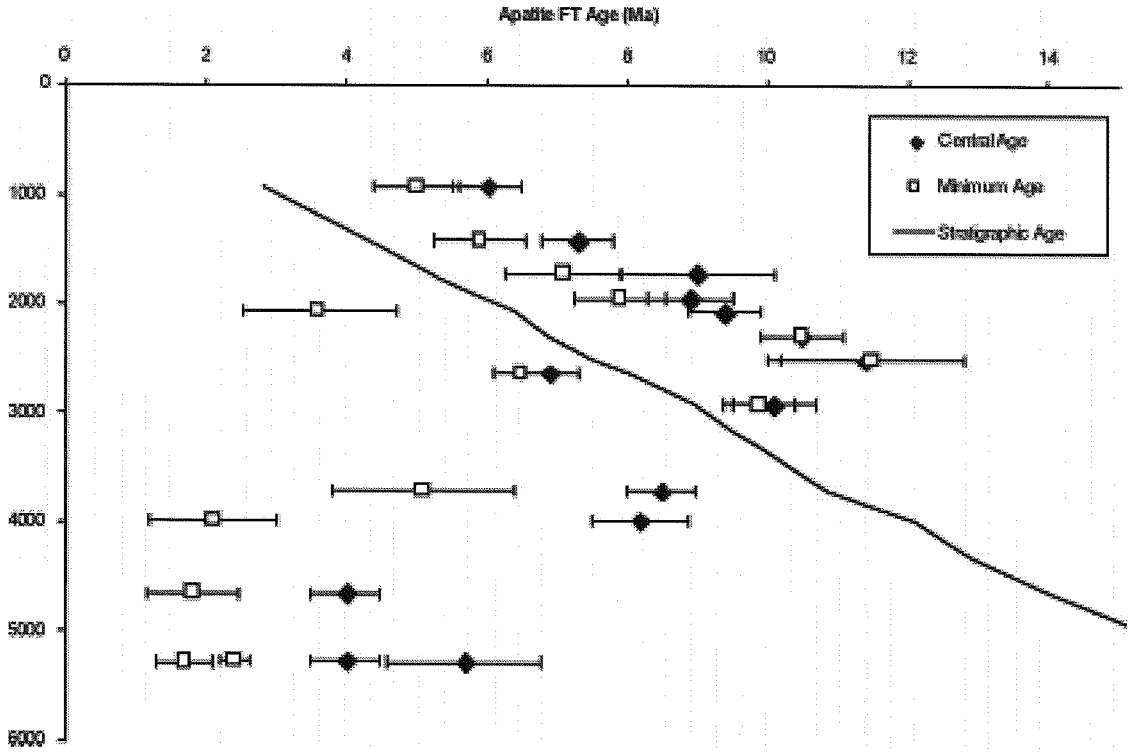

Figure 1. Variation of AFT central age (black diamonds) and minimum peak age (white squares) with stratigraphic depth in the Karnali River section. Continuous black line is stratigraphic age (after Gautam and Fujiwara, 2000). Note constant ~2 My lag time between stratigraphic and minimum AFT age in the upper part of the section (< 2500 m) and consistent 2 Ma minimum age for the lowest 4 samples, providing an estimate for the final exhumation of the section along the Main Frontal Thrust.

APPEL, E., RÖSLER, W. & CORVINUS, G. 1991. Magnetostratigraphy of the Mio-Pliocene Surai Khola Siwaliks in west Nepal. *Geophysical Journal International* 105, 191-198.

BERNET, M., VAN DER BEEK, P.A., HUYGHE, P. AND MUGNIER, J.L.., 2005, Continuous and episodic exhumation of the central Himalayas from detrital zircon fission-track analysis of Siwalik sediments, Nepal. *20th Himalaya-Karakorum-Tibet Workshop* (this issue).

BRANDON, M.T., 1996, Probability density plot for fission track grain-age samples: *Radiation Measurements,* 26, 663-676.

BRANDON, M.T., RODEN-TICE, M.K., AND GARVER, J.I., 1998, Late Cenozoic exhumation of the Cascadia accretionary wedge in the Olympic Mountains, northwest Washington State: *Geological Society of America Bulletin,* 110, 985-1009.

BURBANK, D. W., BLYTHE, A.E., et al. 2003. Decoupling of erosion and precipitation in the Himalaya. *Nature* 426, 652-655.

GAUTAM, P. & RÖSLER, W. 1999. Depositional chronology and fabric of Siwalik Group sediments in central Nepal from magnetostratigraphy and magnetic anisotropy. *Journal of Asian Earth Sciences* 17, 659-682.

GAUTAM, P. & FUJIWARA,Y. 2000. Magnetic polarity stratigraphy of Siwalik Group sediments of Karnali River section in western Nepal. *Geophysical Journal International* 142, 812-824.

ROHRMAN, M., ANDRIESSEN, P. A. M. & VAN DER BEEK, P. A. 1996. The relationship between basin and margin thermal evolution assessed by fission track thermochronology: an application to offshore southern Norway. *Basin Research* 8, 45-63.

FLUID MIXING IN BARITE OF TONS VALLEY, LESSER HIMALAYA, INDIA: USING $\delta^{34}S$ RATIO

Priti VERMA and Rajesh SHARMA

Fluid Inclusion Laboratory, Wadia Institute of Himalayan Geology, 33 G. M. S. Road, Dehra Dun- 248 001 (India)
E-mail: preity_ver@yahoo.com

Sulphur isotope systematic is a complex process due to its variable redox potential and fractionation process. The lighter isotope fractioned for sulphides in comparison to the heavier isotope partitioning for sulphate, infer residual sulphate drives higher isotopic values for seawater. To revealing the source of the sulphate during barite deposition along the nature and the source of the Ba bearing fluid decipher, by using Stable isotopes, $\delta^{34}S$ and $^{87}Sr/^{86}Sr$ ratios of barite has been taken for Tons valley, Lesser Himalaya. The barite of Lesser Himalaya is stratabound in nature principally occurs as veins, lenses, nodules and stringer within the fractures and joints which is hosted by Nagthat siliciclastic rocks.

The observed sulphur isotope ($\delta^{34}S_{CDT}$) data ranges between +26 to +29% for $BaSO_4$ of Tons valley showing similarity between observation made by Claypool et al, 1980 (between + 23 to +30%) and early seawater (+20%) . The observed values of stable isotopes for study area sparingly rule out the possibility of meteorites, basalts, and magmatic or sedimentary source for sulphate. But possibly such a narrow uniform range of data suggests no participation of any biogenic activity for the sulphate configuration and a single continuous source of sulphur in the process. The acquired $^{87}Sr/^{86}Sr$ ratios ranges between 0.720448 to 0.728637 and this value also differs from the mantle Sr ratios (0.70400), seawater (0.70900) and much higher than hydrothermal fluids i.e. 0.7100, this abnormally higher values suggest the involvement of highly radiogenic old crustal source rocks, without influence of magmatic rocks and marine volcanic activity (Sharma et al, 2003).

The obtained results of $\delta^{34}S$ and $^{87}Sr/^{86}Sr$ is considered to be reasonably consistent with the fluid mixing model, where the mixture of endmember A (seawater sulphate) and endmember B (Ba fluid) had take place. A plot of $\delta^{34}S$ with $^{87}Sr/^{86}Sr$ (Fig. 1) for barium sulphate gives a line of mixing of the two fluids from the different source.The initial Sr source suggest the dominance of the crustal source for the Ba bearing fluid. There is no microscopic and field evidence of the presence of any sulphide mineral along with barite, fluid inclusion data also supports the fact for the absence of any H_2S bearing fluid. The fluid inclusion studies also strongly supports the fluid mixing model with homogenization of primary inclusions in the range of 112 – 208 ° C with salinity ranging from 3.71 to 11.9 wt % NaCl and a perfect Th vs salinity trend shows decrease in salinity at the lowering temperatures that infer cooling of fluid along its dilution suggesting the presence of basinal brine.

The stratabound signature reflected from their confinement to host rock has been superimposed by later re- allocation into their fractures and joints. Initial deposition of barite may be linked with the diagenesis of the host rock. Ba released from the silicate minerals like feldspar and mica minerals and gets associated with Nagthat siliciclastic sediment and during diagenesis it assimilate sulphate from the shallow marine environment during Late Proterozic as indicated by sulphur isotope data. It deposit barite in the basin along with siliciclastic host rock and the studied, representative isochors from the fluid inclusion data also reflects higher PT level of the early fluid in barite. The isochors of the successive inclusions at lower PT levels imply effect of tectonic activity during the recrystallization and deformation of barite (Verma, 2004).

In the present case isotope systematic together with the fluid inclusion data provide a strong evidence for the genesis of barite in Tons valley that is closely linked with the physicochemical transport mechanism in the geological environment i.e.:

~ $^{87}Sr/^{86}Sr$ ratio of Ba support crustal derivation
~ $\delta^{34}S$ data +26 to +29% - proven supply of seawater sulphate
~ stratabound deposition of barite within host quartzite
~ later remobilization partly obliterating initial depositional features
~ recrystallization related to isothermal decompressional uplift .

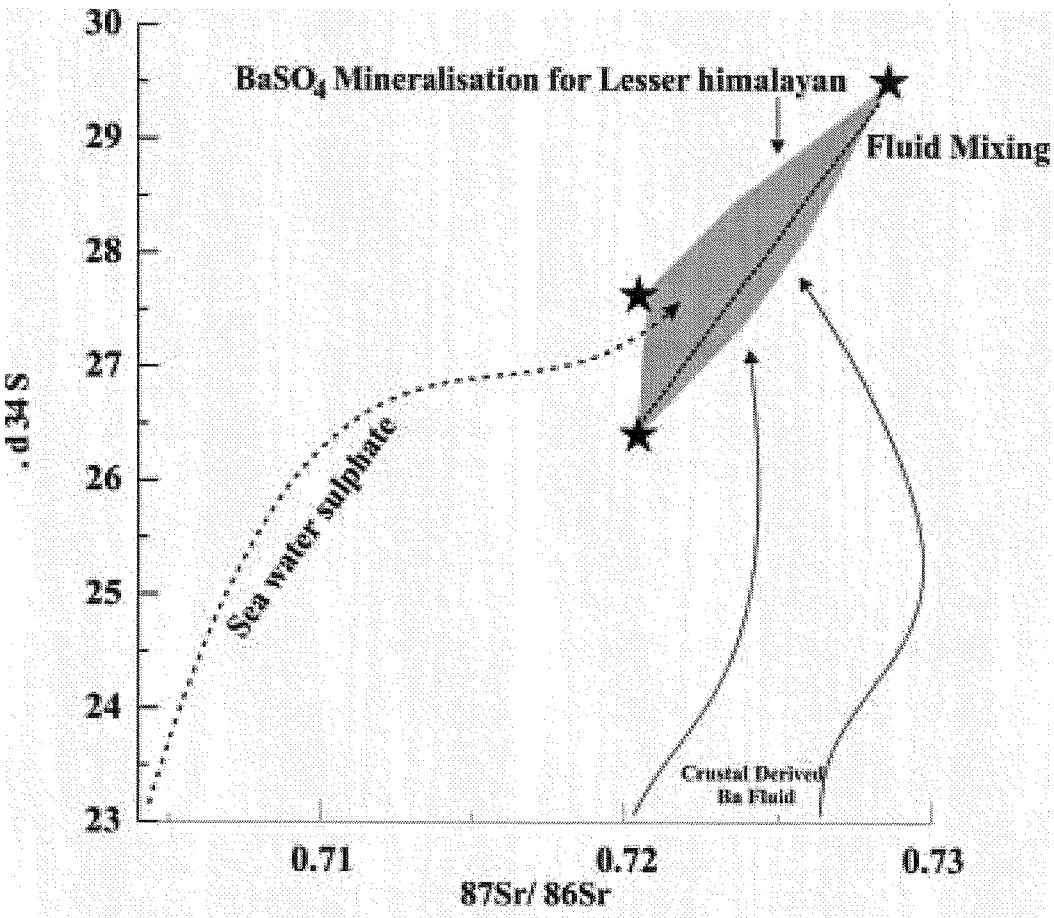

Schematic summery of fluid mixing model of barite from Tons-valley, Lesser Himalaya, Using S and Sr ratio.

References

Claypool., C.E., Holster.W.T. Kaplan. I.R. Sakai. H.& Zak. I. 1980. The age curves of sulfur and oxygen isotopes in marine sulphate and their mutual interpretation. Chem. Geol. 28. 1999- 260.

Sharma., R., Verma. P. & Sachan. H.K. 2003. Strontium isotopic contraints for the origin of barite mineralization of Tons valley, Lesser Himalaya. Curr.Sc. 85 (10). 653- 656.

Verma, Priti. 2004. Genesis of barite in Tons valley and the environmental impact of its exploitation in the Tons valley, Lesser Himalaya. Unpublished Phd Thesis, India.

A GEOLOGICAL RECONNAISSANCE TO SOUTHERN KANGCHENDZONGA MASSIF

Giovanni VEZZOLI (1), Bruno LOMBARDO (2) and Franco ROLFO (3).

(1) Dipartimento di Scienze Geologiche e Geotecnologie, Piazza della Scienza 4, I-20126 Milano (Italy)
(2) CNR, Istituto di Geoscienze e Georisorse, Sezione di Torino. Dipartimento di Scienze Mineralogiche e Petrologiche, Via Valperga Caluso 35, I-10125 Torino, (Italy)
(3) Dipartimento di Scienze Mineralogiche e Petrologiche, Via Valperga Caluso 35, I-10125 Torino, (Italy)

Kangchendzonga, the third-highest and easternmost eight-thousander, sits in a broad synform of regional extent between the Tamar tectonic window to the W and the Rangit tectonic window to the E. The latter cuts deeply through the Himalayan nappe pile, exposing below the Lesser Himalayan Daling schists a well preserved and wholly non-metamorphic sequence of Permo-Carboniferous sedimentary rocks of Gondwana affinity (Damudas). At the northern end of the Rangit tectonic window metamorphic grade increases rapidly from greenschist-facies compatibilities in the uppermost Daling schists (biotite-gneiss) up to sillimanite grade in the MCT zone and finally to Grt-Ky-Sil-Bt migmatites with Grt-bearing leucosomes of the Darjeling Gneiss between Yuksom and Bakhim (Harris et al. 2004).The upper Rathong Chu and Prek Chu valleys are carved in a large body of granite to granodiorite orthogneiss with intercalations of biotite gneiss and rare bodies of amphibolite. Leucogranite sheets first occur south of Bakhim (Harris et al. 2004) but are increasingly abundant in the south face of Rathong and Kabru Dome (Searle and Szulc 2005) and south of Guicha La in the north ridge of Pandim. In the south-west face of this peak a layered sequence of calc-silicate fels and marbles is conspicuous and was noted long ago by Hooker (1854) and Garwood (1903). The layered sequence is associated with biotite schists with quartz-sillimanite nodules and is cut by leucogranite dykes. Leucogranite is homogeneous and in places displays the star-shaped tourmaline clusters typical of Miocene leucogranites throughout the Himalayas.

The lithological association of Pandim is very similar to the banded calc-silicate rocks and marbles occurring in the Mt. Everest region above the Lhotse Shear Zone at the base of the biotite grade North Col. Fm., the lowest member of the Tethys Himalaya sequence. The geological setting we observed at Pandim is also reminiscent of that described by Gansser (1983) in west Bhutan, where a folded shear zone places the biotite grade Cheka phyllites and calc-silicate rocks above sillimanite grade gneisses and migmatites of the Higher Himalaya Crystallines.

(References)

Gansser A. 1983. Geology of the Bhutan Himalaya. Birkhauser, Basel, pp. 181.
Garwood E.J. 1903. The geological structure and physical features of Sikkim. In: Freshfield., D. W. Round Kangchenjunga. London. Arnold. 275-299.
Harris N.B.W., Caddick M., Kosler J., Goswami S., Vance. D. & Tindle G. 2004. The pressure-temperature-time path of migmatites from the Sikkim Himalaya. *J. metamorphic Geol.*, **22**, 249-264.
Hooker J.D. 1855. Himalayan Journals. 2nd edition, London, reprinted 1891, pp. 574.
Searle M. P. & Szulc A.G. 2005. Channel flow and ductile extrusion of the high Himalayan slab-the Kangchenjunga Darjeeling profile, Sikkim Himalaya. *Journal of Asian Earth Sciences*, in press.

ISOTOPIC INHERITANCE IN THE MCT ZONE, ARUN VALLEY, E NEPAL

I.M. VILLA,[1,2] B.LOMBARDO[3]

1 - Università di Milano Bicocca, Milano, Italy; 2 - Isotopengeologie, Bern, Switzerland; 3 – IGG-CNR Torino

The Arun valley in E Nepal is a tectonic window exposing the Lesser Himalayan sequence below the MCT zone and the High Himalayan Crystallines. From the village of Tumlingtar northwards, the following lithotectonic units are exposed:
1) The Tumlingtar Unit (*Nawakot nappes* of Hagen, 1969), a thick sequence of greenschist-facies metasediments, bounded to the north by a syn-metamorphic thrust zone (*Main Central Thrust 1* of Maruo & Kizaki, 1983; *Main Central Thrust Zone* of Meier & Hiltner, 1993).
2) The MCT zone (*Kathmandu nappes* of Hagen, 1969), comprised of staurolite to kyanite grade micaschists and granitic orthogneiss (*Num Orthogneiss* of Lombardo et al., 1993).
3) The Higher Himalayan Crystalline nappe bounded on both side of the Arun tectonic window by thrust sheets defining a major syn-metamorphic thrust (*Main Central Thrust* of Bordet, 1961; *Main Central Thrust 2* of Maruo & Kizaki, 1983).

Metamorphism : The Lesser Himalayan sequence and the MCT zone of the Arun valley (as elsewhere throughout the Himalaya) are characterized by an inverted metamorphism, such that metamorphic grade increases toward structurally higher levels. Mineral assemblages and geothermometric data show an up-structure increase in temperatures. Metamorphic equilibration temperatures rise from 400 °C in Tumlingtar Unit to 500- 650 °C in the MCT zone and over 700 °C in the HHC (Maruo & Kizaki, 1983; Brunel & Kienast, 1986; Pognante & Benna, 1993; Meier & Hiltner, 1993; Goscomb & Hand, 2000). Petrological study of gneisses and amphibolites shows evidence for a clockwise P-T path in upper structural levels of the MCT zone. Peak-P conditions retrieved from mineral cores are around 12 kbar at 720 °C and the thermal peak is recorded from intermediate mineral zones at ca. 9 kbar and 730 °C, at the boundary between the kyanite and sillimanite stability fields. Compositions of mineral rims indicate later cooling to ca. 620 °C at 7 kbar (Lombardo et al., this Workshop).

Petrography: Two samples from the MCT zone were investigated in detail: MK 109, a tourmaline micaschist from the Ahale Danda, north of Tumlingtar and MK 99, a granitic orthogneiss from Seduwa. Both were collected by the late U.Pognante in the 1990 Barun Valley expedition (Pognante & Benna, 1993). MK 109 is from the biotite zone just above the MCT 1. MK 99 is from the upper MCT zone, about 1 km downsection from the MCT 2. Under the microscope MK 109 appears as a muscovite-tourmaline micaschist with thin biotite rims on Mus; tourmaline is zoned, with yellow green cores and blue-green rims. Two Mus-bearing foliations are evident, with an S-C fabric. MK 99 is a garnet-free, biotite-muscovite orthogneiss with cm-sized K-feldspar crystals; biotite is brown and muscovite less abundant than biotite. White mica on the foliation is decussate and in equilibrium with biotite; it is pervasively (but incompletely) recrystallized. Sporadic later muscovite crossing the foliation suggests a high-T reequilibration. Both samples have heterogeneous microtextures; a white mica generation formed during M2 partly survived a pervasive but incomplete M3 recrystallization.

ARGLES T., FOSTER G.L, WHITTINGTON A.B. & GEORGE M.T. (2003). Abstract Volume, 18th HKT workshop, Ascona 2003, p.18. BORDET P. (1961): *Recherches géologiques dans l'Himalaya du Népal, région du Makalu* . Ed. CNRS, Paris, 275 pp. BRUNEL M. & KIENAST J.R. (1986). *Canadian Journal of Earth Sciences*, **23**, 1117-1137. GOSCOMB B. & HAND M. (2000). *Journal of Petrology*, **41**, 1673-1719.
HAGEN T. (1969): *Mém. Soci. Helv. Sc. Nat.*, **86/1**, 185 pp. LOMBARDO B., PERTUSATI P. & BORGHI S. (1993). In: P. J. Treloar & M. P. Searle (eds) - Himalayan Tectonics. *Geol. Soc. Sp. Pub.*, **74**, 341-355. LOMBARDO B., RUBATTO D., ROLFO F. & PERTUSATI P. (2005): This workshop MARUO Y. & KIZAKI K. (1983). In: Shams, F.A. (Ed.) *Granites of Himalayas, Karakorum and Hindu Kush.* Inst. Geology, Punjab Univ., Lahore, 271-286.
MEIER K. & HILTNER E. (1993). In: P. J. Treloar & M. P. Searle (eds) - Himalayan Tectonics. *Geol. Soc. Sp. Pub.*, **74**, 511-523. POGNANTE, U. & BENNA, P. (1993). In: P. J. Treloar & M. P. Searle (eds) - Himalayan Tectonics. *Geological Geol. Soc. Sp. Pub.*, **74**, 323-340. VILLA I.M. (1998): Isotopic Closure. *Terra Nova* **10**, 42-47.

PALEOGENE GYACHALA FORMATION IN GYANGZE, TIBET: IMPLICATION TO THE CLOSING OF NEW TETHYS OCEAN

WANG Chengshan (1), WEI Yushuai (2), JANSA Jansa (3)

(1) China University of Geosciences, Beijing, 100083, China
(2) Chengdu University of Technology, Chengdu, 610059, China
(3) Department of Earth Sciences, Dalhousie University, Halifax, N.S., Canada

In general, the New Tethys Ocean was a huge ocean between southern Eurasia continent and northern India and Africa subcontinents in Mesozoic. At present, it is subdivided into the eastern and western parts by separation of Pamir mountains, in which the eastern part mainly exposes in Himalaya range. It is accepted that the eastern Tethys sea way was closed in Paleogene, however, how and what epoch it close remains questionable. Recently, our geological investigations in the study show a wider distribution of marine upmost Cretaceous and Paleogene sediments, which make initial age research of India collision with Eurasia possible.

The study area lies in the northern Tethys Himalayas (Fig. 1), where was ever at the northern Indian Passive margin. The Gyachala Formation, ca. 900 m thick, is a newly-found marine lithostratigraphic unit in Gyangze area, southern Tibet (Fig.1), dating as Paleocene and Eocene by abundant dinoflagellate, spore and pollen fossils. It is composed of lithoclastic (/quartz) sandstone with intercalated and / interbedded shales and few lenticular limestone. The lithoclastics in sandstones are dominated by andesite and basalt. Three sedimentary cycles of upward fining are recognized. Lots of Bouma turbiditic sequence and sliding and talus structures are also found. Those evidences above indicate a submarine fan environment is relatively eligible. A recycled orogenic background of provenance plus paleocurrent direction recovery (NNW to SSE) suggests the sediment of the formation could be derived the Gandese Arc, and indicates the Tethys oceanic crust had been disappeared during that time and the collision of India with Asia had set off. A comparison among the Balakot Formation in Hazara, Chunglung La Formation and Kong Kesi Formation in Zanskar, the Penqu Formation in Tingri, Zongpubei Formation and Zhepure Formation in Gamba, Barail Formation in north India-Burma mountains, implies the marine sediments of the highest horizons are younger eastward, and the Gyachala Formation had ever been deposited in a remnant sea.

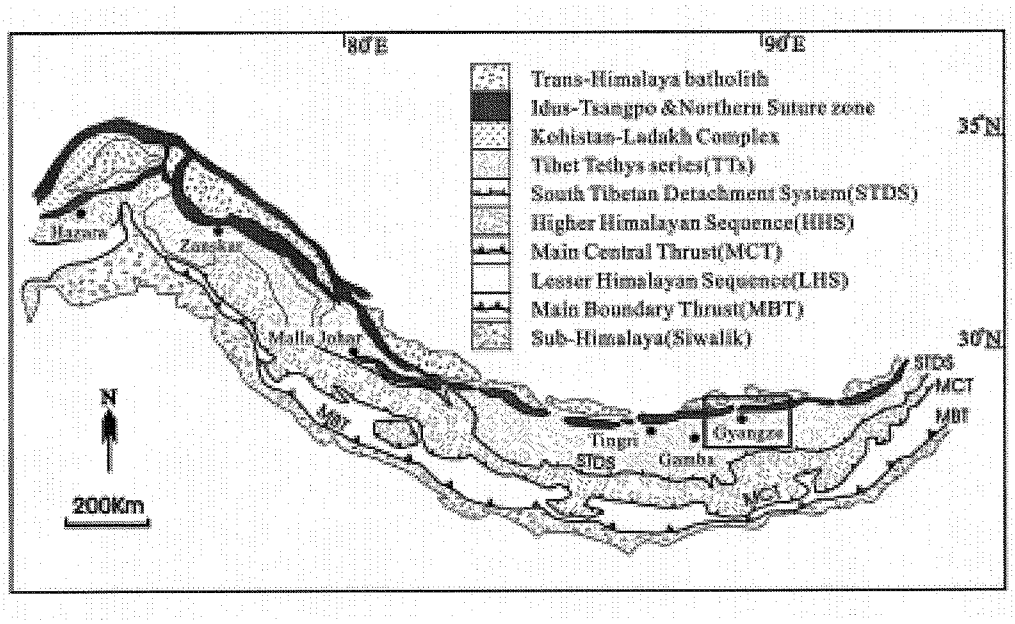

Fig. 1 Geologic sketch of Himalaya with location of study area

ZIRCON U-PB SHRIMP DATING OF HIGH HIMALAYA ROCKS FROM THE SHIBUQI REGION, SOUTHWESTERN TIBET

Yanbin WANG(1), Dunyi LIU(1) and Jinhe LI(2)

(1) Beijing SHRIMP Center, Institute of Geology, Chinese Academy of Geological Sciences,No.26, Baaiwanzhuang Rd,Beijing, 100037, China. E-mail:yanbinw@cags.net.cn
(2) Hebei Institute of Regional Geology and Mineral Resources Survey, Langfang , 065000, Hebei, China

The Shibuqi region lies in southwestern Tibet (roughly 31°N, 79°E) near the China- India boundary. Like much of the High Himalaya mountains, Shibuqi is composed of pelite schists and gneisses, calcareous schists, sillimanite-, kayanite- bearing gneisses, calc-silicates, quartzites, with minor leucosome and amphibolites. The rocks have experienced a clockwise P-T evolution in response to crustal thickening during the collision followed by decompression amd crustal melting. the age of the metasedimentary sequence has not been dated. We establish precise U-Pb zircon SHRIMP ages and Nd isotopic evolution of three samples from the region.

The zircon population displays complex internal structures in dated biotite- sillimanite gneiss samples. The complex crystals have well-preserved magmatic cores and altered rim domains. The core population were dated at about 3221Ma-1124Ma, where the age of the measured rims and altered domains are about 559Ms(Fig1).

The Nd isotopic analyses of the three samples emphasize the Archean Nd modal ages. Zircon separateds from the rocks yield U-Pb dates of 3.2-2.5Ga.

These data on zircons from Shibuqi clearly indicate the that rocks of high Himalaya and the crystaline thrust sheets were regionally metamorphosed during Pan-African periods.

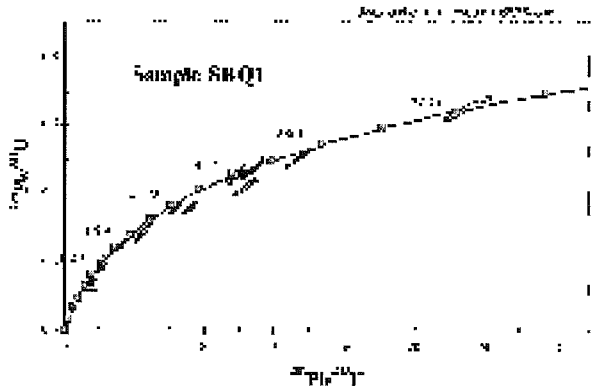

Fig1.U-Pb Weatherill concordia diagrams showing SHRIMP data dor Sample SBQ1. Error ellipses are 1σ.

CATLOS, E.J., HARRISON, T.N., MANNING, C.E., et al., 2001. Journal of Asian Earth Sciences,20,459-479.
DECELLES,P.G., GEHRELS,G.E., QUADE,J., LAREAU,B.N., SPURLIN,M.S., 2000. 288 ,497-499.
GEHRELS,G.E., DECELLES,P.G., MARTIN, A., ET AL.,2003. GSA TODAY, 13,4-9.
MASON, BETSY.,2003.. NATURE, 425
PARRISH, R.R., HODGES, K.V., 1996. GSA BULLETIN,1996, 108,904-

GEOPHYSICSAL CHARACTERISTICS OF THE CRYSTALLINE-BASEMENT IN SONGPAN-ARBA, CHINA

Fangzhi YANG, Yongsheng MA, Xuan ZHU, Tonglou GUO, Zhongyuan LI Guoxiong LI , Tianfa ZHENG, and Guixiang YANG

Southern Petroleum Exploration and Exploitation Co., Sinopec, China

Songpan-Arba locates at the east Tibet, China. Due to the plate interaction among Eurasian, Pacific and Indian, this "triangle" block is surrounded by the Qinling orogenic belt at the north, Longmen mountain belt at the southeast, and the Sanjiang (three rivers) orogenic belt at the southwest. The territory and its neighborhood are featured with very complicated tectonics, such as fold, detachment, under- and over-thrusts etc. The study area has well developed faults, strongly deformed stratum, and the outcrop of Neo-, Paleo-Mesozoic, in which most part is covered by upper mid- and upper Triassic rocks. On the base of the previous work of surface geological survey, we have conducted a series of geophysical exploration including gravity, magnetic, MT and shallow/deep seismic methods, in order to evaluate its potential prospect of oil/gas reservoir.

We have collected outcropped rock samples from seven lines across the study area, with a total profile length over 1000 km. We have selected 805 samples for 40 different formation groups, and measured their density, magnetism, resistivity etc, and established a set of references for the interpretation of gravity, magnetic and electronic data.

For the interpretation of MT data, we have performed 2D inversion using synthetic anneal stealing method, and multi-parameter migration with high vertical resolution. For the analysis of gravity and magnetic data, we have processed the real data using wavelet transform, to improve the resolution.

Figure 1 is the spatial distribution of apparent resistivity at depth of 10 and 15 km. It suggests that the high-resistivity body under the Arba-Ruoergai with shrinking boundary and decreasing size along the depth, and its horizontal shape is nearly a circle. It may be the so-called Ruoergai core. It is separated from neighbouring tectonic units with a wide low-resistivity zone.

For the whole study area, the range of the average thermal gradient is about 15-25°C/km. In the Qilian-Qinling, the thermal gradient is 19-25°C/km. In the Dingxi-Tongren-Wenquan it is 15-18°C/km. In Songpan-Ganzi it is 15-18°C/km. In the Arba-Ruoergai area and the Changdu-Longmenshan area, it is 19-20°and 19-25°C/km, respectively.

Seismic reflection survey has shown three strong reflections above the crystalline-basement, from all three lines of 530 km totally, conducted in November 2002.

Figure 2 is a deep seismic profile between Ruoergai and Hezuo (line RH04-1), conducted in July 2004. It is the first such deep seismic profile across the Qinling orogenic belt and Ruoergai subblock. It has recorded the reflection from the crustal and upper-most of the upper mantle with record length of 30 second, which thereby provides us an image of geological structure down to upper mantle (100 km and deeper). It is of important for the research on lithospheric kinetics and contact relationship between the Qinling orogenic belt and the Ruoergai subblock, and for understanding the coupling relationship between the crust and the mantle.

In summary, the gravity and MT data have revealed high-density, high-resistivity bodies in the Songpan-Arba area, and MT migration result has suggested that such a body under Ruoergai may extend to the maximum of 30km in depth. In addition, deep seismic reflection analysis has indicated that there is no well-developed fault within the crystalline basement. We believe that there is no directly evidence of strong magmatism and that the study area behaves as a relatively stable block.

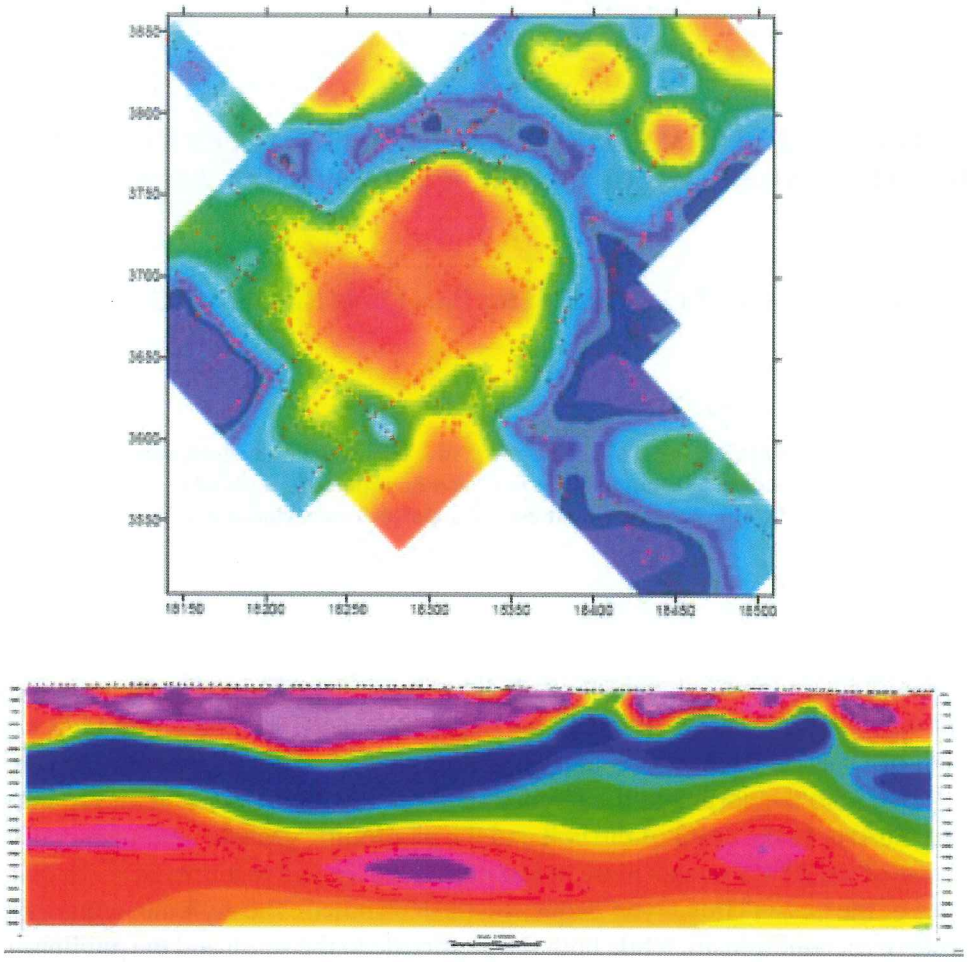

Figure 1. Spatial distribution of the apparent resistivity in the Songpan-Arba area.

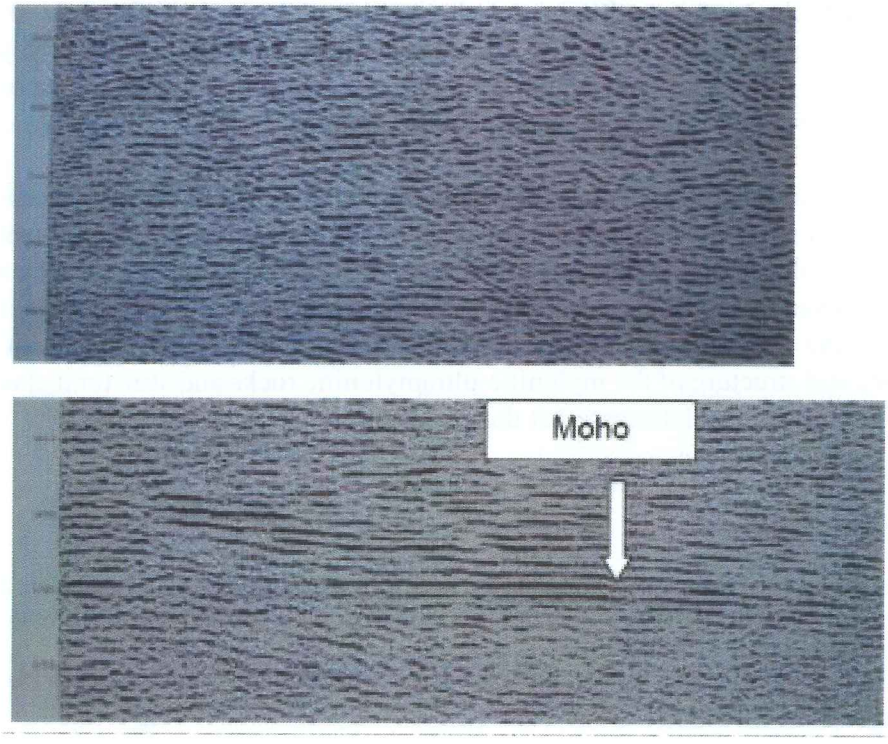

Figure 2. Crustal reflection structure.

MYLONITE AND ULTRAMYLONITE ALONG THE MAIN CENTRAL THRUST IN THE KALIGANDAKI VALLEY AREA, WEST-CENTRAL NEPAL HIMALAYA

Masaru YOSHIDA* (1,2), Santa Man RAI (1) and Bishal Nath UUPRETI (1)

(1) Department of Geology, Tribhuvan University, Trichandra Campus, Kathmandu, Nepal
(2) Gondwana Institute for Geology and Environment, Hashimoto, Japan
* Corresponding author e-mail: gondwana@oregano.ocn.ne.jp

A prominent mylonite-ultra mylonite belt has been identified along the Main Central Thrust zone of the Kaligandaki valley, west-central Nepal Himalaya. The mylonite-ultra mylonite belt occurs south of Dana, in contact with the phyllonitic granite of the Higher Himalayan Crystalline Sequence (HHCS) to the north and the phyllonite of mostly the Lesser Himalayan metasediments to the south. Further to the north of the belt and the phyllonitic granite, heterogeneously mylonitic granitic gneiss of the HHCS occurs more or less continuously, and to the south of the belt, phyllonite and phyllites of the Lesser Himalayan Sequence are distributed. The mylonite-ultramylonite shows middle grade of metamorphism, while both the phyllonite to the south and the phyllonitic granite to the north are low grade.

The phyllonite to the south of the mylonite-ultramylonite belt, for at least some meters southward, carries elongated fragments (augen-shaped) of ultramylonite. Further younger faulting events under further lower grade conditions are also suggested by the occurrence of active faults mostly parallel to S-planes of phyllite and mylonitic granites

The occurrence above indicates that the mylonitization within the MCT zone took place at least twice, except the neotectonic fault movements. The earlier ultramylonite under the middle grade of metamorphism, and the later phyllonitization under the low grade of metamorphism are suggested in this part of MCT. The earlier event may correspond to the early phase activity of MCT in the surrounding area (e.g., Hodges et al., 1996; Catlos et al., 2001). Details of petrography, microstructure and structure of the mylonitic-ultramylonitic rocks and structural characteristics of the belt will be provided and discussed at the presentation.

(References)

Catlos, E.J., Harrison, M.T., Kohn, M.J., Grove, M., Ryerson, F.J., Manning, C.E. and Upreti, B.N., 2001, Geochronologic and thermobarometric constraints on the evolution of the Main Central Thrust, central Nepal Himalaya. J. Geophys. Res., 106, 16177-16204.

Hodges, K.V., Parrish, R.R., and Searle, M.P., 1996, Tectonic evolution of the central Annapurna Range, Nepalese Himalayas. Tectonics, 15, 1264-1291.

SEDIMENTARY CHARACTERISTICS AND ENVIRONMENTS OF SUBMARINE FAN OF THE LOWER CRETACEOUS IN NORTHERN HIMALAYAS

YUE Laiqun 1, SHI Xiaoying 2, WANG Hongzhen 2

1 University of Petroleum, Beijing 102200
2 China University of Geosciences, Beijing 100083

The Lower Cretaceous in northern Himalayas mainly consists of clastic rocks. The submarine fans were well developed in this area. According to the sedimentary minerals, texture and occurrence, the submarine fan can be divided into some subfacies. The differences of subfacies and the arrangements and combinations of subfacies in three dimensions indicate various sedimentary environments. The submarine fan in this area developed stage by stage which was from starting stage, young stage, peak stage, and the disappear stage. The starting and young stages of submarine fan were developed during the Early Age and middle Age of the Early Cretaceous. The sand/mud values of sedimentary materials are much higher than any of other stages. The sedimentary rocks are mainly sandstones with different minerals and textures indicating that the costal plain and shelf were very narrow and the sea bed was dip. The sedimentary conditions were transformed from shelf to slop. The sea level raised. Major tectonic movements were extension, split and subsidence.

During the Late of the Early Cretaceous the submarine fans belong to peak stage. Coastal plain shelves were much wide than before. Sedimentary rocks were black shale and fine-grained clastics with very large thickness. There are many siderite and calcic nodules and a few ammonites fossils in black shales. The values of sand/mud are lower than any of other stages. The sedimentary facies changed transitionally in this area. The sedimentary conditions belong to low energy, gentle slope without clear slope breaks of continental margin. These characteristics prove the significant marine transgression events in northern Himalayas. As the results of the Indian Ocean spreading and the Indian Plate drifting to the north during Early Cretaceous, the passive continental margin was well developed here. The sedimentary chemical conditions were transformed into strong deoxidizing and geographical into slope bottom even bathyal or abysmal sea. Due to the marine regression submarine fans belong to disappear stage in Late Cretaceous and sedimentary rocks changed from shale to coarse sandstone even conglomerate. The sedimentary basins were also developed stage by stage from shelf to extension, split and subsidence basin to slope, and at last to deep sea basin during Early cretaceous.

THE GEOCHEMICAL FEATURES AND U-PB GEOCHRONOLOGY OF LEUCOGRANITE IN CENTRAL GANGTISE, TIBET

ZHAI Qingguo (1)*, LI Cai (1), LI Huimin (2), WANG Tianwu (1)

(1) College of Earth Sciences , Jilin University, Changchun 130061, jilin,China;
(2) Tianjin Institute of Geology and Mineral Resources, China Geological Survey, Tianjin 300170, China)
*E-mail: zhaiqingguo@yahoo.com.cn

Luoza rock batholith is located in the central Lhasa block, Luoza town, Nanmulin County, Tibet. The east-west extended granitic rocks are consisted of two-mica granites, white mica granites, biotite granites and megaphenocryst granodiorites, which intruded into the sandstone and schist of Carboniferous-Permian strata. There are many granitic dikes that intruded into these sedimentary rocks, just like branches, at the verge of the batholith. At the same time, many sandstone and schist xenoliths have been found in the batholith. The chilled and baked border is well preserved at the verge of the granitic rocks. The megaphenocryst granodiorite was formed in later(Lower) Triassic, and was intruded by the later leucogranite(two and white mica granites).

The outcrop of leucogranites are about 350 km^2, which is about 1/2 of the batholith's area. The main components of the leucogranites are k-feldspar, plagioclase, quartz, white mica and biotite, magnetite, zircon, apatite and sphene are accessories. The content of k-feldspar(°¿40%) is more than that of plagioclase(°¿30%), and the total content of the white mica and biotite is about 6%.

According to major element data, trace element data and REE, the leucogranites have the characteristics of high-K calc-alkaline compositions. Besides this, the leucogranites are rich in SiO_2(72.16%~ 75.14%), Al_2O_3(13.75%~14.67%), and low CaO, and FeO_T and MgO is very poor. The A/CNK ratio °›1.11(only one sample is 1.01), the content of corundum exceeds 2.23% through CIPW standard mineral calculating, and the leucogranites lie in the field of peraluminous granites, it suggests that leucogranites are belong to the strong peraluminous granitoids. Concerning trace elements, Rb and Th are much richer than others, and Ba, Ta, Nb, Ga and V are enrichment, on the other hand, Zr, Hf, Y, Sr and Yb are lower. The spidergrams of granitoids normalized to oceanic range granite composations are similar to syn-collision granitoids'. The ratio of °ΔLREE/°ΔHREE is greatness(5.55~17.42), chondrite- normalised REE patterns for the leucogranites show typical LREE enrichment versus HREE depletion and Eu anomalies. In addition, the leucogranites are origin from the earth's crust because of high $^{87}Sr/^{86}Sr$ (0.76929°¿0.00006).

Some single zircon grains were selected from two-mica granite in order to get its ages data in 7km south west of Luoza Town. The sample is unmetamorphosed and its U-Pb ziron age should be the crystal age of the leucogranite. We have obtained four concordant ages: three of them range from 133.2 Ma to 134.7Ma, and one is 127Ma. The average age is 133.9°¿0.9Ma. The age is in agreement with the age of leucogranites(130~140Ma) in the central Gangtise, Chazi and Yangbajing area.

The other important question is about the tectonic implications of the leucogranites. We find that the leucogranites' spots are all in the syn-collisional granite region in terms of the diagram of R_1-R_2 Rb-(Y+Nb) and Nb-Y. There is obviously crustal shortening and thickening due to the collision between the Lhasa and Qiangtang blocks, occurred during the Early Cretaceous, according to newly geologic investigation by Chinese geologists and other data. Murphy et al.(1997) suggested that the shortening is ~60% and the southern Tibetan plateau had obtained an elevation of 3~4km with a crustal thickness of 60~65km during the late Mesozoic. There is lack of Late Jurassic to Early Cretaceous marine strata in most of Lhasa block, and few of these strata(northen rim of the Lhasa block) are interpreted to have been deposited in a narrow seaway induced by thrust loading along the Bangong-Nujiang suture zone. However, this is questionable because the geologic evidence is little, and suggest that the southen Tibetan plateau could have been slightly elevated, but not up to 3~4km during Early Cretaceous time.

The leucogranites of Luoza batholith are belong to the strong peraluminous granitoids and origin from partial melts of metasedimentary rocks in the crust, and its form resemble the one of Himalayas'°£According to the strong peraluminous granitoids, CaO/Na_2O is the index of source composition, and Al_2O_3/Ti_2O is a measure of temperature. Most of CaO/Na_2O ratios of the leucogranite in Luoza batholith are less than 0.3, average 0.23, which indicate that the source of the rock is pelites, and maybe some psammites but only little. Al_2O_3/Ti_2O ratios are between 45.45 and 91.67, average 72.61, which suggest that the partial melting tempereture of leucogranite is larger than 875°Ê, this is in agreement with High-Temperature strong peraluminous granite. So the leucogranite formed by mantle-derved heating of normally thickened crust(°‹50Km) after lithospheric delamination. Therefore, crustal shortening and thickening of Gangdise area during Early Cretaceous is credible, but the crustal thickness is not up to 50km.

In conclusion, the emplacement age of the leucogranite in Luoza batholith central Gangdise is 133.9°¿0.9Ma, which is consistent with the one of Chazi and Yangbajing area's. Taking some other data into account, we suggest that there should be a east-west Early Cretaceous leucogranite belt, which is the result of crustal shortening and thickening of Gangdise area during Early Cretaceous.

Main references

1. BATCHELOR R A, BOWDEN P. 1985. *Chem Geol.*, **48 (1)**: 43-55.
2. DING Lin, Lai Qingzhou. 2003. *Chinese Science Bulletin.*, **48(8)**: 836-842(in Chinese).
3. K J ZHANG, ZHANG Y J, XIA B D. 1998. *Geology.*, **26**: 958-959
4. K.J.ZHANG. 2000. *Cretaceous Research.*, **21**: 23-33
5. LI CAI, WANG TIANWU, LI HUIMIN, et al. 2003. *Geological bulletin of China.*, **22(5)**: 364-366(in Chinese with English abstract).
6. M A MURPHY, A YIN, P KAPP, et al. 2000. *Geology.*, **28**: 451-454..
7. MURPHY M A, YIN A, HARRISON T M, et al. 1997. *Geology.*, **25**: 719-722
8. PEARCE J A, HARRIS N B W, TINDLE A G. 1984. *J Petrol.*, **25**: 956-983.
9. SYLVESTER P J. 1995, *Lithos.* **45**,29-44.
10. TAPPONNIER P,X ZHIQIN,F ROGER,et al. 2001. *Science.*, **294(23)**: 1671-1677.
11. XIZANG BUREAU OF GEOLOGY AND MINERAL RESOURCES. 1993. (in Chinese with English summary).
12. YIN A., HARRISON T M, RYERSON F J,et al. 1994. *Journal of Geophysical Research.*, **99**: 18175-18201.
13. ZHAI QINGGUO, LI CAI, WANG TIANWU, et al. 2004. *Journal of Jilin university(earth science edition).*, **34(1)**: 27-31(in Chinese with English abstract).

GEODYNAMICS PROFILE ACROSS THE INDIAN-EURASIAN PLATE BOUNDARY

ZHAO Junmeng, LIU Hongbing, PEI Shunping

Institute of Tibetan Plateau Research, Chinese Academy of Sciences, Beijing, P. R. China

Up to now, most geophysical profiles in the Tibetan Plateau have been in its eastern and middle parts, while the western part remains lacking in exploration, largely because of its high elevations, harsh natural environment, and poor communication. However, the western Tibetan Plateau, including the western tectonic knot at the west end of the Himalayan arc, is of great importance for research of the region's structure and dynamics. Meanwhile the differences between the eastern and western Tibetan Plateau suggest that they may have dissimilar crustal and upper mantle structures, resulting in varying features at the collision between the Indian Plate with the Eurasian Plate along the tectonic boundary.

The Institute of Tibetan Plateau Research will conduct various geophysical studies from the beginning of 2005 to investigate the geodynamic processes of the Indian-Eurasian Plate collision. The study profile will extend from Bhavnagar on the north coast of the Indian ocean, extending northward to Xayar at the southern Tian Shan, totaling about 3000 km in length (Figure 1). Along this profile the following surveys will be carried out:

(1) Wide-angle seismic reflection/refraction survey

Twenty-four charges (each between 2~15 tone of TNT) will be exploded along the profile. The intervals between receivers will vary from 3~5 km, depending on the specific tectonic settings. As the profile is very long (3000 km), the curvature of the earth will be taken into account, requiring development of new interpretation programs.

(2) Broad-band portable stations along the Burang-Minfeng section (Tibet) of the profile

This profile section is 800 km long (Figure 1). Analyses will utilize the receiver functions, source mechanism solutions, surface wave dispersion methods, and natural earthquake data to constrain the structure and anisotropy of crust and upper mantle. The project plans to deploy 100 sets of Reflak-130 broad-band seismographs every 5~10 km along the profile and record natural earthquakes for about 8 months. Meanwhile these instruments will also record seismic signals from artificial explosions. Through such combined observations, the depth, precision, and accuracy of seismic probing will be greatly improved.

(3) Joint inversion of gravity and magnetism

The available gravity and magnetic data for the study region will be jointly inverted to map the density and magnetization of the crust and upper mantle. Joint inversions will be conducted under the constraints of the gravity and magnetic anomalies and the geometry of the region.

(4) Magnetotelluric (MT) survey

The project will conduct a magnetotelluric survey along the profile. The average interval between measurement sites will be 10 km, varying somewhat depending on the tectonic setting and purpose of the observation. This survey will yield electrical conductivity structures of the crust and upper mantle along the profile, and should delineate the spatial distribution of high-angle faults.

(5) Seismic imaging of the Tibetan Plateau

The target study area lies between 60~110°E, and 20~55°N, extending vertically from the ground surface to a depth of 1000 km. The project plans to use grids of 1°_1°or about 30_50 km. Teleseismic data will be applied as much as possible to enhance resolution. In addition, comparisons will be made between 3D tomographic results, with and without consideration of anisotropy.

(6) Compilation of the geo-transect

The project will compile an integrated geo-transect, based on these new results and those available from the Xayar-Burjin profile[1]. It starts on the north coast of the Indian Ocean, extends northward to southern foot of the Altai mountains (possibly extending as far as Lake Baikal), crosses the Indian and Eurasian Plates, and penetrates the entire Tibetan Plateau to a depth of well over 100 km. An International cooperation is an indispensable part of the project, especially the section between Bhavnagar to Burang. Please let us know if you are interested in this research project.

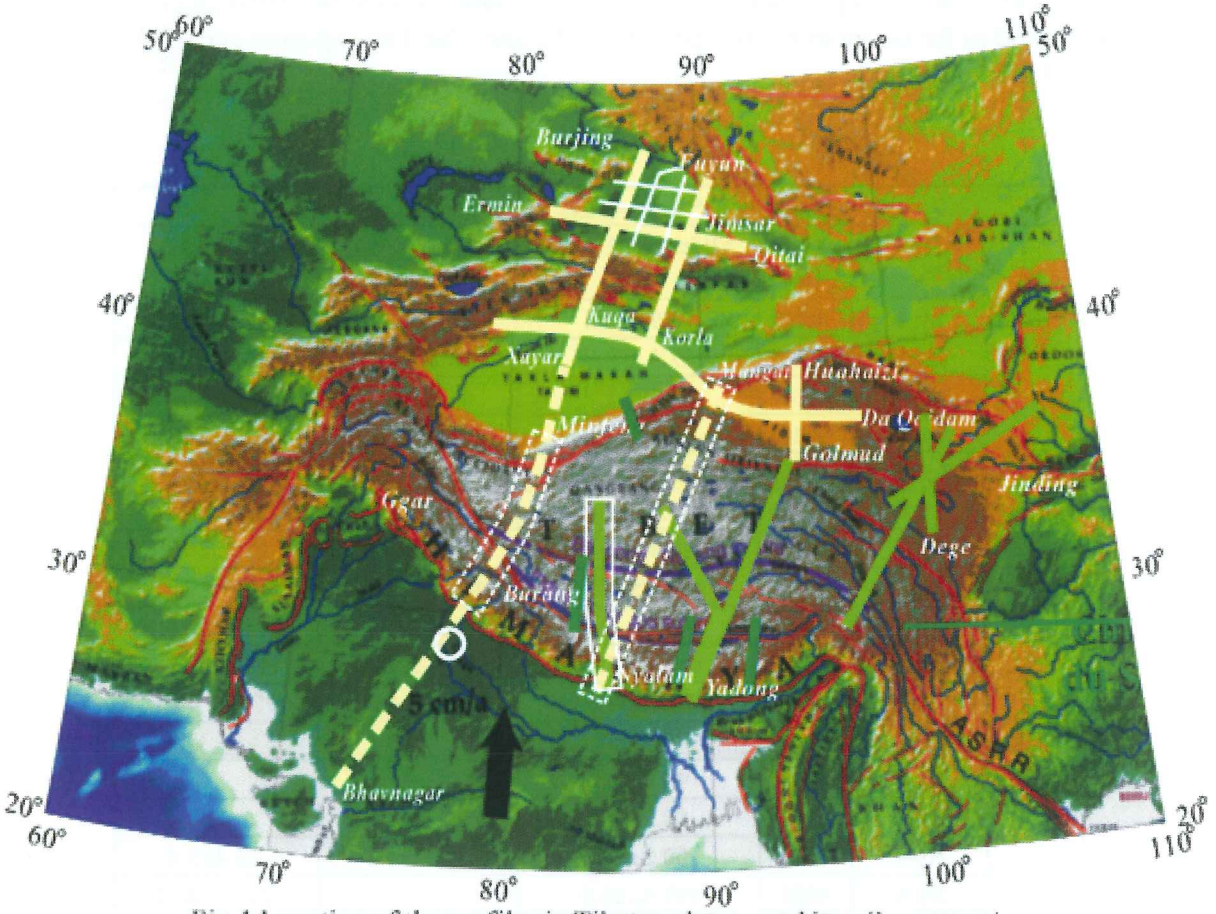

Fig. 1 Location of the profiles in Tibetan plateau and its adjacent regions

Reference:

[1] Zhao Junmeng, Liu Guodong, Lu Zaoxun, Zhang Xiankang, Zhao Guoze, 2003. Lithospheric structure and dynamic processes of the Tianshan orogenic belt and the Junggar basin. ***Tectonophysics*** 376: 199-239

SURFACE EXPOSURE AGE OF THE GLACIATIONS IN TIBET

Zhizhong ZHAO (1), Joerg M. SCHAEFER (2), Silvio TSCHUD (3) and Christian SCHLUECHTER (3)

(1) Institute of Geomechanics, Chinese Acdemy of Geosciences, Beijing 100083, China
(2) ETH Zürich, Isotope Geology and Mineral Resources, NO-C 61,CH-8092 Zürich, Switzerland
(3) Universität Bern, Geologisches Institut, CH-3012 Bern, Switzerland

We chosed three sites to sample in Tibet plateau. One is Haizishan pass of Litang county, second one is near Tanggula pass, and the last is near Nielamu county. We dated glacial boulders in Tibet by method of the cosmogony isotopes ^{10}Be, ^{26}Al, and ^{21}Ne.The exposure age of glaciations in Tibet is as shown in Table 1.

Table 1: ^{10}Be, ^{26}Al and ^{21}Ne exposure ages in Tibet.

Sample		altitude [m]	minimum ^{10}Be-ages [ka]	minimum ^{26}Al-ages [ka]	^{21}Ne-ages [ka]
LITANG	Lit 3	4560	13.9 ± 1.4	15.5 ± 1.4	(29.5 ± 6.0)
	Lit 4a	4560	17.9 ± 2.0	15.5 ± 1.7	(28.4 ± 6.4)
	Lit 4bc	4560	15.0 ± 1.7	15.0 ± 1.7	
	Lit 5a	4610	15.3 ± 1.6	13.8 ± 1.5	(52.9 ± 9.2)
	Lit 5b	4610	15.3 ± 1.5	13.8 ± 3.0	
	Lit 6	4570	15.6 ± 1.4	15.0 ± 2.0	(21.4 ± 4.7)
	Lit 7	4480	13.3 ± 1.4	14.3 ± 3.0	(27.5 ± 7.7)
TANGGU LA	Tan 2	5015	162.3 ± 19.4	171.5 ± 17.2	210.0 ± 20.5
	Tan 4	4925	91.1 ± 9.2	74.2 ± 9.0	102.6 ± 15.1
	Tan 5	4925	164.9 ± 16.6	161.8 ± 16.2	192.0 ± 17.8
	Tan 7	5120	70.5 ± 7.0	68.4 ± 8.2	(77.0 ± 45.1)
NIELAMU	Ny-1		49.9±2.0		
	Ny-2		45.8±2.3		
	Ny-3B	3958	98.2±4.9		
	Ny-4	3930	60.3±3.1		59.4±5.4
	Ny-6	4025	285.4±10.6		232.8±32.9
	Ny-7	4025	51.3±3.8		
	Ny-8		142.3±6.1		142.7±6.3
	Ny-15		101.8±4.3		
	Ny-16		178.9±12.3		148.4±17.5
	Ny-9	4414	15.1±0.9		19.4±4.0
	Ny-10	4425	24.3±1.9		
	Ny-12		10.2±0.6		14.8±3.7
	Ny-13				33.4±7.5
	Ny-14	4436			19.6±5.2

The most extensive glacial advance in Tanggula mountain occurred 180 ka ago, but even this event was of limited extent. All later snowline lowerings in Central Tibet have been even smaller. This finding excludes the Tibetan Plateau as a pacemaker of northern hemisphere ice ages by an initial plateau glaciation. The data strongly contradict the idea that the switch of the Asian monsoon mode during northern hemisphere glacial times, e.g. during the LGM, were caused by an extensive ice-cover on the Tibetan Plateau(Emeis et al., 1995; Sarkar et al., 1990).

In East Tibet, glaciers advanced during Oxygen Isotope Stage 2. However, this event has been much smaller than in other parts of the northern hemisphere, where glacial advances during the Last Glacial Maximum have been on the order of 100km (Rutter, 1995). No more extensive glacial advance occurred on the Eastern Plateau margin later, i.e. neither the Eastern nor the Central Plateau glaciers advanced significantly during the Holocene monsoon precipitation maximum of South Asia. Therefore, the paleoglaciation history of the Himalayas at the western margin of the Plateau, i.e. absence of any glacial event during the peak of the last Northern Hemisphere glaciation but advances in the Holocene, seems to be out of phase with the rest of Tibet. Our study suggests a correlation of the North Atlantic and East Tibet climate, respectively, most likely established by the effect of westerly winds. This finding is in agreement with earlier studies reporting such a climatic link between the North Atlantic on the one hand and northwest Tibet (Thompson et al., 1997) and China (Porter and An, 1995; Wang et al., 1999) on the other. The moderate amplitude of the Tibetan glacial advances and underlying climate changes relative to other northern hemisphere areas in the last 180 kyrs in general and during the LGM time in particular most likely reflects the high sublimation and low precipitation regime of the high-altitude and continental site of the Tibetan Plateau.In southwest Tibet, we finished dating just now. The feature of exposure ages is similar with the other site.

In summary, the result implies that the ice extent on the Tibetan Plateau has been very limited during at least the last two glacial cycles excluding the albedo of the Asian continent as a critical parameter for regional to hemisphere-wide climate changes. However, a detailed glacial chronology especially in the western part of the Tibetan Plateau on time scales of several 100 kyrs still needs to be established by studies similar to the one presented here.

Acknowledgements:
This study is carried out under the programs of the CGS of China (No.200312300034).

(References)

EMEIS K.C., ANDERSON D.M., DOOSE H., et al. 1995. *Quaternary Research*, **43**. 355-361.
SARKAR A., RAMESH R., BATTACHARYA S.K., & RAJGOPALAN G. 1990. *Nature* ,**343**.549-551.
RUTTER N. 1995. *Quaternary International.* **28**.19-37.
PORTER S.C., & AN Z.S. 1995. *Nature*.**375**.305-308.
THOMPSON L.G., YAO T., DAVIS M.E., et al.1997. *Science*.**276**.1821-1825.
WANG L., SARNTHEIN M., ERLENHEUSER H., et al. 1999. *Marine Geology*.**156**.

AGES, ORIGINS AND TECTONIC SETTING OF THE YEBA BIMODAL VOLCANIC ROCKS IN LHASA AREA, SOUTH TIBET

ZHU Dicheng*, PAN Guitang, WANG Liquan, GENG Quanru, LI Guangming, LIAO Zhongli, LIU Bo

Chengdu Institute of Geology and Mineral Resources, 610082, Chengdu, China
*Correspondence should be addressed to Zhu Dicheng (email: cdzdc@cgs.gov.cn)

The Yeba volcanic rocks are distributed between the Luobadui-Milashan fault to the north and the Xietongmen-Angang-Zhigang ductile shear zone to the south and are extended about 280km in the E-W direction from Dazi to Gongbujiangda County, which is geographically located in the central-eastern part of Lhasa area (Fig.1). Ages, origins and tectonic setting of the Yeba volcanism have been problematic for a long time. Key to these problems is generally centralized on the ages that are reported by previous studies at Late Triassic, Middle-Late Jurassic, Cretaceous and Late Cretaceous (Yin Jixiang et al., 1988; Team of integrated geological investigation of Qinghai Province, 1994; Bureau of Geology and Mineral Resources of Xizang Autonomous Region, 1993).

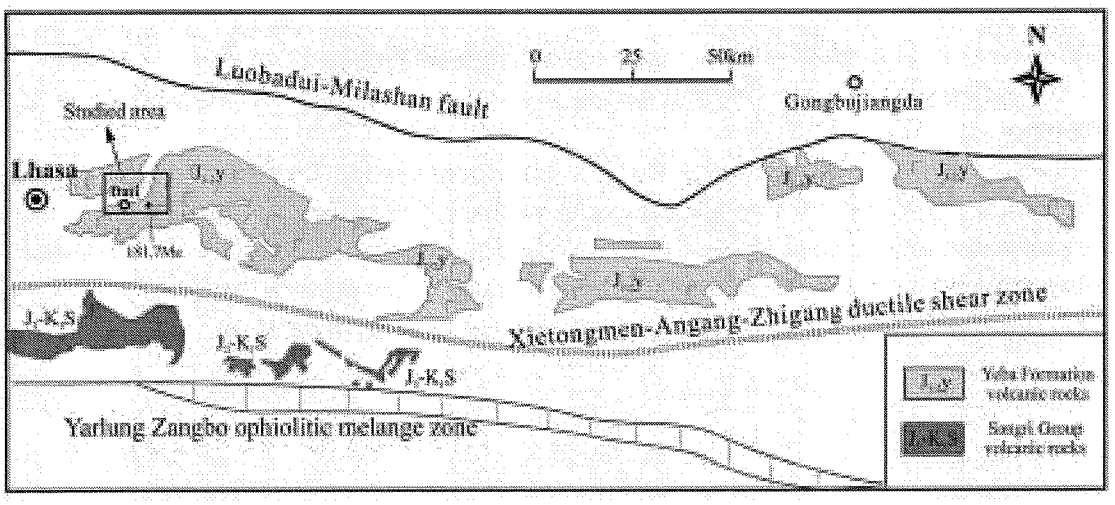

Fig.1 Sketchof the distribution of Yeba Formation volcanic rocks in Lhasa area, south Tibet (modified from Pan et al., 2004)

The Yeba volcanic rocks, which have been affected by low-grade hydrothermal alteration (seawater alteration) and (or) greenschist-facies metamorphism, occur as mafic lavas and felsic metavolcanic rocks and dykes that are generally cropped out as interlayers in metasedimentary rocks. SHRIMP U-Pb zircon dating for the metadacite from the upper part of Yeba Formation and for the subvolcanic dyke from the lower part of Yeba Formation are 181.7±5.2Ma and 188.1±3.4Ma, respectively, providing reliable constraints for the ages of Yeba volcanism occurred at the Early-Middle Jurassic.

The mafic rocks have variable range of SiO_2 contents (SiO_2=40.9% – 50.36%) and affinities with andesitic basalts on immobile Zr/Ti against Nb/Y discrimination diagram. These rocks have markedly negative Nb anomalies relative to Th and La, and moderately negative Zr, Hf, Ti anomalies, moderately fractionation between LREE and HREE ($(La/Yb)_N$=3.74 – 8.31), Th, Sr and other HFSE, as well as a restricted initial Sr, Nd isotopic compositions range from 0.704311 – 0.704827 and 2.44 – 3.20, respectively.

The felsic metavolcanic rocks have restricted range of SiO_2 contents (64.14 – 68.92%) and are therefore dacite or rhyodacite in composition. These felsic rocks are characterized by distinctly negative Nb, Ta, P, Ti anomalies, together with markedly enrichment in Zr, Hf and moderately fractionation between LREE and HREE ($(La/Yb)_N$=3.87 – 7.80), and additionally relatively homogeneous initial Sr, Nd isotopic compositions range from 0.703810 – 0.704923 and 0.36 – 2.86, respectively. The major, trace element characteristics and initial Nd isotopic compositions (¶≈Nd(t)=2.62 – 3.49) of dykes are similar to those of the mafic rocks except for relatively low abundances of REE and high initial Sr isotopic compositions range from 0.705010 to 0.706391, may reflect some degree of alteration.

Obviously, there is a compositional gap between mafic rocks and felsic metavolcanic rocks, indicating that the Yeba volcanic rocks could be considered as a bimodal association of low-grade metabasalts and low-middle grade felsic metavolcanic rocks. In general, the felsic rocks exhibit relatively high Nb, Ta, Zr, and Hf abundances relative to those of the mafic rocks. These, together with other similar trace element signatures within the Yeba volcanic rocks, provide convincing evidences for the felsic metavolcanic rocks are petrogenetically related to the mafic rocks.

The primitive mantle normalized trace element plots of Yeba volcanic rocks are similar to those of island arc volcanic rocks. This conclusion is also supported by the Ta/Yb against Th/Yb diagram (Pearce, 1982; Michael and Eva, 2000), which further confirm that the Yeba volcanic rocks are belonging to island arc calcalkalic volcanic rocks formed at active continental margins. Generally, island arc volcanic rocks can qualitatively be described as a mixture of altered oceanic crust, depleted mantle, and sediment. For the Yeba mafic rocks, however, we need to consider the effects of crustal contamination rather than subducted sediments, as these mafic rocks have not significantly negative Ce anomalies. Further support for crustal contamination is provided by the $(Th/Ta)_{PM}$ against $(La/Nb)_{PM}$ diagram, which illustrate that the plots of the Yeba mafic rocks obviously close to those of the middle and upper crust (Rudnick and Gao, 2003). High Sr/Y ratios, positive Eu anomaly or lacking a negative Eu anomaly and high Sr abundances of Yeba mafic rocks suggest the influence of slab-derived components. The isotopic composition of Sr and Nd of the Yeba mafic rocks mostly fall in the range characteristic for mantle melts although some crustal components may have been involved. Therefore, the petrogenesis of Yeba mafic rocks is most likely related to the partial melting of predominantly mantle- and altered oceanic crust-derived melts and/or fluids and minor crustal components involved during melting and transporting. The petrogenesis of Yeba felsic metavolcanic rocks was dominated by involving extensive fractional crystallization of mafic magmas, with minor amounts of assimilation.

In summary, the trace element and Sr, Nd isotopic evidences of Yeba volcanic rocks display significantly affinities with island arc bimodal suites erupted at active continental margins, and young, comparatively thin continental crust (Pin and Paquette, 1997) could account for the occurrence of volume felsic volcanic rocks genetically related to the mafic rocks.

Acknowledgments: This study is financially supported by the National Keystone Basic Research Program of China (Grant No.2002CB412609), the Integrated Study of Basic Geology in the Blank Area of Southern Tibetan Plateau (Grant No. 200313000025).

References

[1]. Michael P. Gorton and Eva S. Schandl. 2000. From continents to island arcs: a geochemical index of tectonic setting for arc-related and within-plate felsic to intermediate volcanic rocks. The Canadian Mineralogist, vol.38, 1065-1073

[2]. Pan G. T., Ding J., Yao D. S. et al., 1:1500000 Geological map of Qinghai-Xizang Plateau and its adjacent regions, Chengdu: Chengdu Cartographic Publishing House, 2004.

[3]. Pin C and Paquette J L. 1997. A mantle-derived bimodal suite in the Hercynian belt: Nd isotope and trace element evidence for a subduction-related rift origin of the late Devonian Brévenne metavolcanics, Massif Central (France). Contributions to Mineralogy and Petrology, 129: 222-238

CONTENT TABLE

4 Jonathan C. Aitchison, Jason Ali, Badengzhu, Aileen M. Davis, Dei Faustino, Lan Hui, Smriti Safaya, Iain Ross and Zeng Qinggao
The Bangong-Nujiang suture between Gertse and Dong Tso (84°- 85°e) Central Tibet
5 Jason R. Ali and Jonathan C. Aitchison
Greater India: a review
6 Kazunori Arita and Lalu Prasad Paudel
Regional tectonic correlation of central sector of the Himalaya
7 Nicolas Arnaud, Philippe H. Leloup , Stéphane Guillot, Jean Louis Paquette, Franck Valli, Gweltaz Maheo, Haibing Li, Zhiqin Xu, Robin Lacassin, and Paul Tapponier
Geology, magmatism and deformation in west-central Tibet, along the Longmu-co lake.
8 T.N. Bagati
Carbonate platforms through time and space in the Spiti basin
9 S.R.H. Baqri and A. Ul Kaque
The x-ray diffraction studies of Hunza ruby and its host rocks exposed in Karakoram range.
10 Matthias Bernet, Peter Van der Beek, Pascale Huyghe, and Jean-Louis Mugnier
Continuous and episodic exhumation of the central Himalayas from detrital zircon fission-track analysis of Siwalik sediments, Nepal
12 Pierre Bettinelli, Mireille Flouzat, Jean-Philippe Avouac, Laurent Bollinger and Madhab Raj Pandey
Looking for spatial and temporal variations of interseismic strain from GPS monitoring (CGPS and campaign data) across the Himalaya of Nepal
14 Olivier Beyssac, Bruno Goffé, Laurent Bollinger and Jean-Philippe Avouac
Raman spectroscopy of carbonaceous material (RSCM) thermometry as a new tool for geodynamics: application to the lesser Himalayas of Nepal
16 Rajneesh Bhutani and Kanchan Pand
Simultaneous island and continental arc magmatism in northwest Trans-Himalaya, Ladakh, India: inference from ^{40}ar-^{39}ar study
18 R. Bilqees, M. Q. Jan and M.A. Khan
Chemistry of the silicate phases from the Chilas complex, Kohistan magmatic arc, northern Pakistan
20 Pierre Bouilhol, Jean-Pierre Burg, Jean-Louis Bodinier, Shahid Hussain , Hamid Dawood
The ultramafic sequence of Sapat (NE Pakistan): a key in understanding arc building processes and suturing kinematics
22 M. E. Brookfield
River profiles, tectonics and climate in the great Pamir indenter of central Asia.
24 Jean-Pierre Burg, Oliver Jagoutz, Hamid Dawood, Shahid Hussain
Pre-collision tilt of crustal blocks in extended island arcs: structural evidence in the Kohistan arc
26 Rodolfo Carosi, Chiara Montomoli, Dario Visonà
High grade shear zones in the core of the Himalayan belt (western Nepal): consequences on the exhumation of the higher Himalayan crystallines
27 Rodolfo Carosi, Chiara Montomoli, Giovanni Ruggieri
Kinematic and tectonic evolution of the main central thrust zone in lower Dolpo (western Nepal)
28 Jennifer Chambers, Mark Caddick, Andy Richards, Tom Argles, Nigel Harris, Randy Parrish
Isotopic maps of Himalayan units – a framework for metamorphic analysis of channel flow
30 Deepak Chamlagain and Daigoro Hayashi
Stress field and fault development in Thakkhola half graben : a numerical modelling approach
32 Julien Charreau, Yan Chen, Stuart Gilder, Stéphane Dominguez, Jean-Philippe Avouac, Sevket Sen, and Yongan Li
Timing of the late Cenozoic uplift of the chinese TianShan constrained by magnetostratigraphy and rock magnetism from Junggar and Tarim basin
34 François Chauvet, Henriette Lapierre, Delphine Bosch, Georges Mascle, Jean-Claude Vannay
Intraplate volcanism on the southern Tethyan margin (North Arabian and North Indian margins)
36 Zhengle Chen, Xiaofeng Wang, Jian Liu
Sedimentary record reveals uplifting process of mountains in northern edge of the Tibetan plateau
38 Yan Chen, Suart Gilder and Vincent Courtillot
Paleomagnetic contrains on Cenozoic motion of the Altyn Tagh fault, rotation of the Qaidam basin and the northern edge of Tibetan plateau
39 Marie Luce Chevalier, Paul Tapponnier, F. J. Ryerson, R. Finkel, Jérome Van der Woerd, Haibing Li, Qin Liu
Tenfold disparity between decadal insar and millenial morphochronologic slip-rates on the Karakorum fault.
40 Cecily O.J. Chun, Zhifei Liu, Margaret L. Delaney, Xianghui Li and Xinrong Cheng
Marine sedimentary response across the Paleocene-Eocene thermal maximum (PETM) at Tingri, southern Tibet

42 Brian J. Darby, Bradley D. Ritts and Yongjun Yue
Does the Altyn Tagh fault extend beyond the Tibetan plateau?
44 Megh Raj Dithal
Lesser Himalayan Tertiary beds of far west Nepal and their comparison with Chakrata (Saknidhar) and Rautgara formations of Kumaon, India
46 Guochen Dong, Xuanxue Mo, Zhidan Zhao, Tao Chen, Liangliang Wang
Mixing event between the crust and mantle derived magmas: evidences from zircon survidences from zircon shrimp II chronology of the Chushu pluton in southern Gangdese, Tibet
47 Ashok Kumar Dubey
Estimation of crustal shortening in the Himalaya: problems and possible solutions using the model deformation experiments
48 M. Dubille, J. Lavé, R. Pik, E. Labrin
Landscape response in small and large watersheds of central Nepal constrained by thermochronology.
50 Nadine Ellouz
From Himalayan collision to Makran subduction
52 Nadine Ellouz, Siegfried Lallemand, Anne Battani, Philippe Boning, Christophe Buret, Raymi Castilla, Louis Chérel, Muhammad Danish, Guy Desaubliaux, Eric Devill, Jérémie Ferrand, Alexandra Gourlan, Syed Hasany, Pascale Leturmy, Andreas Lugke, Geoffroy Mahieux, Georges Mascle, Guillemette Ménot-Combes, Nicolas Mouchot, Peter Muhr, Laetitia Pichevin, Anne-Catherine Pierson-Wickmann, Philippe Robion, Julien Schmitz, Aamir Hazhad, Aurélie Vantoer, Flavien Waucher
The CHAMAK survey (Pakistan) offshore frontal part of the Makran prism
54 Christian France-Lanord, Albert Galy, Valier Galy, Sunil K. Singh
Modern flux of erosion of the Ganga basin from geochemical budget
55 Maurizio Gaetani
The Triassic in the Karakorum range (Pakistan).
56 Audrey Galve, Alfred Hirn, Martine Sapin, Jiang Mei, Mireille Laigle, Béatrice de Voogd, Josep Gallart
Contrasts in temperature and hydration of the deep crust across present Tibet, and eclogitization (?) of lower crustal material
58 Gao Rui, Ma Yongsheng, Zhu Xuan, Li Qiusheng, Li Zhongyuan, Zeng Tianfa, Li Pengwu, *Wang Haiyan, Zhu Haihua, Zeng Hongwei*
Lithospheric structure of the Songpan block in the northeastern Tibetan plateau— revelation from investigation of the deep seismic profile
60 Eduardo Garzanti, Giovanni Vezzoli, Sergio Andò, Christian France-Lanord, Peter Clift, Gavin Foster, Paolo Paparella and Sunil Singh
Focused erosion at Himalayan syntaxes as documented by the composition of Indus and Brahmaputra river sands
64 E. Gayer, J. Lavé, R. Pik, C. France Lanord
Precise timing of Holocene glaciation and paleoclimatic evolution in Ganesh Himal (central Nepal) constrained by cosmogenic ^{3}He dating of garnets.
66 Johann Genser, Franz Neubauer, Yongjiang Liu, Xiaohong Ge, Gertrude Friedl and Andrea Rieser
An active fault at the northern border of the Qaidam basin, China: implications for extrusion models
68 Vincent Godard, Jérôme Lavé and Rodolphe Cattin
Recent evolution of the Longmen Shan, eastern Tibet: insights from denudation rates and numerical modeling
69 Djordje Grujic, Christopher Beaumont, Rebecca A. Jamieson and Mai H. Nguyen
Extruded domes in the greater Himalayan sequence: model predictions and possible examples
70 Djordje Grujic, Isabelle Coutand, Bodo Bookhagen, Ann Blythe, Stéphane Bonnet and Chris Duncan
Climate leads – tectonics follows: geologic consequences of asynchronous denudation along the Himalaya
71 Carl Guilmette, Réjean Hébert, Céline Dupuis, Viviane Dubois-Coté, Wang Chenshang, Li Zejung
Petrology, geochemistry and geochronology of highly foliated amphibolites underlying the Yarlung Zangbo suture zone ophiolites, southern Tibet ; geodynamical implications for the dismembered dynamothermal sole
72 Daigoro Hayashi
3d strain analysis as a tester for numerical simulation
74 Réjean Hébert, Carl Guilmette, Céline Dupuis, Viviane Dubois-Coté, François Huot, Chengshan Wang, Yalin Li
The Yarlung Zangbo suture zone ophiolites, Tibet : a synthesis
76 Georges Herquel
An overview of crustal and mantle anisotropy in Tibet
78 Alfred Hirn, Audrey Galve, Jiang Mei, Mireille Laigle, Martine Sapin, Béatrice de Voogd, Jordi Diaz
Seismic–inspired model section of crust and mantle wedges and its balancing: time evolution of localization of deformation with depth and across Himalaya-Tibet
80 Pascale Huyghe, Ananta Prasad Gajurel, Jean-Louis Mugnier, Matthias Bernet and Peter Van der Beek
Sedimentological analysis of the Karnali river section (Siwaliks of western Nepal) : implication for the upper Miocene evolution of the Himalayan belt and climate

82 Takeshi Imayama and Kazunori Arita
Sr-Nd isotopic study of main central thrust zone in Nepal Himalaya
84 O. Jagoutz, J.P. Burg, T. Iizuka, T. Hirata, S Maruyama, S. Hussain, H. Dawood, N.M. Chaudhry
The plutonic crust of the Kohistan island arc (NW Pakistan): history from La-icpms U-Pb zircon ages of intrusive units.
86 O. Jagoutz, O.Müntener, J.P. Burg, P.Ulmer, E.Jagoutz, T.Pettke
The zoned ultramafic bodies of the Chilas complex in the Kohistan island arc (NW Pakistan)
88 A. K. Jain, Devender Kumar, Nand Lal, R. M. Manickavasagam, A. K. Choudhary and Sandeep Singh
Erosion vs. tectonic exhumation: FT and Rb-Sr mineral ages for fold-controlled tectonics from Northwest Himalaya
90 M. Qasim Jan and Barry L. Weaver
Petrology of the ultramafic-mafic Tora Tigga complex, Kohistan magmatic arc, northern Pakistan
92 Jiang Wan, Ye Peisheng, Hu Daogong, Wu Zhenhan
Mesozoic phlogopite-bearing olivine websterite in Tethyan-Himalaya
94 Cari L. Johnson and Laura E. Webb
Cenozoic reactivation of the east Gobi fault zone: extrusion tectonics in southeastern Mongolia
96 F. Jouanne, J. L. Mugnier, J. F. Gamond, P. Le Fort, M. R. Pandey, L. Bollinger, M. Flouzat and J. P. Avouac
Current shortening across the Himalayas of Nepal
98 Allah B. Kausar, Christian Picard, Yutaka Takahashi, Masumi U. Mikoshiba, Hiroshi Yamamoto, Said R. Khan, Tahseenullah Khan, and Hafeez U. Rehman
Petrogenetic characeteristics and tectonic setting of Thak Gah and Jijal ultramafic-mafic complexes of Kohistan arc, Pakistan
99 Shan Ke, Zhaohua Luo, Xuanxue Mo
Geochemistry and petrology of Taxkorgan alkaline complex, NW Himalaya
100 Dharma Raj Khadka and Stephen J. Lippard
Resource assessment and hydrocarbon potential of theforeland basin petroleum system of Nepal
102 Muhammad Ahmed Khan
Implications of comagmatic relationship between ganitoids of southeast Kohistan, NW Himalayas, Pakistan.
104 Jessica King, Nigel Harris, Tom Argles, Randy Parrish
Constraints on tectonic models from crustal melt formation in southern Tibet
106 Santosh Kumar and Antonio Castro
Geochemistry and petrogenesis of microgranular enclaves in Cambro-Ordovician granitoids of Champawat region, Kumaun Lesser Himalaya, India
108 J. Lavé, D. Yule, S. Sapkota, K. Basant, C. Madden, M. Attal and R. Pandey
Evidence for a great medieval earthquake (~a.d. 1100) in central Himalaya, Nepal, and seismotectonic behavior of the main Himalayan thrust
110 P.H. Leloup, N.A. Arnaud, B. Vuadelle, R. Lacassin, F. Valli, G. Mahéo, P. Tapponnier
A ductile thrust zone within the Gangdese batholith (South Tibet).
112 Yalin Li, Chengshan Wang, Mou Wang and Haisheng Yi
Rivers geomorphology of the Yangtze river source region and neotectonic movement of north Tibet
114 Tao Liang, Zhaohua Luo
Shrimp U-Pb zircon age of Cenozoic alkali basalts in the Tuyon basin, SW Tien Shan, and its geologic implications
116 Liao Zhongli, Mo Xuanxue, Pan Guitang, Zhu Dicheng, Wang Liquan, Li Guangming, Geng Quanru, Zhao Zhidan, Liu Bo
Characteristics and significance of the accessory minerals from the Tibet peraluminous granites
118 Liao Zhongli, Mo Xuanxue, Pan Guitang, Zhu Dicheng, Wang Liquan, Li Guangming, Geng Quanru, Zhao Zhidan, Liu Bo
Petrogenesis and continental dynamics significance of peraluminous granite in Tibet
120 Jing Liu, Yann Klinger, Xiwei Xu, Cécile Lasserre, Guihua Chen, Wenbing Chen, and Paul Tapponnier
Eight-hundred-year recurrence of large earthquakes on the Haiyuan fault near Songshan, Gansu province, China
121 Xiaohan Liu
Structural feature of Yarlung Zangbo ophiolite zone and its tectonic significance
122 Yan Liu, Wolfgang Siebel, Hans-Joachim Massonne, Xuchang Xiao
Tectonic evolution of the central Higher Himalayan Crystallines in the Kharta area, southern Tibet: new constraints from petrologic and geochronological data
123 Zhifei Liu, Christophe Colin, Alain Trentesaux, Giuseppe Siani, Norbert Frank, Dominique Blamart, Segueni Farid
Late Quaternary climatic control on erosion and weathering in the eastern Tibetan plateau and the Mekong basin

124 Bruno Lombardo, Daniela Rubato, Franco Rolfo and Piero Pertusati
P-T evolution and age of the barrovian metamorphism in the MCT zone of the Arun valley, E Nepal
126 Zhaohua Luo, Xuanxue Mo, Jinfu Deng, Zhongmin Huang, Shan Ke
The relationship of three Cenozoic geodynamic regimes in Tibetan plateau: evidences from the igneous rocks
128 Zhaohua Luo, Yusheng Wang, Xuanxue Mo, Jinfu Deng, Zhongmin Huang
The Cenozoic basalts from Kangxiwar (western Kunlun) and their implications to the uplifting of the Tibetan plateau
130 Gweltaz Mahéo, Jean Philippe Avouac, Aron Meltzner, Laurent Bollinger and Ken Farley
Neogene exhumation of the Palung granite (Lesser Himalaya, Nepal) from (U-Th)/He thermochronology
132 Gweltaz Mahéo, Franck Valli, Philippe Hervé Leloup, Robin Lacassin, Nicolas Arnaud, Jean-Louis Paquette, Alain Ferandez, Li Haibing, Ken Farley and Paul Tapponnier
Timing constraints on the Kung Co pluton and normal fault (South Tibet, P.R.China) based on Ar/Ar and (U-Th)/He thermochronology
134 Jean-Louis Mugnier, Pascale Huyghe
Re-organisation of the Himalayan foreland basin geometry as a result of a break-off of the Indian slab
136 Barun Mukherjee, Himanshu Sachan and Talat Ahmad
A new occurrence of microdiamond from Indus suture zone, Himalaya: possible origin
137 Y. Najman, P. De Celles, G. Gehrels, A. Carter, A. Martin, G. Oliver, E. Garzanti.
Provenance of early foreland basin sediments, Nepal: constraints to the timing and diachroneity of early Himalayan orogenesis.
138 P.S. Negi
Ecological signature of slope instability and its implication in landslide hazard mitigation (lhm) - a case study along MCT zone in himalayan mountains
139 Franz Neubauer, Yongjiang Liu, Johann Genser, Andrea Rieser and Xiaohong Ge
Cenozoic shortening and Lateral extrusion of the Qaidam block at the Northeastern margin of the Tibet plateau: constraints from structural analysis and basin evolution
140 Franz Neubauer, Yongjiang Liu, Johann Genser, Andrea Rieser, Robert Handler, Gertrude Friedl and Xiaohong Ge
$^{40}Ar/^{39}Ar$ detrital white mica ages of Palaeozoic and Mesozoic sandstones from Qilian and Altyn Mountains, China: Constraints
142 Patrick O'Brien
Himalayan eclogite formation: a critical precursor to channel flow?
144 Pan Guitang, Wang Liquan, Li Guangming, Zhu Dicheng, Geng Quanru
Division of tectonic units of the main collisional belt between Indian and Asian continent and its geodynamic setting
146 R.C. Patel, Yogesh Kumar and Nand Lal
Southwestward Extrusion and Exhumation of rocks of the Higher Himalayan Crystallines, Kumaon, NW-Himalaya, India: as revealed from Fission Track and structural studies along Kali-Darma valleys
148 Lalu Prasad Paudel, Takeshi Imayama and Kazunori Arita
Metamorphic History of the Lesser Himalaya in central Nepal recorded by metabasic rocks: New constaints from amphibole chemistry and thermobarometry
150 R. Pik, C. France-Lanord and J. Carignan
Extreme uplift and erosion rates in eastern Himalayas (Siang-Brahmaputra basin) revealed by detrital (U-Th)/He thermochronology
152 Beth Pratt-Sitaula, Douglas Burbank, Arjun Heilsath, Emmanuel Gabet
Impacts of climate change on surface processes, Nepal Himalaya
154 Qiu Ruizhao, Zhou Su, Xiao Qinghui, Deng Jinfu, CaiZhiyong and Zhao Guochun
Discussion on the Basement of Qinghai-Tibetan Plateau, China: evidences from the Nd Isotope of igneous rocks
155 Santa Man Rai, Masaru Yoshida, Prakash Das Ulak and Bishal Nath Upreti
Observation of deformation and metamorphism in the Everest area, Eastern Nepal Himalaya
156 Dhananjay Regmi,Tanaka Shunsuke and Teiji Watanabe
Rock glaciers and the lower limit of discontinuous mountain permafrost in the Langtang valley, Nepal Himalaya
158 Hafiz Ur Rehman and Hiroshi Yamamoto
Mineralogical and textural patterns in HP-UHP eclogites and surrounding felsic/pelitic rocks in Kaghan-Naran valley, Pakistan Himalaya
160 Shoumai Ren,Yongjiang Liu, Dewu Qiao, Xiaohong Ge, Zhenyu Yang, Andrea Rieser
An important geological event in northern Tibetan Plateau: Evidences of ^{36}Cl dating from western Qaidam basin
162 Anne Replumaz, Stéphane Guillot, Pierre Strzerzynski
Himalaya ultrahigh pressure evolution and warped Indian subduction plane
164 Andy Richards, Tom Argles, Nigel Harris, Randy Parrish, Talat Ahmad, Fiona Darbyshire and Erich Draganits
Himalayan architecture constrained by isotopic tracers from clastic sediments

166 Andrea B. Rieser, Franz Neubauer, Yongjiang Liu, Johann Genser, Gertrude Friedl, Robert Handler and Xiaohong Ge
Sediments of the Cenozoic Qaidam Basin in Western China: Linking basin fill with mountains by isotopical and compositional constraints
168 Bradley Ritts, Yongjun Yue and Stephan Graham
Tertiary slip rates of the Altyn Tagh fault and magnitude and timing of shortening and strike-slip in northeast Tibet
170 Franco Rolfo, William McClelland & Bruno Lombardo
Geochronological constraints on the age of the eclogite-facies metamorphism in the eastern Himalaya
171 Yann Rolland, Marc Sosson, Michel Corsini, Taniel Danelian, Ara Avagayan, Gazhar Galoian, Raphael Melkonian and Ruben Jrbashyan.
Tethys: from the Mediterranean to Tibet. Comparisons of ophiolites from Armenia and Kohistan-Ladakh, and their significance for the reconstruction of Tethys history.
172 Ghazala Roohi and S.R.H. Baqri
The correlation of the Fusulinids (Foraminifera) found in the Permian rocks of Salt Range and the Permian rocks of Karakoram Range, Pakistan.
173 Smriti Safaya, Jonathan Aitchison and Jason Ali
Neotectonic faulting along the central Bangong-Nujiang suture zone, central Tibet
174 Mohammad Tahir Shah and Hassan Agheem
Field aspects of the gems and gem-bearing pegmatites of the Shigar valley, Skardu, northern areas of Pakistan
175 Wei Shi, Yinsheng Ma, Yueqiao Zhang, Chunshan Zhang, Huiping Zhang
Characteristics of activity of Maqu fault in the east segment of Kunlun fault
176 Julia de Sigoyer, Manuel Pubellier, Vincent Godard, Wu Xiawei
Preliminaries petrological results on the uplift of the Longmen Shan mountain range (Sichuan, China)
177 Jagmohan Singh, S. Mahanti and Kamla Singh
Geology and evaluation of hydrocarbon prospects of Tethyan sediments in Spiti vally, spiti and Zanskar, Himachal Pradesh
178 Sandeep Singh, A.K. Jain, A.K.Choudhary, Th. Nikunja Bihari Singha
Himalayan migmatite and its relation with collision tectonics
179 Bla Stres, Ivan Mahne, Teiji Watanabe and Ines Mandi-Mulec
Global climate change – the contribution of high altitude soils from the Himalaya
180 Paul Tapponnier, Anne Replumaz, R. D. Van Der Hilst, Gérard Wittlinger, Jérome Vergne
Fate of the lithospheric mantle beneath Tibet : hidden plate tectonics ?
181 Shahina Tariq, Syed Hamidullah and Mohammad Tahir Shah
Environmental geochemistry of the soils of Peshawar basin, Lesser Himalayas, Pakistan
182 V.C. Thakur, N. Suresh and G. Perumal
Late Quaternary landscape evolution in fault-bend fold system, Pinjor Dun, Panjab SubHimalaya, India
183 Rasmus C. Thiede, Rámon Arrowsmith, Bodo Bookhagen, Michael O. McWilliams, Edward R. Sobel and Manfred R. Strecker
From tectonically 'to erosionally controlled development of the Himalayan fold-and-trust belt
184 Rasmus C. Thiede, Rámon Arrowsmith, Bodo Bookhagen, Michael O. McWilliams, Edward R. Sobel and Manfred R. Strecker
Mid Miocene to Recent E-W extension in the Tethyan Himalaya, Leo Pargil dome, NW-India
185 Franck Valli, Nicolas Arnaud, Haibing Li, Robin Lacassin, Edward Sobel, Gweltaz Mahéo, Paul Tapponnier, Philippe Hervé Leloup, Stéphane Guillot, Zhiqin Xu
Deformation along the Karakorum fault, Western Tibet: Ar-Ar, Fission tracks, and U-Th-He geochronological constraints
186 Franck Valli, Jean Louis Paquette, Haibing Li, Philippe Hervé Leloup, Nicolas Arnaud, Stéphane Guillot, Robin Lacassin, Paul Tapponnier, Dunyi Liu, Zhiqin Xu, Etienne Deloule, Gweltaz Mahéo
High Temperature deformation along the Karakorum fault, Western Tibet: U-Th-Pb geochronological constraints
187 Jérôme Van Der Woerd, Frederick J. Ryerson, Paul Tapponnier, Anne-Sophie Meriaux, Xu Xiwei, B. Meyer, and Robert C. Finkel
Rates of crustal uplift and shortening along the northern margin of Tibet based on Pleistocene-Holocene cosmogenic dating of folded alluvial fans and terraces
188 Peter Van der Beek, Jean-Louis Mugnier, Pascale Huyghe, Erika Labrin and Matthias Bernet
Late Miocene – Recent denudation of the Himalayas and recycling in the foreland basin from detrital apatite fission-track analyses of Siwalik sediments, Nepal
190 Priti Verma and Rajesh Sharma
Fluid mixing in barite of Tons valley, Lesser Himalaya, India: using δ^{34} S ratio
192 Giovanni Vezzoli, Bruno Lombardo and Franco Rolfo
A geological reconnaissance to southern Kangchendzonga massif

193 I.M. Villa, B.Lombardo
Isotopic inheritance in the MCT zone, Arun valley, E Nepal
194 Wang Chengshan, Wei Yushuai, Jansa Jansa
Paleogene Gyachala Formation in Gyangze, Tibet: Implication to the closing of New Tethys Ocean
195 Yanbin Wang, Dunyi Liu and Jinhe Li
Zircon U-Pb shrimp dating of High Himalaya rocks from the Shibuqi region, southwestern Tibet
196 Fangzhi Yang, Yongsheng Ma, Xuan Zhu, Tonglou Guo, Zhongyuan Li Guoxiong Li , Tianfa Zheng, and Guixiang Yang
Geophysical characteristics of the crystalline-basement in Songpan-Arba, China
198 Masaru Yoshida, Santa Man Rai and Bishal Nath Uupreti
Mylonite and ultramylonite along the Main Central Thrust in the Kaligandaki valley area, west-central Nepal Himalaya
199 Yue Laiqun, Shi Xiaoying, Wang Hongzhen
Sedimentary characteristics and environments of submarine fan of the Lower Cretaceous in northern Himalayas
200 Zhai Qingguo, Li Cai, Li Huimin, Wang Tianwu
The geochemical features and U-Pb geochronology of leucogranite in central Gangdise, Tibet
202 Zhao Junmeng, Liu Hongbing, Pei Shunping
Geodynamics profile across the Indian-Eurasian plate boundary
204 Zhizhong Zhao, Joerg M. Schaefer, Silvio Tschud and Christian Schluechter
Surface exposure age of the glaciations in Tibet
206 Zhu Dicheng, Pan Guitang, Wang Liquan, Geng Quanru, Li Guangming, Liao Zhongli, Liu Bo
Ages, origins and tectonic setting of the Yeba bimodal volcanic rocks in Lhasa area, South Tibet

Agheem H. 174
Ahmad T. 136 , 164
Aitchison J. 4, 5, 173
Ali J. 4, 5, 173
Andò S. 60,
Argles T. 28, 104, 164
Arita K. 6, 82, 148
Arnaud N. 7, 110, 132, 185, 186
Arrowsmith R. 183, 184
Attal M. 108
Avagayan A. 171
Avouac J.P. 12, 14, 32, 96, 130
Badengzhu 4
Bagati T.N. 8
Baqri S.R.H. 9, 172
Basant K. 108
Battani A. 52
Beaumont C. 69, 70
Bernet M. 10, 80, 188
Bettinelli P. 12
Beyssac O. 14
Bhutani R. 16
Bilqees R. 18
Blamart D. 123
Blythe A. 70
Bodinier J.L. 20
Bollinger L. 12, 14, 96, 130
Boning P. 52
Bonnet S. 70
Bookhagen B. 70, 183, 184
Bosch D. 34
Bouilhol P. 20
Brookfield M. E. 22
Burbank D. 152
Buret C. 52
Burg J.P. 20, 24, 84, 86
Caddick M. 28
Cai Z. 154
Carignan J. 150
Carosi R. 26, 27
Carter A. 137
Castilla R. 52
Castro A. 106
Cattin R. 68
Chambers J. 28
Chamlagain D. 30
Charreau J. 32
Chaudhry N.M. 84
Chauvet F. 34
Chen G. 120,
Chen T. 46
Chen W. 120
Chen Y. 32, 38
Chen Z. 36
Cheng X. 40
Chérel L. 52
Chevalier M.L. 39
Choudhary A. K. 88, 178
Chun C. 40
Clift P. 60
Colin C. 123
Corsini M. 171
Courtillot V. 38
Coutand I. 70
Danelian T. 171
Danish M. 52
Darby B.J. 42
Darbyshire F. 164
Davis A. 4
Dawood H. 20, 24, 84
De Celles P. 137
Dei F. 4
Delaney M. 40
Deloule E. 186
Deng J. 126, 128,154
Desaubliaux G. 52
Deville E. 52
Diaz J. 78
Dithal M.R. 44
Dominguez S. 32
Dong G . 46
Draganits E 164
Dubille M. 48
Dubey A. K. 47
Dubois-Coté V. 71, 74
Duncan C. 70
Dupuis C. 71, 74
Ellouz N. 50, 52
Farid S. 123
Farley K. 130, 132
Ferandez A. 132
Ferrand, F. 52
Finkel R. 39, 187
Flouzat M. 12, 96
Foster G. 60
France-Lanord C. 54, 60, 64, 150
Frank N. 123
Friedl G. 66, 140, 166
Gabet E. 152
Gaetani M 55
Gajurel A.P. 80
Gallart J. 56
Galoian G. 171
Galve A. 56, 78
Galy A. 54
Galy V. 54
Gamond J.F. 96
Gao R. 58
Garzanti E. 60, 137
Gayer E. 64
Ge X. 66, 139, 140, 160, 166
Geng Q. 116, 118, 144, 206
Genser J. 66, 139, 140, 166
Gehrels G. 137
Gilder S. 32,
Godard V. 68, 176
Goffé B. 14
Gourlan A. 52
Graham S. 168
Grujic D. 69
Guillot S. 7, 162, 185, 186
Guilmette C. 71, 74
Guo T. 196
Hamidullah S. 181
Handler R. 140, 166
Haque A. Ul 9
Harris N. 28, 104, 164
Hasany S. 52
Hayashi D. 30, 72
Hazhad A. 52
Hébert R. 71, 74
Heilsath A. 152
Herquel G. 76
Hirata T. 84
Hirn A. 56, 78
Hu D. 92
Huang Z. 126, 128
Hussain S. 20, 24, 84
Huyghe P. 10, 80, 134, 188
Imayama T. 82, 148
Izuka T. 84
Jagoutz E. 86
Jagoutz O. 24, 84, 86
Jain A. K. 88, 178
Jamieson R. A. 69
Jan M. Q. 18, 90
Jansa J. 194
Jiang W. 92
Johnson C.L. 94
Jouanne F. 96
Jrbashyan R. 171
Kausar A. B. 98
Ke S. 99, 126
Khadka D.R. 100
Khan M. A. 18, 102
Khan Said R. 98 T
Khan T. 98
King J. 104
Klinger Y. 120
Kumar D. 88
Kumar S. 106
Kumar Y. 146
Labrin, 188
Lacassin R. 7, 110, 132, 185, 186
Laigle M. 56, 78
Lal N. 88, 146
Lallemand, S. 52
Lan H. 4
Lapierre H. 34
Lasserre C. 120
Lavé J. 48, 64, 68, 108
Le Fort P. 96
Leloup P.H. 7, 110, 132, 185, 186
Leturmy P. 52
Li C. 200
Li G. 116, 118, 144, 196, 206
Li H. 7, 39, 132, 185, 186, 200
Li J. 195
Li P. 58
Li Q. 58
Li X. 40
Li Y. 32
Li YL. 74, 112

Li Z. 58, 196
Li Ze. 71
Liang T. 114
Liao Z. 116, 118, 206
Lippard S. J. 100
Liu B. 116, 118, 206
Liu D. 186, 195
Liu H. 202
Liu J. 36, 120
Liu Q. 39
Liu X. 121
Liu Y. 66, 122, 139, 140, 160, 166
Liu Z. 40, 123
Lombardo B. 124, 170, 192, 193
Lugke A. 52
Luo Z. 99, 114, 126, 128
Ma Y. 58, 175, 196
Madden C. 108
Mahanti S. 177
Maheo G. 7, 110, 130, 132, 185, 186
Mahieux G. 52
Mahne I. 179
Mandi-Mulec I. 179
Manickavasagam R. M. 88
Martin A. 137
Maruyama S. 84
Mascle G. 34, 52
Massonne H.J. 122
Mc Clelland W. 170
Mc Williams M.O. 183, 184
Mei J. 56, 78
Melkonian R. 171
Meltzner A. 130
Ménot-Combes G. 52
Meriaux A.S. 187
Meyer B. 187
Mikoshiba M.U. 98
Mo X 46, 116, 118, 126, 128
Montomoli C. 26, 27
Mouchot N. 52
Mugnier J.L. 10, 80, 96, 134, 188
Muhr P. 52
Mukherjee B. 136
Müntener O. 86
Najman Y. 137
Negi P.S. 138
Neubauer F. 66, 139, 140, 166
Nguyen M. 69
O'Brien P. 142
Oliver G. 137
Pan G. 116, 118, 144, 206
Pande K. 16
Pandey M.R. 12, 96, 108
Paparella P. 60
Paquette J.L. 7, 132, 186
Parrish R. 28, 104, 164
Patel R.C. 146
Paudel L.P. 6, 148
Pei S. 202
Pertusati P. 124
Perumal G. 182
Pettke T. 86
Picard C. 98
Pichevin L. 52
Pierson-Wickmann A.C. 52
Pik R. 48, 64, 150
Pratt-Sitaula B. 152
Pubellier M. 176
Qiao D. 160
Qiu R. 154
Rai S.M. 155, 198
Regmi D. 156
Ren S. 160
Rehman H. U. 98, 158
Replumaz A. 162, 180
Richards A. 28, 164
Rieser A. 66, 139, 140, 160, 166
Ritts B.D. 42, 168
Robion P 52
Rolfo F. 124, 170, 192
Rolland Y 171
Roohi G. 172
Rubato D. 124
Ruggieri G. 27
Ryerson F. J. 39, 187
Sachan H. 136
Sapin M. 56, 78
Sapkota S. 108
Sen S. 32
Schaefer J.M. 202
Schmitz J. 52
Schluechter C. 202
Sharma R. 190
Shi W. 175
Shi X. 199
Shunsuke T. 156
Siani G. 123
Siebel W. 122
Sigoyer J. de 176
Singh J. 177
Singh K. 177
Singh S. K. 54
Singh Sandeep 88, 178
Singh Sunil 60
Smriti S. 4, 173
Sobel E.R. 183, 184, 185
Sosson M. 171
Strecker M.R. 183, 184
Stres B 179
Strzerzynski P. 162
Suresh N. 182
Tahir Shah M. 174, 181
Takahashi Y. 98
Tapponnier P. 7, 39, 110, 120, 132, 180, 185, 186, 187
Tariq S. 181
Thakur V.C. 182
Trentesaux A. 123
Thiede R. C. 183, 184
Tschud S. 202
Ulak P.D. 155
Ulmer P. 86
Upreti B.N. 155, 198
Valli F. 7, 110, 132, 185, 186
Van der Beek P. 10, 80, 188
Van Der Hilst R.D. 180
Van der Woerd J. 39, 187
Vannay J.C. 34
Vantoer A. 52,
Vergne J. 180
Verma P. 190
Vezzoli G. 60, 192
Villa I.M. 193
Visonà D. 26, 27
Voogd B. de 56, 78
Vuadelle B. 110
Wang C. 71, 74, 112, 194
Wang H. 58, 199
Wang L. 46, 116, 118, 144, 206
Wang M. 112
Wang T. 200
Wang X. 36
Wang Y. 128, 195
Watanabe T. 156, 179
Waucher F. 52
Weaver B. L. 90
Webb L. E. 94
Wei Y. 194
Wittlinger G. 180
Wu X. 176
Wu Z. 92
Xiao Q. 154
Xiao X. 122
Xu X. 120, 187
Xu Z. 7, 185, 186
Yamamoto H. 98, 158
Yang F. 196
Yang G. 196
Yang Z. 160
Ye P. 92
Yi H. 112
Yoshida M. 155, 198
Yue Y. 42, 168, 199
Yule D. 108
Zhang C. 175
Zhang H. 175
Zhang Y. 175
Zhai Q. 200
Zhao G. 154
Zhao J. 202
Zhao Z. 46, 116, 118, 204
Zeng H. 58
Zeng Q. 4
Zeng T. 58, 196
Zhou S. 154
Zhu D. 116, 118, 144, 206
Zhu H. 58
Zhu X. 58, 196